


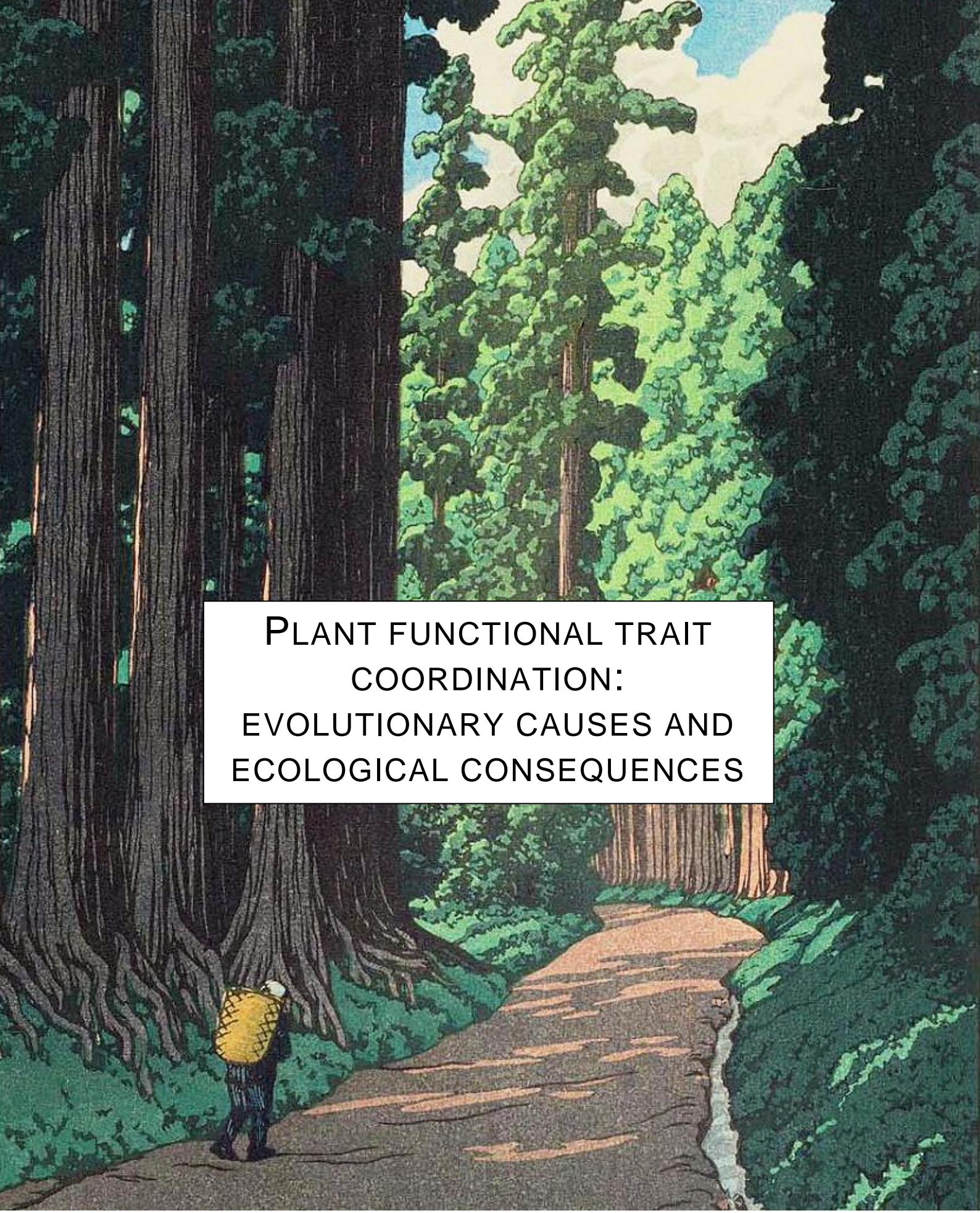


ADVERTIMENT. L'accés als continguts d'aquesta tesi queda condicionat a l'acceptació de les condicions d'ús establertes per la següent llicència Creative Commons:  <https://creativecommons.org/licenses/?lang=ca>

ADVERTENCIA. El acceso a los contenidos de esta tesis queda condicionado a la aceptación de las condiciones de uso establecidas por la siguiente licencia Creative Commons:  <https://creativecommons.org/licenses/?lang=es>

WARNING. The access to the contents of this doctoral thesis it is limited to the acceptance of the use conditions set by the following Creative Commons license:  <https://creativecommons.org/licenses/?lang=en>



PLANT FUNCTIONAL TRAIT
COORDINATION:
EVOLUTIONARY CAUSES AND
ECOLOGICAL CONSEQUENCES

PABLO SANCHEZ MARTINEZ
2023

PLANT FUNCTIONAL TRAIT COORDINATION: EVOLUTIONARY CAUSES AND ECOLOGICAL CONSEQUENCES

DISSERTATION
submitted in partial fulfilment
of the requirements for the doctorate in Terrestrial Ecology

by
Pablo Sanchez Martinez

supervised by **Jordi Martinez-Vilalta and Maurizio Mencuccini**

UAB
Universitat Autònoma
de Barcelona



Centre for Research on Ecology and Forestry Applications (CREAF)
Autonomous University of Barcelona

Barcelona, March, 2023

LA MEVA TESIS

Aquesta tesis ha estat un camí dins d'un bosc.

A vegades, una aventura.

D'altres, un passeig.

Fins i tot ha pogut arribar a ser una petita cursa contra un mateix.

D'aquest camí: els arbres.

La grandesa d'uns éssers que ens son tan aliens que, si nosaltres som de peus a Terra, els ocells al cel, i els fongs a la lluna, ells es trobarien ben be a Mart. Tan estranys com familiars, doncs han estat i son la nostra casa.

Han estat la meva casa des de ben petit. M'hi he trobat a gust, tranquil, segur, al bosc. I ara, que puc entendre una ínfima part de la seva existència, m'hi trobo despert. O més aviat... tot just obrint els ulls.

D'aquest camí: la motxilla.

Porto un bagatge que va creixent a cada passa i en determina la següent. És tan gran aquesta bossa que miro enrere i em costa imaginar-me sense ella. M'ha acabat definint? Tots els organismes la porten, aquesta bossa. Una bossa que acumula, que agafa i que desprèn. Una bossa que, a vegades, fins i tot destria. Aquesta bossa va més enllà de l'individu que camina i es remunta fins que tots els camins es troben. Una bossa que canvia quan els camins es bifurquen i ens donem el "fare well" emocional, físic, ecològic, (filo)genètic... Una bossa que porta l'empremta del passat i és la porta cap al que vindrà.

D'aquest camí: els acompanyants.

Els camins es fan millor en companyia. Una grata companyia ha estat la que jo m'he trobat en aquest petit gran viatge. Primer, una ventada quasi aleatòria va portar a aquesta petita llavor a terra fèrtil. Els meus directors, Maurizio Mencuccini i Jordi Martínez Vilalta, han proporcionat el substrat perfecte per a desenvolupar aquesta aventura. Ells han sabut trobar les paraules que guien i sobretot els somriures que inspiren. M'han obert les portes a un món que ara ja és part de mi. Gràcies per compartir, per la immensa ajuda, pel bon tracte i les oportunitats. Gràcies. Durant aquest camí m'hi he trobat un tercer director de tesi. Ell em va acollir des d'un principi, em va aportar la llum necessària que em va guiar cap a una recerca que he acabat sentint meva. Gràcies, Kyle Dexter, doncs la teva ajuda i predisposició han estat crucials per a la producció d'aquesta petita peça de la que, espero, ens puguem sentir tots ben orgullosos. Altres acompanyants han actuat com a facilitadors, fent d'aquest petit viatge una aventura transoceànica. Vull agrair especialment a David Ackerly i Todd Dawson per la seva hospitalitat, la seva magnífica actitud i la seva dedicació. Gràcies.

Alguns s'han unit a l'aventura de forma momentània, aportant el que per ells i elles segurament ha estat un petit gra de sorra però que per mi s'ha transformat en una gran muntanya d'idees i estímuls. Lucy Rowland, Toby Pennington, Ricardo Segovia Cortés, Raúl Garcia-Valdés, William Hammond, Teresa Rosas, Miquel Riba, Catherine Preece i Joan Pretus, gràcies. Ara, l'aigua. L'aigua que m'ha permès avançar sentint-me ple, acompanyat des de dins. Cada una de les gotes que es fan fortes al unir-se, i llavors mouen cel i terra. Ens hem fet grans junts, ajudant-nos els uns als altres, compartint alegries i decepcions, tristesa i bogeria. Al CREAFuture, a tots i totes vosaltres que ara, després d'aquest temps, ja puc considerar molt més que companys i companyes, ja us considero amics i amigues. Finalment, res d'això hagués estat possible sense l'arrelament que m'ha proporcionat la meva família. Gràcies, mare, pare, germans, germana tiets i avis, i a la meva parella, Andreanna, pel vostre suport.

Als companys i companyes d'aventura

PREFACE

I, Pablo Sanchez Martinez, confirm that the work presented in this thesis is my own. Where information has been derived from other sources, I confirm that this has been indicated in the thesis.

All the work described in this thesis was carried out in the Centre for Research on Ecology and Forestry Applications (CREAF), under the supervision of Jordi Martinez Vilalta and Maurizio Mencuccini. This dissertation is my own work and contains nothing which is the outcome of work done in collaboration with others except as specified in the text and summarised in the Statement of Contributions.

This dissertation is not substantially the same as any that I have submitted, or is being concurrently submitted, for a degree or diploma or other qualification at the Autonomous University of Barcelona or any other University or similar institution except as declared in the Preface and specified in the text. It does not exceed 100,000 words, including footnotes, tables, and figures but excluding bibliography, appendices, and supporting data.

ABSTRACT

Comparative plant ecology seeks to understand the spectrum of different ways of making a living, that is, the combinations in which plant traits occur, and the incidence of trait constellations in different environments (Ackerly and Donoghue 1995). However, knowledge on species ecological strategies will not be complete until evolutionary causal explanations are elucidated. While the role of evolutionary history shaping contemporary ecology has long been of interest, its quantitative examination has only been recently possible thanks to methodological innovations together with the availability of representative phenotypic and genotypic data (Pagel 1999, Losos 2008, Ackerly 2009, Pennell and Harmon 2013). So, we now have the opportunity to enrich ecological knowledge by including the evolutionary perspective making use of phylogenies, letting us explore which processes have shaped lineage diversification (Ackerly and Donoghue 1995). In this dissertation, I present a methodological and conceptual framework to study evolutionary patterns in plant functional strategies and I elucidate some emerging ecological consequences focusing on plant functional traits and drought responses. Results show how functional strategies are generally organized in a phylogenetically structured manner and in response to current environmental conditions, describing a pattern of phylogenetic niche conservatism (Losos 2008) which may emerge from phylogenetically conserved adaptation and the effect of environmental filtering on species distribution. Moreover, functional traits show a high degree of evolutionary interdependence conforming evolutionary modules, where a module indicates a group of coordinated traits that evolve together representing a specific functional strategy. These functional strategies are related to life history strategies and these relationships present a phylogenetically conserved component. Under a scenario of phylogenetic conservatism, individual trait variability is expected to be evolutionarily constrained, and then, we do not expect rapid adaptation to happen. If this is true, rapid environmental changes could bring populations outside their ecological niches, as it has been already observed in some areas where vegetation shows

clear signs of stress which eventually can lead to mortality in some cases (Hammond et al. 2022). In this thesis I show how including the functional perspective at the community-level can be highly informative in relating physiological drought stress and drought-induced mortality patterns. More concretely, I show how communities with a higher hydraulic risk tend to present higher drought-induced mortality, improving its prediction at global scale. This thesis proposes a new evolutionarily explicit framework in ecophysiology that can be used to understand evolutionary patterns in functional traits, how they relate with ecological strategies and scale them at the community and ecosystem levels to better understand vegetation responses to climate.

IMPACT STATEMENT

The linkage between evolutionary biology and ecophysiology is crucial to elucidate adaptability of plants to climate, understanding specific mechanisms influencing individual responses to the environment and the *causa ultima* of their distribution through space and time. Determining which processes are related to fitness components (growth, survival and reproduction), measuring them in an efficient way (e.g., by using functional traits) and understanding the drivers influencing their distribution will allow to improve our knowledge on climate change impacts on vegetation at different scales. Here I develop a framework to perform such a linkage, applying tools to different sources of data in an integrated way to elucidate evolutionary patterns in functional strategies and how they translate into ecological responses to environmental forcing. This work can be used to guide ecosystem management by, for instance, informing restoration decisions by placing species traits and their changes in an evolutionary context and understanding their adaptive capability.

STATEMENT OF CONTRIBUTIONS

The work presented in this thesis would not have been possible without the contributions of many brilliant people, to whom I am very grateful. These people are **Dr. Jordi Martinez Vilalta, Dr. Maurizio Mencuccini, Dr. Kyle G. Dexter, Dr. David D. Ackerly, Dr. Todd E. Dawson.** Due to the collaborative and interdisciplinary nature of this project, some of the data presented was acquired with the help of other people. I want to specifically mention **Teresa Rosas**, who compiled the first version of the dataset hydraTRY, **William Hammond**, who compiled the actualized version of the xylem database and the ATDN (Amazonian Tree Diversity Network) and TRY plant trait database groups*, specifically **Kyle Dexter, Hans Ter Steege** and **Freddie Draper.**

Next, I state the contribution of other people to each chapter:

Chapter 1: written by Pablo Sanchez-Martinez (PSM) with revisions of Jordi Martinez-Vilalta (JMV) and Maurizio Mencuccini (MM).

Chapter 2: designed by PSM, JMV and MM, Kyle G. Dexter (KGD) and Ricardo Segovia Cortés (RSC) provided the phylogeny, JMV and MM and Teresa Rosas provided the hydraulics database, PSM analysed the data with inputs from MM, JMV and KGD and wrote the first draft of the manuscript. All authors contributed substantially to revisions.

Chapter 3: designed by PSM, JMV, MM, David D. Ackerly (DDA) and Todd E. Dawson (TED), JMV and MM and Teresa Rosas provided the database, PSM analysed the data with inputs from MM, JMV, KGD, DDA and Jarrod Hadfield and wrote the first draft of the manuscript. All authors contributed substantially to revisions.

Chapter 4: designed by PSM, KGD, Freddie Draper (FD) and Hans Ter Steege (HTS), ATDN and TRY members* provided the data, PSM analysed the data with inputs from KGD, FD and HTS and wrote the first draft of the manuscript. All authors contributed substantially to revisions.

Chapter 5: designed by PSM, JMV, MM and Raúl García-Valdés (RGV), William Hammond (WH) provided the hydraulics database, PSM analysed the data with inputs from MM, JMV, RGV, WH and KGD and wrote the first draft of the manuscript. All authors contributed substantially to revisions.

Chapter 6: written by Pablo Sanchez-Martinez (PSM) with revisions of Jordi Martinez-Vilalta (JMV) and Maurizio Mencuccini (MM).

**ATDN and TRY members: Kyle G. Dexter, Freddie C. Draper, Chris Baraloto, Iéda Leão do Amaral, Luiz de Souza Coelho, Francisca Dionízia de Almeida Matos, Diógenes de Andrade Lima Filho, Rafael P. Salomão, Florian Wittmann, Carolina V. Castilho, Marcelo de Jesus Veiga Carim, Juan Ernesto Guevara, Oliver L. Phillips, 16 William E. Magnusson, Daniel Sabatier, Juan David Cardenas Revilla, Jean-François Molino, Mariana Victória Irueme, Maria Pires Martins, José Renan da Silva Guimarães, José Ferreira Ramos, Olaf S. Bánki, Maria Teresa Fernandez Piedade, Dairon Cárdenas López, Nigel C.A. Pitman, Layon O. Demarchi, Jochen Schöngart, Bruno Garcia Luizé, Evelyn Márcia Moraes de Leão Novo, Percy Núñez Vargas, Thiago Sanna Freire Silva, Eduardo Martins Venticinqué, Angelo Gilberto Manzatto, Neidiane Farias Costa Reis, John Terborgh, Katia Regina Casula, Euridice N. Honorio Coronado, Abel Monteagudo Mendoza, Juan Carlos Montero, Flávia R.C. Costa, Ted R. Feldpausch, Adriano Costa Quaresma, Nicolás Castaño Arboleda, Charles Eugene Zartman, Timothy J. Killeen, Beatriz S. Marimon, Ben Hur Marimon-Junior, Rodolfo Vasquez, Bonifacio Mostacedo, Rafael L. Assis, Dário Dantas do Amaral, Julien Engel, Pascal Petronelli, Hernán Castellanos, Marcelo Brilhante de Medeiros, Marcelo Fragomeni Simon, Ana Andrade, José Luís Camargo, William F. Laurance, Susan G.W. Laurance, Lorena Maniguaje Rincón, Juliana Schietti, Thaiané R. Sousa, Emannelle de Sousa Farias, Maria Aparecida Lopes, José Leonardo Lima Magalhães, Henrique Eduardo Mendonça Nascimento, Helder Lima de Queiroz, Gerardo A. Aymard C., Roel Brienén, Pablo R. Stevenson, Alejandro Araujo-Murakami, Bruno Barçante Ladvoat Cintra, Tim R. Baker, Yuri Oliveira Feitosa, Hugo F. Mogollón, Joost F. Duivenvoorden, Carlos A. Peres, Miles R. Silman, Leandro Valle Ferreira, José Rafael Lozada, James A. Comiskey, José Julio de Toledo, Gabriel Damasco, Nállarett Dávila, Roosevelt García-*

Villacorta, Aline Lopes, Alberto Vicentini, Fernando Cornejo Valverde, Alfonso Alonso, Luzmila Arroyo, Francisco Dallmeier, Alvaro Duque, Vitor H.F. Gomes, Eliana M. Jimenez, David Neill, Maria Cristina Peñuela Mora, Janaína Costa Noronha, Daniel P. P. de Aguiar, Flávia Rodrigues Barbosa, Yennie K. Bredin, Rainiellen de Sá Carpanedo, Fernanda Antunes Carvalho, Fernanda Coelho de Souza, Kenneth J. Feeley, Rogerio Gribel,7 Torbjørn Hangaasen, Joseph E. Hawes, Marcelo Petratti Pansonato, Marcos Ríos Paredes, Domingos de Jesus Rodrigues, Jos Barlow, Erika Berenguer, Izaias Brasil da Silva, Maria Julia Ferreira, Joice Ferreira, Paul V.A. Fine, Marcelino Carneiro Guedes, Carolina Levis, Juan Carlos Licon, Boris Eduardo Villa Zegarra, Vincent Antoine Vos, Carlos Cerón, Flávia Machado Durgante, Émile Fonty, Terry W. Henkel, John Ethan Householder, Isau Huamantupa-Chuquimaco, Marcos Silveira, Juliana Stropp, Raquel Thomas, Doug Daby, William Milliken, Guido Pardo Molina, Toby Pennington, Ima Célia Guimarães Vieira, Bianca Weiss Albuquerque, Wegliane Campelo, Alfredo Fuentes, Bente Klitgaard, José Luis Marcelo Pena, J. Sebastián Tello, Corine Vriesendorp, Jerome Chave, Anthony Di Fiore, Renato Richard Hilário, Luciana de Oliveira Pereira, Juan Fernando Phillips, Gonzalo Rivas-Torres, Tinde R. van Andel, Patricio von Hildebrand, William Balee, Edelcilio Marques Barbosa, Luiz Carlos de Matos Bonates, Hilda Paulette Dávila Doza, Ricardo Zárate Gómez, Therany Gonzales, George Pepe Gallardo Gonzales, Bruce Hoffman, André Braga Junqueira, Yadvinder Malhi, Ires Paula de Andrade Miranda, Linder Felipe Mozombite Pinto, Adriana Prieto, Agustín Rudas, Ademir R. Ruschel, Natalino Silva, César I.A. Vela, Stanford Zent, Eglé L. Zent, Angela Cano, Yrma Andreina Carrero Márquez, Diego F. Correa, Janaina Barbosa Pedrosa Costa, Bernardo Monteiro Flores, David Galbraith, Milena Holmgren, Michelle Kalamandeen, Guilherme Lobo, Luis Torres Montenegro, Marcelo Trindade Nascimento, Alexandre A. Oliveira, Maihyra Marina Pombo, Hirma Ramirez-Angulo, Maira Rocha, Veridiana Vizoni Scudeller, Maria Natalia Umaña, Geertje van der Heijden, Emilio Vilanova Torre, Manuel Augusto Abuite Reategui, Cláudia Baider, Henrik Balslev, Sasha Cárdenas, Luisa Fernanda Casas, William Farfan-Rios, Cid Ferreira, Reynaldo Linares-Palomino, Casimiro Mendoza, Italo Mesones, Germaine Alexander Parada, Armando Torres-Lezama, Ligia Estela Urrego Giraldo, Daniel Villarroel, Roderick Zagt, Miguel N. Alexiades, Edmar Almeida de Oliveira, Karina Garcia-Cabrera, Lionel Hernandez, Walter Palacios Cuenca, Susamar Pansini, Daniela Pauletto, Freddy Ramirez Arevalo, Adeilza Felipe Sampaio, Elvis H. Valderrama Sandoval, Luis Valenzuela Gamarra, Lourens Poorter, , Masha van der Sande, Hans ter Steege

CONTENTS

1 Introduction	1
1.1 Plant functional strategies	2
1.2 Evolutionary patterns of plant functional strategies	8
1.2.1 Phylogenetic conservatism and evolutionary lability in plant functional traits	9
1.2.2 From traits to trait modules: a multivariate perspective	14
1.3 Ecological consequences of evolutionary patterns in plant functional traits	16
1.3.1 Functional constraints on species distributions and species assemblage	18
1.3.2 Function-environment mismatches	21
1.4 Towards an evolutionary framework in plant functional ecology.....	22
1.5 Research aims and outline.....	23
2 Adaptation and coordinated evolution of plant hydraulic traits	25
2.1 Abstract.....	26
2.2 Introduction	26
2.3 Materials and methods.....	31
2.3.1 Data sources	31
2.3.2 Phylogeny.....	33
2.3.3 Statistical analyses	34
2.4 Results	38
2.4.1 Phylogenetic signal in hydraulic traits.....	38
2.4.2 Environmental drivers of hydraulic traits	41
2.4.1 Correlated phylogenetic signal.....	44
2.5 Discussion	46
2.5.1 Phylogenetically conserved adaptation in hydraulic traits	46
2.5.2 Evolutionary modules in hydraulic traits	48
2.6 Conclusion.....	50
3 A unified framework to study and predict functional trait syndromes	51
3.1 Abstract.....	52
3.2 Introduction	53

3.3	Materials and methods.....	57
3.3.1	Trait Variance-covariance partition.....	57
3.3.2	Networks.....	61
3.3.3	Imputation algorithm.....	62
3.3.4	Application.....	65
3.4	Results.....	69
3.4.1	Variance covariance partition results.....	69
3.4.2	Imputation results.....	75
3.5	Discussion.....	77
3.5.1	A new framework to study functional syndromes evolution....	77
3.5.1	Leaf economics and hydraulic traits conform to two phylogenetically conserved modules integrated in response to aridity.....	78
3.5.1	Using information on traits evolution to perform data imputation	81
4	Plant functional traits are evolutionarily coordinated with life history traits in the Amazon basin	83
4.1	Abstract.....	84
4.2	Introduction.....	85
4.3	Materials and methods.....	88
4.3.1	Data.....	88
4.3.2	Principal components analyses.....	89
4.3.3	Phylogenetic signal calculation.....	89
4.3.4	Correlations calculation.....	90
4.4	Results.....	92
4.4.1	Functional and life history conform to two main axes of variation	92
4.4.2	Phylogenetic signal in functional and life history strategies.....	95
4.4.1	Phylogenetic conservatism and evolutionary lability in functional and life history traits integration.....	96
4.5	Discussion.....	102
4.5.1	Leaf acquisitiveness is integrated with survival and reproduction and stature is integrated with growth.....	102
4.5.1	Leaf acquisitiveness, survival and reproduction integration is phylogenetically conserved and independent of size-growth integration, which presents evolutionary lability.....	104

4.5.1	The meaning of evolutionary lability and phylogenetic conservatism in ecological strategies	105
4.5.1	Caveats and future directions.....	107
5	Increased hydraulic risk in assemblages of woody plant species predicts spatial patterns of drought-induced mortality	109
5.1	Abstract.....	110
5.2	Introduction	110
5.3	Results and discussion	113
5.3.1	Low hydraulic safety margins are widespread in woody plant species	113
5.3.2	Species-level hydraulic risk is a poor predictor of species-level drought induced mortality	116
5.3.3	Using information from species assemblages to characterize site-specific hydraulic risk	116
5.3.4	Species-assemblage hydraulic risk is positively related to drought-induced mortality occurrence.....	122
5.3.5	Spatial patterns in the probability of DIM occurrence	124
5.3.6	Future directions.....	126
5.4	Materials and methods.....	127
5.4.1	Species distribution data	127
5.4.2	Hydraulic data	127
5.4.3	Environmental data.....	128
5.4.4	Mortality database.....	130
5.4.5	Phylogenetic information	130
5.4.6	Hydraulic traits predictions using phylogenetic and edaphoclimatic data	131
5.4.7	Geographical projection of hydraulic traits and calculation of pixel-level species assemblages hydraulic metrics	133
5.4.8	Assessing the predictive capacity of hydraulic risk against mortality records.....	134
5.4.9	Projecting mortality risk using maximum entropy models.....	137
6	General discussion and conclusions	139
6.1	Insights from an evolutionarily explicit framework in ecophysiology	140
6.2	Phylogenetic niche conservatism in functional syndromes.....	142

6.3	Ecological consequences of functional strategies evolution	145
6.3.1	Functional strategies relationship with life history strategies	145
6.3.2	Effects of functional strategies on vegetation responses to climate	147
6.4	Conclusions	149
6.5	Future directions.....	150
7	References	153
8	Appendixes	187
8.1	Chapter 2	188
8.1.1	Supplementary tables and figures	188
8.1.2	Supplementary methods	202
8.1.3	Analyses using a species-level phylogeny	206
8.1.4	Evolutionary correlations reported by genus-level phylogenetic models using observations available for the species-level phylogeny and evolutionary correlations reported by species-level phylogeny pruned at the genus level	209
8.2	Chapter 3	211
8.2.1	Supplementary tables and figures	211
8.2.2	Supplementary methods	214
8.3	Chapter 4	215
8.3.1	Supplementary tables and figures	215
8.4	Chapter 5	220
8.4.1	Supplementary tables and figures	220

FIGURES

Figure 1.1 Representation of the basis and effects of functional traits.	3
Figure 1.2 Differences in vessel diameter and hydraulic conductivity between angiosperms and gymnosperms.....	7
Figure 1.3 Evolutionary patterns.....	12
Figure 1.4 Evolutionary patterns and community composition.....	20
Figure 2.1 Hypotheses	30
Figure 2.2 and 2.3 Phylogenetic reconstruction of hydraulic traits.....	39
Figure 2.4 Environment-trait relationships	42
Figure 2.5 Correlated phylogenetic signals	45
Figure 3.1 'Traits' variance-covariance conceptual framework.....	55
Figure 3.2 Imputation algorithm scheme.....	64
Figure 3.3 Simulated data structure.....	66
Figure 3.4 Total correlation among variables	68
Figure 3.5 and 3.6 Simulated trait networks	72
Figure 3.7 Plant functional trait networks.....	74
Figure 3.7 Imputation performance.....	76
Figure 4.1 Functional, life history and integrative axis of variation	94
Figure 4.2 Correlation and phylogenetic signal.....	96
Figure 4.3 Variance-covariance networks	98
Figure 4.4 Functional and life history axis correlations	101
Figure 5.1 Phylogenetic distribution of the data	114
Figure 5.2 Global distribution of species-assemblage hydraulic metrics.....	119
Figure 5.3 Relationship between drought-induced mortality occurrence and species-assemblage hydraulic metrics	123
Figure 5.4 Projection of drought-induced mortality occurrence probability..	125
Figure 5.5 Methodology.....	131
Figure S2.1	188
Figure S2.2.....	190
Figure S2.3.....	190
Figure S2.4 and S2.5.....	192
Figure S2.6.....	193

Figure S2.7	194
Figure S3.1	211
Figure S3.2	212
Figure S4.1	218
Figure S5.1	221
Figure S5.2	223
Figure S5.3	225
Figure S5.4	226
Figure S5.5	227
Figure S5.6	228
Figure S5.7	229
Figure S5.8	230
Figure S5.9	231
Figure S5.10	232

TABLES

Table 2.1.....	37
Table S2.1	195
Table S2.2	196
Table S2.3	197
Table S2.4	197
Table S2.5	198
Table S2.6	200
Table S2.7	206
Table S2.8	207
Table S2.9	209
Table S2.10	210
Table S3.1	213
Table S3.2	213
Table S4.1	215
Table S4.2	216
Table S5.1	233
Table S5.2	236
Table S5.3	237
Table S5.4	239
Table S5.5	241
Table S5.6	242

1 INTRODUCTION

1.1 PLANT FUNCTIONAL STRATEGIES

Functional traits are phenotypic characters (e.g., leaf size) influenced by a genetic basis related to a strategy of resource uptake and utilization that affects performance (e.g., vegetative growth rate), having an impact on fitness and undergoing adaptive evolution (Ackerly et al. 2000, Geber and Griffen 2003, Violle et al. 2007). As so, functional traits mediate the relationships between organisms and environment, responding to external conditions through biochemical, physiological, morphological, developmental, or behavioural mechanisms to optimize physiological responses that will allow them to persist. Then, functional traits have a central role in the evolutionary play, positioning organisms in the ecological scene by defining their responses to the environment and directly affecting the fate of their carriers under a given set of conditions.

From a functional perspective, any living organism can be seen as an aggrupation of functional traits conforming a strategy that has been selected in favour. This group of functional trait values can be referred to as functional trait syndrome (Reich et al. 2003) (box 1.1). Then, a functional trait syndrome represents a description of a successful strategy mediating the relationship between organisms and external conditions, understanding “success” as the capability to perpetuate by means of survival and reproduction and “failure” as the removal from a given system. Therefore, trait syndromes will determine the range of potential physiological responses (e.g., hydraulic conductivity) that organisms can display to modulate their functions (e.g., water transport to leaves) with external conditions, affecting performance responses (growth, reproduction, and survival) that will subsequently determine their life history strategy (Grime et al. 1997, Westoby et al. 2002, Reich et al. 2003). In their interaction with the environment, these functional strategies will shape the ecological niche of a given taxonomic entity, understood as the n-dimensional environmental space where their members can survive and evolve (Hutchinson 1957), constraining their distribution and

abundance and then, influencing species assemblage which will affect in turn ecosystem properties (Figure 1.1).

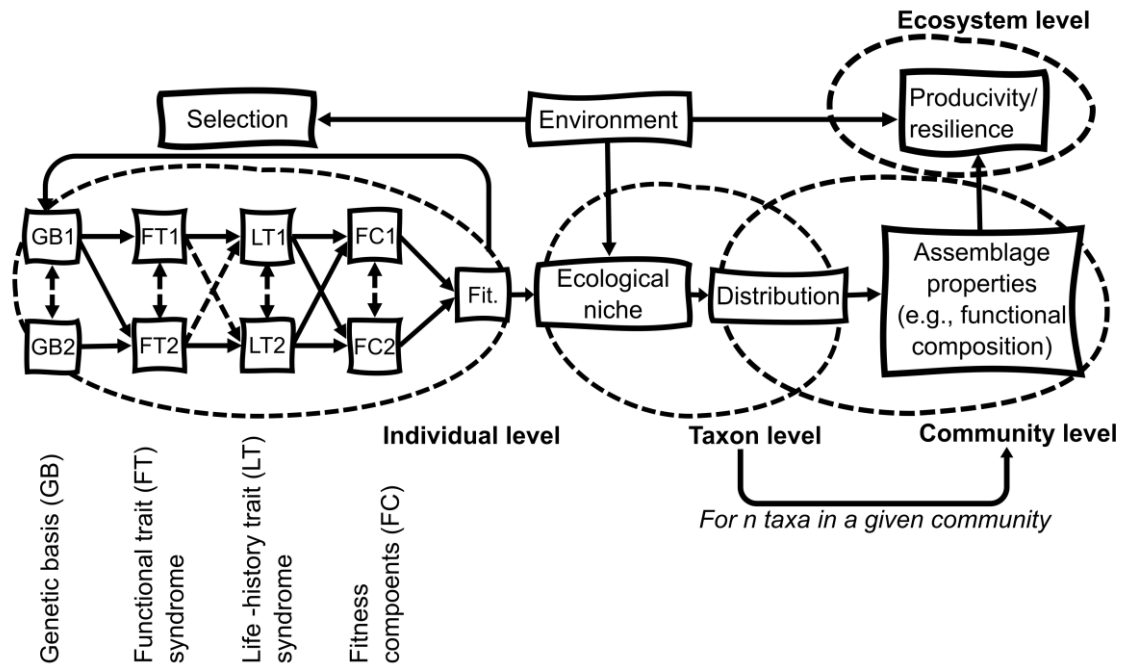


Figure 1.1 Representation of the basis and effects of functional traits. Contextualization of the genetic origin in the expression of functional traits and their relationship with fitness (Fit.) and the environment. Some ecological consequences of trait response to the environment by means of natural selection and impacts on fitness is shown by scaling these relationships from individual to taxon (e.g., species), community and ecosystem-level.

Under this premise, an amalgam of different strategies can emerge under a given set of environmental conditions, as different combinations of traits may represent successful strategies. To illustrate that, let us imagine a plant community situated in a location with seasonal drought, being water a potential limiting resource during the dry season. Under these conditions, we can find species which tend to escape drought by completing their life cycles before the period of scarcity, presenting a functional strategy to uptake and use resources rapidly (i.e., acquisitive functional strategy) (Wright et al. 2004, Reich 2014). However, in this community we can also find some species that are adapted to tolerate dry periods and keep functioning during the dry season, which

would be stressful for the group of species with an acquisitive functional strategy. These species will be adapted to tolerate stress, presenting a slow resource uptake and use (Wright et al. 2004, Reich 2014). These contrasted strategies and many others can co-occur, meaning that even when external conditions are the same, living entities can respond in diverse ways to maintain different resource requirements needed to perpetuate in space and time.

The diversity of successful strategies is constrained by environmental conditions, acting as environmental filters on a pool of functional syndromes. An extreme resource scarcity may constrain the number of successful functional trait syndromes, filtering species pools depending on how suitable their functional strategies are to cope with environmental conditions (Swenson et al. 2012). For instance, in extremely arid sites with a few days of precipitation per year, most species may present a desiccation tolerance strategy, which consists in tolerating leaf moisture content equal to ambient during long dry periods and revive only during rehydration. Under these extremely arid conditions, all other strategies to face drought may be filtered out. As the dry period shorten, other drought response strategies may become successful, such as maintaining the hydraulic function under dry conditions by presenting a highly resistant xylem able to move water to the leaves under high tension (dehydration or drought tolerance) or investing in deep roots to uptake water from the water table (dehydration or drought avoidance) (Volaire 2018).

Another constrain on the diversity of strategies present in a given site is the evolutionary legacy of species present, as functional strategies are likely to be at least partially inherited from ancestors (Cavender-Bares et al. 2016). This is based on the fact that different strategies may have appeared in distant lineages (i.e., long time since divergence), constraining descendant species strategies when rapid evolution is not happening. The appearance of key features can produce a divergence in strategies that will differentiate and evolve towards different adaptive optima, strongly influencing the functional space that descendant species can explore to conform successful strategies.

A clear example of such divergence is the appearance of xylem vessels in angiosperms, which allowed an increase in hydraulic conductivity compared to gymnosperms' tracheid (Figure 1.2), acting as evolutionary enablers for other functional possibilities such as larger leaf sizes (Sperry et al. 2006). The co-occurrence of angiosperms and gymnosperms under a given set of conditions (Jacobsen et al. 2007) demonstrate how different strategies can be successful under the same environment and that trait syndromes can be strongly constrained by species evolutionary legacy.

Box 1.1 Trait terminology

Physiological response. Variable related to a physiological process (e.g., photosynthesis or water transport) that can be measured at the individual level and that present variability within and among individuals in space and time (e.g., photosynthetic rates or stem hydraulic conductivity).

Functional trait. Variable describing individual phenotype under some degree of genetic control (i.e., presenting heritability) which is expected to affect individual performance, influencing fitness and being under selection. A functional trait is expected to characterize a giving taxonomic entity (individual, population, species, genus), so the within-entity variability should be lower than the among-entity variability (e.g., maximum photosynthetic rates and maximum hydraulic conductivity).

Performance response. Variable representing a component of individual fitness (i.e., growth, reproduction or survival) that can be measured at the individual level and that presents variability within and among individuals in space and time (e.g., individual growth rates).

Demographic response. Variable describing population dynamics that present variability in space and time (e.g., mortality rates).

Life history trait. Variable characterizing performance or demographic responses of a giving taxonomic entity (normally, species or supra-specific level). A life-history trait is expected to present higher among-entity variability than within-entity variability (e.g., mean mortality rates).

Functional trait syndrome. Group of functional trait values that co-occur in a given taxonomic entity (e.g., individual, population, species or genus) involved in a functional strategy describing aspects related to resource uptake and utilization.

Life history trait syndrome. Group of life-history trait values that co-occur in a given taxonomic entity (e.g., individual, population, species or genus) involved in a life-history strategy describing aspects related to growth, survival or reproduction.

Ecological syndrome. Group of traits that co-occur in a given taxonomic entity (e.g., individual, population, species or genus) involved in an ecological strategy describing its interaction with the environment through space and time.

Divergence in function among taxa from different environments and convergence in taxa from similar environments has been a central topic in biogeography, ecology, and evolution (Grime and Hunt 1975, Ehleringer and Monson 1993, Garnier and Laurent 1994, Beerling and Kelly 1996, Ackerly and Donoghue 1998, Ackerly and Reich 1999, Cunningham et al. 1999, Reich et al. 1999). Understanding the drivers of the relationships among functional strategies and environmental conditions is crucial to better elucidate constraints on species distributions, impacts of environmental forcing on their persistence and the scaling of underlying processes from organs within individuals to communities and ecosystems. This knowledge will help us understand and predict the distribution of functional strategies, which is expected to be crucial to better understand impacts of climate change on vegetation by improving modelling frameworks that aim to assess the potential impacts of environmental forcing on ecosystem services. In the current thesis I analyse various sources of data covering functional traits, phylogeny, environmental conditions, species distributions, life history traits, and data on climate change impacts on vegetation to build a framework to study the drivers of functional strategies, their spatial distribution, and the ecological consequences in terms of vegetation responses to climate.

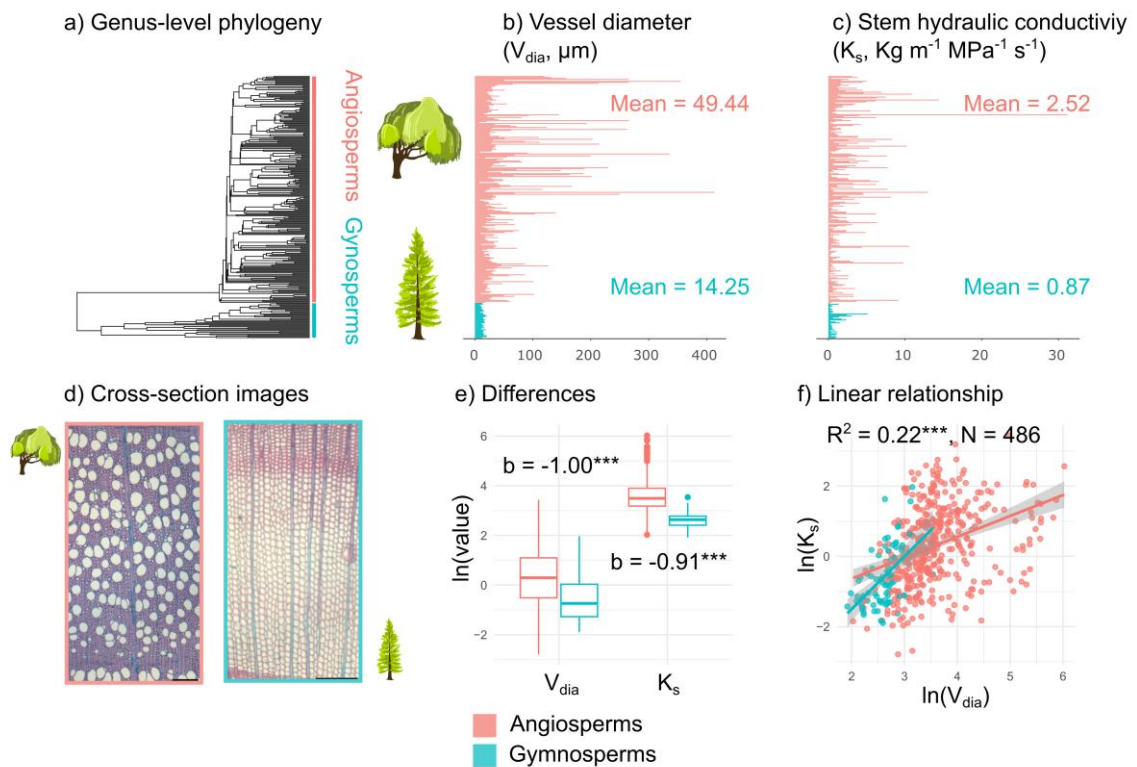


Figure 1.2 Differences in vessel diameter and hydraulic conductivity between angiosperms and gymnosperms. Representation of the values and relationship between vessel diameter (V_{dia}) and stem hydraulic conductivity (K_s) in angiosperms and gymnosperms. In this analysis, data from an actualized version of the xylem traits global dataset has been used (Hammond et al. 2021). a) Genus-level phylogeny for woody plant species with data for both V_{dia} and K_s , b and c) genus-level means for V_{dia} and K_s , respectively. Mean for each group is displayed. d) Images of xylem conduits extracted from Sperry et al. (2006). e) Boxplots representing mean and dispersion for species-level values of K_s and V_{dia} for angiosperms and gymnosperms. Differences and their significance were reported by means of a general linear model. f) Scatterplot and linear relationship between K_s and V_{dia} for gymnosperms and angiosperms. R^2 represents the variance explained of K_s including V_{dia} , angiosperm-gymnosperm affiliation and their interaction as predictors. N show the number of species-level values used in the analysis.

1.2 EVOLUTIONARY PATTERNS OF PLANT FUNCTIONAL STRATEGIES

Variation in plant functional traits present a genetic basis that can be inherited from ancestors (Ackerly et al. 2000, Pereira and Des Marais 2020). This genetic component can be quantified by the heritability of a given trait, which represents the amount of variance that can be attributed to genetic effects (i.e., genetic variance, VAR_g) compared to the total variance, which is composed of genetic and environmental (VAR_e) variances.

$$\textit{Heritability } (H^2) = \frac{VAR_g}{VAR_g + VAR_e}$$

Functional traits have been shown to present significant levels of heritability, meaning that the genetic composition is an important factor determining their values compared to developmental determination in response to the environment (i.e., phenotypic plasticity) (Geber and Griffen 2003). This is not to say that plasticity is not important in functional traits, and in fact, it can be an important component determining their values particularly in plants (Sultan 2000). However, the fact that some heritability exists in functional traits opens the door to the use of phylogenies as a proxy of their evolutionary history, as genes involved in trait values are transmitted from ancestors to descendants over evolutionary timescales.

1.2.1 Phylogenetic conservatism and evolutionary lability in plant functional traits

At the macroevolutionary level (i.e., species or supra-specific level), we can use the phylogenetic signal (box 1.2) as an analogue of heritability. At first sight this might not be evident, as the phylogenetic signal is a measure of the tendency for evolutionary related organisms to resemble each other (Blomberg and Garland 2002), while heritability is related to the genetic component of a given trait which is transferable from one generation to the next. However, if we further develop the idea of phylogenetic signal, we realize that it can be seen as a measure of the relationship of trait values with the evolutionary history of species carrying them. When more than one species is considered, shared evolutionary history can be seen as shared evolutionary time, which is expected to be related to the overall genetic similarity. Then, phylogenetic signal is showing the amount of variance in a trait that is related to broad genetic similarity among species (i.e., phylogenetic variance, VAR_{phylo}) over total variance (VAR_{total}) (Pagel 1999).

$$\text{Phylogenetic signal } (\lambda) = \frac{VAR_{phylo}}{VAR_{total}}$$

A high phylogenetic signal represents a pattern showing how closely related species tend to resemble each other in a given trait. This can be understood as phylogenetic conservatism, meaning that values are phylogenetically structured, so there may be some constraints on their evolution maintaining ancestral states (Losos 2008) (box 1.2). Contrarily, traits with a low phylogenetic signal can present very different values for closely related species, pointing that ancestral states do not strongly determine descendant ones. In this latter case, we expect traits to present a more labile evolution, as they can drastically change their values over short evolutionary times (e.g., within-genera) (Figure 1.3). Then, from a broad and unifying perspective, phylogenetic signal,

as heritability, is a measure of the amount of influence that ancestral values exert on descendant values for a given trait or trait syndrome, acting as constraints on their values.

Phylogenetic conservatism and evolutionary lability appear as contrasted concepts describing patterns in functional traits that may arise under different evolutionary scenarios (Blomberg and Garland 2002, Blomberg et al. 2003). Then, we expect evolutionary processes shaping traits to differ depending on which one of these two scenarios is predominant. Phylogenetic conservatism may appear under a scenario of lineage-specific stabilizing selection, meaning that mean values of a given trait will be maintained and transmitted to descendants (Crisp and Cook 2012). This scenario is compatible with a slow evolution of traits and the existence of strong environmental filtering determining the environmental space that species occupy (Losos 2008). If stabilizing selection and environmental filtering are involved as processes leading to this pattern, we would expect phylogenetic conservatism in functional traits to be related to environmental variables describing the species ecological niche. In this case, trait values will be restricted to those conditions where they conform to successful strategies. Under this scenario, we do not expect rapid evolutionary changes in populations adapting to new environmental spaces. Instead, closely related species will tend to occupy similar ecological spaces and respond to the environment by means of similar functional strategies. This pattern of constrained adaptation is referred as phylogenetic niche conservatism (Losos 2008, Crisp et al. 2009, Crisp and Cook 2012).

Phylogenetic conservatism can also arise from processes not related to species adaptation. For instance, a lack of genetic diversity in crucial genes involved in trait expression can lead to evolutionary stasis that can be lineage-specific (lower within lineage genetic variability), leading to a relationship between the phylogeny and trait values that is not underlined by adaptive processes. Genetic drift can also cause lineages to gradually differ in their functional strategies and occupy different ecological spaces (Crisp and Cook 2012). This may also lead to phylogenetic conservatism in functional traits which can be related to environmental variables but without a causal relationship

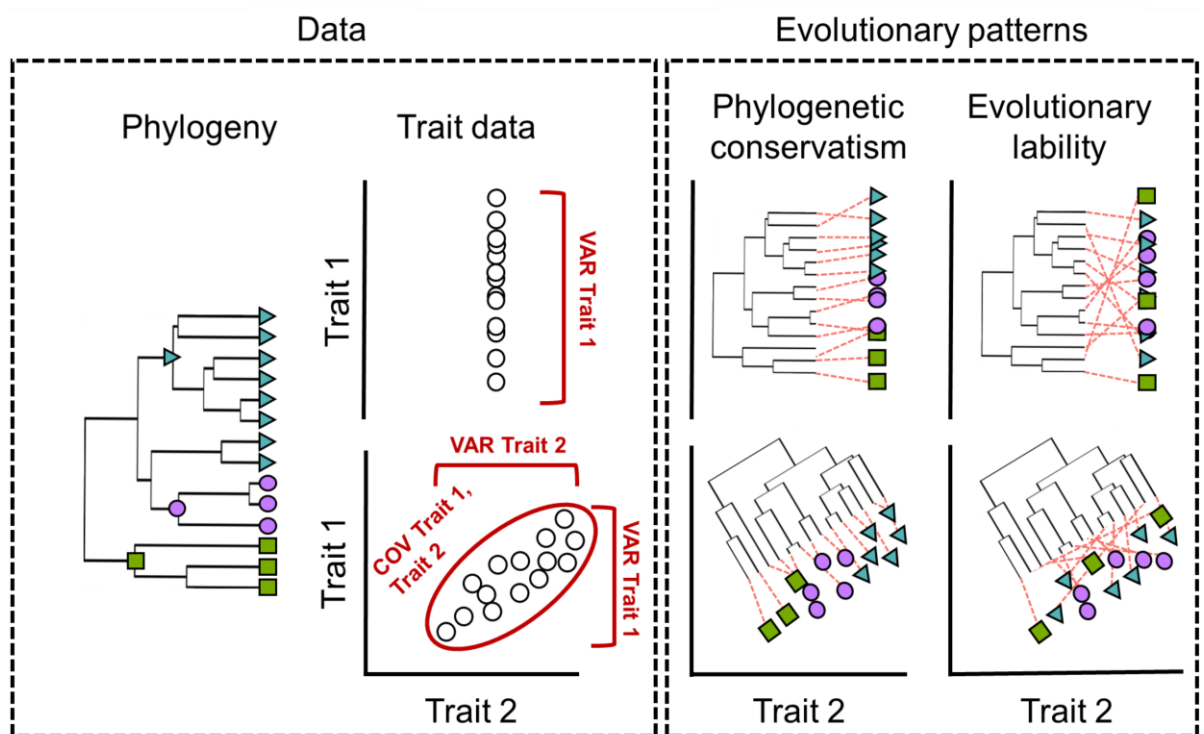
among them. Genetic correlation among traits could also lead to adaptive traits driving values in non-adaptive traits, conforming to a correlation with selective pressures that may not be underlined by adaptation. Therefore, it is crucial to have some previous knowledge on the physiological meaning of traits under different situations to clarify their adaptive meaning before exploring macroevolutionary patterns.

Evolutionary lability may appear in a scenario where evolution is less constrained so trait values of descendants can rapidly diverge from ancestral ones. This scenario is compatible with rapid evolution, which can be adaptive, leading to patterns such as adaptive radiation when ancestral populations are exposed to different selective pressures (Ackerly et al. 2000, Ackerly 2009). For instance, we expect disruptive selection in ancestral populations of a given lineage to be a process shaping a pattern of evolutionary lability, leading to diversification of trait values in closely related taxa. Under this adaptive scenario, we expect traits to be related to environmental variables exerting selective pressures in a non-phylogenetically structured way, with closely related taxa presenting different strategies that allow them to survive under different conditions.

Ecologists and evolutionary biologists have recently showed substantial interest in understanding phylogenetic conservatism and evolutionary lability in functional traits (Losos 2008, Ackerly 2009, Crisp and Cook 2012). However, there is still a generalized lack of information on the degree of conservatism and lability in functional trait syndromes as well as their relationship with environmental components. This may be partially due to a lack of a clear conceptual and methodological framework to analyse and interpret these patterns, specially from a multivariate perspective. One of the aims of this thesis is to fill this gap by providing a unified framework to study phylogenetic conservatism and evolutionary lability in trait syndromes specifically focusing on their relationship with environmental components related to species niche. This framework can be used at the macroecological and macroevolutionary scale but also at the micro-

ecological and micro-evolutionary scale, seeking to close the gap between these two perspectives.

Figure 1.3 Evolutionary patterns Representation of the two main evolutionary patterns studied in this thesis from phylogenetic and functional trait data.



Box 1.2 Evolutionary terminology

Phylogenetic conservatism. Pattern describing closely related taxa resembling each other in a given variable or group of related variables. It can be detected by a high degree of phylogenetic structure in a given variable variance or covariation among variables. It is related to a maintenance of the common ancestor value in one or more variables.

Phylogenetic niche conservatism. Pattern of phylogenetic conservatism related to the environmental space that a given taxonomic entity occupy (ecological niche).

Evolutionary lability. Pattern describing disparification in closely related for a given variable or a group of related variables. It can be detected by phylogenetically independent variance in a given variable or covariation among variables. It is related to a low degree of relation between ancestral and descendent values.

Phylogenetic signal. Measure of phylogenetic autocorrelation of a given variable. It represents a measure of phylogenetic conservatism.

Correlated phylogenetic signal. Measure of phylogenetic covariance between two variables relative to their individual phylogenetic variance (i.e., magnitude and direction of the shared phylogenetically conserved covariance).

Phylogenetic correlation. Measure of phylogenetic covariance between two variables relative to their total variances (i.e., contribution in magnitude and sign of phylogenetic covariance to total covariance).

Evolutionarily labile correlation. Measure of phylogenetically-independent covariance between two variables relative to their total variances (i.e., contribution in magnitude and sign of phylogenetically independent covariance to total covariance). Labile correlation and phylogenetic correlation sum to total correlation.

Environmental phylogenetic conservatism. Amount of phylogenetic conservatism in a variable or a group of related variables that is related to one or more specific environmental variables. It is expected to be a component of phylogenetic niche conservatism and then, to be related to a phylogenetically conserved pattern of adaptation in response to one or more specific selective pressures.

Non-attributed phylogenetic conservatism. Amount of phylogenetic conservatism in a variable or a group of related variables that cannot be attributed to one or more potential selective pressures. It may be explained by non-measured causes or by non-adaptive evolutionary processes.

Evolutionarily labile environmental effects. Amount of evolutionary lability in traits or a group of related variables that is related to one or more specific environmental variables. It is expected to be related to recent adaptation in response to one or more selective pressures causing disparification in closely related taxa with different selective backgrounds.

1.2.2 From traits to trait modules: a multivariate perspective

Functional traits can be related because of different underlying structures or mechanisms which lead to the existence of a linkage among them, which can be shallow or tightly hardwired depending on the nature of the relationship. At the macroevolutionary scale, this lead to the existence of a correlation between traits, meaning that species can be positioned into an axis or a spectrum describing variation in these non-independent traits based on their trait values (Díaz et al. 2016) (box 1.3).

Box 1.3 Trait relationships

Integration. Pattern that describes the co-dependence among elements measured at a given taxonomic level (e.g., traits at the species level). Two traits are integrated at the species level when species-level values are not independent, presenting a correlation that may be underlined by a phenotypical or genetic basis.

Trade-off (-+). Pattern of integration represented by a negative correlation among traits involved, so lower values in a given trait are related to higher values in another trait at a given taxonomic level.

Coordination (++, --). Pattern of integration represented by a positive correlation among traits involved, so higher values in a given trait are related to higher values in another trait or lower values in a given trait are related to lower values in another trait at a given taxonomic level.

Functional module, axis, continuum, or spectra. Group of integrated traits from a network perspective (module) or a unidimensional perspective (axis, continuum, or spectra).

Several underlying processes can lead to a pattern of correlation between traits. First, functional traits can be related as a consequence of their physiological relationship. For instance, maximum xylem hydraulic conductivity is expected to be related to photosynthetic capacity as a higher amount of water supply will allow for a higher carbon uptake and a higher productivity of chloroplasts (Reich et al. 2003). Then, we do not expect to find high photosynthetic rates in species with low maximum xylem hydraulic conductivity due to their physiological coordination (i.e., positive correlation).

Functional traits can also be related due to a common phenotypic cause. For instance, maximum xylem hydraulic conductivity and its resistance to embolism have long been hypothesized to present a trade-off (negative correlation) due to the impact of an anatomical feature on both traits: the structure of inter-conduit pit membranes. Xylem conduits are connected by pits, which present a central membrane separating them. The thicker this membrane, the higher the embolism resistance, as it exerts resistance to the spread of air bubbles among connected vessels provoking generalized embolism. However, thick membranes are also expected to diminish maximum xylem hydraulic conductivity, as they also exert resistance on water flow (Li et al. 2016, Lens et al. 2022). Then, we do not expect species presenting xylem with both high maximum hydraulic conductivity and embolism resistance at the conduit level (Tyree and Zimmermann 2002, Venturas et al. 2017), even though at the tissue level, other traits may compensate this relationship, weakening the trade-off (Gleason et al. 2016). Finally, traits can also be correlated at the genetic level (Etterson and Shaw 2001). Genetic correlation can happen, for instance, when different genes impacting different traits are co-selected and tend to co-occur or when the same gene is impacting different traits (pleiotropy) (Cruzan 2018). As an example, genetic trait co-variance was found in leaf traits in *Populus trichocarpa*, pointing to the fact that they are evolving together due to a relationship at the genetic level (Chhetri et al. 2019).

It has been shown that functional traits are related to fitness through their integrated effect on higher-level traits describing performance (Ackerly et al. 2000) (Figure 1.1). Then, functional trait syndromes may be integrated with life history syndromes describing individual and demographic performance conforming to ecological syndromes (box 1.1). Functional traits positively correlated with performance are expected to present the same pattern of selection, while negatively correlated traits will show opposing patterns of selection. This may lead to the evolutionary integration among traits at distinct levels (e.g., functional and life history traits). Then, adaptation may happen in a multivariate way, involving trait syndromes at distinct levels that are

correlated due to the joint effects of selection. Under this scenario, knowledge of trait covariance is essential to predictions of adaptive evolution (Geber and Griffen 2003).

It is then crucial to understand trait evolution not only individually but also jointly. To do so, it may be useful to move beyond the unidimensional perspective of trait spectra and continuums, into the more multidimensional perspective provided by trait network modules. The elucidation of phylogenetic conservatism, evolutionary lability and their relationship with environmental components not only in individual traits but also in groups of traits can be very useful to frame the big question of functional strategies evolution. This will lead to the identification of integrated adaptation in functional traits and the existence of independent modules responding to selective pressures. In this thesis, such perspective is developed, presenting novel conceptual and methodological tools to study trait syndromes and their drivers, and providing some results in this regard.

1.3 ECOLOGICAL CONSEQUENCES OF EVOLUTIONARY PATTERNS IN PLANT FUNCTIONAL TRAITS

Trait syndromes determine the environmental space that a given living entity occupy, affecting its performance in response to external conditions. The combination of functional strategies and environmental conditions related to resource availability will then affect growth, survival, and reproduction. Then, trait syndromes are expected to constrain life history strategies describing individual performance responses (e.g., growth rates) and demographic responses (e.g., mortality rates), influencing community-level characteristics such as species composition and abundances which are crucial in determining ecosystem functioning (Adler et al. 2014, Salguero-Gómez et al. 2016, Salguero-Gómez 2017). Let us see how functional traits constrain life history by retaking a previous example. In a given plant community, different functional trait syndromes can coexist leading to the occupation of different ecological niches by

different species. Some species may present an acquisitive functional syndrome, meaning that they acquire and use resources rapidly (e.g., high hydraulic conductivity and photosynthetic capability). This strategy is expected to be related to high and fast growth when resources are not scarce and a rapid reproduction which may lead, for instance, to a rapid dominance of the community after a disturbance. This is what is referred as a fast strategy (Reich 2014) whereby population growth is expected to be more influenced by growth and/or fecundity (Adler et al. 2014). Once a canopy is established, new micro-environmental conditions appear as shade develops, opening a new ecological space with a lower availability of resources (e.g., light). This space may be occupied by species with more conservative trait syndromes, with a slow resource uptake and use but a higher conservation capability. These species will present a slow growth but a higher resistance to resource scarcity (higher stress tolerance), what is referred to as a slow strategy, with a higher survival and a delayed reproduction (Reich 2014). In this case, population growth is expected to be more influenced by survival than by growth and fecundity (Adler et al. 2014). Therefore, due to intrinsic constraints of plant function on growth, survival and reproduction, a conservative uptake and use of resources may constrain life history traits so species cannot present, for instance, high growth and rapid fecundity. Consistently, we will not expect acquisitive resource uptake and use to present a high stress tolerance (related to a high survival). Even though some general frameworks describe the relationship between functional and life history strategies (Adler et al. 2014, Reich 2014, Salguero-Gómez et al. 2017), variability in functional traits and life history traits can be more complex and several axes of variation may appear in different biogeographical regions in relation to environmental limiting factors and evolutionary legacies of species present. In this regard, a trait network perspective can be useful to better elucidate the relationship between functional and life history strategies in a multivariate way. In this thesis, such a perspective is taken to elucidate the relationship between functional and life history traits in trees from the Amazon Region.

1.3.1 Functional constraints on species distributions and species assemblage

At the species and supra-specific levels, functional trait syndromes can be seen as adaptive toolkits that allow species to perpetuate under a given range of conditions. Then, we expect individual traits and their relationships to be related to species distributions over environmental space (Figure 1.1), which will determine their geographical ranges at evolutionary timescales, where dispersal is not expected to strongly constrain species distributions (Crisp et al. 2009, Segovia et al. 2020). Some functional traits mediating the response to environmental factors such as water availability can become crucial in determining the environmental boundaries within which a given species can survive and evolve (Stahl et al. 2014, Laughlin et al. 2020, Kunstler et al. 2021). This will determine the geographical boundaries of species distributions and then, will affect the composition of communities, influencing species assemblage by applying environmental filtering on functional strategies.

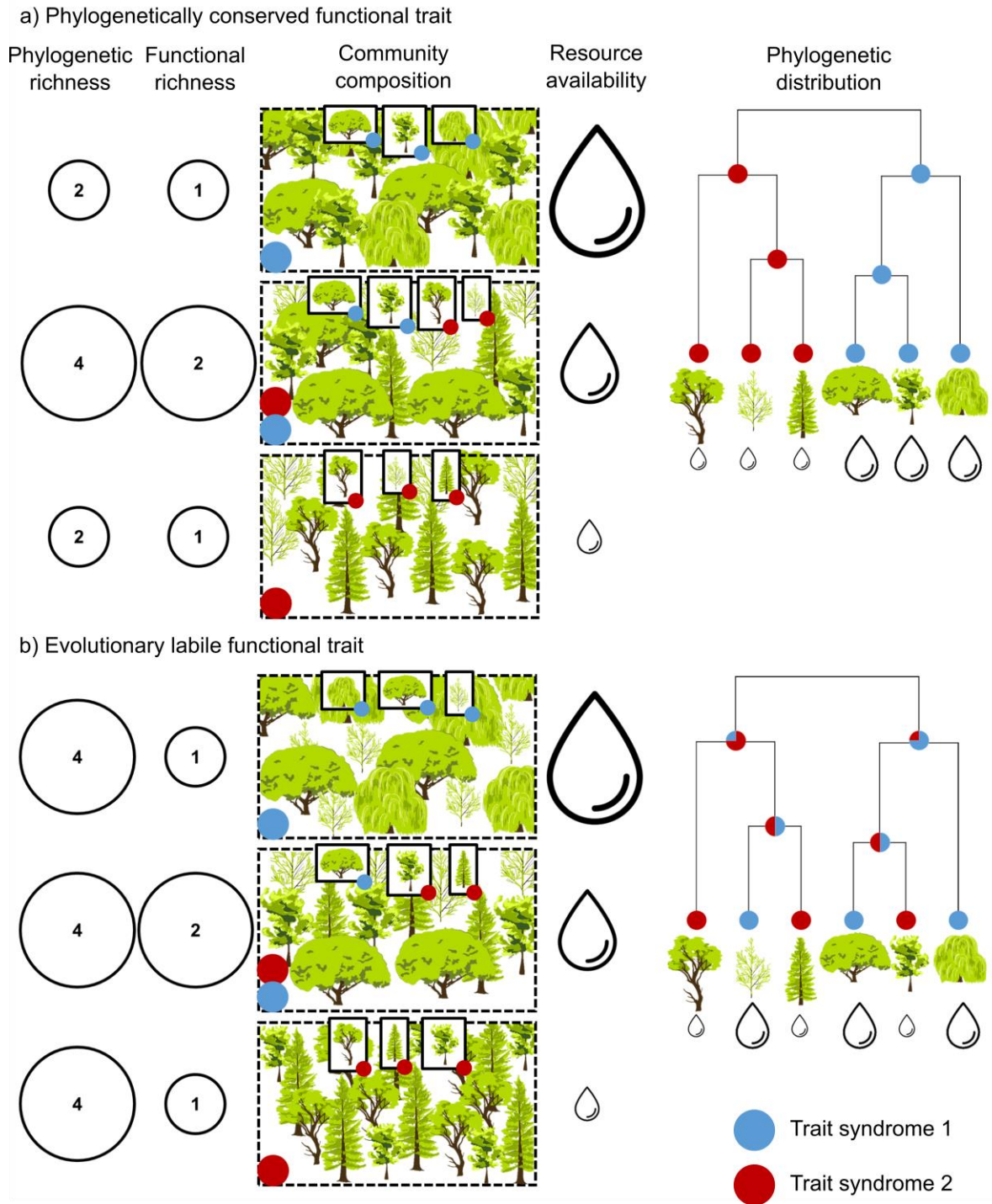
Evolutionary processes shaping species functional trait syndromes are expected to influence species assemblage patterns. Under a phylogenetic niche conservatism scenario, we expect closely related species to occupy areas with similar environmental conditions and to respond to them by means of similar strategies (Crisp et al. 2009, Crisp and Cook 2012). This phylogenetic structure will not only happen across geographical gradients of environmental variables, but also at the within-site level, in relation to micro-environmental variation. This would mean that environmental filtering is strongly affecting species distributions, as rapid adaptation may not be happening, and species will tend to occupy environmental spaces similar to those occupied by their ancestors. In this case, phylogenetic diversity of communities will be related to functional diversity and to environmental conditions both within and among sites (Figure 1.4). This pattern indicates that species may not be able to track drastic environmental forcing by changing their functional strategies. Then, community-level changes over evolutionary timescales will be more strongly influenced by dispersal of

new species which find the new conditions suitable. This pattern has already been observed in the case of drought at ecological timescales (Batllori et al. 2020, Trugman et al. 2020), but its relationship with underlying evolutionary patterns of functional traits are not clear yet.

Contrarily, under an evolutionary labile scenario, sister taxa may occupy quite different environmental spaces as a consequence of recent and relatively rapid adaptation and/or plastic acclimation. In this situation, we do not expect phylogenetic diversity to be strongly related to functional diversity either within or among sites (Figure 1.4). In this case, species may be more likely to track environmental changes, even though their capacity to persist under environmental changes will depend on the lability of crucial traits and to the degree of environmental forcing (Trugman et al. 2020).

Site-specific functional composition and diversity are expected to be related to ecosystem functioning, structure and response to environmental forcing (García-Valdés et al. 2020, Trugman et al. 2020). Then, elucidating biogeographical patterns in crucial functional traits is needed to better assess potential impacts of environmental forcing on species persistence. In this thesis, I provide an example illustrating the value of including the geographical perspective to better elucidate macroevolutionary patterns of functional traits and its effects at community and ecosystem levels.

Figure 1.4 Evolutionary patterns and community composition Example of evolutionary patterns translation to community characteristics.



1.3.2 Function-environment mismatches

Currently, environmental conditions are rapidly changing in some areas all over the globe (IPPC 2022). More concretely, global warming is expected to increase the frequency and intensity of drought events and heat waves (Stocker et al. 2013). This environmental forcing can push populations outside of the comfort zone of their ecological niches, generating mismatches between external conditions and their capability to maintain physiological processes that allow individuals to maintain viable populations (Parmesan and Yohe 2003, Thomas et al. 2004). This may be specially the case under a scenario in which crucial functional traits are evolutionarily constrained and then, are not expected to respond to environmental forcing by means of an adaptive response.

Climate change-induced mortality may be preceded by a decrease in growth and reproduction driven by a regulation in more labile traits (Niinemets 2010, Mundim and Pringle 2018). However, some specific phenomena may impact rapidly on survival under strong and/or persistent environmental forcing. This may be the case of hydraulic failure, a generalized disruption of plant transport system (xylem) that happens when severe drought strikes, interrupting water transport to leaves and producing relatively fast mortality in species with a low degree of stress tolerance (Hammond 2020, McDowell et al. 2021). Functional traits related to species drought tolerance are expected to be crucial to elucidate individual species and communities' response to ongoing environmental forcing (Anderegg et al. 2015, McDowell et al. 2021). A better characterization of species drought response strategies, its evolution and its relationship with the environment is crucial to better understand drought-induced mortality events, helping to assess impacts of climate change on vegetation and allowing us to anticipate them. In this thesis, I show how evolutionary patterns in crucial functional traits can be useful to better understand climate change impacts on vegetation.

1.4 TOWARDS AN EVOLUTIONARY FRAMEWORK IN PLANT FUNCTIONAL ECOLOGY

The consideration of evolutionary processes when discussing patterns in functional traits can be highly insightful to approximate their mechanistic basis and upscale their consequences. If functional traits present heritability, these patterns of variation emerge, at least partially, from genetic composition, which is then influenced by mechanisms related to selective pressures, mutation, gene flow and genetic drift shaping their variability at the micro-evolutionary scale (i.e., intraspecific variability). This variability is then translated at the macroevolutionary scale, where successful strategies can be described from the co-occurrence of functional trait values (i.e., functional syndromes). Variation in functional syndromes can be related to environmental factors and to evolutionary legacies of species influencing current values. As we have seen, the importance of these elements explaining functional diversity can be highly insightful to elucidate processes shaping it, which is crucial to better assess climate change impacts on ecosystems at different scales.

Even if methodologies that explicitly consider phylogeny to study patterns in functional traits already exist (e.g., independent contrasts, phylogenetic least squares or phylogenetic principal component analyses), they are normally focused on defining evolutionary relationships as those that are not explained by divergence of lineages (Felsenstein 1985, Revell 2009, Blomberg 2016). However, phylogenetic conservatism in relationships between traits may bring some insights to determine evolutionary patterns in functional strategies and their impact on ecological processes. To my knowledge, a clear methodological and conceptual framework to study phylogenetic conservatism jointly with evolutionary lability from a multivariate perspective and including environmental components is still lacking. This thesis aims to fill this gap by providing a new methodology to study trait syndrome diversity and their association with phylogenies and environment, seeking to elucidate the degree of phylogenetic

conservatism and evolutionary lability in plant functional strategies. This will lead to a better understanding of how functional strategies distribute and why, which is of great interest to elucidate vegetation responses to climate change. Moreover, disentangling potential drivers of plant function may be very useful to improve predictions on functional traits and their distributions, which are also increasingly demanded by process-based models predicting climate change dynamics and their potential impacts on society (De Cáceres et al. 2021a). Finally, such an overview of evolutionary patterns in plant physiological strategies may guide next steps focusing on the relationship between functional traits and genetic precedence as well as their response to environmental conditions and environmental forcing that will help closing the gap between plant function, its genetic basis, and its interaction with the environment.

1.5 RESEARCH AIMS AND OUTLINE

In this thesis I aim to elucidate macroevolutionary patterns in plant functional traits including the evolutionary perspective using phylogenies. Then, I aim to relate these patterns to ecological consequences such as performance related to growth, survival and reproduction. Finally, I aim to elucidate some potential effects of function and environment mismatches. To do so, I defined specific objectives addressed in each one of the chapters introduced below.

In the second chapter, I aim to elucidate the degree of phylogenetic niche conservatism in plant hydraulic traits, their relationship and in their response to environmental conditions related to water availability. I report that hydraulic traits show a pattern of phylogenetically conserved integrated adaptation. I also show how hydraulic traits conform to two hardwired modules: the drought exposure-tolerance coordination and the conductivity-allocation to sapwood relative to leaf trade-off.

In the third chapter, I aimed to develop a conceptual and methodological framework to study functional trait syndromes and predict missing values. In this framework, evolutionary patterns in individual traits and their relationships are elucidated, considering potential drivers related to environmental conditions and evolutionary legacies. Then, this information is used to inform a newly derived machine learning algorithm which implements predictions on functional trait missing values based on the previously presented relationship with phylogeny, environment, and other traits. This methodology is applied to the relationship between leaf economics spectrum (Wright et al. 2004) and plant hydraulics, showing a pattern of phylogenetic niche conservatism in the integration among leaf economics and hydraulics.

In the fourth chapter, I aimed to elucidate the relationship between some functional traits and performance traits describing life history strategies in tropical trees, focusing on clarifying the degree of evolutionary lability and phylogenetic conservatism in these individual traits and their relationship. I show how functional and life history traits are evolutionarily integrated conforming to two main axes. The first one represented the relationship between resource use, reproduction, and mortality, and it showed to be phylogenetically conserved. The second axis represented the relationship between size and growth and showed to be partially phylogenetically conserved and partially evolutionarily labile.

In the fifth chapter, I aimed to relate patterns of functional strategies to ecological consequences related to environmental forcing effects on vegetation. To do so, I focused on drought exposure-tolerance coordination to estimate and map species assemblage hydraulic risk, which is shown to present a positive relationship with drought-induced mortality.

2 ADAPTATION AND COORDINATED EVOLUTION OF PLANT HYDRAULIC TRAITS

Sanchez-Martinez, P., Martínez-Vilalta, J., Dexter, K. G., Segovia, R. A., & Mencuccini, M. (2020). Adaptation and coordinated evolution of plant hydraulic traits. Ecology Letters, 23(11), 1599–1610. <https://doi.org/10.1111/ele.13584>

2.1 ABSTRACT

Hydraulic properties control plant responses to climate and are likely to be under strong selective pressure, but their macroevolutionary history remains poorly characterized. To fill this gap, I compiled a global dataset of hydraulic traits describing xylem conductivity (K_s), xylem resistance to embolism ($|P_{50}|$), sapwood allocation relative to leaf area (H_v) and drought exposure ($|P_{min}|$) and matched it with global seed plant phylogenies. Individually, these traits present medium to high levels of phylogenetic signal, partly related to environmental selective pressures shaping lineage evolution. Most of these traits evolved independently of each other, being co-selected by the same environmental pressures. However, a correlated phylogenetic signal between $|P_{50}|$ and $|P_{min}|$ and between K_s and H_v show signs of deeper evolutionary integration because of functional, developmental, or genetic constraints, conforming to deep evolutionary modules. We do not detect evolutionary integration between conductivity and resistance to embolism, rejecting a hardwired trade-off for this pair of traits.

2.2 INTRODUCTION

Water transport in plants occurs under negative pressure and is driven by the process of transpiration at the leaf-atmosphere interface, which generates a water potential gradient throughout the plant (cohesion-tension theory) (Dixon 1914). A key source of vulnerability for the water transport system is the formation of xylem embolism, resulting from the breakage of the water columns caused by cavitation (the phase change from liquid water to gas), which reduces hydraulic conductivity and may lead to plant death through hydraulic failure (Tyree and Zimmermann 2002). This process is more likely to occur during drought events, as low water availability results in low soil plant water potentials, and becomes more pronounced also with high

temperatures, which provoke an increase in atmospheric evaporative demand (Venturas et al. 2017). A wealth of research over the last decades has established that hydraulic failure is a principal mechanism triggering tree mortality under drought (Adams et al. 2017). Therefore, drought and high temperatures, together with other important sources of selection such as freezing temperatures (Zanne et al. 2014), have been considered among the primary forces shaping plant evolution by acting directly on hydraulic traits (Maherali et al. 2004). However, global patterns in the evolution of hydraulic traits remain only partly characterized and their relationship with relevant environmental selective pressures poorly identified.

Species differ greatly in their exposure to low water potentials and in their capacity to operate under such conditions. The actual hydraulic risk is normally represented by the hydraulic safety margin (HSM) (Choat et al. 2012). HSM integrates both drought stress exposure at the tissue level, measured as the minimum leaf water potential registered for a given species (referred as an absolute value, $|P_{\min}|$), and resistance to embolism, quantified as the water potential that causes a 50% reduction in stem hydraulic conductivity (referred as an absolute value, $|P_{50}|$) ($HSM = P_{\min} - P_{50}$). Plants with low (or even negative) safety margins experience large amounts of embolism (Choat et al. 2012, 2018b). $|P_{\min}|$ emerges from the balance between soil water availability, the rate of water loss, and the capacity of the plant transport system to supply water to leaves, and it is thus determined by plant functional properties such as rooting strategy, leaf phenology and stomatal control as well as by abiotic factors such as soil water availability and atmospheric evaporative demand (Bhaskar and Ackerly 2006). Meanwhile, $|P_{50}|$ is primarily explained by xylem anatomical features (Venturas et al. 2017). $|P_{50}|$ and $|P_{\min}|$ are known to co-vary, leading to relatively invariant HSMs at the global scale and to respond to similar environmental selective pressures related to water availability (Choat et al. 2012, Maherali 2004). For instance, stem $|P_{50}|$ has been reported to be negatively related with precipitation for 10 conifer species from different habitats (Brodribb and Hill 1999) and for the gymnosperm genus *Callitris* (Larter et al. 2017) and $|P_{\min}|$ has been negatively related to variables determining water

availability (Bhaskar & Ackerly 2006) and positively to soil particle size during drought for Great Basin shrubs (Sperry and Hacke 2002). Since the risk of hydraulic failure is likely to be under greater selective pressure than $|P_{\min}|$ and $|P_{50}|$ *per se*, these two latter traits are expected to be integrated over the evolutionary history of lineages, specifically meaning that they evolve in a coordinated fashion (i.e., non-independently from each other), representing an evolutionary module.

Xylem conductive capacity is another key determinant of hydraulic function, usually quantified as the maximum, stem-specific hydraulic conductivity (K_s). This property has been reported to be positively related to temperature and precipitation at a global scale (He et al. 2020b). Because the structural properties of xylem conduits and pit membranes associated with increased embolism resistance (quantified here as $|P_{50}|$) are also expected to reduce conductive capacity, a trade-off between $|P_{50}|$ and K_s has long been hypothesized (often referred to as the hydraulic safety-efficiency trade-off) (Tyree & Zimmermann 2002). According to this hypothesis, evolutionary processes associated with frequent drought occurrence would have driven an increase of xylem resistance to embolism, allowing taxa to bear lower water potentials and maintain water transport at the expense of xylem conductive capacity. In contrast, increased xylem conductivity could have evolved in wetter and warmer environments, where higher water transport was adaptive and selective pressures favouring expensive safety features were weaker (Maherali et al. 2004). Although this trade-off has been shown to be relatively weak across species (Maherali et al. 2004, Gleason et al. 2016), it remains unknown whether it reflects independent responses of each trait to similar selective pressures related to climate conditions and soil properties, or a deeper evolutionary integration.

The role of hydraulic conductivity is more nuanced when considered at the whole plant level, where transport capacity needs to match water demand, which is in turn strongly influenced by leaf area (Mencuccini et al. 2019b). Consequently, xylem conductive capacity is frequently expressed in a relativized manner as a measure of

hydraulic sufficiency (leaf-specific hydraulic conductivity; K_l , $K_l = K_s * H_v$, see below) (Tyree & Zimmermann 2002). From this perspective, plants may adapt to drought stress prioritizing supply over demand by reducing the ratio of leaf area relative to cross-sectional sapwood area (i.e., increasing its inverse, the Huber value; H_v) and thus ensuring the maintenance of hydraulic sufficiency under water scarcity. Contrarily, lineages not exposed to drought stress and with no restriction to evolve towards a more conductive xylem may be able to supply water to a higher leaf area by using a relatively low sapwood area, potentially allowing for higher productivity (Mencuccini et al. 2019b). Therefore, we would also expect xylem conductivity and sapwood-to-leaf allocation to be integrated over evolutionary timescales, evolving in a coordinated manner to maintain hydraulic sufficiency (Reich et al. 2003).

In this study, I aim to elucidate the global macroevolutionary patterns of hydraulic traits, disentangling (1) the degree to which trait values are phylogenetically conserved, (2) the extent to which trait conservatism is related to environmentally driven selection and (3) whether traits evolve in a correlated manner because of their responses to environmental conditions or because of a deeper integration. I hypothesize that closely related species will have similar trait values (Losos 2008) and that this phylogenetic conservatism will be partly explained by environmental selection (Figure 2.1). In addition, I hypothesize that some pairs of traits will show signs of a deep evolutionary relationship (evolutionary modules) reflecting a deep functional, developmental or genetic integration. Specifically, I expect to find three deep evolutionary modules consistent with previously hypothesized trait integration (namely, $|P_{50}| / |P_{min}|$, $|P_{50}| / K_s$, K_s / H_v) (Figure 2.1).

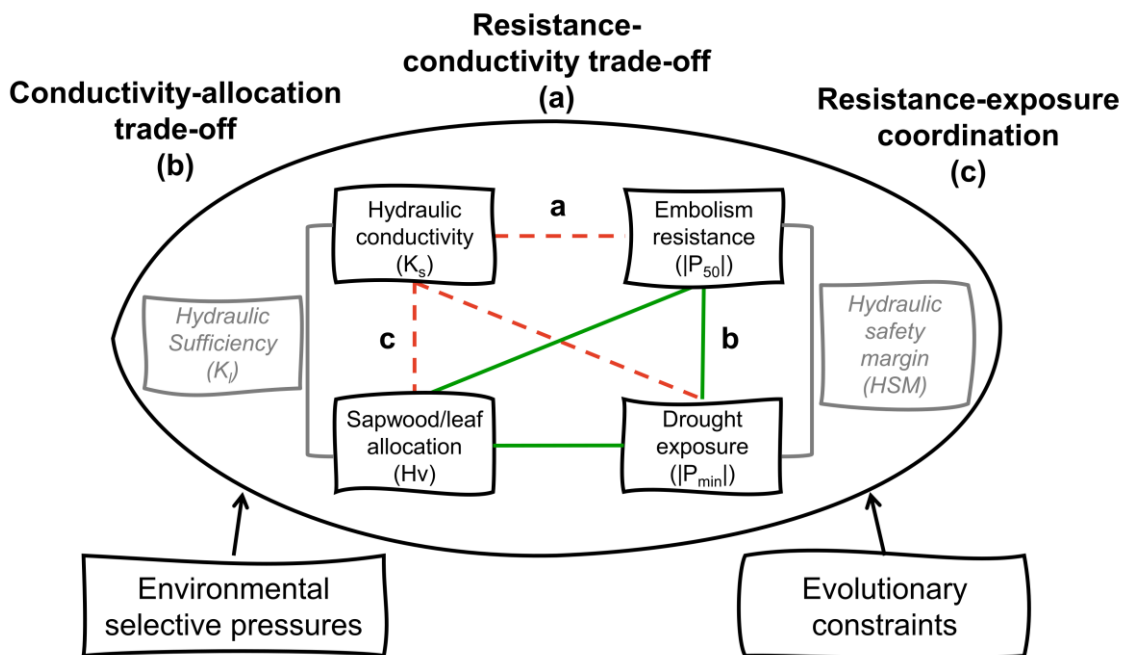


Figure 2.1 Hypotheses Lines represent potential correlation involving key hydraulic traits. Red dashed lines represent negative correlations and solid green lines represent positive correlations. Hydraulic safety margin (HSM) is the relationship between $|P_{min}|$ and $|P_{50}|$, and hydraulic sufficiency (K_i) which is the relationship between K_s and H_v . Hypothesised coordination between traits are specifically referred (a, b and c).

2.3 MATERIALS AND METHODS

2.3.1 Data sources

We extracted detailed hydraulic trait data from a database covering 2,027 species (1,888 angiosperms and 139 gymnosperms), representing 817 genera from 161 families. The data come from previously published databases (Liu et al. 2019a, Mencuccini et al. 2019b). Species names were matched against accepted names in The Plant List using the *taxonstand* R package (Cayuela et al. 2012). Then, the *taxonlookup* R package (Pennell et al. 2016) was used to complete species information at the genus, family, order and major evolutionary affiliation (angiosperms vs. gymnosperms) levels. The database covers all major biomes (Figure S2.1 in appendix 8.1.1).

I used data of four hydraulic traits that were represented across sufficiently large numbers of species ($N > 550$): (1) maximum stem-specific hydraulic conductivity (K_s , $\text{kg m}^{-1} \text{MPa}^{-1} \text{s}^{-1}$) as a measure of xylem conductive capacity; (2) stem water potential at 50% loss of hydraulic conductivity measured in terminal branches (referred as an absolute value, $|P_{50}|$, MPa) as a measure of xylem resistance to embolism; (3) branch-based Huber value (H_v ; $\text{cm}^2 \text{m}^{-2}$), defined as the sapwood cross-sectional area to leaf area ratio, as a measure of allocation; and (4) minimum midday leaf water potential recorded for species (referred as an absolute value, $|P_{\min}|$ MPa) as a measure of exposure to drought stress at the tissue level. I also included two additional variables integrating two pairs of the four selected traits, specifically, (5) maximum leaf-specific hydraulic conductivity (K_l , $\text{kg m}^{-1} \text{MPa}^{-1} \text{s}^{-1}$) as the hydraulic capacity per unit leaf area ($K_s * H_v$) and (6) the hydraulic safety margin (HSM, $\text{HSM} = P_{\min} - P_{50}$) (Table S2.1). When multiple measures for one species were available, mean values were used for all traits, except for $|P_{\min}|$, where the absolute minimum was used (c.f. Choat et al. 2012). For all variables, I excluded data from seedlings and studies in greenhouses or experimental gardens, data obtained on roots and leaves (Liu et al. 2019; Mencuccini et

al. 2019b) and $|P_{50}|$ values corresponding to extreme, r-shaped vulnerability curves, following previously used criteria (Choat et al. 2012).

I note that all study traits are subject to methodological uncertainty in their determination and in aggregation to species level, and sample sizes differ among species. Estimates of species-specific $|P_{\min}|$ in particular are sample-size dependent and likely biased to an unknown extent for some species. It is likely that the sampling period will miss droughts with a long return interval at some sites. It is also likely that long-lived species (e.g. several gymnosperms) will encounter more severe drought events throughout their lives with consequently greater biases. HSM combines uncertainties in both $|P_{50}|$ and $|P_{\min}|$ determination, which is problematic because of direct methodological issues in the case of $|P_{50}|$ (Jansen et al. 2015) and because of the inherent difficulty in characterizing extreme values in the case of $|P_{\min}|$ (Head et al. 2012). Finally, in the case of K_s , although it is normalized by sapwood area, it might still depend upon stem size to some degree.

Sixteen environmental variables were compiled (11 related to climate and five to soil properties) (Table S2.1). Climatic variables were extracted from WorldClim (Fick and Hijmans 2017) (www.worldclim.org; accessed on February 2019) except for Moisture Index, which was extracted from the global aridity and potential evapotranspiration (PET) database (Trabucco & Zomer 2019) (www.cgiar-csi.org, data accessed on February 2019) at a resolution of 30 arcsec. Soil data were extracted from SoilGrids (Hengl et al. 2017) (www.soilgrids.org, accessed on February 2019) at the same resolution. Occurrences for all species were obtained from the Global Biodiversity Information Facility (www.gbif.org, accessed on February 2019) and the Atlas of Living Australia (www.ala.org.au, accessed on February 2019) using the *rgbif* (Chamberlain et al. 2023) and the *ALA4R* (Westgate et al. 2023) R packages, respectively. Potentially incorrect species occurrence records were filtered using the *CoordinateCleaner* R package (Zizka et al. 2019).

2.3.2 Phylogeny

I used a genus-level phylogeny instead of a species-level one to avoid issues with species misidentifications, which are particularly common in the tropics (Baker et al. 2017), and from where a considerable amount of our hydraulics data come. The genera in the phylogeny covered a greater number of species present in our database than the best-sampled species-level phylogeny available (Smith and Brown 2018). Some models, however, were also fitted using a species-level phylogeny (Smith and Brown 2018) to assess the robustness of our results to the taxonomic resolution of our phylogenetic data. To construct the genus-level phylogeny, sequences of the *rbcL* and *matK* plastid gene for 707 angiosperm tree genera were obtained from Genbank (www.ncbi.nlm.nih.gov/genbank) building on previous efforts (Dexter & Chave 2016; Neves et al. 2020; Segovia et al. 2020). Sequences were aligned using the *MAFFT* software (Katoh and Standley 2013). “Ragged ends” of sequences that were missing data for most genera were manually deleted from the alignment. The two chloroplast markers were concatenated, and a maximum likelihood phylogeny for the genera was estimated in the *RAxML v8.0.0* software (Stamatakis et al. 2008), on the CIPRES web server (www.phylo.org), using General Time Reversible (GTR) + categorical Gamma (G) model of sequence evolution. The tree was constrained following order-level relationships proposed by the angiosperm Phylogeny Group IV (Chase et al. 2016). Sequences of *Nymphaea alba* (Nymphaeaceae) were included as an outgroup.

The resulting maximum likelihood phylogeny for angiosperms was temporally calibrated using the software *treePL* (Smith and O’Meara 2012). Age constraints for internal nodes were implemented for most families and orders (Magallón et al. 2015). The rate smoothing parameter (λ) was set to 10 based on a cross-validation procedure. Finally, the newly-derived angiosperm phylogeny was fused with an existing gymnosperm phylogeny (Leslie et al. 2018). I manually added the genera *Gnetum* and *Ginkgo* according to ages found in the literature, 174 Ma for the Gnetales (Ran et al. 2018) and 265.2 Ma for Ginkgoaceae (Tank et al. 2015).

2.3.3 Statistical analyses

All analyses were carried out in R (3.6.0) (R Core Team 2020). Some variables were transformed to achieve normality (using absolute values in the case of P_{50} and P_{\min}) (Table S2.1). A Principal Components Analysis (PCA) on the 16 variables was performed using the R package *stats* (R Core Team 2020) to reduce the number of axes summarizing environmental variation. The first principal component (PC1) explained 51% of the variance in the environmental data, representing variation in water availability and some related variables such as soil pH, soil clay content, soil water content and temperature seasonality, with high values characterizing more humid locations with leached acidic soils characteristic of non-seasonal wet tropical habitats. The second principal component (PC2) explained 20% of the variance, representing variation in energy input, with high values characterizing low solar irradiation, low maximum temperatures and low atmospheric water demand. Finally, the third principal component accounted for 9% of the variance and largely reflected soil depth and, to a lower extent, wind velocity, with high values indicating deeper soils with low sand content and low maximum wind velocities (Table S2.2, Figure S2.2 and Figure S2.3). The remaining components explained a low proportion of variance ($<7\%$), so the first three axes were used to characterize the environmental niches of species in the following analyses.

Uni-response and bi-response Bayesian phylogenetic mixed models, alternatively including or excluding fixed effects of environmental principal components, major evolutionary affiliation (angiosperm vs. gymnosperm) and their interactions were fitted using the *MCMCglmm* R package (Hadfield 2010a) (see Table S2.3 for models description). All models accounted for the occurrence of multiple measurements in each genus by the inclusion of genus identity as a random effect. Moreover, genus-level phylogenetic relationships were taken into account as a second random effect using the previously presented phylogeny. The inclusion of these random effects allowed us to partition the residual variance from models into three components: the inter-generic

variance caused by phylogenetic relationships; the non-phylogenetic, inter-generic variance; and the intra-generic variance. The inter-generic phylogenetic variance quantifies the variability explained by the relationships among taxa as given by our phylogenetic hypothesis and, when divided by the total variance, gives a measure of the phylogenetic signal (λ) (Lynch 1991). Non-phylogenetic inter-generic variance (γ) accounts for the proportion of among-genus variability not explained by the phylogeny, and the intra-generic variance (ρ) provides a measure of the proportion of variability caused by intra-generic trait variation (plus any residual error) (Hadfield and Nakagawa 2010) (see appendix 8.1.2 for a more formal description).

To partition variances of phylogenetic and non-phylogenetic components, I implemented uni-response models without fixed effects for the six selected hydraulic traits and for the three environmental PCA axes as response variables (Table 2.1, Table S2.4 to see non-phylogenetic model variance partitions). To identify relationships between hydraulic traits and environmental PCA axes, I then ran uni-response models with hydraulic traits as response variables and single environmental principal components as fixed effects, both accounting and not accounting for phylogenetic relationships affecting the response trait. To examine the effect of the major split between angiosperms and gymnosperms, additional models included a binary variable describing major evolutionary affiliation and the interaction between affiliation and environment, allowing us to detect statistical differences between angiosperms and gymnosperms in the overall mean values of traits and in their relationships with environmental axes. For each group of nested models, the best fitting one in terms of DIC (Deviance Information Criterion) was selected (Table S2.5 to see DIC values). Models within 4 DIC units of each other were considered equivalent in terms of fit, and the simplest one was selected.

Subsequently, to characterize phylogenetic covariation between the hydraulic traits and between each hydraulic variable and the three environmental principal components, bi-response models were used. In these models, two response variables

and their phylogenetic structure were considered simultaneously, resulting in a variance-covariance matrix from which the correlated phylogenetic signal (see box 1.2) between the two variables could be calculated (see supplementary methods in appendix 8.1.2). Correlated phylogenetic signal was calculated for all combinations of trait pairs, including, and excluding the three environmental components, evolutionary affiliation, and their interactions as fixed effects (Figure S2.1 shows data coverage for each combination of traits). Finally, I also estimated correlated phylogenetic signal between traits and single environmental principal components including and excluding evolutionary affiliation as a fixed effect (Table S2.6 to see all correlations). Bi-response models were also implemented using a species-level phylogeny (Smith and Brown 2018) and available in the R package *V.PhyloMaker* (Jin and Qian 2019), to ensure consistency with genus-level results (see appendix 8.1.3). As data availability for the species-level phylogeny was lower due to the coverage of the phylogeny, I replicated the bi-response genus-level models using the same reduced dataset to ensure that potential differences between results were not due to different species coverage. I also performed analyses using the species-level phylogeny pruned at the genus-level, to ensure that potential differences between results were not explained by differences in the topologies of our custom-made genus-level phylogeny and the available species-level phylogeny (see appendix 8.1.4).

Models were specified to achieve convergence while minimizing correlation between iterations (appendix 8.1.2). Marginal variance explained (R^2_m , variance explained by the fixed effects) and conditional variance explained (R^2_c , variance explained by both fixed and random effects) were calculated for the uni-response models (Nakagawa and Schielzeth 2013). P-values were calculated for correlated phylogenetic signals using a previously published methodology (Makowski et al. 2019). Finally, reconstructions of the six traits and the three environmental principal components evolution under a Brownian motion model were mapped along the phylogeny using maximum likelihood ancestral state reconstructions (Schluter et al. 1997) by means of the *Phytools* R package (Revell 2013).

Table 2.1 Variance partitioning for six hydraulic traits and three environmental principal components. N: number of species used in each case, phylogenetic variance (phylogenetic signal, λ), non-phylogenetic intergeneric variance (γ) and intra-generic variance plus measurement error (ϱ). Mean and lower and upper 95% credible intervals (HPD) are shown for each component.

variable	N	λ	Lower HPD	Upper HPD	γ	Lower HPD	Upper HPD	ϱ	Lower HPD	Upper HPD
Embolism resistance, $\ln(P50)$	868	0.484	0.305	0.697	0.225	0.085	0.360	0.291	0.205	0.368
Drought exposure, $\ln(Pmin)$	541	0.745	0.572	0.874	0.066	0.000	0.179	0.189	0.129	0.273
Hydraulic conductivity, $\ln(Ks)$	1026	0.515	0.363	0.680	0.086	0.000	0.174	0.399	0.303	0.493
Sapwood/leaf allocation, $\ln(Hv)$	1271	0.446	0.291	0.594	0.191	0.097	0.294	0.363	0.276	0.449
Hydraulic safety margin, HSM	326	0.449	0.201	0.722	0.163	0.000	0.339	0.388	0.246	0.546
Hydraulic sufficiency, $\ln(Kl)$	827	0.432	0.244	0.592	0.036	0.000	0.113	0.532	0.399	0.675
Water availability PC1	1911	0.820	0.767	0.870	0.063	0.030	0.099	0.117	0.093	0.139
Energy input PC2	1911	0.686	0.599	0.766	0.028	0.000	0.069	0.286	0.230	0.341
Soil depth PC3	1911	0.841	0.798	0.876	0.007	0.000	0.027	0.152	0.124	0.182

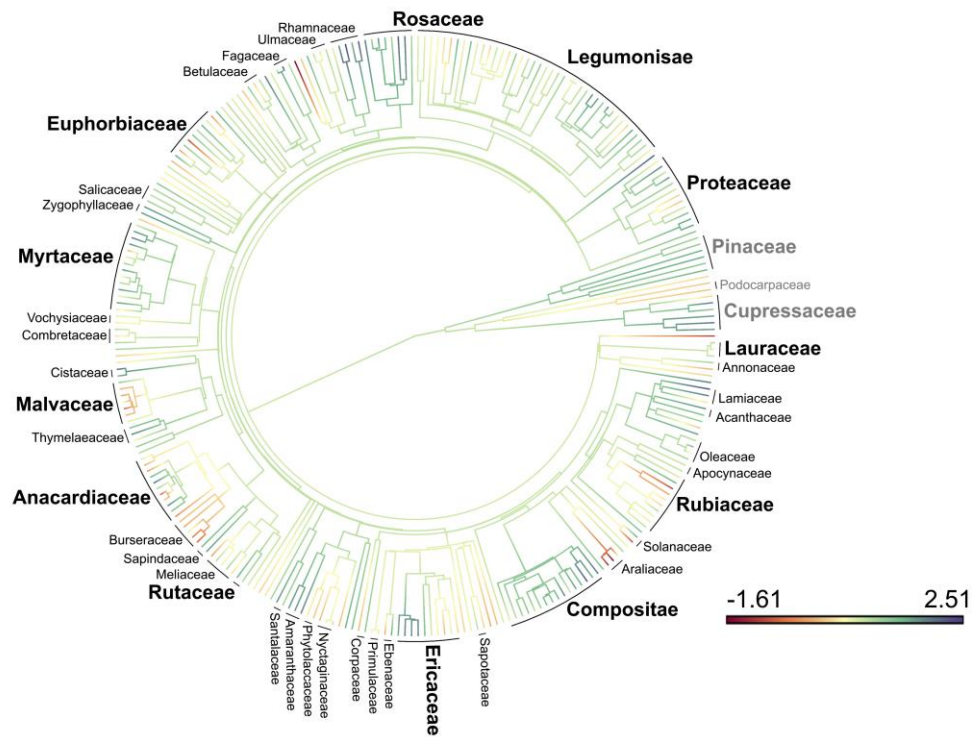
2.4 RESULTS

2.4.1 Phylogenetic signal in hydraulic traits

All six selected traits showed a significant phylogenetic signal. The proportion of variance that was explained by the inter-generic phylogenetic structure (λ) ranged from 0.432 (K_1) to 0.745 ($|P_{\min}|$) (Table 2.1). This means that 43.2-74.5% of trait variances can be attributed to relatively deep evolutionary differences among genera, with the rest being attributed to non-phylogenetic inter-generic (γ) and intra-generic (ρ) variances. Intra-generic variances (ρ) ranged from 0.189 ($|P_{\min}|$) to 0.532 (K_1), being the second most important variance component in all cases except K_1 (where it was the most important), indicating that trait diversification within genera is a substantial part of global trait variability. Analyses using the species-level phylogeny confirmed that variation within genera also had strong phylogenetic patterns (see analysis using a species-level phylogeny in the appendix 8.1.3). Finally, inter-generic, non-phylogenetically related variances (γ) ranged from 0.036 (K_1) to 0.225 ($|P_{50}|$) and accounted for the lowest proportion of the variance in all cases (Table 2.1). Phylogenetic mapping of hydraulic traits qualitatively confirmed the findings reported above, showing more gradual changes in highly conserved traits such as $|P_{\min}|$ and changes more concentrated at the tips of the phylogeny for variables showing a lower phylogenetic signal, such as H_v , which also showed higher intra-generic variance (Figure 2.2, Figure 2.3 and Figure S2.4).

Importantly, the phylogenetic signal of the three environmental principal components was also very high, particularly for PC1, representing water availability (0.820) and PC3, mainly represented by soil depth (0.841) (Table 2.1, Figure S2.5)

a) Drought exposure ($\ln|P_{\min}|$)



b) Embolism resistance ($\ln(|P_{50}|)$)

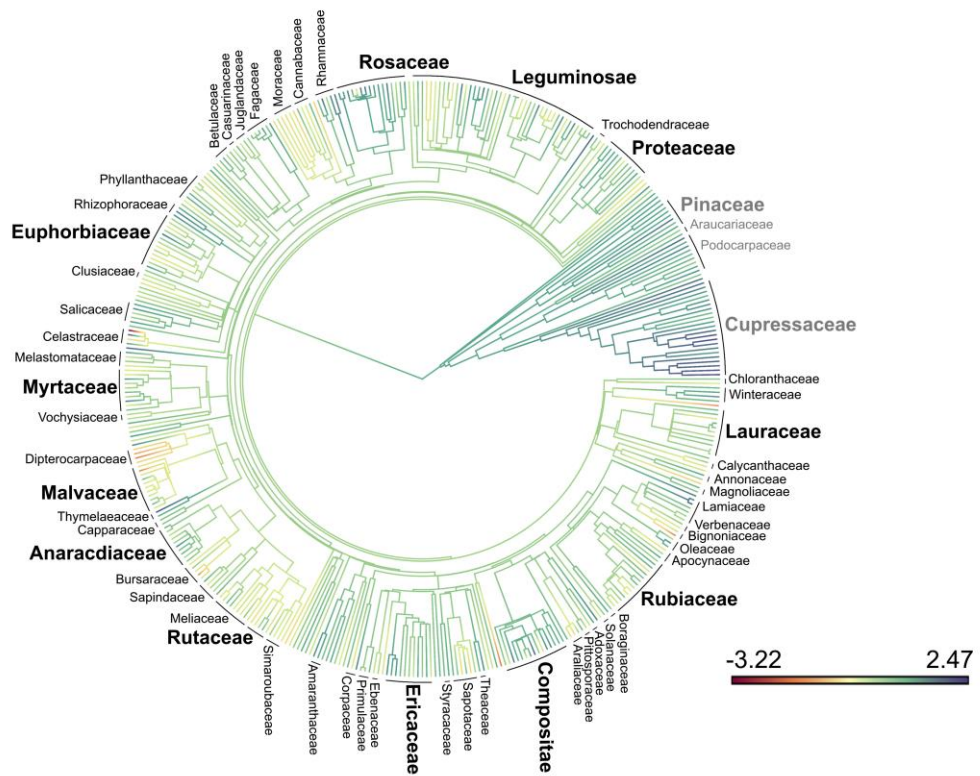
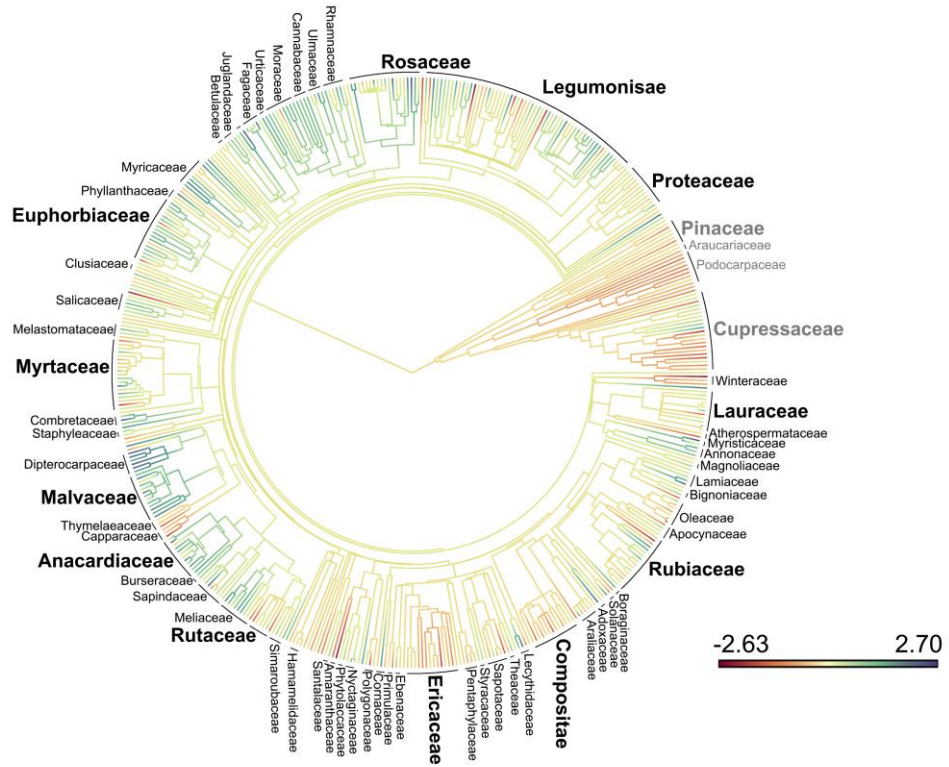
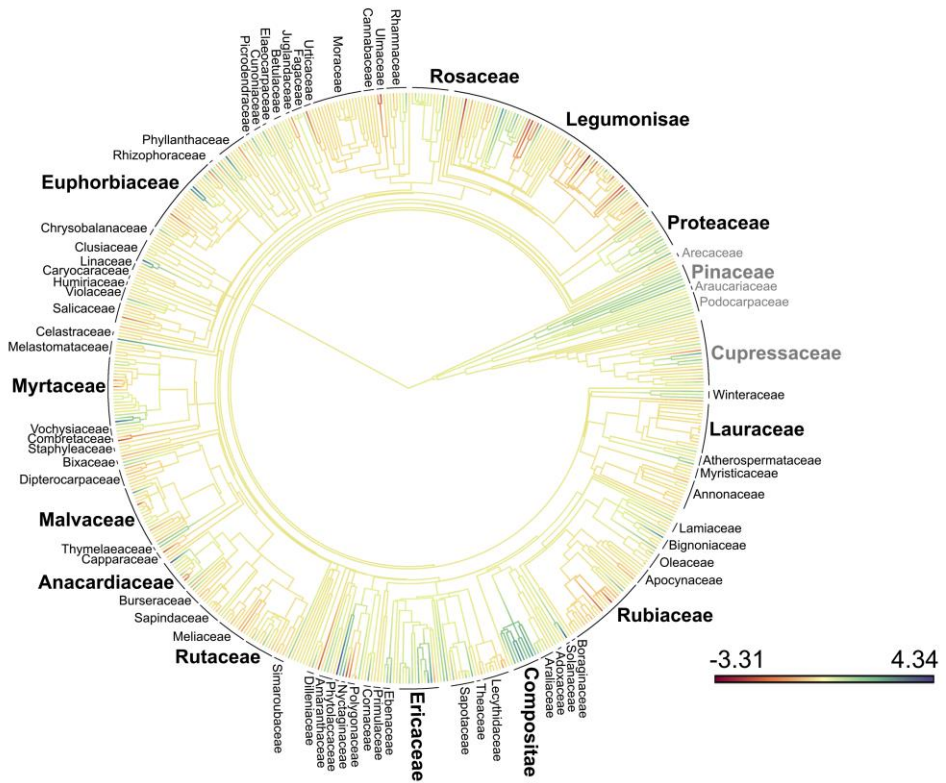


Figure 2.2 and 2.3 Phylogenetic reconstruction of hydraulic traits

c) Hydraulic conductivity, $\ln(K_s)$



d) Sapwood/leaf allocation, $\ln(H_v)$

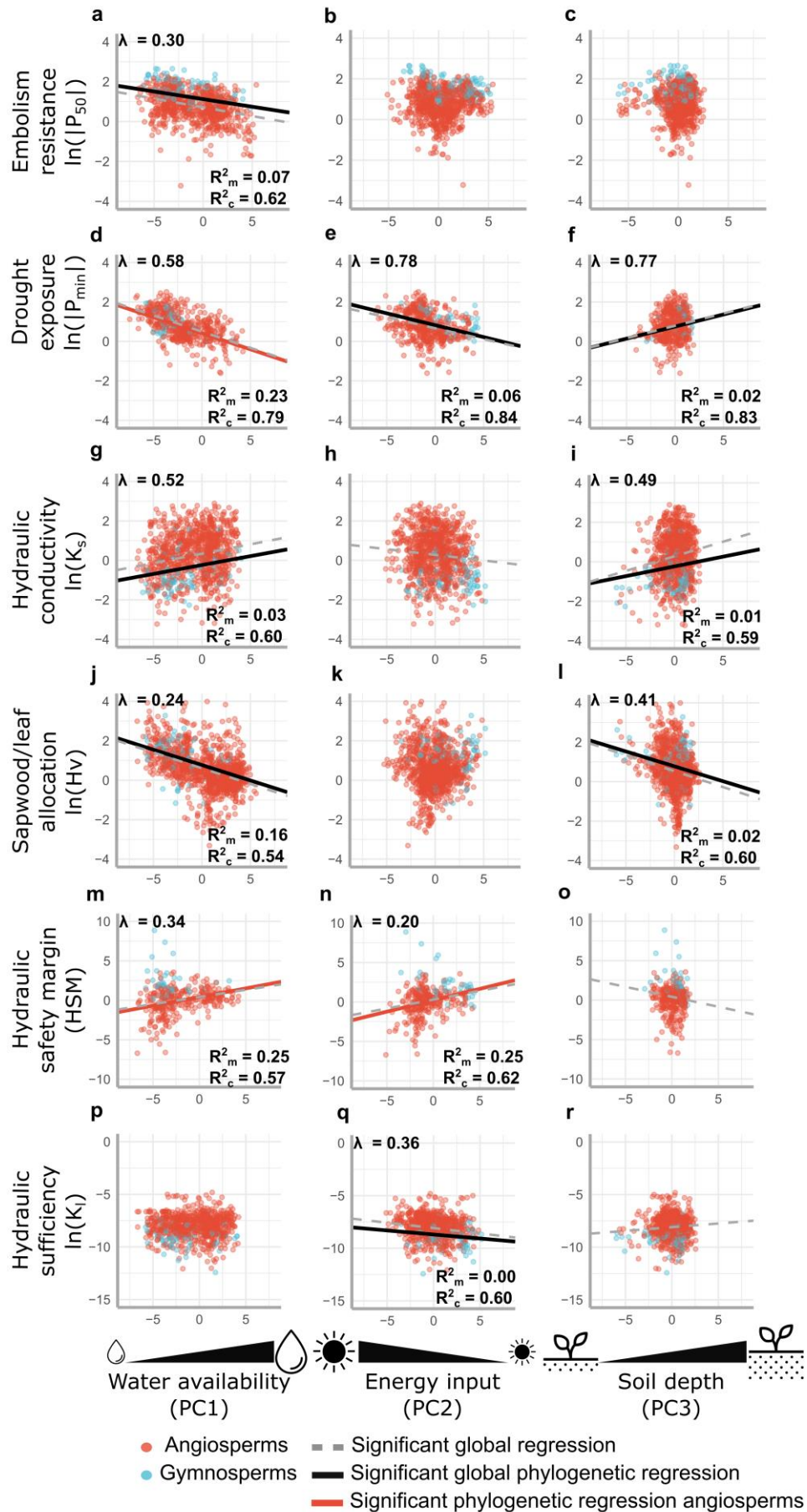


2.4.2 Environmental drivers of hydraulic traits

In models that accounted for phylogenetic structure, all hydraulic traits showed significant relationships with at least one of the three environmental axes defined by the PCA (Figure 2.4). Conditional explained variances (R^2_c) were notably higher than marginal explained variances (R^2_m), indicating that accounting for the phylogenetic relationships was crucial to improve model fit (Figure 2.4). Consistent with the fact that environmental axes were highly phylogenetically conserved, we also found that the phylogenetic signal of traits (Table 2.1) diminished when accounting for environmental effects (Figure 2.4, lambdas (λ)), thus indicating that environmental conditions explain part of the phylogenetic variance.

Xylem resistance to embolism ($|P_{50}|$) was only negatively related to PC1 (water availability). Minimum water potential at midday ($|P_{min}|$) was negatively related to PC1 and PC2 (declining energy input) and positively to PC3 (soil depth). However, the relationship with PC1 was only significant for angiosperms. Xylem conductivity (K_s) was found to be positively related to PC1 and PC3, being negatively related with PC2 only in non-phylogenetic models. Sapwood to leaf area ratio (Hv) was negatively related to PC1 and PC3. The hydraulic safety margin (HSM) was positively related to PC1 and PC2 only for angiosperms and the relationship between HSM and PC3 was only significant (and negative) for non-phylogenetic models. Finally, Leaf-specific conductivity (K_l) was only related to PC2 (negatively) in phylogenetic models, but a positive relationship with PC3 was also found when using non-phylogenetic models (Figure 2.4).

Figure 2.4 Environment-trait relationships Grey-dashed lines represent the significant global relationship without accounting for the phylogenetic structure and black-, and red-solid lines significant relationship once phylogenetic structure is considered for all the data and angiosperms (only when statistical differences with gymnosperms were reported). Residual phylogenetic signal (λ) of hydraulic traits once environmental effects are accounted for in each case is reported when relationships are significant. R^2_m is the variance explained by the fixed effects and R^2_c by the fixed and random effects for the phylogenetic mixed models. Signif. codes: “***”: $P < 0.001$; “**”: $P < 0.01$; “*”: $P < 0.05$ “.”: $P < 0.1$ “ ”: $P > 0.1$.



2.4.1 Correlated phylogenetic signal

Significant correlated phylogenetic signal was reported between $|P_{\min}|$ and $|P_{50}|$ (positive), K_s and H_v (negative), H_v and $|P_{50}|$ (positive) (Figure 2.5). These correlated phylogenetic signals were confirmed when the species-level phylogeny was used, which also showed a significant correlated phylogenetic signal between $|P_{50}|$ and K_s (negative), $|P_{\min}|$ and H_v (positive) and K_s and $|P_{\min}|$ (negative) (Figure S2.6). The emergence of these correlated phylogenetic signal was not explained by the lower number of species available for the species-level phylogeny compared to the genus-level one, nor by differences in topology between phylogenies (appendix 8.1.4), so it is likely due to the large amount of phylogenetic covariance between traits within genera. Only two correlated phylogenetic signals between traits remained once environmental factors and major evolutionary affiliation of species were accounted for, coinciding with two of the three hypothesized evolutionary modules. These were the ones involving $|P_{50}|$ and $|P_{\min}|$ (positive correlation) and K_s and H_v (negative correlation) (Figure 2.5, Figure S2.6). While $|P_{50}|$ and $|P_{\min}|$ presented a highly conserved covariation pattern, the evolutionary integration between K_s and H_v was less strong. The latter was marginally significant when using the genus-level phylogeny (Figure 2.5), but clearly significant when intra-generic phylogenetic covariation between traits was additionally considered by using the species-level phylogeny (Figure S2.6).

Consistent correlated phylogenetic signals were also observed between certain hydraulic traits and environmental principal components in the bi-response models: K_s was positively correlated with PC1 (water availability), and PC3 (soil depth) while its relationship with PC2 (energy input) was only significant at the genus-level and disappeared when considering major evolutionary affiliation. H_v was negatively correlated with PC1 and PC3; and both $|P_{50}|$ and $|P_{\min}|$ were negatively correlated with PC1 (Figure 2.5).

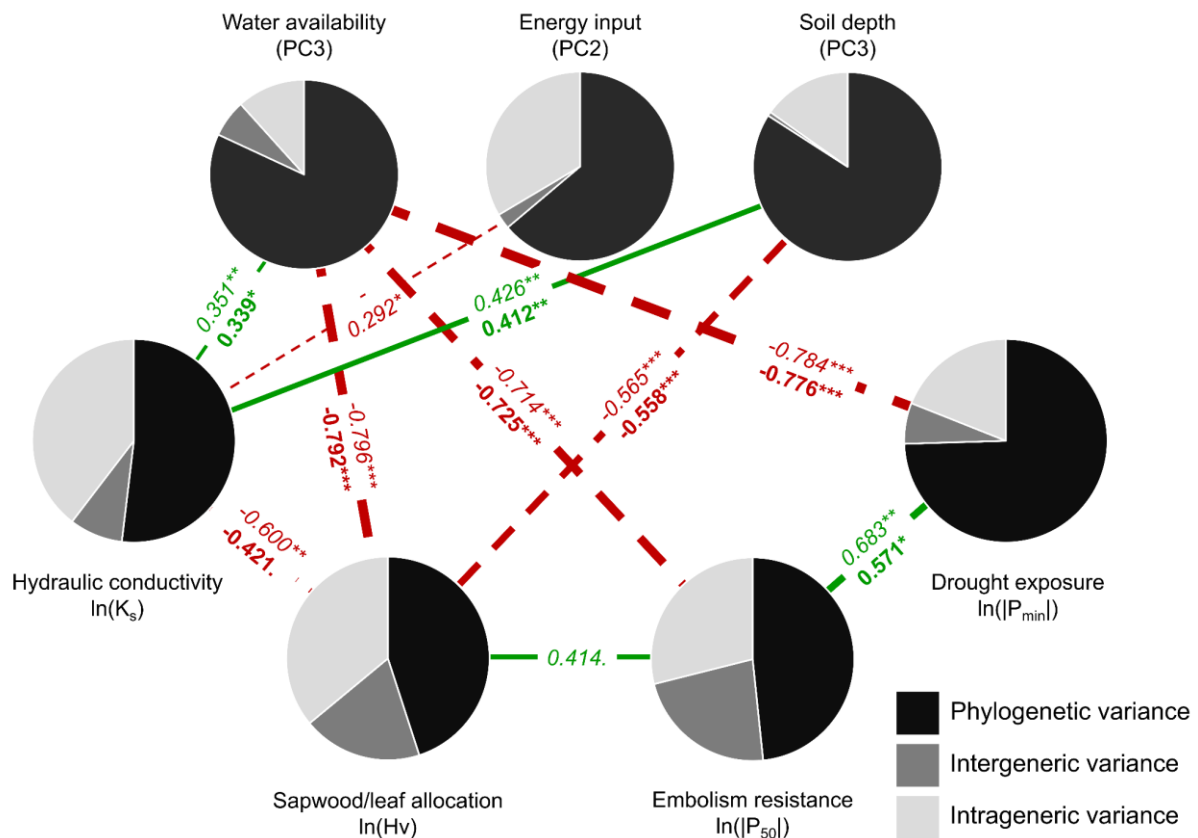


Figure 2.5 Correlated phylogenetic signals Correlated phylogenetic signals involving species-level hydraulic traits and environmental principal components using a genus-level phylogeny. Environmental variables represent orthogonal PC axes and as such are not correlated. Lines represent significant correlated phylogenetic signals. Red dashed lines represent negative correlations and green solid lines indicate positive correlations. Significant correlation coefficients are shown in italics and are proportional to the thickness of the line. Significant correlation coefficients between traits including environmental components and evolutionary affiliation as fixed effects are shown in bold (in the case of the relationships between environmental axes and traits, only evolutionary affiliation was considered as a fixed effect). P-values are also displayed for each coefficient. P-values are also displayed for each coefficient. Signif. codes: “****”: $P < 0.001$; “***”: $P < 0.01$; “**”: $P < 0.05$; “*”: $P < 0.1$; “.”: $P > 0.1$.

2.5 DISCUSSION

2.5.1 Phylogenetically conserved adaptation in hydraulic traits

I found a clear pattern of phylogenetic conservatism for hydraulic traits, suggesting that the legacy of traits found in species' evolutionary ancestors is an important determinant of trait values in extant species. While we cannot formally rule out Brownian motion evolution operating over long evolutionary timescales as the source of present-day trait variability on the basis of our single trait variance partitioning (Revell et al. 2008), our finding of correlated phylogenetic signals of traits with environmental variables indicates a key role for non-neutral evolutionary processes. Consistently, environmental components explained part of traits' phylogenetic variance when accounted for as fixed effects (Figure 2.4). Therefore, our analyses indicate that adaptive processes have driven the diversification of hydraulic traits, but the prevalent pattern of phylogenetic niche conservatism suggests that evolutionary constraints have limited the range of trait values within lineages. Thus, lineages have been largely tracking environments similar to those their ancestors were already adapted to, retaining ancestral traits because of stabilizing selection (Ackerly 2009), while occasionally adapting to novel environmental conditions.

We do observe a wide range of trait values across lineages (including among genera), indicating that they adaptively diverged in deep evolutionary time (Figure 2.2, Figure 2.3, Figure S2.4 and Figure S2.5). Further, substantial trait variation can also arise over shorter evolutionary timescales (i.e., in recent evolutionary time) via species adapting to environmental changes, as supported by the significant degree of trait variance at the intra-generic level (Table 2.1), which also appears to have a phylogenetic component (Figure S2.6). As a result, lineages that have been evolving in dry habitats have adapted to a higher exposure to drought stress by increasing their xylem resistance

to embolism, being able to maintain water transport at low water potentials (Choat et al. 2012). These species are also selected to ensure water supply to leaves by using a relatively high sapwood area with a low hydraulic conductivity (Mencuccini et al. 2019b). As water become less limiting, lineages are less exposed to low water potentials and are not selected to increase xylem resistance to embolism, while switching their allocation priority to a high leaf area maintained by a smaller area of highly conductive sapwood (Figure 2.4).

However, substantial variability in species exposure to drought stress within a given environment reflects the fact that plant characteristics such as stomatal control (Brodribb and McAdam 2017), deciduousness (Wolfe et al. 2016) or rooting depth (Canadell et al. 1996) are also determining hydraulic trait evolution. This may explain the lack of a clear relationship between PC1 (water availability) and $|P_{\min}|$ and HSM in gymnosperms, a clade mainly represented by Pinaceae and Cupressaceae (Figure S2.7) that are known to adopt contrasting strategies under drought. While Pinaceae avoid exposure to low water potentials by closing their stomata and possibly disconnecting from the soil (Poyatos et al. 2018a), Cupressaceae tolerate them by presenting a high resistance to embolism (Brodribb et al. 2014). Differences between angiosperms and gymnosperms could also be due to an underestimation of drought stress exposure for long-lived gymnosperms, especially in the case of the highly stress resistant Cupressaceae, for which the observation window may not have been long enough to adequately capture $|P_{\min}|$. Therefore, different evolutionary processes may be dominant depending on the taxon studied. For instance, xylem embolism resistance has been reported to be extremely labile for the genus *Callitris* (Larter et al. 2017) and to be conserved for *Juniperus* (Willson et al. 2008), while showing a high canalization for *Pinus* species (Lamy et al. 2014). It is also worth noting that our global eco-evolutionary overview may be limited by the availability of hydraulic data and its methodological uncertainties, as well as by the difficulty of upscaling traits at the whole-plant level, which remains a challenge (Mencuccini et al. 2019a).

2.5.2 Evolutionary modules in hydraulic traits

Traits can evolve in an integrated fashion conforming to evolutionary modules because of their response to similar selective pressures, but relationships between them may also arise from functional, developmental, or genetic constraints. We found two sets of traits for which an evolutionary correlation cannot be explained by similar responses to environmental conditions or by fundamental differences between angiosperms and gymnosperms. These sets of traits represent a deeper evolutionary integration. The first evolutionary module involves species exposure to drought and resistance to embolism ($|P_{50}|/|P_{min}|$), and it is strongly conserved over evolutionary scales. The second one involves xylem conductivity and sapwood to leaf area allocation (K_s/Hv), the integration of which appears stronger when quantified in more recent evolutionary time (c.f. results for genus- vs. species-level phylogenies in Figure 2.5 and Figure S2.6). The third evolutionary module we hypothesized ($K_s/|P_{50}|$) appears to be explained exclusively by separate trait responses to similar selective pressures, confirming previous results (Maherali et al. 2004). Therefore, a direct evolutionary trade-off between K_s and $|P_{50}|$ can be rejected based on available data, further indicating that K_s and $|P_{50}|$ cannot be determined by a single common anatomical feature (e.g., the size distribution of pores in the inter-conduit pit membranes) at the tissue level (Baas et al. 2004). I suggest that K_s and $|P_{50}|$ depend on several anatomical properties that may be coordinated under strong selective pressures, but do not necessarily co-evolve when pressures are relaxed over evolutionary timescales. Our results likely reflect the fact that some species may present strategies that do not rely on maximizing xylem conductivity or resistance to embolism, especially when water is not the most limiting resource and survival does not depend on fast resource use (Reich 2014). However, the detailed structural and physiological conditions allowing the independent evolution of these two traits remains to be elucidated.

Traits involved in the same evolutionary module are likely to be functionally, developmentally, or genetically integrated. Deep functional integrations over evolutionary timescales can be explained by the need to optimize HSM and K_I under a given environmental context, as the maintenance of positive safety margins and a sufficient hydraulic supply to leaves are likely to be closely linked to survival (Choat et al. 2018a) and under a strong stabilizing selection. Therefore, events of coordinated selection on the involved trait pairs described above might take place over evolutionary times in order to maintain HSM and K_I values close to the adaptive peak.

Integration might also be influenced by phylogenetic conservatism in underlying physiological processes and anatomical features. For example, conservatism in stomatal control (Brodribb and McAdam 2017) and leaf phenology (Davies et al. 2013) might explain the evolutionary covariation between $|P_{\min}|$ and $|P_{50}|$ beyond environmental forcing, with some lineages being able to avoid low water potentials by rapid stomatal closure (Martin-StPaul et al. 2017) or drought-deciduousness (Kolb and Davis 1994).

Finally, these functional and developmental integrations may be underpinned by genetic integration, specifically meaning that processes such as genetic correlation (Etterson and Shaw 2001), linkage disequilibrium and pleiotropy (Cheverud 1996) might be affecting the anatomical and structural determinants of the traits involved, leading to the observed evolutionary integration. As a result, the evolution of traits in the same module might be genetically constrained (Wagner 1996). Further work on the causes and consequences of the evolutionary integration of hydraulic traits, and the meaning of their conservatism through evolutionary time, will be crucial to characterize global trait syndromes and assess species adaptive potential under changing environmental conditions.

2.6 CONCLUSION

Diversity in species level hydraulic traits appear to be largely determined by deep-time evolutionary changes driven by adaptation to divergent environmental conditions, potentially limited by evolutionary constraints. I have found evidence for evolutionary integrations not explained by common environmental drivers, conforming to two hardwired evolutionary modules: the xylem resistance-exposure module ($|P_{\min}|/|P_{50}|$), which is highly conserved over evolutionary scales, and the conductivity-allocation module (Hv/K_s), which is more evident in recent evolutionary timescales. Results do not support a hardwired module describing the resistance-conductivity trade-off ($K_s/|P_{50}|$). The underlying mechanisms shaping these evolutionary modules and their role in species functional and evolutionary diversification remain to be elucidated. More phylogenetically explicit studies of individual clades (including intraspecific genetic, anatomical, and functional variation) under different environmental contexts will allow further characterization of plant trait syndromes as a network of integrated units that respond to natural selection.

3

A UNIFIED FRAMEWORK TO STUDY AND PREDICT FUNCTIONAL TRAIT SYNDROMES

*A unified framework to study and predict functional trait syndrome. Pablo Sanchez-Martinez,
David Ackerly, Maurizio Mencuccini, Jordi Martínez-Vilalta, Kyle G. Dexter and Todd Dawson.
Submitted to Methods in Ecology and Evolution.*

3.1 ABSTRACT

The evolution of traits does not happen in isolation but often as part of integrated trait syndromes, yet the relative contribution of environmental effects and evolutionary history on traits and their integration is not easy to resolve. In this chapter, I develop a methodological framework to elucidate eco-evolutionary patterns in functional trait syndromes. I do so by separating the amount of variance and covariance related to the phylogeny and environmental variables (***environmental phylogenetic conservatism***), only the phylogeny (***non-attributed phylogenetic conservatism***) and only to the environmental variable(s) (*evolutionarily labile environmental effects*). Variance-covariance structures are displayed as networks. Then, I use this framework to guide a newly derived imputation method based on machine learning models that predict trait values for unsampled taxa, considering environmental and phylogenetic information as well as trait covariances. *TrEvol* is presented as an R package providing a unified set of methodologies to study and predict multivariate trait patterns and improve our capacity to impute trait values. To illustrate its use, I use both simulated data and data on traits of woody angiosperm species related to hydraulics and the leaf economics spectrum. This conceptual framework can be employed to examine issues ranging from the evolution of trait adaptation at different phylogenetic resolutions to within-species trait variation.

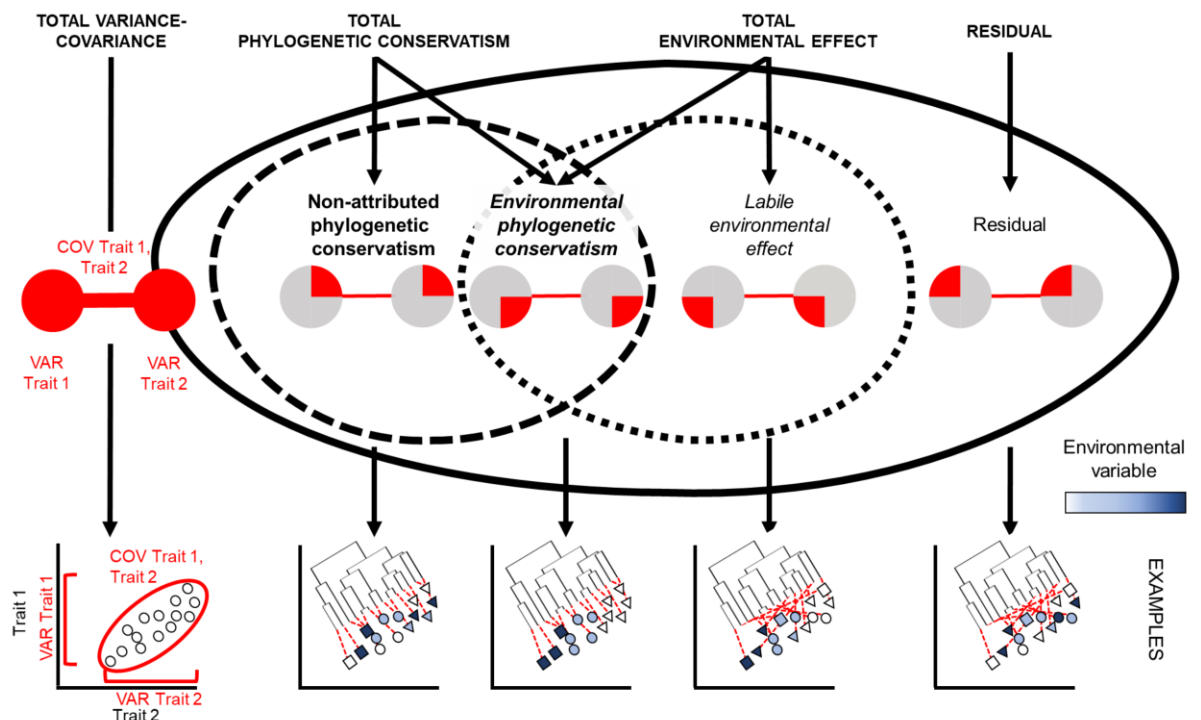
3.2 INTRODUCTION

Functional traits can be defined as morpho-physio-phenological attributes which impact fitness indirectly via their effects on individual performance (Violle et al. 2007). As such, they are likely to undergo adaptive evolution in response to environmental drivers (Ackerly et al. 2000). The functional significance of any one trait depends on coordination with others, creating functional strategies referred as trait syndromes that contribute to success under different environmental conditions (Reich et al. 2003, Wright et al. 2004, Sanchez-Martinez et al. 2020). Then, a trait syndrome is a combination of functional trait values that occur in a given taxonomic unit (e.g., a species) and that can be shared with others (e.g., group of species). Variability in functional strategies can lead to the conformation of trait modules (also referred as trait axes or trait spectra), which are groups of traits that covary potentially responding to environmental conditions and may be influenced by evolutionary legacies (Reich et al. 2003, Cavender-Bares et al. 2016). While the relationships among some functional traits (e.g., Wright et al. 2004, Mencuccini et al. 2019), their relationship with environmental variables (e.g., Bhaskar and Ackerly 2006, Flo et al. 2021) and trait phylogenetic conservatism (e.g., Ackerly 2009, Flores et al. 2014) have been widely studied, to my knowledge, a unified framework to study trait syndromes from an eco-evolutionary perspective is still lacking. I posit that a phylogenetically explicit framework describing the multivariate structure of traits and their relationship with environmental variables will improve our capacity to understand the ecological and evolutionary nature of trade-offs and coordination regulating trait syndromes. In turn, this framework may be used to predict plant functional trait values for unsampled taxa, which can help in determining vegetation responses to environmental changes (Choat et al. 2018b, Anderegg et al. 2021), particularly in the common situation where sparse trait data undermine the ability to make predictions in understudied locations or vegetation types (e.g., Trugman et al. 2020, García-Valdés et al. 2021).

Variation in environmental conditions underlies adaptive variation in trait syndromes (Reich et al. 2003). This adaptive variation can be phylogenetically conserved, describing a pattern of phylogenetic niche conservatism, which arises when ecological opportunities are occupied by species that are already adapted to similar conditions (Losos 2008). As a result, adaptive evolutionary change may be limited over short evolutionary timescales leading to closely related species retaining similar functional and ecological characteristics that are highly constrained by common ancestry. I refer to this pattern as the *environmental phylogenetic conservatism* of a given trait or trait syndrome in response to one or more environmental axis related to species ecological niche. In contrast, environmental variation can be related to functional traits and their covariation in a phylogenetically independent manner, describing a scenario where closely related species are not constrained to occupy similar environmental spaces and functional strategies (Ackerly 2009). I refer to this pattern as *evolutionarily labile environmental effect* of one or more environmental axis of the ecological niche on trait syndromes.

A pattern of phylogenetic conservatism in trait variation and covariation can also appear as a product of evolutionary constraints that are un-related to environmental variables. These potentially non-adaptive processes can lead to a slow and constrained evolution as a result of genetic correlation, linkage disequilibrium, pleiotropy, lack of genetic variability or homogenizing gene flow, among others (Ackerly 2009). This conservatism may also be related to lineage-specific biophysical constraints on trait values or unmeasured environmental axes, although one would generally aim to include the environmental variables that are expected to be relevant to the traits under study. Therefore, I suggest referring to this conservatism in the data that is not related to a given set of measured environmental effects of interest as *non-attributed phylogenetic conservatism* (in relation to one or more environmental axes) (Figure 3.1).

Figure 3.1 Traits' variance-covariance conceptual framework Variance and covariance partition into the different components related to **non-attributed phylogenetic conservatism**, **environmental phylogenetic conservatism**, *labile environmental effects* and residual. Note how **non-attributed phylogenetic conservatism** and **environmental phylogenetic conservatism** sum to TOTAL PHYLOGENETIC CONSERVATISM and **environmental phylogenetic conservatism** and *labile environmental effect* sum to TOTAL ENVIRONMENTAL EFFECT. Examples representing two traits in each case are presented as networks (showing variance results as pie charts in nodes and covariance as edges). At the bottom, examples for different traits showing extreme cases maximizing each one of the components are shown as scatterplots, representing two different hypothetical traits in each case and the phylogeny relating different points, showing the phylogenetic group for each terminal taxon value (different shapes for different major lineages) and an environmental variable as the filling colour. We can see how in the **non-attributed phylogenetic conservatism** scenario only the phylogeny is related to variance and covariance patterns; in the **environmental phylogenetic conservatism** one, both the phylogeny and the environmental variable are related to the variance and covariance patterns and in the *labile environmental effect* one, only the environmental gradient is related to the variance and covariance patterns.



A better knowledge on functional trait relationships and their drivers can improve predictive power to infer unmeasured trait values. Previous methodologies allow one to predict missing values by using phylogenetic information (Swenson 2014) and statistical covariation among traits and environmental variables (Poyatos et al. 2018b). However, in some cases, traits and their relationship are highly phylogenetically conserved, such that phylogeny is highly informative in predicting missing values, while in other cases traits present a more labile relationship in response to environmental variables, and these variables are better predictors of missing functional trait values. In addition, the organization of traits in modules (i.e., groups of tightly related traits) indicates that not all traits are equally informative for inferring the values of other traits. In this chapter, I propose an imputation method that implements a data-driven procedure to select which predictors to include in each case, based on trait covariation and relationships with phylogeny and environmental data.

The methodology described here uses phylogenetic mixed models to separate the contribution of *environmental phylogenetic conservatism*, **non-attributed phylogenetic conservatism**, and *labile environmental effect* to trait variances and covariances, helping to elucidate their relative importance in shaping patterns in comparative data. Then, this methodology is used to optimize the use of available data in a newly derived machine learning algorithm that predicts missing values for functional traits, and which I compare with alternative imputation methods. The reliability of this framework is first tested using simulated data, and it is then applied to a real dataset hydraulic and leaf economics spectrum (LES) traits (Wright et al. 2004) covering woody angiosperm species. The methodology presented here is implemented in an accompanying R package named *TrEvol* (from Traits Evolution).

3.3 MATERIALS AND METHODS

The proposed method consists of two separate elements. The first one consists of characterizing variance-covariance structures of pairs of traits by elucidating their association with environmental factors as well as their phylogenetic structure. I represent these results as trait networks to describe the partition of trait variance-covariance structures for a given set of traits, differentiating *environmental phylogenetic conservatism*, *non-attributed phylogenetic conservatism*, and *labile environmental effects*. Then, network metrics can be calculated for each case, which can prove helpful to efficiently elucidate the multivariate nature of evolutionary patterns in trait syndromes. The second component consists of an imputation algorithm which uses the previously described variance-covariance structures to make the most accurate prediction of missing values using available information on the phylogeny, the environment and traits.

3.3.1 Trait Variance-covariance partition

I developed a framework to estimate trait variance-covariance related to a set of measured environmental variable(s) and to the phylogeny so that the individual contribution of these elements (i.e., *labile environmental effect* and **non-attributed phylogenetic conservatism**, respectively) as well as their combined contribution (*environmental phylogenetic conservatism*) can be calculated. To do so, I used multi-response phylogenetic mixed models implemented in the *MCMCglmm* R package (Hadfield 2010b). For a given list of traits, the *computeVarianceCovariancePartition* function selects all pairwise combinations between traits and a single given environmental variable and builds models including them as response variables (i.e., tri-response models, two traits and one environmental component). When more than two traits are included, the function iterates and does all possible pairwise combinations between different traits. For each trait-trait-environmental variable combination, the model

estimates the amount of phylogenetically dependent (u) and phylogenetically independent (e) variances and covariances. Given two traits (T1 and T2) and a continuous environmental variable (E), the model structure is the following:

$$(T1, T2, E) \sim u + e$$

From this model, the following two variance-covariance matrices are estimated:

Matrix u (phylogenetically dependent)	T1	T2	E
	T1	VAR_u^{T1}	$COV_u^{T1,T2}$
	T2	VAR_u^{T2}	$COV_u^{T2,E}$
	E		VAR_u^E
Matrix e (phylogenetically independent)	T1	T2	E
	T1	VAR_e^{T1}	$COV_e^{T1,T2}$
	T2	VAR_e^{T2}	$COV_e^{T2,E}$
	E		VAR_e^E

The elements of these matrices are used to calculate the environmental phylogenetic variance ($VAR_{env,phylo}$), the non-attributed phylogenetic variance (VAR_{phylo}), the labile environmental variance (VAR_{env}) and the residual variance (VAR_{res}). Then, these variance components can be aggregated to calculate **Total Phylogenetic Variance** (VAR_{total_phylo}), **Total Environmental Variance** (VAR_{total_env}) and **Total Variance** (VAR_{total}) for a given trait (e.g., T1), as follows (in bold, aggregation of variance estimates):

1. $VAR_{env,phylo}^{T1} = \left[\frac{COV_u^{T1,E}}{VAR_u^E} \right]^2 VAR_u^E$
2. $VAR_{phylo}^{T1} = VAR_u^{T1} - VAR_{env,phylo}^{T1}$
3. $VAR_{env}^{T1} = \left[\frac{COV_e^{T1,E}}{VAR_e^E} \right]^2 VAR_e^E$
4. $VAR_{res}^{T1} = VAR_e^{T1} - VAR_{env}^{T1}$
5. $VAR_{total_phylo}^{T1} = VAR_{phylo}^{T1} + VAR_{env,phylo}^{T1}$
6. $VAR_{total_env}^{T1} = VAR_{env}^{T1} + VAR_{env,phylo}^{T1}$

$$7. \mathbf{VAR}_{total}^{T1} = \mathbf{VAR}_u^{T1} + \mathbf{VAR}_e^{T1} = \mathbf{VAR}_{total_env}^{T1} + \mathbf{VAR}_{phylo}^{T1} + \mathbf{VAR}_{res}^{T1}$$

The same applies to trait 2. Similarly, elements of the two matrices were used to calculate environmental phylogenetic covariance ($COV_{env,phylo}$), non-attributed phylogenetic covariance (COV_{phylo}), labile environmental covariance (COV_{env}), and residual covariance (COV_{res}) between all pairwise combinations of traits. Then these covariance components can be aggregated to calculate **Total Phylogenetic Covariance** (COV_{total_phylo}), **Total Environmental Covariance** (COV_{total_env}) and **Total Covariance** (COV_{total}) for a given pair of traits (e.g., T1 and T2), as follows (in bold, aggregation of variance estimates):

$$8. COV_{env,phylo}^{T1,T2} = \frac{COV_u^{T1,E} COV_u^{T2,E}}{VAR_u^E}$$

$$9. COV_{phylo}^{T1,T2} = COV_u^{T1,T2} - COV_{env,phylo}^{T1,T2}$$

$$10. COV_{env}^{T1,T2} = \frac{COV_e^{T1,E} COV_e^{T2,E}}{VAR_e^E}$$

$$11. COV_{res}^{T1,T2} = COV_e^{T1,T2} - COV_{env}^{T1,T2}$$

$$12. \mathbf{COV}_{total_phylo}^{T1,T2} = \mathbf{COV}_{phylo}^{T1,T2} + \mathbf{COV}_{env,phylo}^{T1,T2}$$

$$13. \mathbf{COV}_{total_env}^{T1,T2} = \mathbf{COV}_{env,phylo}^{T1,T2} + \mathbf{COV}_{env}^{T1,T2}$$

$$14. \mathbf{COV}_{total}^{T1,T2} = \mathbf{COV}_u^{T1,T2} + \mathbf{COV}_e^{T1,T2} = \mathbf{COV}_{total_env}^{T1,T2} + \mathbf{COV}_{phylo}^{T1,T2} + \mathbf{COV}_{res}^{T1,T2}$$

When no environmental effect is specified, the function calculates Total Variance and Covariance and Total Phylogenetic Variance and Covariance, the difference being the Total non-phylogenetic Variance and Covariance. The function allows for representation of variances and covariances in absolute or relative terms. When *showRelativeResults* = TRUE (which is the default), the proportion of explained variance from the total variance is reported and covariation is reported as correlations:

$$Corr = \frac{COV^{T1,T2}}{\sqrt{VAR^{T1} * VAR^{T2}}}$$

The function retrieves a list containing a table with the variance results and a table with the covariance results jointly with individual model outputs. As *MCMCglmm* uses a Bayesian framework, values shown in the tables are means of posterior distributions of estimates. The list also contains posterior distributions for each estimate from which convergence, effective sample sizes and autocorrelation can be elucidated. From these posterior distributions, p-values corresponding to the probability of the credible intervals to contain 0 are calculated using the *bayestestR* package (Makowski et al. 2019). The *TrEvol* package also includes an alternative methodology that allows for consideration of more than one environmental variable at the same time and also can account for non-continuous environmental variables by means of the *computeVariancePartition* and the *computeCovariancePartition* functions, for variance and covariance, respectively (see supplementary methods).

These three functions to compute variance and covariance partitions share the same input structure. Inputs needed are:

- *traits*: character vector containing the names of the traits to be considered.
- *environmental.variables*: character vector containing the names of the continuous environmental variables to be considered (if using the alternative methodology, it can be of length > 1 and does not need to be continuous; see supplementary methods in 8.2.2). These variables need to be in the dataset.
- *dataset*: data frame containing traits, environmental variables, and taxon names (e.g., species or genus names).
- *phylogeny*: *phylo* object containing species present in the dataset. The function matches internally the dataset with the phylogeny, so it allows missing values in the data frame and some species present or absent in the phylogeny. The

function will use complete cases for each pair of traits, so only data with complete phylogenetic and environmental observations will be used.

3.3.2 Networks

To optimize the representation of the multivariate structure, variance-covariance structures can be plotted as networks by the function *plotNetworks* included in the *TrEvol* package, which shows trait explained variance (i.e., variance related to the environment, phylogeny or their combination) in each case as pie charts and correlations as edges for each one of the pairs of traits included. A given network represents the structure related to ***environmental phylogenetic conservatism***, ***non-attributed phylogenetic conservatism*** or *labile environmental effect*.

The function also calculates and displays network metrics described in (He et al. 2020a) and performed by the *igraph* R package (Csardi and Nepusz 2006). These measures are the number of modules (NM) showing how many independent groups of intercorrelated traits exist; edge density (ED) describing the proportion of actual connections among nodes out of all possible connections; maximum absolute correlation ($|r|_{\max}$) and mean absolute correlation ($|r|_{\text{mean}}$). In this framework, NM represents the number of trait modules, high ED represents high coordination between all traits and high $|r|_{\max}$ and $|r|_{\text{mean}}$ represent networks with a higher dependence among related traits. At the node level, degree (i.e., number of connections per node) can be also calculated and displayed as node size when the argument *displayDegreeAsNodeSize* is set to TRUE, which is the default. Traits with a higher degree (i.e., higher node size in the visualisation) are considered hubs.

3.3.3 Imputation algorithm

The package presented here includes an imputation algorithm performed by the function *imputeTraits* which uses the previously described variance-covariance structures to guide the trait imputation process. Inputs needed are:

- *dataset*: a data frame containing traits with missing values and optionally environmental factors for a set of terminal taxa. The dataset must contain a column named “taxon” which indicates the name of the taxon (e.g., species names). Note that more than one observation per taxon can be included (intra-taxon variability).
- *Phylogeny*: a “phylo” object including all terminal taxa present in the dataset (or a tree representing populations genetic structure variability at the intraspecific level).
- *imputationVariables*: character vector indicating the name of the variables to be imputed as they appear in the dataset.
- *predictors*: character vector indicating the list of environmental factors included in the dataset (without missing values) that may be considered as potential predictors (see below).

Phylogenetic information is included as predictors by calculating phylogenetic coordinates for each terminal taxon. To calculate phylogenetic coordinates, the algorithm first calculates the phylogenetic distance matrix by means of the *cophenetic.phylo* function and then calculates principal coordinates by means of the *pcoa* function, both from the *ape* package (Paradis and Schliep 2019). Phylogenetic coordinates are stored internally so the algorithm does not need to calculate them each time that it is run for a given dataset, which can be time consuming specially for big datasets. However, it will recalculate them if the argument *forceRun* is set to “TRUE”. All principal coordinates

explaining more than one per cent of the variance are subsequently considered as predictors (see below). However, users can also control the number of phylogenetic coordinates to be considered as predictors by using the *numberOfPhyloCoordinates* argument (which must be lower than the number of phylogenetic axes explaining more than one per cent of the variance). Note that all terminal taxa present in the input dataset need to be also present in the phylogeny.

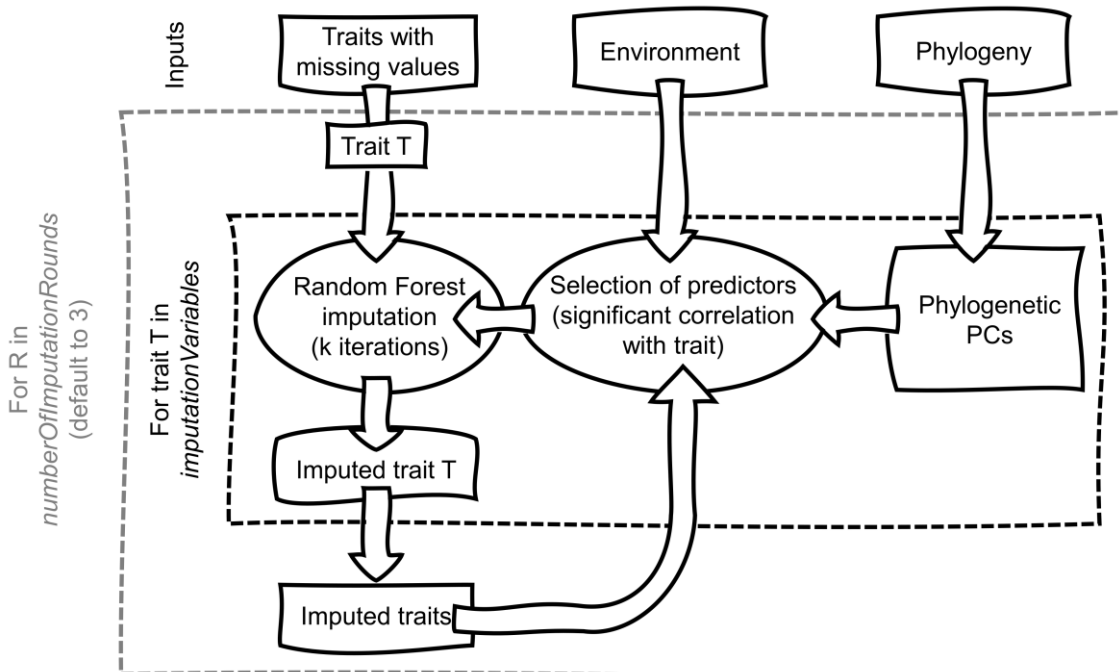
The algorithm included in the *imputeTraits* function uses trait relationship as well as the phylogenetic structure and, optionally, environmental factors to predict missing values by performing three chained imputation rounds. In the first round, individual trait missing values are predicted by using complete data on environmental variables and phylogeny as predictors when they are informative (i.e., when they present statistically significant relationship with trait variance). In the second round, individual trait missing values are predicted using environmental variables, phylogeny, and other traits (including values imputed in the first round) as predictors when they are informative. In the third round, individual trait missing values are predicted using environmental variables, phylogeny and other traits (imputed in the second round) as predictors when they are informative (Figure 3.2). Preliminary analyses showed that imputation performance improved in some cases if a third round of imputation was performed, and it was thus implemented. To elucidate which variables are informative and thus included as predictors in each case, *computeVarianceCovariancePartition* function is computed internally to calculate phylogenetic and environmental effects for each trait as well as the covariance between the traits to be imputed. Users can also include the results of the *computeVarianceCovariancePartition* manually using the *varianceResults* and the *covarianceResults* arguments.

In each imputation round, imputation of trait missing values is performed for each one of the traits of interest. Each imputation model is iterated several times (controlled by the *numberOfIterations* argument, set to 10 by default). From each imputation round, an imputed matrix is obtained by calculating the mean for all

iterations for each predicted value. Standard deviations of predicted values and individual model results are also reported.

The algorithm uses random forests models to predict missing values by means of the *randomForest* function of the *randomForest* R package (Liaw and Wiener 2002). These models calculate out of bag errors (OOB), which are supplied also as a measure of imputation error reported as the normalized root mean square error (NRMSE). Moreover, the developed algorithm calculates cross validation R^2 values by randomly creating NAs in the traits to be imputed, predicting values, and then comparing predictions with observed values. The proportion of NAs that are randomly created to calculate cross validation R^2 is controlled by the *prodNAS* argument of the function (between 0 and 1, set to zero by default). When *prodNAS* = 0, cross validation R^2 is not calculated. Parallel processing is enabled in the function, when the *parallelization* argument is set to “TRUE”, which is the default. The parallelization method is based on previous implementations of random forests in R programming (Stekhoven and Bühlmann 2012), so users can set the number of clusters that they want to use in the *clustersNumber* argument, set to two by default.

Figure 3.2 Imputation algorithm scheme



3.3.4 Application

To test the methodology, I first applied it to 10 simulated traits, each one with 100 observations (simulated species) with a known variance-covariance structure (Figure 3.3, Table S3.1). I also simulated a pure-birth stochastic phylogeny using the *pbtree* function of the *phytools* package (Revell 2012) for the 100 simulated species. Five traits were simulated to present a phylogenetic component in their variance-covariance structure by means of *simulate_bm_model* function of the R package *castor* (Louca and Doebeli 2018) including the simulated phylogeny and the variance-covariance matrix (Table S3.1) as the diffusion matrix. The remaining five traits were simulated using the same variance-covariance matrix (Table S3.1) to present a variance-covariance structure not-explicitly related to the phylogeny by using the function *rnorm_multi* of the R package *faux* (DeBruine Lisa 2021).

Traits conformed to four trait modules (i.e., traits presenting correlation among them but not with others). The first correlation module (*M1*) was constituted by *Phylo Trait 1*, *Phylo Trait 2*, the variance-covariance structure of which was expected to be related to the phylogeny and to the simulated environmental variable *Phylo Env* (i.e., **environmental phylogenetic conservatism due to Phylo Env**). The second correlation module (*M2*) was constituted by *Phylo Trait 3* and *Phylo Trait 4*, whose variance-covariance was also expected to be related to the phylogeny but not to traits in *M1* nor to the environmental variable *Phylo Env* (i.e., **non-attributed phylogenetic conservatism** given *Phylo Env*). The third correlation module (*M3*) was constituted by *Non Phylo Trait 1*, *Non Phylo Trait 2*, whose variance-covariance was not expected to be related to the phylogeny but was expected to be related to *Non Phylo Env* (i.e., *labile environmental effect*). The fourth correlation module (*M4*) was constituted by *Non Phylo Trait 3* and *Non Phylo Trait 4*, whose variance-covariance was also not expected to be related to the phylogeny nor to the previously presented environmental variables (i.e., expected to be detected as residual variances and covariance) (Figure 3.3). Note that “*Env*” variables were considered as environmental effects but the procedure to obtain

them was not different from the one implemented with the rest of the simulated variables. The expectations for results were summarized *a priori* (Table S3.2, Figure 3.3). Trait simulations were performed by using the *simulateDataSet* function of the R package presented here, which by default produces the simulated data used in this study.

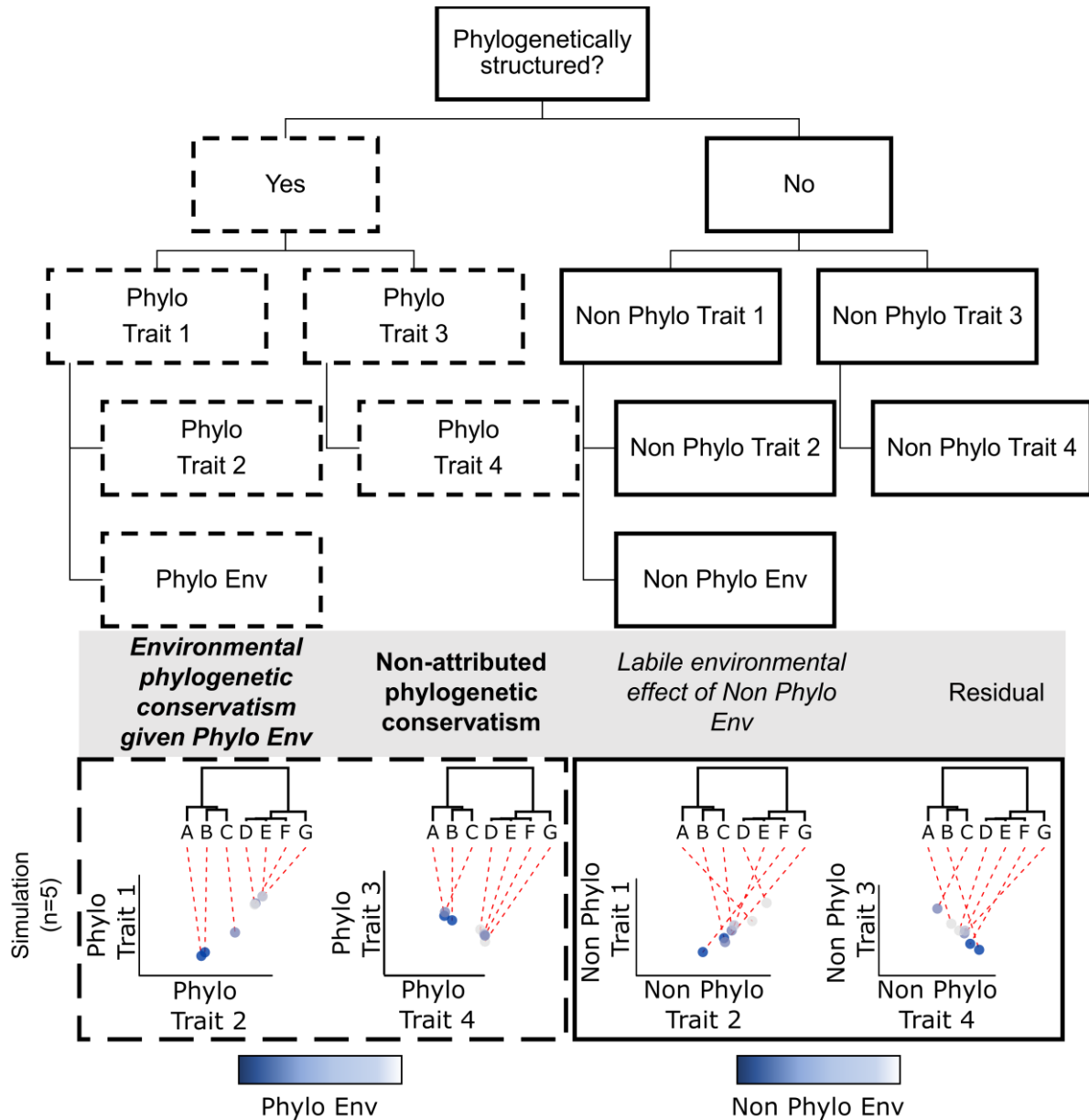


Figure 3.3 Simulated data structure Scheme representing the expected relationships between simulated traits linking it to the presence or absence of phylogenetic structure. Scatterplot for simulated traits for 5 species following the simulation structure described in the text is also shown, coloured by the simulated environmental variable of interest in each case.

Next, I applied the methodology to real data on woody-plant species functional traits related to hydraulic function and the leaf economics spectrum. I used data covering seven leaf traits for woody plant angiosperms coming from a previously published dataset (Mencuccini et al. 2019b). Functional traits included were specific leaf area ($\text{cm}^2 \text{g}^{-1}$, SLA, number of species = 1,183), leaf nitrogen (mg g^{-1} , number of species = 930), maximum photosynthetic rate per area as a measure of photosynthetic capacity ($\text{micromole CO}_2 \text{ m}^{-2} \text{ s}^{-1}$, A_{area} , number of species = 206), leaf lifespan (months, LL, Number of species = 198), midday leaf xylem tension as a measure of drought exposure (Martínez-Vilalta et al. 2021) (MPa, $|P_{\text{min}}|$, number of species = 636), xylem tension at the turgor loss point as a measure of drought tolerance (Delzon 2015) (MPa, $|P_{\text{tlp}}|$, number of species = 556) and leaf-specific maximum hydraulic conductivity as a measure of hydraulic sufficiency ($\text{Kg m}^{-1} \text{MPa}^{-1} \text{s}^{-1}$, K_i , number of species = 878). To test for the effects of one potential selective pressure on trait phylogenetic patterns I considered the aridity index (AI), obtained from CGIAR (Trabucco and Zomer 2018) in a previously published analyses (Sanchez-Martinez et al. 2020). Note that low values of AI represent regions with low water availability and high atmospheric water demand. All variables were transformed by calculating the natural logarithm of absolute values, as it improved their normality.

As a unique predictor was considered (AI), results are reported by the *computeVarianceCovariancePartition* function described in the main text. Total correlation networks and partitioned traits networks for simulated data and for LES traits were obtained. Then, the imputation method was implemented both for simulated and for LES traits, considering environmental effects described in each case as potential predictors as well as the phylogeny. In the real data case, a species level phylogeny was built using the *V.PhyloMaker* R package (Qian and Jin 2016). The rest of the arguments of the function *imputeTraits* were maintained as default.

To compare results obtained by *imputeTraits* with existing imputation methodologies, we performed a cross validation procedure by using 80-20% and 50-

50% (Figure S3.2) of the data to test and train, respectively, for each one of the methodologies, including *imputeTraits*. These methodologies include mean imputation (i.e., mean for each one of the traits to be taken as imputed values); *MICE* imputation (van Buuren and Groothuis-Oudshoorn 2011), which uses the covariation of multiple traits to be imputed as well as other complete environmental variables to predict missing values; and a phylogenetic imputation by means of the *phylopars* R package, which uses trait phylogenetic variance-covariance to predict missing values (Goolsby et al. 2017). Thus, predictive performance results reported are not the ones reported internally by the *imputeTraits* function but calculated outside the algorithm in order to use the same cross validation data for all the imputation methods compared. The cross-validation process was iterated ten times in each case.

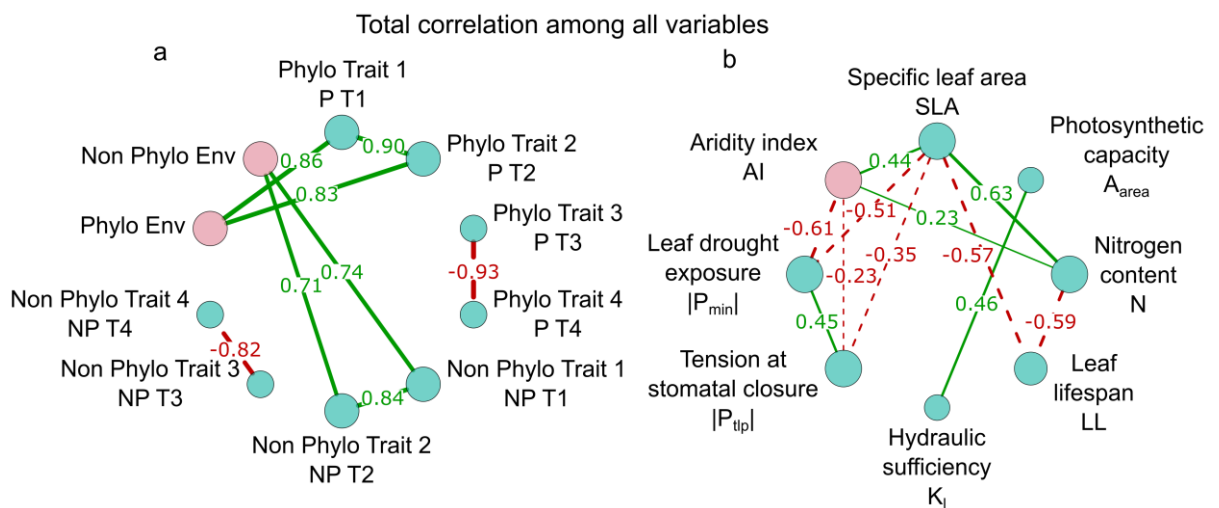


Figure 3.4 Total correlation among variables a) Total correlation among simulated variables and b) total correlation among plant functional traits. Pink represents environmental variables and blue represent traits.

3.4 RESULTS

3.4.1 Variance covariance partition results

Results obtained by applying the described methodology for a set of simulated traits matched those expected given the variance-covariance matrix used to simulate data, detecting the four hypothesized modules (Table S3.1 and Figure 3.3, Figure 3.4a). The methodology successfully detected the amount of variance and covariance related to the phylogenetic structure of the data, as is the case for the covariance between *Phylo Trait 1* and *Phylo Trait 2*, between *Phylo Trait 3* and *Phylo Trait 4* and their variances (edges and pie charts in Figure 3.5 and 3.6). Moreover, it successfully detected the independence between these two modules of phylogenetically correlated traits. The methodology also successfully separated the variance and covariance that is uniquely attributed to shared evolutionary heritage (**non-attributed phylogenetic conservatism**) from **environmental phylogenetic conservatism** due to *Phylo Env* (Figure 3.5 b and c). Finally, the methodology successfully detected the *labile environmental effect* (i.e., phylogenetically independent effect) of *Non Phylo Env* on variances of *Non Phylo Trait 1* and *Non Phylo Trait 2* traits as well as on their covariance (Figure 3.6 d), while the correlations not related to the phylogenetic structure nor to the given environmental variables were placed within the unexplained or residual component of the covariance (Figure 3.5 e and 3.6 e). Networks presenting a higher contribution to the covariation pattern had higher edge density (ED); those presenting a strong relationship between connected nodes showed a high maximum absolute correlation ($|r|_{\max}$) and mean absolute correlation ($|r|_{\text{mean}}$) and the number of modules related to each one of the components was also successfully detected by the methodology (NM) (Figure 3.5 and 3.6).

When applied to the dataset of traits of woody angiosperms species, I found that leaf economics traits and leaf hydraulic traits conformed to two main modules (Figure

3.7a), that trait variances and covariances were mainly phylogenetically conserved and that this conservatism was partially due to aridity (Figure 3.4b, Figure 3.7b, c, d and e). The first module relates the leaf resource uptake and use strategies (i.e., leaf economics) with drought exposure (quantified as the absolute value of the minimum water potential measured in the xylem, $|P_{\min}|$) and tolerance (quantified as the absolute value of the water potential at stomatal turgor loss point, $|P_{\text{tp}}|$). This module represents variation in an axis describing acquisitive leaves with low drought exposure-tolerance to leaves with conservative resource uptake and use with high drought exposure and tolerance (specific leaf area is positively related to nitrogen content, negatively related to leaf lifespan and negatively related to drought exposure and tolerance). This module presents phylogenetic conservatism and part of this conservatism is due to aridity, which is specially related to correlations involving drought exposure and tolerance (Figure 3.7c). Contrarily, most of the phylogenetic conservatism in leaf economic traits and their relationship (specific leaf area, nitrogen content and leaf lifespan) is not attributed to aridity (Figure 3.7b). The second module relates hydraulic sufficiency with photosynthetic capacity (higher maximum hydraulic conductivity related to higher photosynthetic capacity). This module showed phylogenetic conservatism which was not attributed to aridity (Figure 3.7b).

The two modules described showed to be integrated in response to aridity (Figure 3.7c). More concretely, specific leaf area showed to be positively related to hydraulic sufficiency and negatively related to photosynthetic capacity and drought exposure showed to be negatively related to hydraulic sufficiency. Then, the integration between these two modules is mediated by specific leaf area and xylem drought exposure, which show a high degree (number of connections presented by a node) and function as hubs of plant functional trait syndromes in woody angiosperm species. These correlations are related to aridity in a phylogenetically structured manner, describing a pattern of *environmental phylogenetic conservatism* due to aridity in the integration between plant hydraulics and leaf economics.

Trait networks supported the predominant pattern of phylogenetic conservatism in functional traits of woody angiosperm species. Networks representing **non-attributed phylogenetic conservatism** and *environmental phylogenetic conservatism* due to aridity showed higher values of edge density (ED), maximum absolute correlation ($|r|_{\max}$) and mean absolute correlation ($|r|_{\text{mean}}$) compared to the labile environmental effect of aridity. The number of modules proved to be useful to detect the number of independent groups of correlated traits, showing the integration of the two modules in response to aridity (Figure 3.7c). The higher ED in the phylogenetic part of trait relationships indicates that most of trait correlations are phylogenetically conserved. The higher $|r|_{\max}$ and $|r|_{\text{mean}}$ in these networks indicates that phylogenetically conserved relationships are stronger (Figure 3.7b and c).

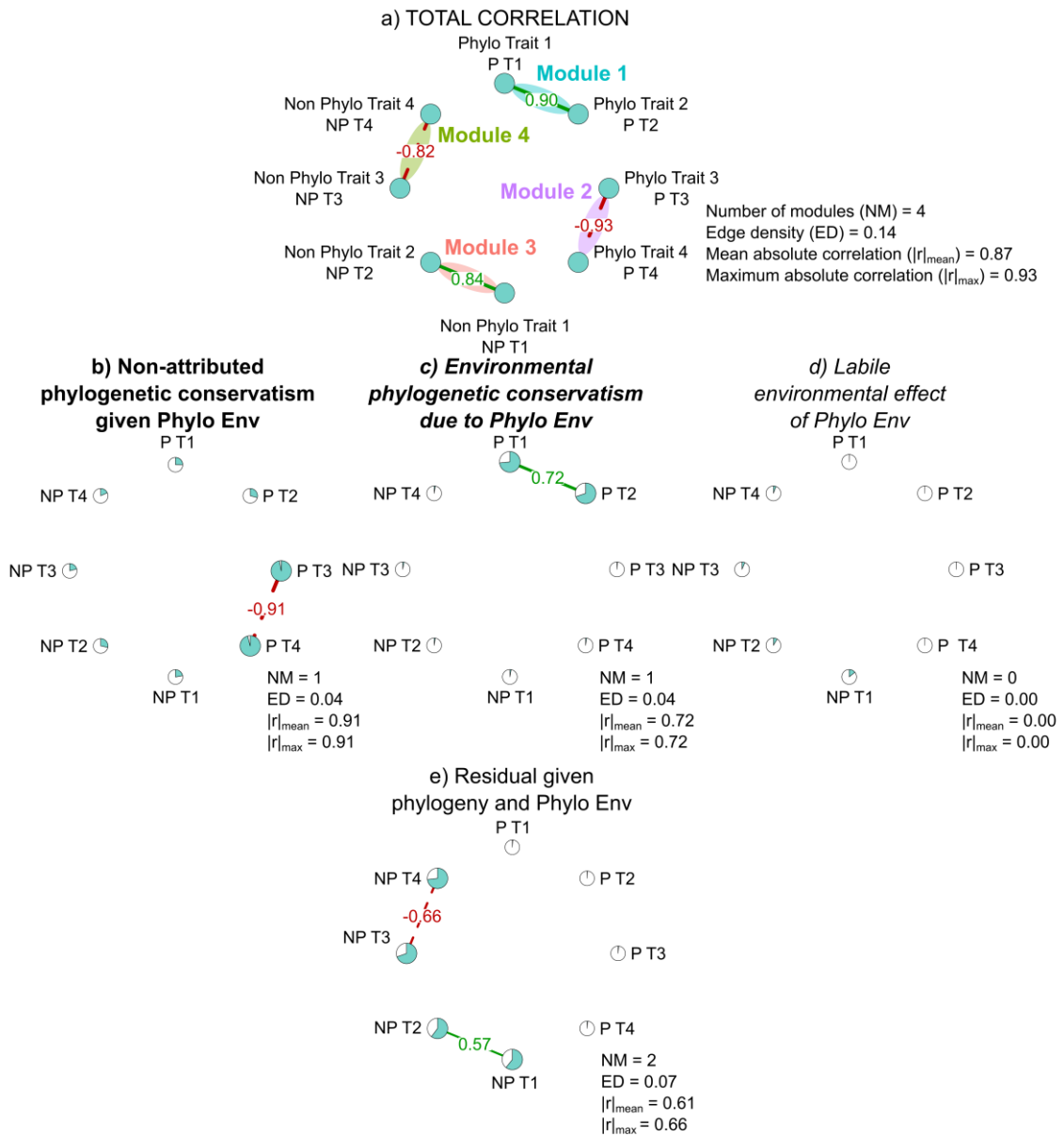
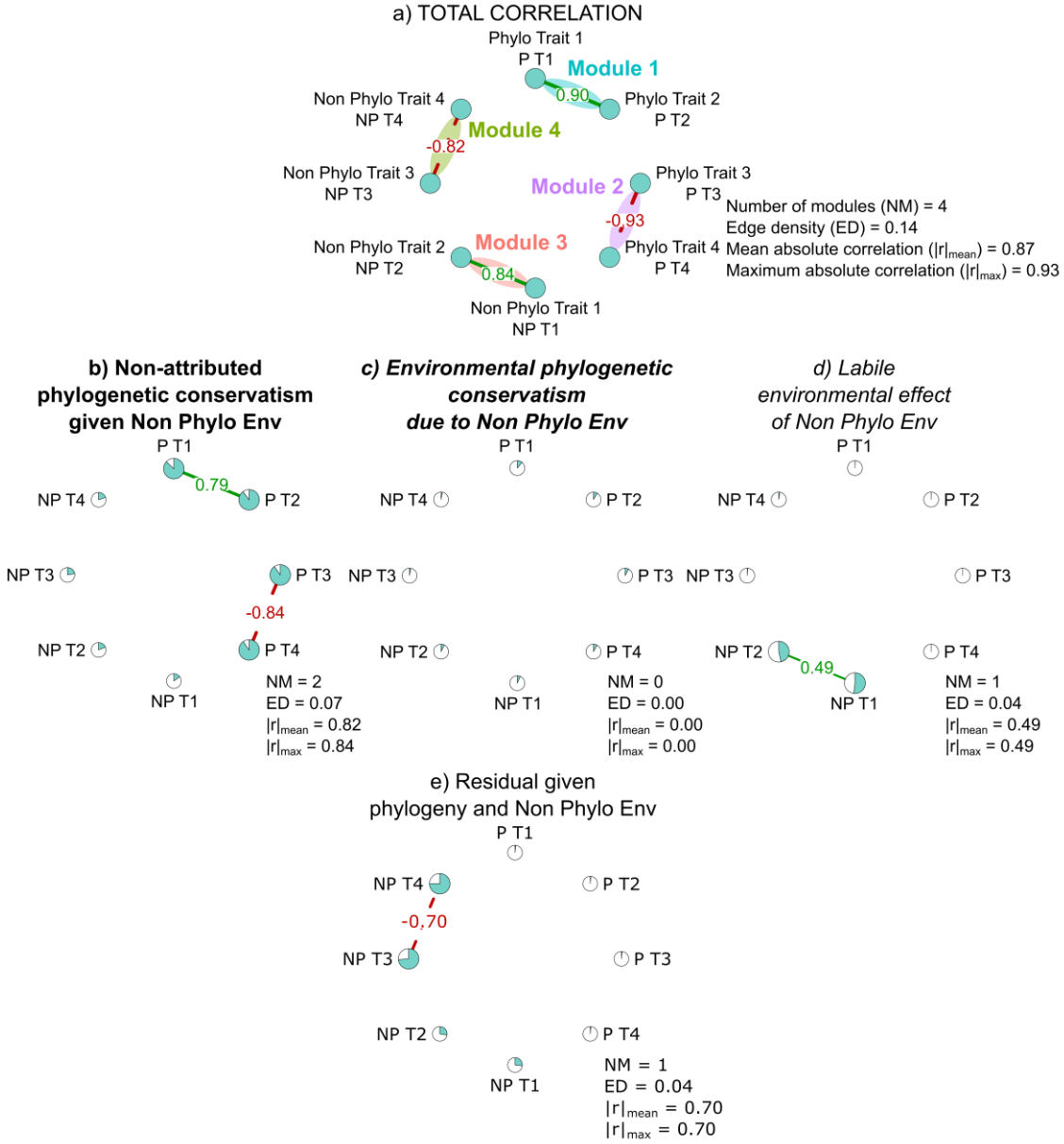


Figure 3.5 and 3.6 Simulated trait networks Simulated data networks considering phylogenetically conserved and independent environmental variables (*Phylo Env* and *Non Phylo Env*). Pie charts represent the variance and edges represent the covariance related to each one the components (**non-attributed phylogenetic conservatism**, **environmental phylogenetic conservatism**, *labile environmental effect* and residual). Green-solid edges represent positive correlations and red-dashed ones negative correlations with a width proportional to the correlation coefficient. Node size is proportional to node degree (number of connections). Network metrics are also shown in each case.



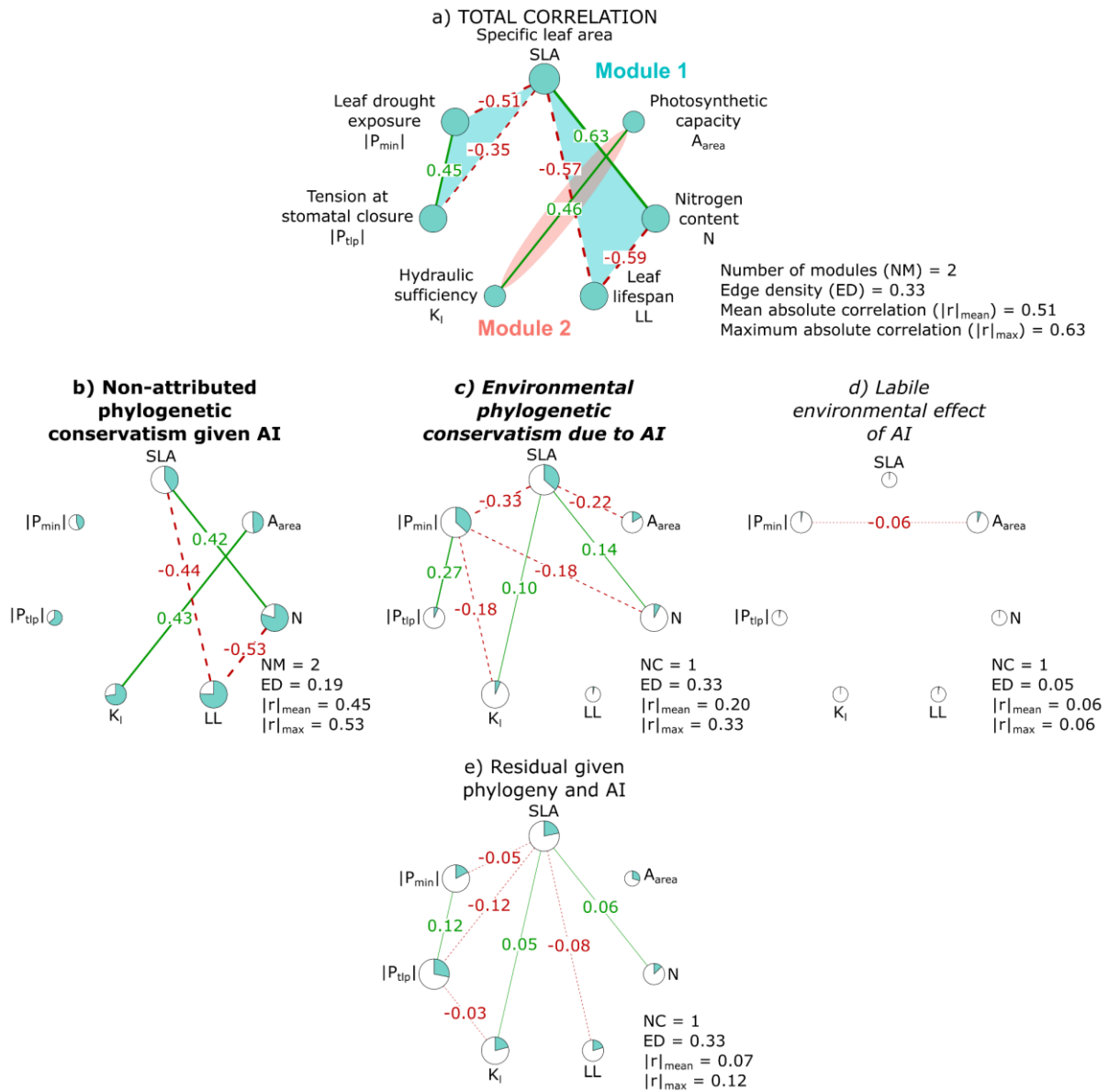


Figure 3.7 Plant functional trait networks Trait networks considering aridity (aridity index, AI) as the environmental variable of interest. Pie charts represent the proportion of the variance for each variable related to each one of the components (**non-attributed phylogenetic conservatism**, **environmental phylogenetic conservatism**, *labile environmental effect* and residual) and edges represent the covariance related to each one of these components shown as correlations (green-solid lines represent positive correlations and red-dashed line represent negative correlations with a width proportional to the correlation coefficient). Node size is proportional to node degree (number of connections). Network metrics are also shown.

3.4.2 Imputation results

The predictive performance of the presented imputation algorithm improved when informative imputed traits were considered as shown by the higher cross-validation R^2 and lower cross-validation NRMSE of the second and third imputation rounds compared to results obtained using only phylogenetic and environmental data (first round) (Figure S3.1). The *imputeTraits* algorithm outperformed previously described imputation procedures in the case of the mean imputation and the *MICE* imputation using all environmental and traits covariation and performed similarly to *phylopars* imputation using all environmental and traits phylogenetic covariation when traits show phylogenetic structure. The new algorithm outperformed *phylopars* approach when the correlation among simulated data was not phylogenetically structured and when applied to real data (Figure 3.7). Thus, across all simulation scenarios, the new algorithm proposed here was the most effective, especially when imputing real data.

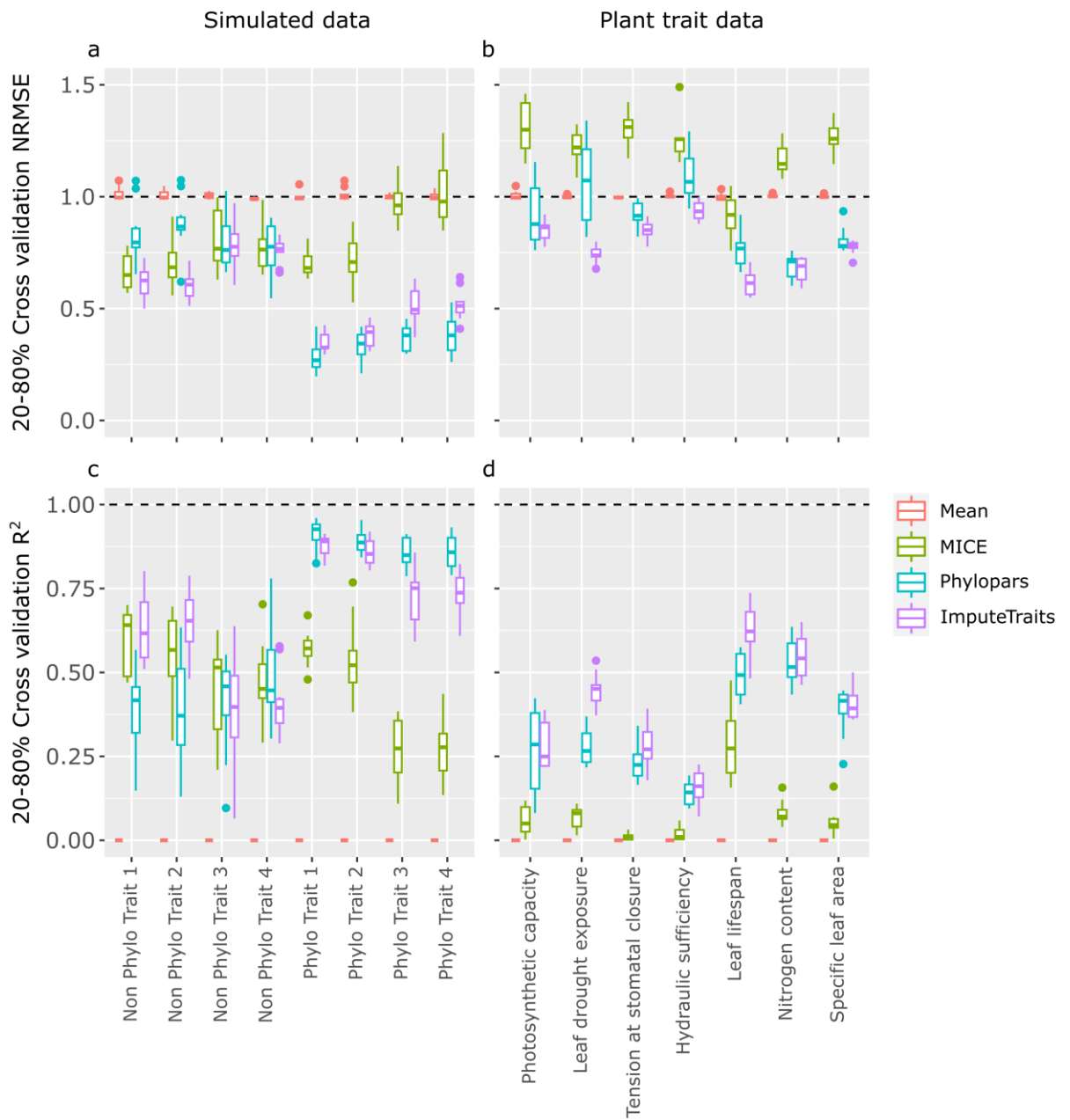


Figure 3.7 Imputation performance Predictive performance of the imputation framework. Results for mean imputation (red), *MICE* imputation (blue), *phylopars* imputation (green) and *imputeTraits* imputation (purple) are shown. a) and b) show normalized root mean square error (NRMSE) for simulated and leaf traits, respectively. b) and d) show R² for simulated and leaf traits, respectively. NRMSE and R² were calculated from a cross validation procedure using 80% of the data to train models and 20% to test.

3.5 DISCUSSION

3.5.1 A new framework to study functional syndromes evolution

In this chapter, I developed a new methodological framework to study eco-evolutionary patterns in multiple functional traits. This methodology allows to separate variances and covariances related to the phylogeny from those that are phylogenetically independent, complementing previous methods such as phylogenetic independent contrasts and phylogenetic least squares, which allowed to control by the phylogenetic structure when analysing trait relationships (Felsenstein 1988, Blomberg 2016). By using this methodology, evolutionary patterns can be elucidated not only from phylogenetically independent contrasts results as done in previous studies (e.g., Ackerly and Reich 1999, Maherali et al. 2004, Zheng et al. 2019), but also from the phylogenetically conserved component of evolutionary relationships (Sanchez-Martinez et al. 2020). Furthermore, our methodology allows testing whether phylogenetically conserved and phylogenetically independent structures are related to potentially driving environmental variables. Therefore, this method allows quantifying which part of trait variance and covariance is related only to the phylogeny given environmental variable(s) (**non-attributed phylogenetic conservatism**), only to these environmental variable(s) (*labile environmental effect*) and to the phylogenetically conserved environmental effect (***environmental phylogenetic conservatism***). The latter represents (co)variation that is related to both environment and phylogeny. These three components show patterns reflecting different evolutionary processes which cannot be distinguished using previously published frameworks, which were not able to consider multiple traits, their phylogenetic structure, and their relationship with environment all at once, as done here. This approach also allows partitioning networks and calculating network metrics such as number of module (NM), edge density (ED), maximum

absolute correlation ($|r|_{\max}$) and mean absolute correlation ($|r|_{\text{mean}}$) for each component, showing how the multivariate structure is related to the phylogeny and to the environment.

Even if it is beyond the scope of the current work, the proposed methodology also allows further elucidation of patterns at the intraspecific scale. The usage of within species variability in future works will better allow quantification of the extent to which variability within species is phylogenetically structured and related to specific environmental axis. It is also worth to note that even if here we are interested in environmental variables related to trait syndromes, other variables could be included to test for phylogenetic patterns in their relationship with trait syndromes.

3.5.1 Leaf economics and hydraulic traits conform to two phylogenetically conserved modules integrated in response to aridity

Implementing the new methodological approach allows to show how the leaf economics spectrum and plant hydraulics are evolutionarily integrated, conforming to two evolutionary modules across species at global scale. The first module describe the trade-off between xylem drought exposure-tolerance (Sanchez-Martinez et al. 2020) and leaf acquisitiveness (Wright et al. 2004). The second module describe the coordination between hydraulic sufficiency and photosynthetic capacity (Scoffoni et al. 2016). Our results show how these two modules are integrated following a pattern of ***environmental phylogenetic conservatism*** due to aridity. This integration is mainly mediated by specific leaf area and drought exposure, which act as functional hubs relating the two modules previously presented in response to aridity. However, some phylogenetic conservatism in individual trait variability, the integration among leaf economic traits and the integration between hydraulic sufficiency and photosynthetic capacity was not attributed to a response to macroevolutionary patterns of aridity. Then,

these functional traits and their integration may be related to other environmental components of species niche or may be caused by hardwired relationships at the phenotypical or genetic level.

From these results we can better understand the generalities of angiosperms woody plants adaptation to aridity. Angiosperm lineages exposed to low water potential and high evaporative demand will tend to present a higher capability to maintain stomata open under low water potentials, allowing maintenance of leaf growth and plant productivity under dry conditions (i.e., anisohydric strategy), presenting a higher drought exposure in the xylem in consequence (Volaire 2018). These lineages will tend to present an embolism resistant xylem that will allow maintaining water transport under low water potentials (see the second chapter, Sanchez-Martinez et al. 2020). Drought resistant lineages will tend to have smaller and/or thicker leaves as an adaptation to tolerate water stress (Wright et al. 2017), with lower nitrogen content and higher leaf lifespan, conforming to a conservative strategy of resource acquisition and processing (Wright et al. 2004, Reich 2014). Importantly, these lineages will also tend to present a relatively higher photosynthetic capacity in response to aridity, pointing that even if there is a phylogenetically conserved coordination between conductivity and productivity, this coordination may disappear when focusing on the macroevolutionary response to aridity. This means that under dry conditions, lineages with a lower specific leaf area may tend to present a higher photosynthetic capacity independently of their hydraulic sufficiency as an adaptation to maintain productivity per unit area under low water availability. Then, a drought resistant functional strategy may compensate for the lower hydraulic sufficiency and the lower leaf area by increasing its photosynthetic capacity. This result contradicts lineage specific results reporting that hydraulic sufficiency is evolutionarily coordinated with photosynthetic capacity in response to aridity (Scoffoni et al. 2016) but supports other evidence pointing that photosynthetic capacity may increase under dry conditions (Ramírez-Valiente and Cavender-Bares 2017, Green et al. 2020). However, these traits presented the lowest data availability from all the combination of traits used (118 species with both traits),

which may limit the capability to extract global patterns from them. Then, future work on the integration of photosynthetic capacity with other functional traits is needed to further elucidate its adaptive role.

The reported results show that leaf economic and hydraulic traits are not evolving independently and that their evolution may be constrained, leading to a pattern of phylogenetic conservatism where closely related species tend to present similar functional strategies. These constraints are at least partially related to species niche characterization, specifically to aridity, leading to a pattern of phylogenetic niche conservatism (Losos 2008). Based on these results, we expect adaptation in leaf and hydraulic trait syndromes of woody angiosperms to happen in a slow and conserved manner, maintaining their relationships and multivariate structure, with closely related species tending to occupy similar ecological and functional spaces (i.e., similar trait syndromes). It seems likely that environmental filtering related to variables related to water availability constrains the set of trait syndromes that can be present under a given set of conditions and a hardwired relationship between traits constrain individual trait variation at the macroevolutionary scale. Elucidating the directionality of these relationships in future works will help better understand which traits are responding to selective pressures directly and which are indirectly related to them as a result of trait integration.

3.5.1 Using information on traits evolution to perform data imputation

The presented statistical framework also enables new approaches to imputation and achieved high predictive performance, especially when trait covariances are considered. The proposed imputation methodology optimizes the usage of available data by including phylogenetic, environmental, and functional trait data as predictors when they show a significant relationship with the variable to be imputed. This method provides a framework for users that are not familiarized with phylogenetic methods, internally testing for the importance of the phylogenetic structure, and including it when informative. Moreover, it allows the consideration of multiple environmental variables which will only be included when informative. Finally, it allows for the consideration of functional traits data with missing values as predictors by performing imputation on them and then including them in predictive models, when informative.

This methodology outperformed *mean* and *MICE* imputations while performing similar to *phylopars* in most cases, outperforming it in non-phylogenetically conserved simulated traits and in most of the plant functional traits. However, it slightly underperformed *phylopars* in simulated phylogenetically conserved traits. This may be due to the fact that we include phylogenetic data by means of a low number of principal components describing most of the phylogenetic structure, which may lead to relatively lower predictive performance in highly phylogenetically structured traits compared to methods that include the whole phylogeny such as *phylopars*. Across scenarios, we show how the presented methodology is a good option, especially when using real data, which may be more complex than the data simulated in this study.

The fact that this methodology uses widely available information such as phylogenetic and environmental data will allow it to be widely applicable, particularly given the generalized scarcity of functional data at global scales. Finally, it is important to note that the macroevolutionary perspective may be undermining the within-species

variability. Even if it is beyond the scope of the current work, it is worth mentioning that this methodology allows one to include within species variability in environmental data and functional traits. Thus, the application of the current framework by including intraspecific variability will be of great interest to better characterize species adaptive capability and should be considered as soon as data availability increases at the global scale.

4 PLANT FUNCTIONAL TRAITS ARE EVOLUTIONARILY COORDINATED WITH LIFE HISTORY TRAITS IN THE AMAZON BASIN

Plant functional traits are evolutionarily coordinated with life history traits in the Amazon basin.

Pablo Sanchez-Martinez, Kyle G. Dexter, Freddie C. Draper, Hans ter Steege, ATDN and TRY groups (see statement of contributions)

4.1 ABSTRACT

Plants functional traits describing resource acquisition and processing are related to life history traits describing growth, reproduction, and survival strategies, but the evolutionary nature of these relationships is largely unknown. In this study, I shed light on the degree of phylogenetic conservatism and evolutionary lability in these traits and their relationships for tree genera across environmental gradients in the Amazon Region. Functional and life history traits are aligned primarily along two main axes of variation representing the integration between (1) functional acquisitiveness, longevity, and reproductive strategy and (2) size and growth. Leaf and wood economics conform a phylogenetically conserved module with reproduction and survival, meaning that closely related genera tend to present similar economic, reproduction and survival strategies, suggesting a constrained, integrated evolution. Contrarily, the relationship between size and growth presents a more labile evolutionary pattern, with both characteristics changing jointly over evolutionary time. These results clarify the evolutionary interdependence of functional and life history strategies, illuminate the principal ecological strategies for tropical trees and serve to elucidate general patterns of adaptation in woody plants of the Amazon Region.

4.2 INTRODUCTION

Life history theory predicts functional traits describing resource uptake, use and storage to be related with life history traits describing growth, survival and reproduction following the fast-slow continuum (Stearns 1999, Reich 2014). At one end, acquisitive species will prioritize fecundity over survival, presenting productive leaves and fast-growing wood with rapid turnover. This strategy will generally imply a lighter wood with lower resistance to disturbances that may lead to a higher mortality (Chave et al. 2009). This strategy is often linked to rapid and cheap reproduction where a high number of small seeds are produced (Poorter et al. 2008, Adler et al. 2014). In the tropics, species presenting this characteristics are identified as the pioneers, with a high capability to reach and colonize disturbed areas, and a low tolerance to stress (Turner 2001). At the other end, conservative species will prioritize survival over fecundity, presenting well-defended leaves and wood long lifespan and revenue stream, but which can constrain growth rates (Adler et al. 2014). A slower growth will ultimately produce denser wood which will be resistant to disturbances (Chave et al. 2009) and then these species will reach big sizes by presenting a high lifespan. These species are often linked to a higher investment per unit of seed which constrains the amount of seeds that a given individual can produce, but increasing the seed and seedling's probability to survive (Moles and Westoby 2006). This strategy is identified as the stress-tolerant strategy in the tropics (Turner 2001).

Previous studies have shown that this general theory may not always hold in the tropics, where different combinations between functional and life history traits may appear. For instance, the coordination between leaf economics (Wright et al. 2004) and wood economics (Chave et al. 2009) may not always hold for tropical species (Baraloto et al. 2010, Fortunel et al. 2012). Then, species with a slow return on investment of nutrients and dry mass in leaves will not always present a stress-resistant dense wood with slow water transport and species with a fast return on investment in leaves will not be constrained to present stress-vulnerable light wood with fast water transport.

Similarly, it has been shown that species presenting a fast strategy can also reach big sizes (Poorter et al. 2008). Other studies show reproductive strategy to be independent to the fast-slow continuum describing the growth-survival trade-off (Salguero-Gómez et al. 2016) and may instead be related to stature, describing a stature-recruitment axis (Rüger et al. 2018). Evolutionary processes leading to patterns in ecological strategies in the tropics may lead to some degree of independence between different functional and life history axis of variation.

Functional traits are often good predictors of life history traits, which suggests that functional strategies are important in determining which life history strategies species can adopt (Adler et al. 2014). However, whether these relationships are fully explained by common ancestry, or they appear multiple times in closely related species remains unknown. Both functional traits (Flores et al. 2014, Sanchez-Martinez et al. 2020) and life history traits (Coelho de Souza et al. 2016) have been reported to present phylogenetic conservatism. This phylogenetic conservatism in individual traits indicate that there may be some processes constraining their evolution. However, whether these processes are independent for each trait or shared among traits cannot be elucidated from individual trait patterns. To face this issue, it may be useful to quantify phylogenetic conservatism in traits relationship, which will shed light on the independence of potential processes constraining traits evolution. Related traits are co-evolving, and when their relationship is phylogenetically structured, it may be underlined by the same processes constraining their evolution. Contrarily, when trait relationships are independent of the phylogeny, processes leading to their covariation may be acting in more recent evolutionary timescales (e.g., within taxonomic families), pointing to a more labile evolution.

Phylogenetic conservatism in functional and life history traits and their relationship describe a pattern of closely related species presenting similar functional and life history strategies. This in turn means that ancestral trait syndromes are constraining descendent ones, pointing to a slow evolution that may not be able to

undergo relatively rapid changes in response to selective pressures (Losos 2008). Under this scenario, closely related species will tend to occupy similar ecological spaces and changes in the distribution of ecological strategies in response to environmental forcing will be mainly influenced by changes in lineage composition (understanding lineage as closely evolutionarily related taxa), and not to rapid adaptation of the species present in a given area. Contrarily, if ecological strategies present evolutionary lability, rapid changes may happen over evolutionary timescales (e.g., disparification within families). This will lead to a pattern of closely related taxa presenting a higher variability in functional and life history strategies (Ackerly et al. 2000). Under this scenario, we expect species to be more capable to modulate their ecological strategies, with closely related species occupying different ecological spaces. In this case, changes in the distribution of ecological strategies may be more influenced by the evolution of species present in a given site in response to changes in selective pressures.

To my knowledge, a quantification of the phylogenetic conservatism and evolutionary lability in integrative ecological strategies, which we define to include functional and life history strategies and their relationships, is still lacking. In this chapter, I explore the relationships among a range of functional and life history traits across hundreds of Amazon tree taxa within an evolutionarily explicit framework. First, I describe the general strategies that emerge from available data, quantifying phylogenetic conservatism in functional, life history and integrative (i.e., functional and life history) axes of variation. Then, I further explore the degree of phylogenetic conservatism and evolutionary lability in trait-trait correlations. This knowledge will be crucial to understand and predict ecological strategies of tropical species, an important step forward that will lead to better understand vegetation changes in the Amazon basin, which are expected to have important impacts on carbon and water cycles from regional to global scales (Bonan 2008, Hilker et al. 2014).

4.3 MATERIALS AND METHODS

4.3.1 Data

I compiled species-level data on plant functional traits and demographic rates from previous publications (Coelho de Souza et al. 2016, Kattge et al. 2020). I then calculated genus-level mean trait values, and matched them with a previously published genus-level phylogeny (Neves et al. 2020) by using the *ape* R package (Paradis and Schliep 2019). Overall, I obtained trait values for 1,036 genera which were represented in the phylogeny (Table S4.1 to see the number of genera with data for each trait).

Functional traits included in the present study were specific leaf area ($\text{m}^2 \text{kg}^{-1}$, SLA), leaf nitrogen, phosphorous and carbon content (mg g^{-1} , N, P and C, respectively), wood density (g cm^{-3} , WD) and maximum diameter as a proxy of whole plant size (cm, D_{max}). Life history traits were characterized in the present study by maximum growth rate (cm yr^{-1} , GR_{max}), mortality rate ($\% \text{ year}^{-1}$, MR) and seed mass (g, SM) as a proxy of reproductive strategy. The later was obtained as an ordinal categorical variable, and we treated it as a quasi-continuous variable. I acknowledge that seed mass could be classified as a functional trait instead of a life history trait, but given the lack of data on reproductive strategies, I decided to use it as a proxy of reproductive strategy based on its widely reported positive relationship with seedling emergence and successful sapling recruitment (Mazer 1990, Westoby et al. 1996, Henery and Westoby 2001, Moles and Westoby 2006). All variables were checked for normality, and mortality rate, maximum growth rate and maximum diameter were subsequently log-transformed to improve normality.

4.3.2 Principal components analyses

I implemented principal component analyses on functional traits (SLA, N, P, C, WD and D_{\max}) and life history traits (GR_{\max} , MR and SM) separately and jointly using the *prcomp* function of the *stats* R package (R Core Team 2020) (Figure 4.1 to see biplots showing the two first principal components in each case, generated by using the *factoextra* R package (Alboukadel Kassambara and Fabian Mundt 2020)). Principal component analyses were conducted using those genera with complete observations for all the variables ($N = 197$).

4.3.3 Phylogenetic signal calculation

I calculated the phylogenetic signal (λ) of principal components and individual traits. To do so, I used the *computeVarianceCovariancePartition* function of the package *TrEvol* (see chapter 3), which uses Bayesian phylogenetic mixed models (BPMMs) from the *MCMCglmm* R package (Hadfield 2010a) to estimate phylogenetic variance (V_{phylo} , amount of variance related to the phylogenetic structure) and residual variance (V_{res} , non-phylogenetically related variance). Phylogenetic signal (λ) is described as the amount of variance for a given variable that is related to the phylogeny, divided by the total trait variance, and is calculated as it follows:

$$\lambda = \frac{V_{phylo}}{V_{phylo} + V_{res}}$$

As the Bayesian framework operates with posterior distributions of estimates, I calculated the phylogenetic signal for the posterior distributions of the variance components, obtaining a distribution for each phylogenetic signal from which mean and credible intervals were calculated. P-values related to the probability that the distribution contained zero were calculated in *TrEvol* package (see chapter 3) importing functions from the *BayesR* R package (Makowski et al. 2019).

4.3.4 Correlations calculation

I calculated total correlation among variables, which was decomposed into a phylogenetic correlation and an evolutionarily labile correlation. The phylogenetic correlation refers to the proportion of the total correlation that is phylogenetically structured, while the evolutionarily labile correlation is the proportion of the correlation which is independent of the phylogenetic structure. The phylogenetically conserved and phylogenetically independent correlations components sum to the total correlation. To calculate these coefficients I used the *computeVarianceCovariancePartition* function of the *TrEvol* package, which uses BPMMs from the *MCMCglmm* R package (Hadfield 2010a) to partition the amount of variance-covariance on pairwise traits related to the genus-level phylogeny (Neves et al. 2020). Correlation coefficients are calculated as it follows:

$$\text{Total correlation} = \frac{COV_{phylo}^{T1,T2} + COV_{res}^{T1,T2}}{\sqrt{(V_{phylo}^{T1} * V_{phylo}^{T2}) + (V_{res}^{T1} * V_{res}^{T2})}}$$

$$\text{Phylogenetic correlation} = \frac{COV_{phylo}^{T1,T2}}{\sqrt{(V_{phylo}^{T1} * V_{phylo}^{T2}) + (V_{res}^{T1} * V_{res}^{T2})}}$$

$$\text{Labile correlation} = \frac{COV_{res}^{T1,T2}}{\sqrt{(V_{phylo}^{T1} * V_{phylo}^{T2}) + (V_{res}^{T1} * V_{res}^{T2})}}$$

Where $COV_{phylo}^{T1,T2}$ and $COV_{res}^{T1,T2}$ are phylogenetic and non-phylogenetic (residual) covariances between two traits (T1 and T2), V_{phylo} and V_{res} are phylogenetic and non-phylogenetic (residual) variances for each trait. As with the analyses of phylogenetic signal, I obtained a distribution of correlation estimates in each case from which mean and credible intervals were calculated as well as a p-value related to the probability of the distribution containing zero as described before by using the *BayestestR* package (Makowski et al. 2019). Note that even if phylogenetic and labile correlations sum to the total correlation, they can be significant even when the total correlation is not. Correlation coefficients were calculated for each pair of traits as well

as for each pair of principal components coming from different principal component analyses.

I used the *plotData* function of the *TrEvol* R package to plot principal components on the phylogeny. I used the *plotVcv* and the *plotNetworks* functions of the *TrEvol* package to display phylogenetic signal and correlation results. In the latter case, the function calculates network metrics (He et al. 2020a). These measures are the number of modules (NM); edge density (ED) describing the proportion of actual connections among nodes out of all possible connections; the maximum absolute correlation coefficient ($|r|_{\max}$) and mean absolute correlation ($|r|_{\text{mean}}$) as measures of the strength of the correlation among traits in a given network. In this framework, high NM will represent a high modularity pointing to the existence of independent groups of correlated traits; high ED represents high coordination between all traits and high $|r|_{\max}$ and $|r|_{\text{mean}}$ represent networks with a higher dependence among related traits (i.e., higher maximum and mean correlation among related traits, respectively). At the node level, degree (i.e., number of connections per node) is displayed as node size. Traits with a higher degree value (i.e., higher node size in the visualisation) are considered hubs.

4.4 RESULTS

4.4.1 Functional and life history conform to two main axes of variation

The first two functional principal components explained more than the 60% of the variance in the six functional traits considered (specific leaf area, SLA; leaf nitrogen, N; leaf phosphorous, P; leaf carbon, C; wood density, WD and maximum diameter, D_{\max}). The first functional principal component, explaining 40% of the variance represented the coordination between the leaf economic spectrum (Wright et al. 2004) and the wood economic spectrum (Chave et al. 2009), with higher values representing genera with lower SLA, leaf N and P, and higher WD (conservative) and low values presenting genera with higher SLA, N and P and lower WD (acquisitive). The second functional principal component explained 20% of the functional variance and was mainly related to D_{\max} and leaf C, with low values indicating larger-sized genera and high leaf C and high values indicating smaller-sized genera with low leaf C values (Figure 4.1).

The two first life-history principal components explained 82% of the variance in the three life history traits (mortality rate, MR; maximum growth rate, GR_{\max} and seed mass, SM). The first life history principal component, explaining 55% of the variance, was mainly related to the seed mass/mortality trade-off, with low values representing genera with lower seed mass and higher mortality (R strategy hereafter) and high values representing genera with higher seed mass and lower mortality (K strategy hereafter) (MacArthur and Wilson 1967, Pianka 1970). The second life history principal component, explaining 27% of the variance was interpreted as a growth axis, with low values representing genera with higher maximum growth rates and higher values representing genera with lower maximum growth rates. (Figure 4.1).

When considered altogether in the same principal component analysis, functional traits and life history traits represented variation in plant ecological strategy through two main axes referred to hereafter as integrative principal components. The first axis represented the trade-off between resource acquisitiveness, longevity, and investment per seed (explaining 31% of the variance) and the second axis represented the coordination between individual growth capability (GR_{max}) and size (D_{max}) (explaining 20% of the variance). Ecological strategies of tropical tree genera were broadly characterized by the four extremes described by these two axes, and represented as the four corners of the biplot shown in Figure 4.1c. At the top left corner (i.e., negative values for PC1 and positive for PC2), genera were characterized by an acquisitive function (A), short lifespan and seed mass (R strategy), big size (B) and fast growth (FG), represented by genera such as *Ficus*, *Ceiba* and *Sapium* (A R – B FG). At the top right corner (i.e., positive values for both PC1 and PC2), genera were characterized by a conservative function (C), high lifespan and seed mass (K strategy), big size (B) and fast growth (FG), represented by genera such as *Manilkara*, *Hymenaea* and *Couma* (C K – B FG). At the bottom left corner (i.e., negative values for both PC1 and PC2), genera were characterized by an acquisitive function (A), an R strategy, small size (S) and slow growth (SG), represented by genera such as *Quararibea*, *Lunania* and *Lindackeria* (A R – S SL). Finally, at the bottom right corner (i.e., positive values for PC1 and negative values for PC2), genera were characterized by a conservative function (C), K strategy, small size (S), and slow growth (SG), represented by genera such as *Psidium*, *Myrcia* and *Cheiloclinium* (C K – S SG). However, note that these groups represent the extremes of the combination of the two main axis and then, intermediate strategies are more common.

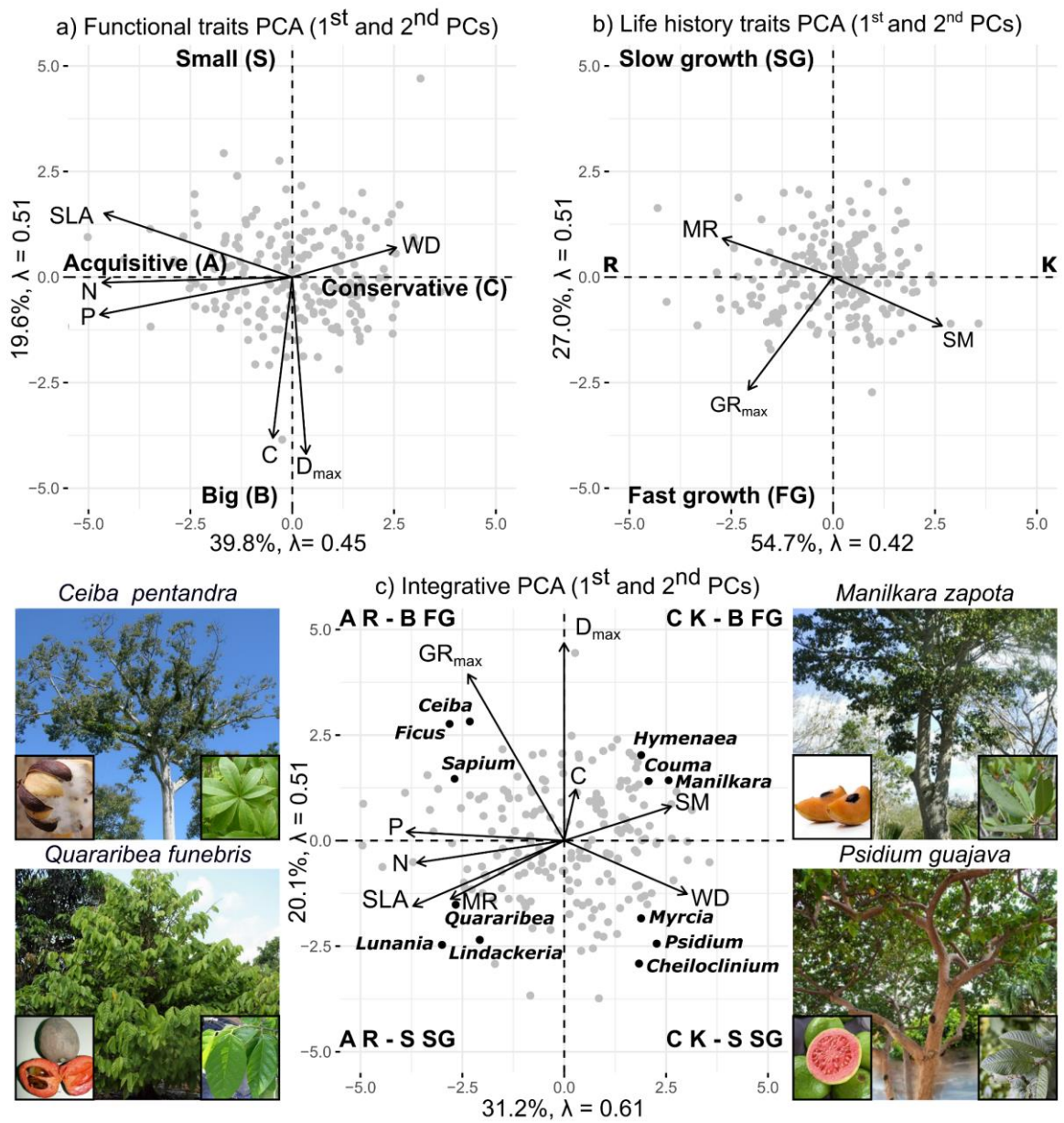


Figure 4.1 Functional, life history and integrative axis of variation First principal components using functional traits (a), life history related traits (b) and all traits (c). Only genera with complete data for all variables are represented (197 genera). Variable contributions are shown as arrows. Principal axis interpretation is shown in bold letters. Phylogenetic signal (λ) and amount of variance explained by each axis in percentage are shown for each axis.

4.4.2 Phylogenetic signal in functional and life history strategies

Functional, life history and integrative axes presented significant phylogenetic signal (Figure 4.1, Figure 4.2a diagonal). The first functional axis describing variability in leaf and wood economics presented a phylogenetic signal of 0.45, meaning that 45% of its variance is related to the phylogenetic structure. The second functional axis describing variability in plant size presented a phylogenetic signal of 0.51 (i.e., 51% of its variance was phylogenetically structured) (figure 4.1a). The first life history axis representing the reproduction-survival trade-off (R-K strategies) presented a phylogenetic signal of 0.42 (i.e., 42% of its variance was phylogenetically structured). The second life history axis describing variability in growth presented a phylogenetic signal of 0.51 (i.e., 51% of its variance was phylogenetically structured) (figure 4.1b). Finally, the first and second integrative traits representing variability in functional and life history strategies presented a phylogenetic signal of 0.61 and 0.51, respectively (61% and 51% of their variance was phylogenetically structured, respectively) (figure 4.1c). Individual traits also presented significant phylogenetic signal, ranging from 0.30 (mortality rates, MR) to 0.79 (seed mass, SM) being the most important source of variation (i.e., >50% of variation) in 4 out of 9 traits. Then, evolutionary lability of individual traits was the most important source of variation in 5 out of 9 traits analysed (Figure 4.2b diagonal, Figure 4.3b and c, pie charts, Table S4.1).

4.4.1 Phylogenetic conservatism and evolutionary lability in functional and life history traits integration

Phylogenetic correlation was the main component of total correlation in 24 out of 27 significant total correlations found (Figure 4.2, Table S4.3), consistent with the phylogenetic conservatism of the previously presented principal components.

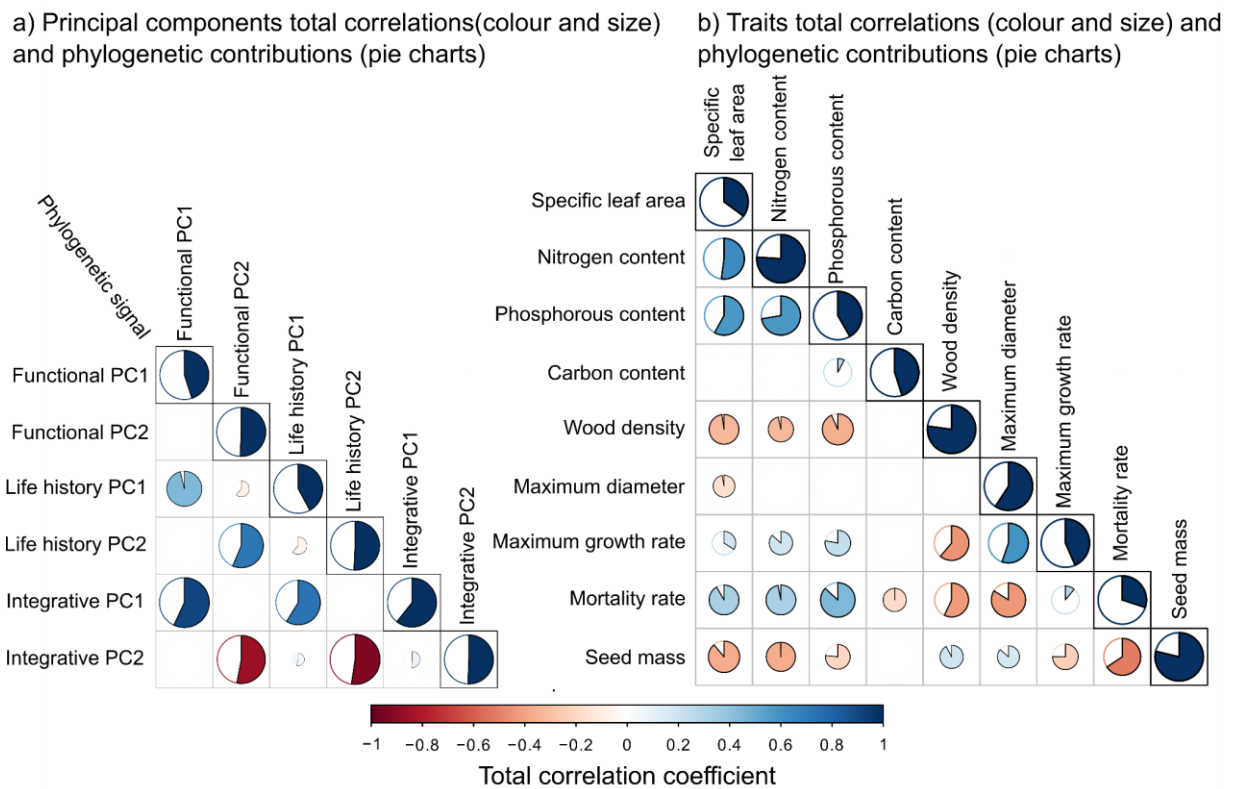


Figure 4.2 Correlation and phylogenetic signal Significant total correlation (colour and size, values between -1 and 1) and contribution of phylogenetic conservatism (filled) to significant total correlations (pie chart, values between 0 and 1) for PCs (a) and traits (b). Phylogenetic signal is also displayed in the diagonal pie charts (values between 0 and 1). Contributions are represented as the proportion of the total correlation that is related to phylogeny (dark colour of pie charts).

We complemented the principal components perspective by means of a trait network perspective. By doing so, we show how functional and life history traits conform to one unique module (Figure 4.3). Thus, even if traits may present different degrees of correlation leading to the conformation of the previously described main axis of variation, there may be some traits acting as links between these axes leading to a relatively hardwired pattern of covariation.

Leaf traits present a high and consistent coordination describing the leaf economics spectrum (LES) (positive correlation between specific leaf area, leaf nitrogen and phosphorous) (Wright et al. 2004). These correlations showed both a phylogenetically conserved and an evolutionarily labile component (Figure 4.3). LES showed a phylogenetic correlation with the wood economics spectrum (WES, represented by wood density), describing how lineages with acquisitive leaves tend to present low wood density while those with conservative leaves tend to present a high wood density. This relationship was not evident in the evolutionarily labile component. LES and WES relationships with life history traits were also mainly phylogenetically conserved, describing how lineages presenting acquisitive leaves and light wood tend to present higher mortality rates (MR), lower seed mass (SM) and higher growth rates (GR_{max}) (Figure 4.3b). However, some degree of evolutionary lability was also patent in some of these correlations. LES present an evolutionarily labile positive correlation with seed mass, while WES present evolutionary labile negative correlations with mortality and growth rates (Figure 4.3c).

Plant size showed a positive correlation with maximum growth rate, and this relationship presents both phylogenetically structured and evolutionarily labile components. These results point that plants that reach high stature tend to present high maximum growth rates, and this pattern is not fully explained by common ancestry. Contrarily, the negative correlation between plant size and mortality rates is fully explained by the phylogenetic component, describing how lineages with higher stature tend to present lower mortality rates. It is also worth mentioning that in our study, no

correlation between wood density and maximum size was detected. Instead, both functional traits are consistently correlated to maximum growth rates, so lineages with higher maximum growth rates tend to present lighter wood and higher sizes. These correlations present both a phylogenetically conserved and an evolutionarily labile component.

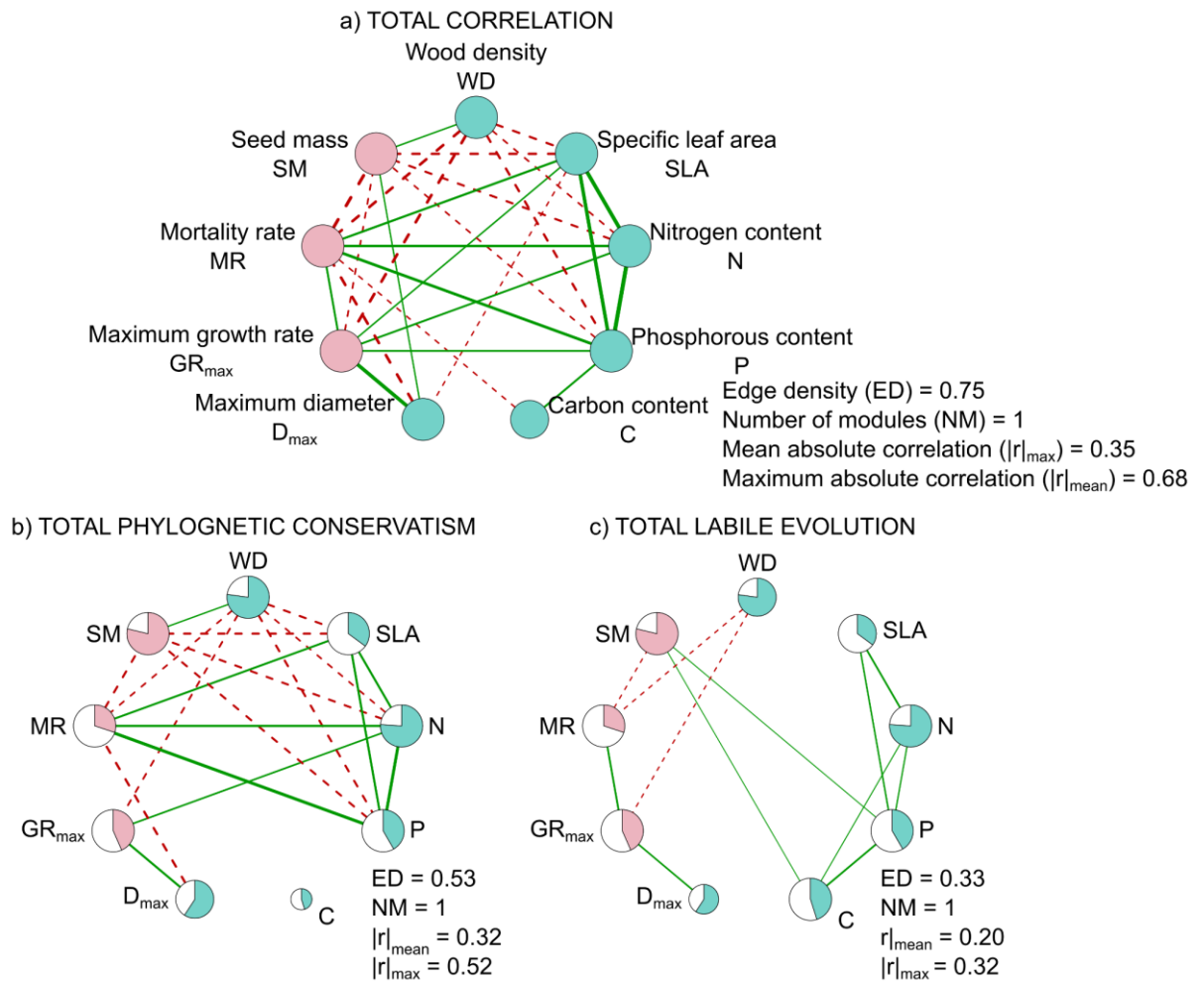


Figure 4.3 Variance-covariance networks Edges represent total correlation (a), phylogenetic correlation (a) and labile correlations (c). Solid green and dashed red lines represent statistically significant positive and negative correlation coefficients, respectively. Line width is proportional to the absolute value of the correlation coefficient. Pie charts in b and c represent trait phylogenetic signal, and circles are coloured by trait type (i.e., functional traits are light blue, life history traits are pink). Node size is proportional of the number of connections per node.

Relationships between life history traits present both phylogenetic conservatism and evolutionary lability. The negative correlation between seed mass and mortality presents both phylogenetically structured and evolutionarily labile components, describing how lineages with higher seed mass tend to have a lower mortality. However, the positive correlation between mortality rates and maximum growth rates is fully explained by the labile component, describing how species that grow fast tend to have higher mortality, and that closely related taxa can present different growth-survival strategies. Finally, seed mass and maximum growth rate appear to vary independently, being indirectly related through other traits.

Most of the significant phylogenetic and labile correlations maintain the same direction. As a result, a phylogenetic principal component analysis was not extremely different from the one reported here, meaning that the direction of the relationships was consistent both in the phylogenetically conserved and the evolutionarily labile components (Figure S4.1). However, wood density appeared to be more orthogonal to leaf economic spectrum in the phylogenetic principal component analysis, consistent with the fact that their relationship may be mainly driven by common ancestry. Even if it was not the norm, in some specific cases, the direction of the phylogenetically conserved and evolutionarily labile components of the correlation changed. For instance, leaf phosphorous (P) and SM show a negative correlation (Figure 4.3a) which is consistent with the phylogenetic component (Figure 4.3b), its main driver, but a positive evolutionarily labile correlation was discovered between these traits (Figure 4.3c).

We also tested for phylogenetic conservatism and evolutionary lability in the relationships between functional and life history principal components. We reported that the first functional component (acquisitive to conservative economics) is correlated to the first life history component (R to K strategy) and that the second functional component (big to small statured) is correlated to the second life history component (high to low growth). The correlation between the first functional component and the first life history principal component was completely phylogenetically structured. In contrast, the correlation between the second functional component and the second life history component, was as much due to evolutionary lability as to phylogenetic conservatism (Figure 4.4).

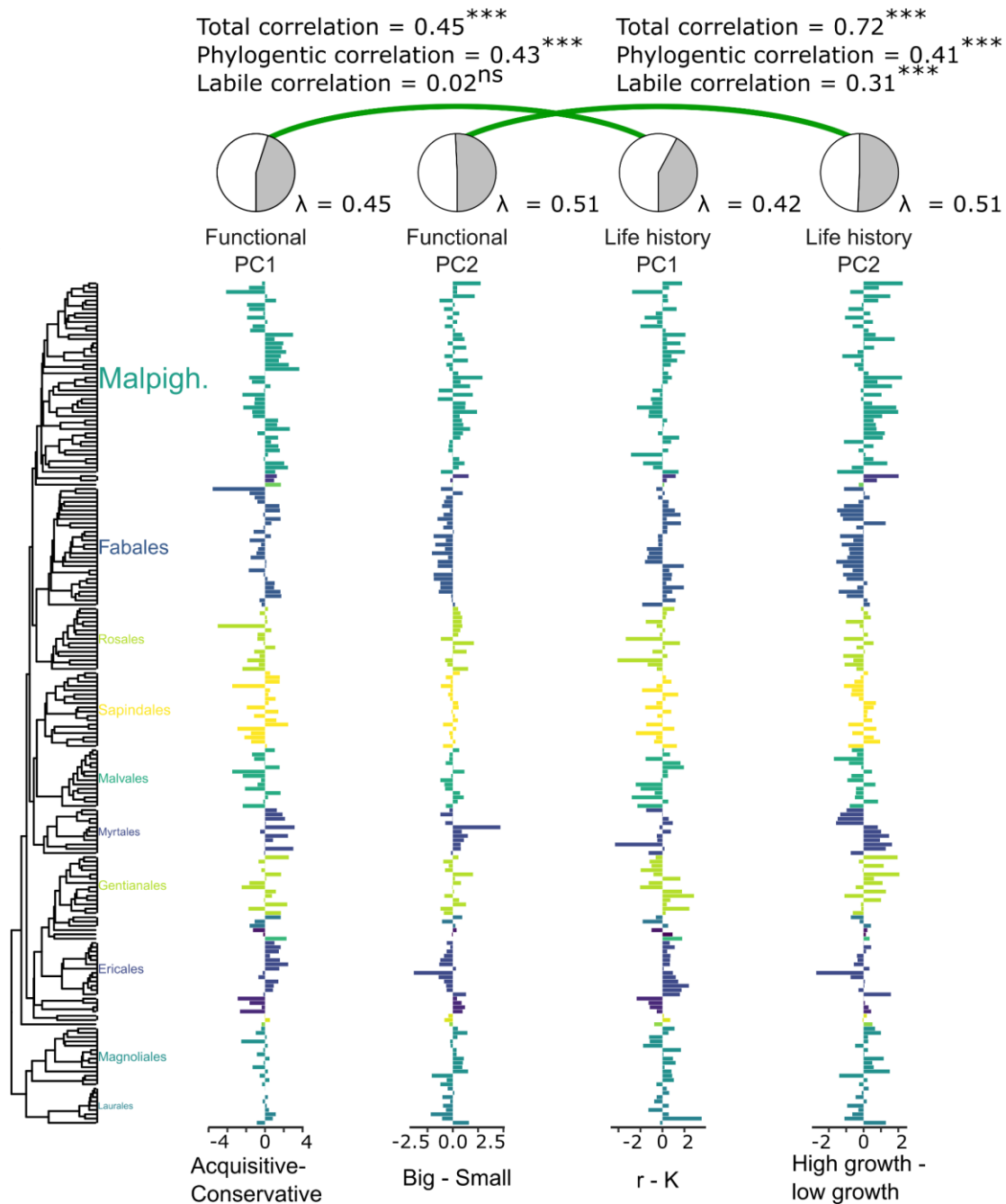


Figure 4.4 Functional and life history axis correlations Total, phylogenetic and labile correlations between functional and life history principal components. Phylogenetic signal λ is also shown and represented as pie charts for each principal component. Values for genera with complete observations are plotted on the genus-level phylogeny. Bars are coloured by taxonomic order and the most important taxonomic order names are shown. Signif. codes: “***”: $P < 0.001$; “**”: $P < 0.01$; “*”: $P < 0.05$; “.”: $P < 0.1$; “ns”: $P > 0.1$.

4.5 DISCUSSION

4.5.1 Leaf acquisitiveness is integrated with survival and reproduction and stature is integrated with growth

In this chapter, I show that functional traits and life history traits are broadly aligned along two axes of variation representing diversity in ecological strategies across Amazonian tree genera. The first axis showed the integration between leaf economics (Wright et al. 2004) and reproductive and survival strategies. This axis describes how genera with acquisitive leaves have a higher probability to suffer mortality potentially related to their lower stress tolerance, while presenting a fast and cheap reproduction (low seed mass). Contrarily, genera with conservative leaves will have lower mortality rates potentially related to their higher stress tolerance (see the relationship between SLA and drought tolerance in chapter 3), while presenting a higher investment per seed (Adler et al. 2014). The second axis represents the coordination between maximum growth rates and maximum size, showing how species with a higher maximum growth capability tend to reach higher stature independently of their resource use strategy, lifespan, or reproductive strategy. These results suggest that functional traits related to leaf and wood economics (Wright et al. 2004, Chave et al. 2009) may be constraining life-history traits related to survival and reproduction, while they are relatively independent of an axis related to size and growth. Then, these results are not aligned with the existence of a plant economic spectrum (Reich 2014) in Amazon trees at the genus level, as growth rates are disconnected from leaf acquisitiveness, reproduction and mortality, even though there is a weak link between these axis mediated by leaf nitrogen.

Following these two axes of variation describing variability in integrative ecological strategies, tropical tree genera can be broadly characterized by their position in reference to four different ecological extremes regarding functional acquisitiveness,

reproduction, survival, growth, and size. The first group is characterized by an Acquisitive R strategy with Big size and Fast Growth (AR-BFG) and can be identified as a big-pioneer strategy (e.g., *Ceiba*). The second group presents a Conservative K strategy with Big size and Fast Growth (CK-BFG) and can be identified as a big stress-tolerant strategy (e.g., *Manilkara*). The third group displays an Acquisitive R strategy with Small size and Slow Growth (AR-SSG) and can be identified as a small-pioneer strategy (e.g., *Quararibea*). Finally, the fourth group shows a Conservative K strategy with Small size and Slow Growth (CK-SSG) and can be identified as a small stress-tolerant strategy (e.g., *Psidium*). Note that these groups represent extreme relationships as describe by the two integrative axis and then, intermediate strategies are common. These results correspond partially to the previously reported shade-tolerance and size axis (Turner 2001) and to the fast-slow continuum (Stearns 1999). However, in the present study, I show how the fast (pioneer) to slow (stress-tolerant) continuum is mainly decoupled from maximum growth rate and maximum size, the latter of which are in turn correlated. Note that we characterized size as maximum size (i.e., adult size), related to access to light in the reproductive stage, which may not be always a good predictor of juvenile growth (Needham et al. 2022). We do not detect an independence of the reproductive strategies from fast-slow continuum as previously reported (Salguero-Gómez et al. 2016, Rüger et al. 2018). However, we acknowledge that the characterization of reproductive strategies in our study is limited and may not be representing all its variability.

Trait-to-trait relationships support the described main axes of variation, but further show how these two axes are connected by means of the positive relationship between growth rates and leaf nitrogen and by a negative relationship between growth rates and wood density. Then, higher nitrogen in leaves is related to higher growth rates which lead to lower wood density, acting as a link between the main axes described above.

4.5.1 Leaf acquisitiveness, survival and reproduction integration is phylogenetically conserved and independent of size-growth integration, which presents evolutionary lability

The first axis related to leaf acquisitiveness, reproduction and survival is strongly phylogenetically structured. This suggests that the relationship between leaf economics strategies, survival and reproduction may be evolutionarily constrained by common factors or by their interdependence. As a result, their covariation is conserved through evolutionary time leading to a pattern of phylogenetic conservatism that involves functional and life history components of the ecological strategy. Under this scenario, lineages may not be able to rapidly change their functional and life history strategies related to reproduction and survival, leading closely related species to present similar strategies (Losos 2008). This pattern may emerge from conserved and slow adaptation in response to environmental variables (Crisp and Cook 2012), leading to a predominant effect of environmental filtering influencing the distribution of these strategies over environmental gradients (among and within sites, the latter being light availability gradients). As a result, phylogenetic position is expected to be informative on resource economics, survival and reproductive strategies in Amazonian trees.

Contrarily, the relationship between size and growth presents a higher evolutionary lability, with closely related genera presenting different values along this axis. This pattern suggests that the evolution of different maximum growth rates and size are not strongly evolutionarily constrained. Then, lineages may be able to adapt to different conditions by diversifying in their growth rate, which is related to variability in maximum size in a non-phylogenetically conserved manner. However, maximum size showed a relatively high phylogenetic signal, meaning that it may be evolutionarily constrained by other factors influencing its values. One of these factors may be its relationship with mortality rates, which is negatively phylogenetically correlated with

maximum size. Then, phylogenetic conservatism in maximum size may also be influenced by its phylogenetically conserved relationship with lifespan or to some underlying mechanisms leading to this pattern, describing how closely related species presenting a lower mortality will tend to present a higher maximum size, even when presenting low growth rates.

Overall, these results suggest that the distribution of leaf and wood economics, survival and reproductive strategies over environmental gradients has likely been constrained by environmental filtering both in the present and over evolutionary timescales. In contrast, changes in growth rates may allow species to adjust to various levels of resource availability, mediating events of rapid adaptation to different conditions over evolutionary times, being mainly disconnected from leaf economics. From these results we can see how traits are interconnected and how their variability is potentially determined by multiple processes, leading to a mixed pattern where evolutionary lability and phylogenetic conservatism coexist. The quantification of the contribution of each one of these components in individual traits and their relationship as done here is crucial to better elucidate patterns of adaptation and hypothesize potential processes shaping them.

4.5.1 The meaning of evolutionary lability and phylogenetic conservatism in ecological strategies

Even though evolutionary lability is evident in some individual traits' evolution such as specific leaf area or mortality rates, phylogenetic conservatism was the main pattern emerging from the analyses of relationship among traits in this study. This points that trait syndromes may evolve in a phylogenetically conserved manner, meaning that relationships among traits are conserved even though individual traits may present some degree of evolutionary lability. Traits pairs for which their correlation is entirely phylogenetically structured may not actually have a direct functional

relationship (Felsenstein 1988). Instead, this correlation may appear as an effect of common factors constraining evolution of the two traits, leading to phylogenetic autocorrelation in trait syndromes. This may be the case for the relationship between leaf economics and wood economics, the relationship of leaf economics with survival and reproduction and the relationship between wood economics and seed mass. However, this phylogenetic conservatism in traits relationship could also be the output of a conserved pattern in adaptation if it is itself related to common environmental factors influencing their values (i.e., phylogenetic niche conservatism) (Sanchez-Martinez et al. 2020). Future studies should consider the potential environmental axes explaining these patterns of phylogenetic conservatism to shed additional light on their adaptive meaning. This is a challenge of course as the most impactful environmental gradients that tree species experience in the Amazon Region are likely in edaphic and light conditions, and it would be a massive undertaking to consistently quantify these conditions across many tree species over the entire region.

Some relationships among traits appear to consistently have both phylogenetically structured and evolutionarily labile components, such as within the leaf economics spectrum or the relationship between wood economics and growth rates. These traits relationship may present a hardwired relationship potentially underlined by adaptive processes. Then, these traits may present some slow adaptation related to the general characterization of species ecological niche, but also more recent adaptation related to more subtle changes in environmental conditions. A lower number of trait correlations appear only in the evolutionary labile component, although one notable case is the relationship between growth rates and mortality. This evolutionary labile relationship may indicate that taxa with high mortality and high growth rates appear in multiple lineages and that closely related species are not constrained to present similar values for these traits.

4.5.1 Caveats and future directions

The current study has some caveats, such as the usage of genus-level data, which may be underestimating intra-generic functional and life history diversity as well as phylogenetic structure. Moreover, our data on maximum growth rates may be strongly influenced by tree size. In future works, using relative growth rates may complement results shown here. Also, characterizing reproductive strategies by means of seed mass is an oversimplification due to a lack of reproductive data for Amazon tree taxa. In future works, the inclusion of other important axis of variation determining reproductive strategies such as number of seeds or recruitment may help better characterize them. Nevertheless, this work has helped to quantify the phylogenetic conservatism in tropical tree taxa, where high resolution data is still lacking, in a continuous and multivariate way. By doing so, it improved our knowledge of life history evolution, with important implications for their macroevolutionary patterns of adaptation. The inclusion of environmental data in future works will help elucidate the adaptive meaning of the strategies described. Finally, the phylogenetic relationships described in the present work can be used to predict and impute trait values for those species without measured data, potentially helping parameterise land surface models in the Amazonian Region (Swenson et al. 2017, Anderegg et al. 2021), which in turn may help with the current data scarcity for both functional and life history traits in this biome.

5 INCREASED HYDRAULIC RISK IN ASSEMBLAGES OF WOODY PLANT SPECIES PREDICTS SPATIAL PATTERNS OF DROUGHT- INDUCED MORTALITY

Pablo Sanchez-Martinez, Maurizio Mencuccini, Raúl García-Valdés, William M. Hammond, Josep M. Serra-Diaz, Wen-Yong Guo, Ricardo A. Segovia, Kyle G. Dexter, Jens-Christian Svenning, Craig Allen, Jordi Martínez-Vilalta. Under review in Nature Ecology and Evolution.

5.1 ABSTRACT

Predicting drought-induced mortality (DIM) of woody plants remains a key research challenge under climate change. Here, I integrate information on species' edaphoclimatic niches, phylogeny, and hydraulic traits to estimate the hydraulic risk of woody plants globally. I also combine these models with species distribution records to produce the first global maps projecting the hydraulic risk faced by local species assemblages and to test for its relationship with observed DIM. Our results show that local assemblages modelled as having higher hydraulic risk present a higher observed probability of DIM, and that metrics characterizing this hydraulic risk improve DIM predictions globally, relative to models accounting only for environmental predictors or broad functional groupings. The methodology I present here allows wall-to-wall mapping of functional trait distributions and elucidation of global macroevolutionary and biogeographical patterns, improving our ability to predict potential global impacts on vegetation.

5.2 INTRODUCTION

A substantial number of woody plant communities worldwide are experiencing increased mortality due to rising drought severity and temperature (termed drought-induced mortality, DIM), driven by anthropogenic climate change (Allen et al. 2010, Hartmann et al. 2018, Hammond et al. 2022). Such mortality modifies ecosystem composition, structure and functioning (Batllori et al. 2020), with large potential impacts on biodiversity and biogeochemical cycles (Bonan 2008, Brodribb et al. 2020). Generally, DIM is triggered by hydraulic failure (Anderegg et al. 2012, Rowland et al. 2015, Adams et al. 2017, McDowell et al. 2021), a physiological process causing loss of functionality of the plant conductive tissue (xylem), eventually leading to desiccation

and death. Previous studies have shown that plant hydraulic traits have the potential to improve our capacity to understand and predict DIM (Anderegg et al. 2016) and drought impacts on ecosystem fluxes (Anderegg et al. 2018a, Eller et al. 2020), as well as the community dynamics (Trugman et al. 2020, García-Valdés et al. 2021) emerging from these processes. Accordingly, hydraulic schemes are being incorporated into forest vulnerability assessments (Lecina-Diaz et al. 2020, Peters et al. 2021) and vegetation models, from the regional (Venturas et al. 2020, De Cáceres et al. 2021b) to the global (De Kauwe et al. 2020) scale. However, these models' predictive capacity is still poor (Venturas et al. 2020, Rowland et al. 2021, Trugman et al. 2021), potentially reflecting lack of high-quality hydraulic data or insufficient understanding of the mechanisms involved.

Hydraulic dysfunction happens when drought stress exceeds the capability of the xylem to tolerate low water potentials, leading air emboli in conduit lumens to disrupt water flow. This disruption can lead to hydraulic failure if embolism propagates (Tyree and Zimmermann 2002). The probability of suffering hydraulic failure (i.e., hydraulic risk) (Anderegg et al. 2016, Choat et al. 2018b) is commonly quantified with the hydraulic safety margin (HSM), which is the difference between the minimum water potential in the xylem (P_{\min} , a measure of drought exposure reflecting plant hydraulic regulation at the tissue level) and the water potential causing 50% or the 88% of hydraulic conductivity loss (P_{50} and P_{88} , measures of vulnerability to xylem embolism) (Choat et al. 2012, Delzon and Cochard 2014, Hammond et al. 2019). HSM is thus an individual- and site-specific physiological metric which is likely to be associated with drought induced mortality. However, data availability of P_{\min} and P_{50} at broad spatial scales is sparse both across and especially within species, and available values frequently do not reflect local conditions. Not surprisingly, species-level HSM is generally a poor predictor of mortality, only marginally improving existing models (Venturas et al. 2020, Rowland et al. 2021).

The distribution of HSM values within woody plant assemblages has been shown to relate to responses to extreme drought events (Skelton et al. 2015, Anderegg et al. 2018b) and to the maintenance of productivity under increasing drought (García-Valdés et al. 2021). This functional variability is likely explained by the variety of existing species-specific mechanisms to cope with drought (Kannenberg et al. 2021), influenced in turn by environmental filtering and evolutionary legacies present in any species assemblage (Cavender-Bares et al. 2016). Here, I posit that our capacity to predict where mortality is more likely to occur will be improved by considering the variability of hydraulic risk at the local level (assemblages of potentially co-occurring species), and not only the average hydraulic risk of individual species in the assemblage. Currently, P_{50} and P_{\min} data are available for 1,678 and 819 woody plant species, respectively, representing less than 1.5% of the world's estimated number of woody plant species. Nonetheless, I have recently shown that P_{\min} and P_{50} are phylogenetically conserved to a significant degree and are related to edaphoclimatic affiliations (see chapter 2) (Sanchez-Martinez et al. 2020). Including phylogenetic and edaphoclimatic information is therefore likely to improve the trait imputations required to provide global trait coverage. These results, together with increased availability of plant distribution data, pave the way towards predictions of hydraulic risk metrics that cope with the data scarcity problem, moving from individual species predictions to analyses of species assemblages at global scales.

Here, I use a newly global database of hydraulic traits (Hammond et al. 2021) and edaphoclimatic and phylogenetic information coupled with random forest modelling to predict xylem minimum water potentials (P_{\min}) and xylem embolism vulnerability (P_{50}), and hence hydraulic safety margins (HSM) as a measure of hydraulic risk, for 44,901 woody plant species. I georeferenced these predictions using existing data on species distributions (Serra-Diaz et al. 2017) and map aggregated hydraulic metrics for species assemblages at a 5-km resolution, globally. Then, I use linear models to test which metrics of hydraulic risk characterization (species assemblage mean and minimum

HSM, its variability and the number of species with high hydraulic risk) can predict observed drought induced mortality, using precisely georeferenced records on its occurrence (Hammond et al. 2022). Finally, I use maxent models (Phillips and Dudík 2008) to project drought induced mortality occurrence probability worldwide using different environmental predictors and the newly derived hydraulic metrics. I hypothesize that species-assemblage hydraulic risk will predict drought induced mortality occurrence, reflecting both the fact that species with lower hydraulic safety margin incur greater mortality risk and that assemblages with a higher number of species at hydraulic risk will experience more mortality. I also expect that measures of hydraulic risk of the entire species assemblage will outperform the species-level metrics of hydraulic risk in predictive models, as the former leverages information contained in spatial differences among species assemblage distributions and the associated phylogenetic patterns. By applying this framework, I provide the first global projection of woody plant hydraulic risk and associated drought induced mortality.

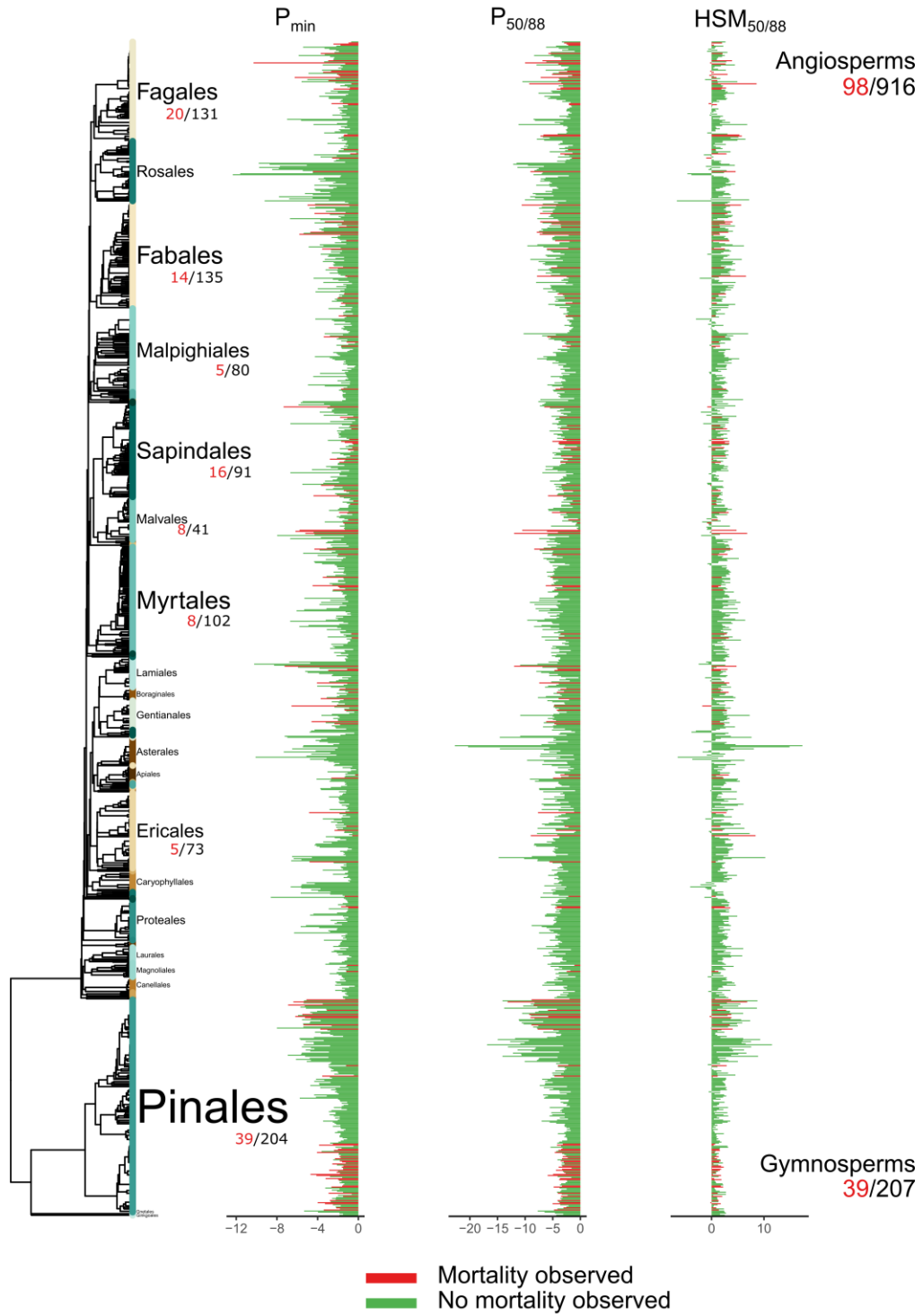
5.3 RESULTS AND DISCUSSION

5.3.1 Low hydraulic safety margins are widespread in woody plant species

Random-forest models, considering phylogenetic data jointly with edaphoclimatic affiliations and trait covariation, had substantial predictive power for species-specific minimum water potential in the xylem (P_{\min}) and its embolism vulnerability (P_{50}) values with a cross-validation R^2 of 0.60 ± 0.10 and 0.54 ± 0.12 , respectively (mean and standard deviation, Table S5.1, see methods). Hydraulic safety margins (HSM) estimated at the species level was related to observed HSM values, with an R^2 of 0.51. Overall, 7,024 out of 44,901 species (15.5%) presented negative HSM values, 66.2% of all species had $HSM < 0.5$ MPa, and 95.9% of all species had $HSM < 1$ MPa (Figure

5.1a, Figure S5.1 and Figure S5.2). These results generalize previous studies (Choat et al. 2012) indicating convergence towards low HSM in woody plants, pointing to a prevalent strategy of maximizing the usage of available water at the expense of increasing hydraulic risk. Negative HSM implies that species may experience embolism levels above 50%, which are expected to be stressful, especially for gymnosperms (Hammond et al. 2019). Some species (particularly angiosperms) may be adapted to recover from embolism by refilling conduits, resprouting from branch nodes below dead tissues or radial growth following drought relief (Anderegg et al. 2016), even though a significant loss of hydraulic conductivity can also lead them to mortality (Anderegg et al. 2015, 2016). When using P_{88} instead of P_{50} for angiosperms, which may be a more realistic hydraulic failure threshold for species in this group ($P_{50/88}$ results hereafter) (Hammond et al. 2019), only 165 species out of 44,901 species (0.37%) presented negative $HSM_{50/88}$ values (i.e., HSM calculated using P_{50} for gymnosperms and P_{88} for angiosperms, Figure S5.3).

Figure 5.1 Phylogenetic distribution of the data Phylogenetic distribution of observed and imputed hydraulic traits for species with observed data for xylem minimum water potential (P_{min}) and/or xylem embolism vulnerability (P_{50}). In red, species with observed mortality and in green species without observed mortality. The most important order names are shown with size proportional to the number of species represented. The total number of species with trait data is shown in black and the number in red is the number of those species that have an observed mortality event. The number and percentage of species showing hydraulic safety margin (HSM) values below zero, 0.5 and 1 are also shown.



5.3.2 Species-level hydraulic risk is a poor predictor of species-level drought induced mortality

I did not find significant relationships ($p > 0.3$) between species-level HSM or $HSM_{50/88}$ and species-level drought-induced mortality (DIM) occurrence. This result supports the lack of a strong relationship at broad spatial scales between species' mean hydraulic risk and their probability to suffer mortality (Venturas et al. 2020). However, I found significant negative relationships between species-level HSM (slope = -0.16, standard error = 0.03, $p < 0.001$) and $HSM_{50/88}$ (slope = -0.34, standard error = 0.02, $p < 0.001$) with the number of recorded DIM events per species. These relationships were significant for both angiosperms and gymnosperms, even though their predictive power was low (pseudo- $R^2 < 0.15$ and AUC < 0.57 in both cases). Equivalent results were obtained when using only observed HSM values (i.e., excluding imputed values). These results suggest that even though species with low HSM tend to present a higher number of recorded DIM events, this information is not sufficient to predict with reasonable accuracy the probability that a species will suffer DIM. This may be due to the fact that not only mean species hydraulic risk, but also its intraspecific variability and local environmental conditions are playing a crucial role in determining DIM risk. Then, incorporating a geographical perspective may improve predictive capacity of DIM occurrence.

5.3.3 Using information from species assemblages to characterize site-specific hydraulic risk

I aggregated imputed (i.e., observed and predicted) data for species xylem minimum water potential (P_{min}) and embolism vulnerability (P_{50} and P_{88}) into species assemblages in 5 km x 5 km grid cells using species distribution data (Figure S5.4a and b) (Serra-Diaz et al. 2017) (see Methods). Areas with drought incidence such as the Mediterranean basin, SW of Africa, SW of USA, and SW Australia presented species assemblages with

lower vulnerability to embolism (i.e., lower mean P_{50}) but not necessarily lower hydraulic risk (constant mean hydraulic safety margin, HSM) (in Figure 5.2b and c, note that hydraulic risk is represented as negative hydraulic safety margin so higher values represent higher risk). This pattern underlines the importance of tissue-level drought exposure (P_{\min} , Fig. S5.5) in determining hydraulic risk, as species can converge towards similar HSM even when being exposed to very different levels of climatic drought or present very different HSM under the same conditions depending on their functional strategies (Bhaskar and Ackerly 2006).

Maintaining a reasonably high HSM can imply very different strategies, including high embolism resistance, but also deep roots, tight stomatal regulation, or drought deciduousness to limit P_{\min} . The implications of these strategies may not be equivalent, which is a matter that requires further study. For example, in the case of stomatal and leaf area regulation, the carbon balance is also impacted directly, which could potentially result in indirect effects on the hydraulic system that could promote dehydration in the longer term or carbon starvation (McDowell et al. 2008, 2021, Sala et al. 2012). Even though carbon starvation has been shown to be not as important as hydraulic dysfunction in determining drought induced mortality (Rowland et al. 2015, Choat et al. 2018a), consideration of this process by including drought length and intensity in future studies would be useful to deepen our understanding of the consequences of changing drought intensities.

The functional richness of species assemblages was further characterized by estimating the variability of strategies in a community (trait variance at the grid cell level). The highest variability for both P_{50} and HSM was found in species assemblages occurring in grid cells with relatively high drought incidence (e.g., the Mediterranean basin, W USA, N Mexico, S Australia, Turkey, and S Red Sea in Figure 5.2d, e). This result generalizes previous results found at regional scales (Martínez-Vilalta et al. 2002, Choat et al. 2003, Jacobsen et al. 2007, Johnson et al. 2018). We observed a spatial decoupling at the global scale between hydraulic trait variability and species richness

(Figure S5.4). While species richness peaks in highly favourable habitats without water limitations (Weiser et al. 2007) (Figure S5.4), hydraulic trait variability is higher where water scarcity leads to different physiological solutions to cope with drought in different plant lineages, resulting in a wide range of hydraulic trait values (Martínez-Vilalta et al. 2002, Jacobsen et al. 2007). These results are in contrast with the favourability hypothesis (Fischer 1960) and previous results showing a higher functional diversity towards the equator in some traits (Swenson et al. 2012), but are aligned with other results showing that evolutionary, and potentially functional, diversity peaks under intermediate precipitation (Neves et al. 2020). Then, functional richness may increase in sites with some degree of resource limitation that in turn allows the coexistence of lineages presenting variable drought-coping strategies (e.g., the case of the coexistence of gymnosperms such as *Pinus spp.* and angiosperms such as *Quercus spp.* in Mediterranean forests, with their divergent hydraulic strategies) (Martínez-Vilalta et al. 2002, Martínez-Vilalta et al. 2004). However, this particular result may be influenced by a higher sampling in these areas with higher drought and needs to be confirmed by further studies.

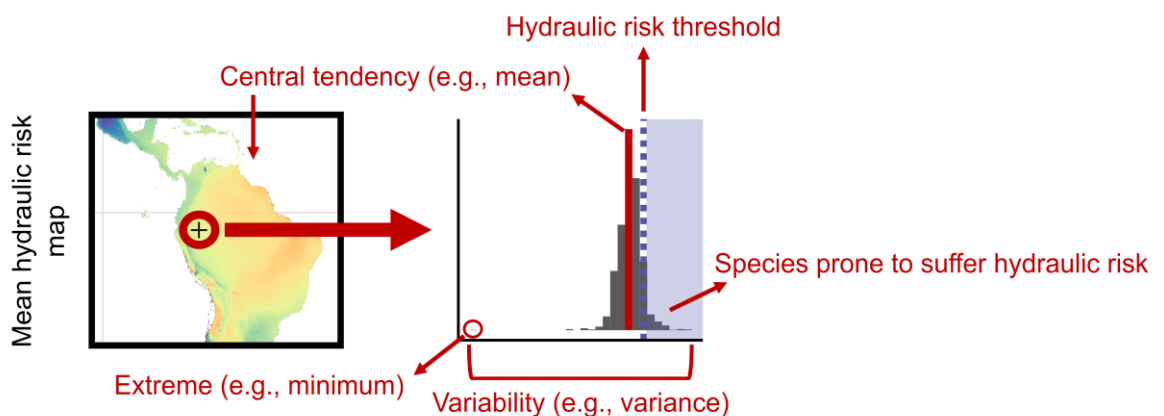
I further characterized the hydraulic risk of species assemblages by calculating the number of species presenting $HSM < 0$, which was considered to be a justified hydraulic risk threshold. The number of species with high hydraulic risk was highly variable (Figure 5.2f), showing a great potential to characterize species-assemblage hydraulic risk. This metric represents the number of species expected to experience hydraulic dysfunction, potentially providing meaningful information on the likelihood of a site experiencing drought induced mortality (DIM). Projections showed that species assemblages with a high number of species with $HSM < 0$ occur both in dry and mesic places (e.g., Mexico and W Amazonia, respectively). However, species presenting the highest hydraulic risk were found in places with high drought incidence (e.g., the Mediterranean basin, W USA, Mexico, SW Australia, S Africa, Figure 5.2g), reflecting that in these places some species are prone to experience high levels of embolism. The

occurrence of invariant minimum values over some large areas likely results from species with particularly low HSM values having widespread distributions. However, in some cases these results may be influenced by limited data availability (e.g., boreal forests in Russia).

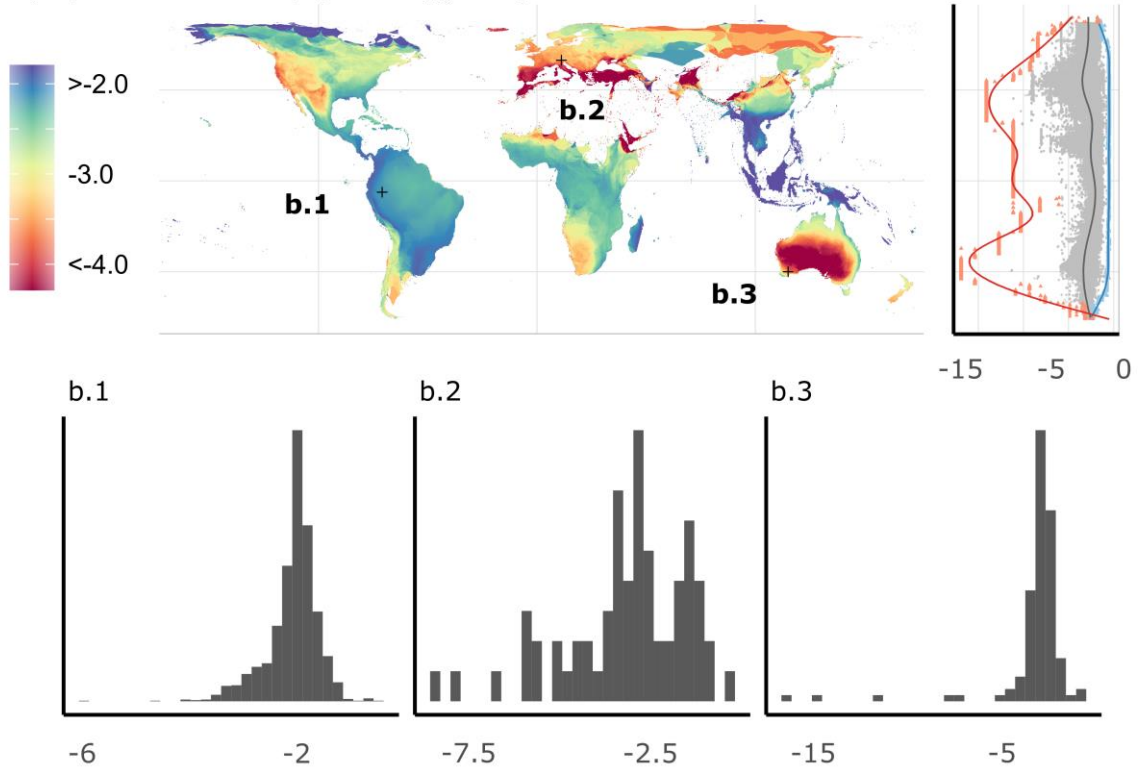
Results based on $HSM_{50/88}$ projections were similar but, as expected, showed a lower total number of species with negative values. $HSM_{50/88}$ results show lower hydraulic safety margins in boreal forests, which may be due the dominance of gymnosperms in this biome and that P_{50} (the value used for gymnosperms for $HSM_{50/88}$) may be easier to surpass compared to P_{88} (the value used for angiosperms) (Figure 5.6).

Figure 5.2 Global distribution of species-assemblage hydraulic metrics a) example on the hydraulic risk composition for a given species assemblage, from which the plotted metrics are calculated. b) mean P_{50} and c) hydraulic risk represented as negative hydraulic safety margin; d) and e) P_{50} and HSM variance; f) the number of species with negative HSM and g) maximum hydraulic risk represented as negative minimum HSM. The distribution of species-level values for a sample of three representative pixels are shown in histograms in b) and c). Lateral scatterplots in b) to g) show the distribution of pixel values by latitude in grey, and absolute minimum and maximum values by latitude as red and blue, respectively.

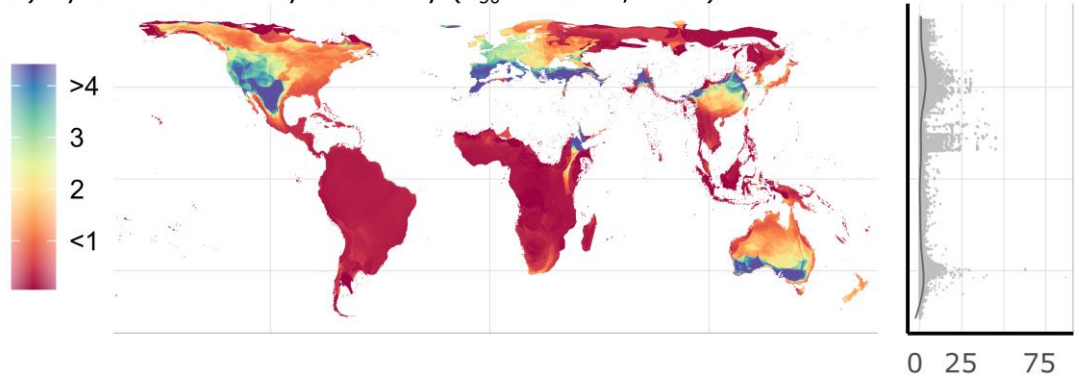
a) Example of species assembly hydraulic risk composition



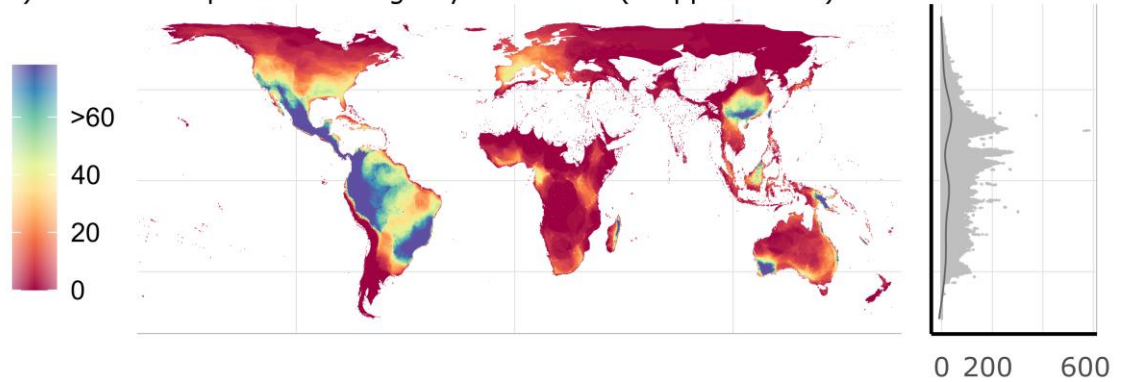
b) Xylem vulnerability (Mean P_{50} , MPa)



d) Xylem vulnerability variability (P_{50} variance, MPa^2)

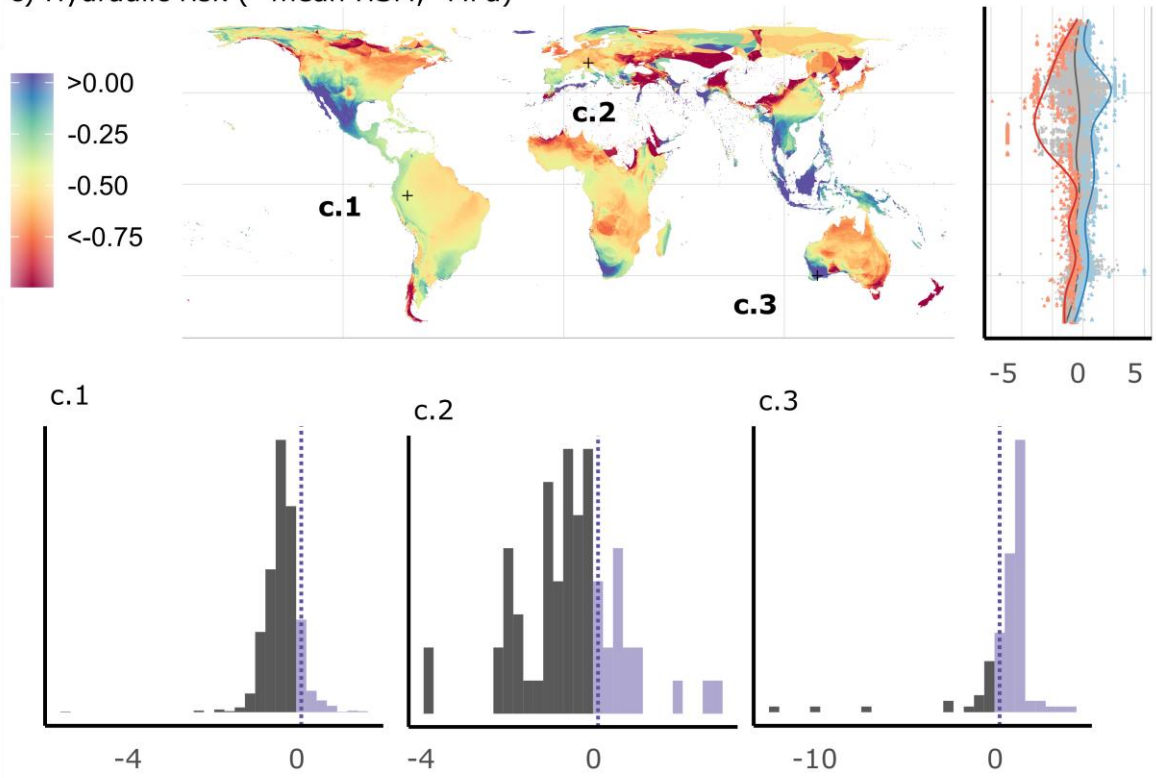


f) Number of species with high hydraulic risk (N spp. HSM<0)

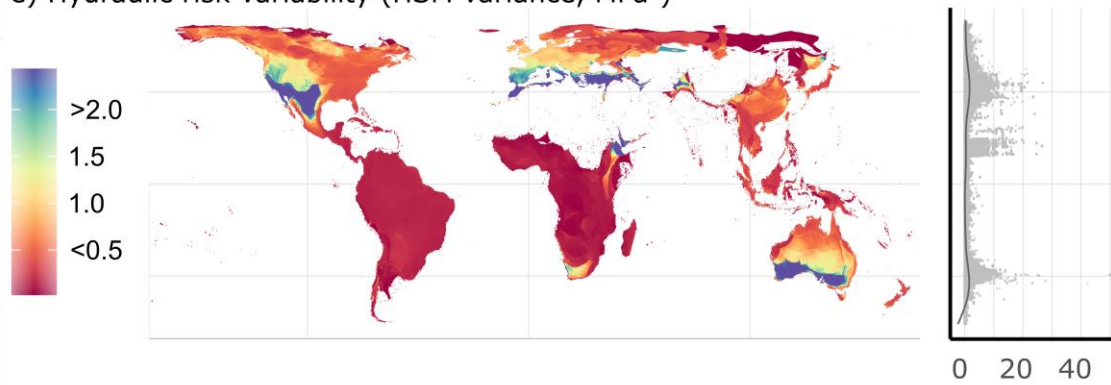


● Mean — Trend for maximum
 — Trend for mean — Trend for minimum

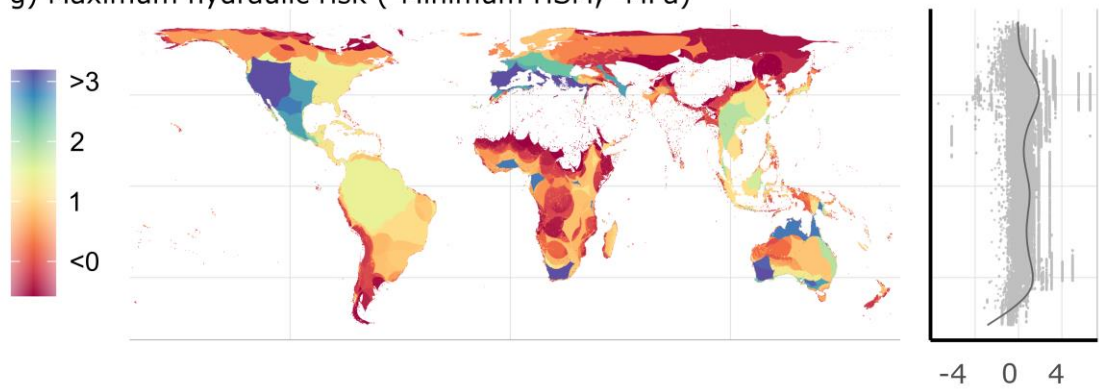
c) Hydraulic risk (- mean HSM, -MPa)



e) Hydraulic risk variability (HSM variance, MPa²)



g) Maximum hydraulic risk (-Minimum HSM, -MPa)



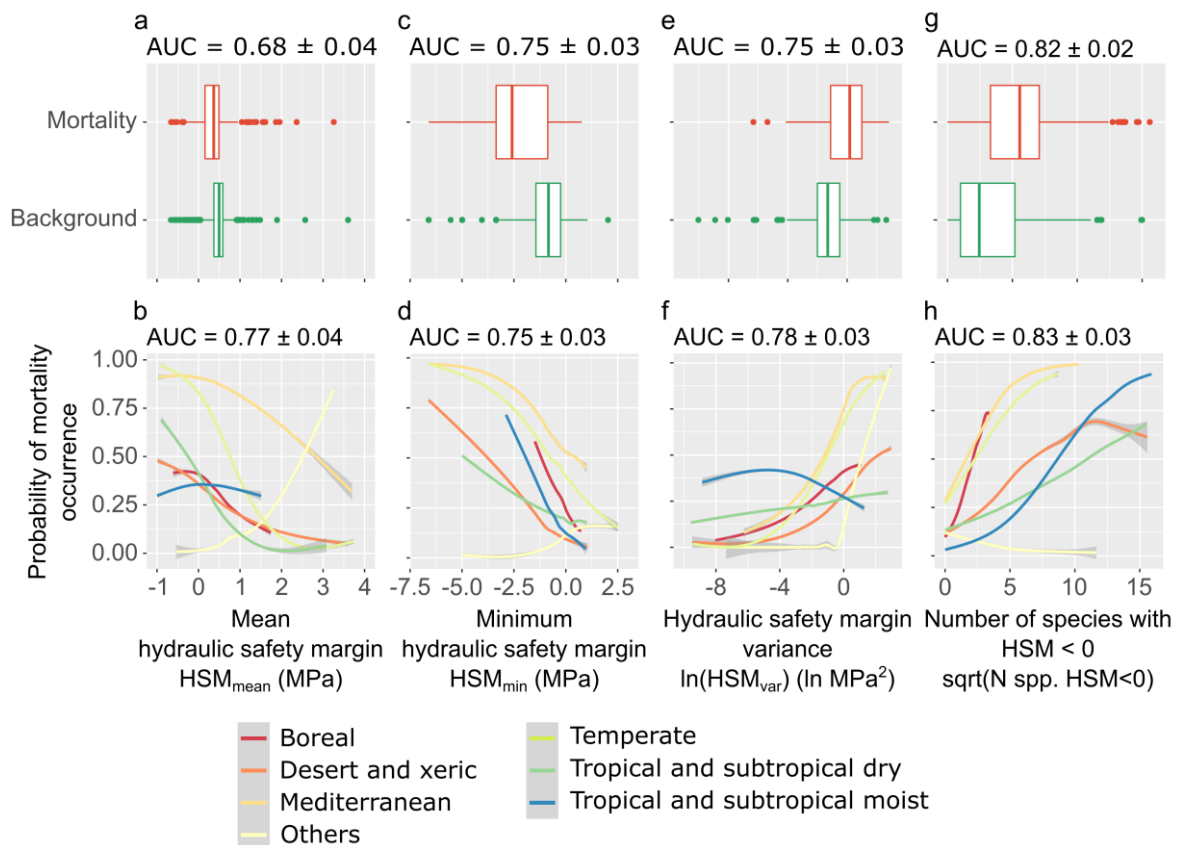
5.3.4 Species-assemblage hydraulic risk is positively related to drought-induced mortality occurrence

I found significant relationships ($p < 0.01$) between species-assemblage hydraulic risk metrics and drought-induced mortality (DIM) occurrence (Figure 5.3). Compared to species-level hydraulic safety margins, species-assemblage hydraulic risk metrics had higher predictive power for DIM occurrence (pseudo- R^2 between 0.14 and 0.36, AUC between 0.68 and 0.84) and far outperformed the predictive power of a climatic aridity index, annual precipitation, and maximum temperature (pseudo- $R^2 < 0.02$, AUC < 0.6) (Table S5.2). The relationships of species assemblages' hydraulic metrics with DIM occurrence remained significant even after the climatic aridity index was included in the models as a covariate (Table S5.3 and S5.4). These results indicate that metrics related to the hydraulic risk of local species assemblages incorporate meaningful information beyond the local drought status. The relationships between DIM occurrence and species assemblage's hydraulic risk metrics were highly consistent across different biomes and plant functional types (PFTs) (Figure 5.3, Figure S5.7, Table S5.3, Table S5.4, Table S5.6).

Overall, sites comprising species assemblages with higher hydraulic risk (i.e., lower mean and minimum HSM and higher number of species with HSM < 0) exhibited higher DIM occurrence probability. In the case of the relationship between the number of species with HSM < 0 , the effect remained significant when species richness was included as a covariate. In fact, species richness itself was not a strong predictor of DIM occurrence. Thus, the relationship between the number of species with HSM < 0 and DIM occurrence was not driven by species number *per se*, but by the relationship between the number of species with high hydraulic risk and DIM. I show that places with higher HSM variance tend to present higher DIM occurrence. This pattern was largely explained by the strong correlation between HSM variance and minimum HSM, the latter being related to DIM probability. Our results show that species with the highest hydraulic risk of an assemblage may be under a higher mortality risk. Their

removal could generate directional functional changes (Pérez-Navarro et al. 2021), decreasing site-specific functional richness and potentially amplifying negative effects on ecosystem functioning (García-Valdés et al. 2018, Esquivel-Muelbert et al. 2019, Batllori et al. 2020).

Figure 5.3 Relationship between drought-induced mortality occurrence and species-assembly hydraulic metrics a) and b) mean HSM, c) and d) minimum HSM, e) and f) HSM variance and g) and h) the number of species with HSM < 0 excluding and including their interaction with biome (top and bottom rows, respectively). Results summarize 100 iterations of each model. In each iteration, a different random set of background points was sampled. In the top row, boxplots show species-assembly metrics values for pixels with mortality compared to background locations. In the bottom row, mean response curves for individual species-assembly metrics for each biome.

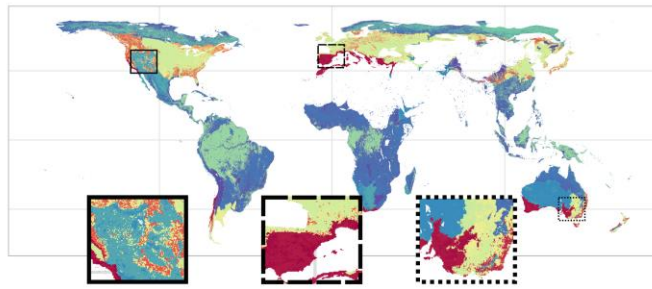


5.3.5 Spatial patterns in the probability of DIM occurrence

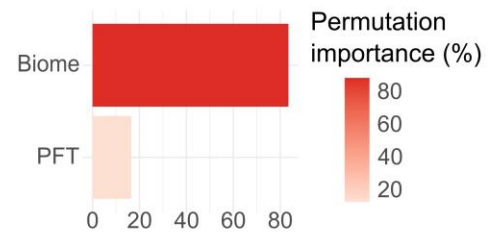
I built on our significant predictive models described above to estimate DIM occurrence probability worldwide with maximum entropy models (Phillips and Dudík 2008). Our results supported the usefulness of the newly derived hydraulic risk metrics at the species assemblage level to predict DIM occurrence, increasing predictive performance compared to models based only on environmental variables, biome, and broad plant functional types (PTFs) (Figure 5.4). The number of species with HSM < 0 was the most important explanatory variable in these models. Results showed that high DIM risk is predicted in e.g., the Mediterranean Basin, southern Australia, western North America and western tropical South America. Models including hydraulic risk metrics better constrained DIM occurrence probability in places with abundant mortality information (e.g., the Iberian Peninsula), limiting the environmental space where mortality is predicted to occur by considering the functional characterization of species assemblages. However, differences between models are more difficult to interpret in regions where mortality data are scarce or absent (Figure S5.4c), such as the African continent and Russian boreal forests. In these cases, the inclusion of the functional perspective may be over-constraining the model, leading to an underestimation of the probability of DIM occurrence.

These results show the capability of functional data to improve the predictive capacity for vegetation responses to climate change at broad spatial scales. By considering geographical variability in functional composition, physiological mechanisms involved in species responses to the environment can be characterized and the vulnerability of communities can be better assessed.

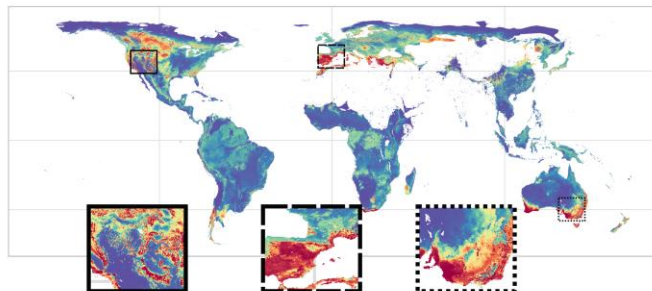
a) Biome and functional type predictors



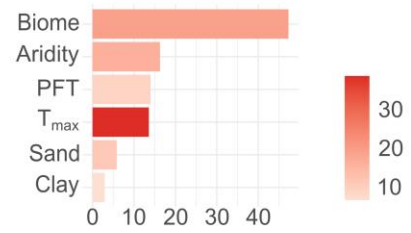
AUC = 0.77 ± 0.03



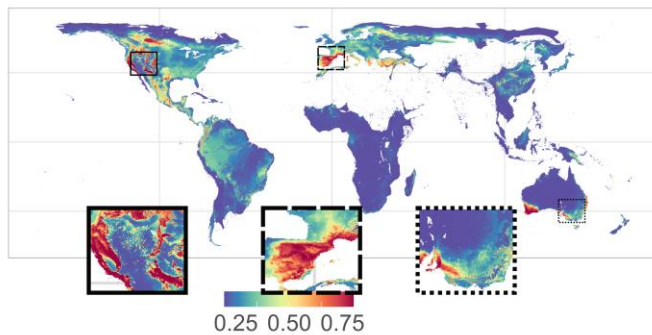
b) Biome, functional type and environmental predictors



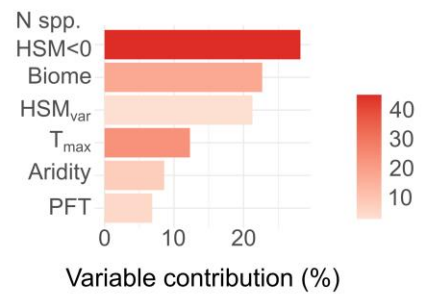
AUC = 0.84 ± 0.01



c) Biome, functional type, environmental and hydraulic risk predictors



AUC = 0.88 ± 0.02



Drought-induced mortality occurrence probability

Figure 5.4 Projection of drought-induced mortality occurrence probability Model's performance (test AUC), variables contribution and their permutation importance are displayed. Predictors used in each case are indicated (see methods).

5.3.6 Future directions

Future efforts to improve the monitoring of observed drought-induced mortality (DIM) as well as the characterization of hydraulic risk under different climate change scenarios will enable better assessments of when and where high mortality is to be expected, and the corresponding impacts on ecosystem composition, structure, and function. Better knowledge on eco-evolutionary relationships among functional traits will improve predictive models, leading to lower imputation error and a better functional characterization of species assemblages. Furthermore, inclusion of intraspecific variability is clearly important to better assess geographical patterns in functional traits and associated environmental responses. Including data on species abundances will also lead to a more realistic characterization of the hydraulic safety margin (HSM) distribution within each species assemblage. In fact, results obtained here substantially differed from HSM projections using community weighted means for a smaller region (USA) (Trugman et al. 2020), even though they were reasonably consistent for P₅₀ mean projections as well as for metrics that are not based on abundances, such as trait ranges (Figure S5.9). In addition, HSM can be considered a static proxy for hydraulic risk at a given site, but any temporally explicit prediction of DIM risk would need to consider the characteristics of specific droughts in terms of duration and intensity, and their impact on tissue-level exposure. Finally, considering additional ecological and historical factors such as the likelihood of biotic attacks, land use change, extreme event legacies, and microclimatic conditions (McDowell et al. 2008, Trugman et al. 2021) should further improve predictions of DIM probability.

In conclusion, I show that species assemblage hydraulic metrics are related to DIM and improve DIM prediction at the global scale, particularly compared to species-level mean values or projections based on climate and coarse functional classifications. I show that locations with higher numbers of species with high hydraulic risk tend to present higher DIM. The approach presented here also represents a step forward in predicting plant functional trait values, providing continuous multi-layer maps that

supplement environmental and coarse plant functional type characterisations. Further, the geographical characterization of functional trait distributions provided here is likely of broad interest to improve the parametrization of terrestrial biosphere models (De Kauwe et al. 2020, Eller et al. 2020), and complements other recent efforts using model inversion to predict hydraulic traits at the global scale (Liu et al. 2020). However, the mortality projections presented are limited by the availability of spatially explicit hydraulic and mortality data as well as tree abundance data and should be seen as a starting point to improve global-scale mortality projections.

5.4 MATERIALS AND METHODS

5.4.1 Species distribution data

Spatially-explicit alpha-hull terrestrial range distributions of 44,901 species derived from compilations of species presence records (Serra-Diaz et al. 2017) were used to determine species assemblages within 5 km grid cells. Species nomenclature was standardized using the *Taxonstand* R package (Cayuela et al. 2012) and species taxonomy was filled using the *taxonlookup* R package (Pennell et al. 2016), both following The Plant List nomenclature.

5.4.2 Hydraulic data

I extracted values from the recently updated xylem traits database (Hammond et al. 2021) for minimum water potential recorded in the xylem (P_{\min}) and water potential at the 50% and 88% loss of conductivity (P_{50} and P_{88}) for 685, 1,376 and 735 species, respectively, measured in stems of mature individuals. P_{50} and P_{88} included only observations with values $< -0.5\text{MPa}$ that originated from S-shaped vulnerability curves. Taxonomic standardization was conducted as described above.

P_{\min} estimated as the absolute minimum xylem water pressure recorded for a given species can be prone to biases (Martínez-Vilalta et al. 2021), so I tested for its relationship with soil minimum water availability and maximum vapour pressure deficit within the distribution of the species, which were considered to be among the main environmental drivers of its variation. Soil minimum water potential ($P_{\min \text{ soil}}$) was calculated and projected worldwide at 5 km resolution using the minimum soil water content at 0-100cm depth over the last 40 years from ERA5-Land monthly averaged data (Muñoz-Sabater et al. 2021), soil texture information for the same depth layers (Hengl et al. 2017) and following Saxton & Rawls (Saxton and Rawls 2006) using the *medfate* R package (De Cáceres et al. 2021b). Then, $P_{\min \text{ soil}}$ values were extracted for all pixels using species distributions and summarized by calculating mean values per species. The cross-species relationship between soil and plant minimum water potentials was positive and significant ($R^2 = 0.12$; Figure S5.10). The large scatter around this relationship likely reflects differences in rooting depth (and hence explored soil volume) across species, as well as substantial methodological uncertainties for both P_{\min} estimation approaches. P_{\min} also showed a significant relationship with maximum vapour pressure deficit (VPD_{\max}), as expected, with more negative minimum water potentials under a higher atmospheric water demand ($R^2 = 0.20$, Figure S5.10).

5.4.3 Environmental data

To characterize edaphoclimatic affiliations for all the species for which we had range distributions, I downloaded global layers describing climatic variables from Worldclim v2 (Fick and Hijmans 2017) and soil characteristics variables from SoilGrids (Montzka et al. 2017) at a resolution of 2.5 arcmin. I then extracted the values for each species using species range distributions data and the *sf* and *raster* R packages (Pebesma 2018, Hijmans 2021). Environmental variables were selected based on their importance in a previous study (Sanchez-Martinez et al. 2020). The following layers describing species' historical climate (averaged values for 1970-2000) (Fick and Hijmans 2017)

were considered: mean annual temperature (°C), minimum temperature of the coldest month (°C), mean temperature of the wettest month (°C), mean temperature of the driest month (°C), isothermality (unitless), temperature seasonality (°C), annual precipitation (mm), precipitation of the wettest month (mm), precipitation of the driest month (mm), precipitation seasonality (mm), precipitation of the warmest quarter (mm), precipitation of the coldest quarter (mm), mean solar radiation ($\text{kJ m}^{-2} \text{day}^{-1}$), mean vapour pressure (kPa) and mean wind speed (m s^{-1}). I also extracted monthly maximum temperature values and the vapour pressure for the same months to calculate maximum vapour pressure deficit (kPa) for each species distribution using the *SVP* function from the *humidity* R package (Cai 2019). Layers describing soil characteristics were absolute depth to bedrock (cm), soil water content at 200 cm depth (percentage), cation exchange capacity at 30 cm depth (cmolc/kg), clay content at 30 cm depth (percentage), organic carbon at 30 cm depth (permille) and pH at 30 cm depth (pH).

Mean values for each species range were calculated for each environmental variable and were transformed to achieve normality when needed (ln or square root-transformed). To summarize environmental information, I implemented a principal component analysis on species mean values for the whole set of variables using the *princomp* function from the *stats* R package (R Core Team 2020). The first five principal components explained 82.3% of the variance and were used in further analyses.

Additional environmental information required in some analyses (see the last two methods sections below) was downloaded separately. This included the aridity index (Trabucco and Zomer 2018), historical maximum temperature for 1970-2000 (Fick and Hijmans 2017), as well as biome identity (Dinerstein et al. 2017) and pixel-level plant functional type (ERA Copernicus 2019 land cover version 2.1.1) (Muñoz-Sabater et al. 2021). All these environmental layers were aggregated to a 5 km² resolution for further use with the *raster* R package (Hijmans 2021).

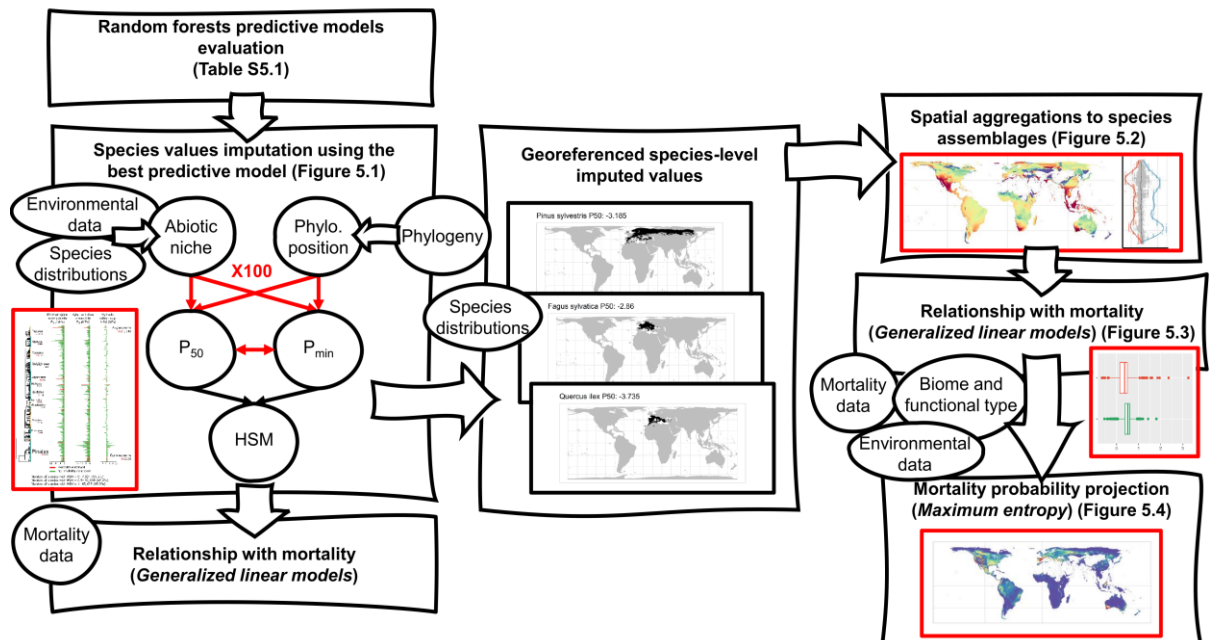
5.4.4 Mortality database

I used a global database on forest die-off events related to drought and/or heat (Allen et al. 2010, Hammond et al. 2022), which is an updated and geographically referenced version of the Allen et al. (2010) dataset. This new database was a spatial points data frame covering 1,303 mortality events records (Figure S5.4c), with documented affected species in each instance (> 400 tree species worldwide). Taxonomic standardization was conducted for species in the mortality database as described above.

5.4.5 Phylogenetic information

To include species phylogenetic information, I used a newly-derived genus-level phylogeny covering 3,488 genera (Segovia et al. 2020) to construct a phylogenetic distance matrix between taxa using the *cophenetic.phylo* function of the *ape* R package (Paradis and Schliep 2019). The distance matrix was used to calculate phylogenetic principal coordinates values for each genus using the *pcoa* function of the *ape* R package (Paradis and Schliep 2019). Then, coordinate values were assigned to each species. Overall, I generated a dataset covering 44,901 species with complete environmental and phylogenetic data and some sparse data on hydraulic traits distributed throughout the phylogeny. I also constructed a species-level phylogeny using the *V.PhyloMaker* R package (Jin and Qian 2019) matching our species list. I used the species-level phylogeny only for plotting purposes because it contained many polytomies and because genus-level approaches can be considered more reliable, especially for tropical clades where species misidentification can be an issue (Baker et al. 2017).

Figure 5.5 Methodology Scheme of the methodology implemented, and the data used in each case. The data used is shown in black circles. The main results obtained in each step are also referred in red boxes.



5.4.6 Hydraulic traits predictions using phylogenetic and edaphoclimatic data

I used random forest models as implemented by the *missForest* R package (Stekhoven and Bühlmann 2012) to predict and impute species-level P_{\min} and P_{50} values for the 44,901 woody plant species with available distribution data. Before performing the imputations, I tested the predictive performance of a set of models including different combinations of phylogenetic principal coordinates, environmental principal components and including or excluding major evolutionary affiliation (angiosperms vs gymnosperms). I built models that predicted one trait at a time, or both (P_{\min} and P_{50}), within the same model (in the latter case, trait covariation was explicitly considered). To do so, I used the subset of species for which hydraulic measurements were available and calculated R^2 values following a 10-fold cross-validation procedure using different

proportions of train and test observations in each case (from 10 to 70% of data used to test and the remaining to train). Each model was iterated 100 times using a random selection of training and test points, maintaining the proportions in each case. I calculated the mean R^2 and its standard deviation in each case (Table S5.1), and the model with the highest mean R^2 was subsequently used to predict trait values with all available data as training data and was iterated 100 times. The best predictive model included the first five phylogenetic principal coordinates and the first five environmental principal components, while considering the covariation between traits and major evolutionary affiliation, reaching mean R^2 of 0.60 ± 0.10 and 0.54 ± 0.12 for P_{\min} and P_{50} , respectively (Table S5.1, see Figure 5.5 for a schematic description of the process leading to the results presented in the main text). As some studies have pointed out that P_{88} may be a better hydraulic failure threshold for angiosperm species (Hammond et al. 2019), I also performed predictions using P_{88} instead of P_{50} for angiosperms ($P_{50/88}$ and $HSM_{50/88}$ hereafter).

Imputed values were summarized at the species level, calculating the mean and the standard deviation from the 100 iterations of the predictive model, and HSM values were calculated from imputed mean-hydraulic trait values in each case ($HSM = P_{\min} - P_{50}$). Imputed values were plotted on a species-level phylogeny (Figure 5.1 shows hydraulic traits imputation at the species-level for those species with at least one trait with observed values) as well as on the genus-level phylogeny (by averaging values per genera) (Figure S5.1 and Figure S5.2 to see mean and standard deviation of data aggregated at the genus level, respectively). To assess model uncertainty related to the identity and number of species used to train the predictive model, I repeated it 100 times, randomly excluding 20% of species with observed data each time and calculating the standard deviation of the predicted values for each species.

The predictive framework was also implemented using P_{50} values for gymnosperm species and P_{88} values for angiosperm species ($P_{50/88}$), calculating $HSM_{50/88}$ (Figure S5.3). I obtained a lower predictive performance, reaching a mean R^2 of 0.43 ± 0.12

(mean and standard deviation for $P_{50/88}$ from the previously described cross-validation procedure), probably because of a higher error in P_{88} estimates and lower data availability compared to P_{50} . Given the lower performance of $HSM_{50/88}$ models, the lower data availability for $P_{50/88}$ compared to P_{50} and considering that P_{88} was highly related to P_{50} ($R^2 = 0.69$, Figure S5.10), I used P_{50} and standard HSM to report the main results.

5.4.7 Geographical projection of hydraulic traits and calculation of pixel-level species assemblages hydraulic metrics

In order to plot hydraulic metrics for species assemblages, I first spatially referenced species-level imputed data for 44,901 species using their spatial range distribution (Serra-Diaz et al. 2017) (Figure S5.4a and b to see species range distribution coverage for imputed and observed traits data, respectively). Spatial projections were implemented by assuming fixed trait values at the species level (as I expect intraspecific variability to be much lower than interspecific variability for hydraulic traits) (Anderegg 2015, Rosas et al. 2019, Skelton et al. 2019). Then, I aggregated trait values for species with overlapping distributions at the pixel level by calculating their mean, minimum, and variance as a measure of functional variability by using the *fasterize* function of the *fasterize* R package (Ross n.d.), and the *rasterize* function of the *raster* R package (Hijmans 2021) in the case of the variance. By doing so, I obtained 5 km² raster layers for P_{50} and HSM mean and their variability (Figure 5.2), minimum HSM (Figure 5.2), P_{\min} mean and its variability (Figure S5.5), $P_{50/88}$ and $HSM_{50/88}$ mean and their variability (Figure S5.6). Note that mean HSM and minimum HSM were reported as negative HSM so higher values represent higher hydraulic risk. This was performed for consistency with P_{50} plots, as higher P_{50} represents higher embolism vulnerability. These maps should be interpreted as predicted values, and then will only be relevant in areas with woody plant vegetation.

I also spatially aggregated cross-species P_{50} and HSM standard deviations by calculating the mean from the 100 iterations of the predictive model including all species (Figure S5.8a, c and e) and excluding the 20% of species with observed trait data in each iteration (Figure S5.8b, d and f). Then, I report two measures of model uncertainty aggregated at the spatial scale: the first one showing the uncertainty of the predictive model at the species level and the second one the uncertainty linked to the identity of the species represented in the training data used. The uncertainty due to the identity of the species used to train models is higher than the model uncertainty (Figure S5.8). For HSM and $HSM_{50/88}$ spatially referenced values, I also calculated the number of species with negative values per pixel at 5 km² resolution using the same approach (Figure 5.2 and Figure S5.6 for HSM and $HSM_{50/88}$, respectively).

In order to better visualize variability in raster plots, I restricted values using the *clamp* function from the *raster* R package (Hijmans 2021), setting the 0.05 quantile as the lower value and the 0.95 quantile as the upper value.

5.4.8 Assessing the predictive capacity of hydraulic risk against mortality records

First, I tested the relationship between imputed species-level HSM values and the presence-absence of observed mortality as well as the number of mortality events recorded per species as reported in the global mortality database (Hammond et al. 2022). I used generalized linear models through the *glm* function of the *stats* R package (R Core Team 2020), setting the family parameter to *binomial* in the first case and to *Poisson* in the second one. To see the effects of angiosperm-gymnosperm affiliation in this relationship, I included the major evolutionary affiliation as an explanatory factor interacting with HSM. As the number of species without observed mortality was much higher than the number with observed mortality, I randomly selected the same number of species without observed mortality events to match the number of species with

mortality events (i.e., 482). I repeated this procedure 100 times and averaged the results in both cases.

To explore the relationship between the spatial projection of hydraulic metrics and mortality occurrence as reported by the global DIM database (Hammond et al. 2022), I used binomial generalized linear models with the *glm* function of the *stats* R package (R Core Team 2020). I kept one mortality event per square kilometre, reducing the number of geographical points with observed DIM from 1,303 to 882 to avoid over-representing areas with a higher sampling effort. In order to assess the degree of spatial autocorrelation of models, I performed Mantel tests on all models' residuals using the function *mantel.rtest* of the *Ade4* package (Dray and Dufour 2007). The spatial autocorrelation was <0.06 in all cases. The response variable in our models was mortality occurrence (1 for pixels with at least one mortality event observed and 0 for the same number of randomly sampled pixels without observed mortality). Backgrounds could include some presences, so to deal with the lack of absence points I repeated models 100 times randomly changing background points and averaged results. The explanatory variables included HSM-derived variables related to the hydraulic risk of species assemblages (pixel mean, minimum, variance, and number of species with $HSM < 0$), as well as their interaction with biome and plant functional type (e.g., broadleaf deciduous, broadleaf evergreen, needle leaved, etc.) (Figure 5.3, Figure S5.7). An aridity index, annual precipitation and maximum temperature were also included as predictors in a separate model to assess their individual predictive power (Table S5.2). Biome and functional type categories were reclassified to maintain as many observations per category as possible (Table S5.5). I included biome and functional type as factors in the models to check for changes in the magnitude and direction of the relationships between species-assemblage hydraulic metrics and DIM as well as to improve predictions by better representing broad vegetation types (e.g., see the Amazon Basin in Figure 5.4). Note that our data have a low number of observations in some biome and functional type groups, so no firm conclusions were drawn from the differences among factor levels.

The number of species per pixel was also included as a covariate in a model using the number of species with HSM < 0 to check for the effect of species number on its relationship with DIM occurrence. HSM variance and HSM minimum as well as their interaction were also considered together in the same model to better understand their non-independent relationship with DIM occurrence. Trend significance was tested by using the *emmeans* R package (Lenth 2021) (Table S5.6). Each model was run 100 times using a different set of background points and pseudo-R² values were calculated using the *rml* R package (Harrel 2020) (Table S5.2). Test AUC values were also calculated using the *dismo* R package (Hijmans et al. 2017) following a cross-validation procedure with 80% of the data to train and 20% to test. All models were re-run including aridity index values extracted from mortality and background points as a co-variate to test whether trait effects remained significant when the climate was considered, which was the case. To check for variable significance, I implemented ANOVA tests using the *anova* function from the *stats* R package (R Core Team 2020) (Table S5.3 and S5.4 to see the mean results calculated from 100 iterations in each case for models excluding and including aridity index as a covariate, respectively). As a further check, I repeated the same procedures but I was more restrictive in aggregating mortality data to avoid over-representing areas with higher sampling intensity (W USA, SW Australia and Europe) (Varela et al. 2014). When I kept only one mortality occurrence per 10 km² (Varela et al. 2014), reducing the number of occurrences from 1,303 to 517, the results did not differ.

5.4.9 Projecting mortality risk using maximum entropy models

I used maximum entropy models (Phillips and Dudík 2008) as implemented by the *dismo* R package (Hijmans et al. 2017) to predict and project drought-induced mortality (DIM) probability at the global scale. I used this methodology instead of the previous binomial generalized linear models as it accounts better for presence/background point data under a predictive framework. This allowed us to better characterize the background by including more background points than presences, a procedure not recommended with generalized linear models (Elith et al. 2006). Moreover, this technique presents higher predictive performance than generalized linear models because of its capability to account for non-linearities and multiple interactions between predictors (Merow et al. 2013). Three types of models were run: (a) using only functional type and biome distributions as predictors, (b) as in “a” plus continuous environmental variables and (c) as in “b” plus the projected hydraulic metrics as predictors. In order to maximise predictive performance while keeping the lowest number of predictors, only continuous variables with high predictive power that presented Pearson cross-correlation coefficients among themselves lower than 0.75 were included in models “b” and “c”. These variables were maximum temperature, aridity index, soil sand and clay content for models including environmental variables and the number of species with HSM < 0, HSM variance, maximum temperature and aridity index for models including both hydraulic traits and environmental variables. In all cases, biome and functional type were included as predictive factors. Note that none of the environmental variables used to predict mortality was included in the environmental principal components used to predict species-level hydraulic traits from which species assemblage hydraulic metrics were calculated. Models “b” and “c” were constructed to contain the same number of predictors in order to facilitate their comparability.

In this instance, mortality data was aggregated to keep one occurrence per 10 km² to avoid overfitting (Varela et al. 2014) (N occurrences = 517) while standardizing the spatial resolution with the layers used as predictors. Models were trained using the *hinge* option (similar to GAM) with 10,000 randomly sampled background points (but models were also trained using 1,000 and 50,000 randomly sampled background points to assess model consistency). To evaluate model performance, each model was trained using 80% of the data and tested using the remaining 20%, and this procedure was repeated 100 times in each case (randomly changing training and test data points) and test AUC values were calculated and summarized by calculating their mean and standard deviation to assess performance (Figure 5.4). I made sure to include both points with observed mortality and background points in all cases by sampling the 80% and the 20% in each of these groups separately and then unifying the datasets, following previous implementations (Sanchez-Martinez et al. 2021). Finally, a single model trained using all observations was implemented for model types “a”, “b” and “c” (see above) and used to project mortality occurrence probability geographically (Figure 5.4). Variable importance was assessed by its relative (percentage) contribution to the fit of the models as generated by the *maxent* jack-knife procedure, which compares the training gain for each variable in isolation to the training gain of the model with all variables (Figure 5.4). Permutation importance was also calculated for each environmental variable by randomly permuting presence and background values, re-evaluating the model and calculating the resulting drop in training AUC, normalized as a percentage (Figure 5.4).

6 GENERAL DISCUSSION AND CONCLUSIONS

6.1 INSIGHTS FROM AN EVOLUTIONARILY EXPLICIT FRAMEWORK IN ECOPHYSIOLOGY

In this thesis, I demonstrate the insightful results that can be obtained by considering phylogenies to estimate the effect of evolutionary histories in the current diversity of plant functional strategies and their relationship with species niche. The novelty of the framework presented resides in the capability to separate phylogenetically conserved and evolutionary labile patterns in functional traits individually, as well as in their relationship and in their individual and integrated response to environmental conditions. By doing so, the evolution of functional trait syndromes can be better understood, and this information can be used to scale functional aspects from species to communities and ecosystems.

Previous methodologies focused on the so-called evolutionary correlations, which are relationships among functional traits that are not explained by major lineage divergences and then, are hypothesized to present a functional cause (Felsenstein 1988). Evolutionary correlations are based in the cladistic perspective, where only derived characters are related to adaptation and any inherited ancestral state needs no further explanation (Hansen 1997). Under this framework, trait coordination and trade-offs will appear as a result of an optimization of plant function in response to selective pressures. Then, deviations from the optimal value of traits can be attributed to evolutionary inertia (*sensu* Blomberg, (Blomberg and Garland 2002)) of lineages, understood as the lineage-specific contingencies that is adding noise to adaptation patterns and needs to be factored out. This perspective has showed to be highly insightful in a number of studies showing how phylogenetically corrected traits relate (Ackerly and Reich 1999, Maherali et al. 2004, Martínez-Vilalta et al. 2014). However, this methodology undermines the effect of stabilizing selection and environmental filtering, which are important processes shaping species adaptive response (Hansen 1997). These two processes can lead to a pattern of phylogenetic conservatism in adaptation. Then, the

phylogenetic structure of functional traits syndromes can be of interest by itself to elucidate which processes are leading to species adaptation under different conditions. In this thesis, I propose and apply a complementary method to the evolutionary correlation framework that can provide extra insights on the evolution of functional strategies.

Under an evolutionary perspective, species can achieve different adaptive optima in response to the same conditions, as diversification of lineages and disparification of traits can lead to different successful strategies. Then, trait values will be not only affected by external conditions but also by the evolutionary history of a given taxa, describing the evolutionary paths taken by ancestors which constrain the adaptive options that are available for descendants. In fact, one could hypothesize that, if functional syndromes evolution is constrained (e.g., traits under stabilizing selection), the weight of evolutionary history of trait syndromes on the conformation of adaptive optima may be higher than that of environmental conditions. If this is true, most species inhabiting a given community will rarely reach the hypothetical optima expected from their relationship with the environment. Instead, these species will adopt suboptimal functional traits values that allowed them to survive and reproduce under a given set of conditions, but that cannot fully reach the optima due to evolutionary constraints. The integration between traits can itself be constraining the optimization of a given trait, diminishing its degrees of freedom by limiting the potential values that it can take based on other trait values. Under suboptimal conditions, functional trait values may not be able to maximize performance responses related to growth, reproduction and survival and then, their life history will be modulated accordingly. In this scenario, eco-evolutionary processes shaping community functional composition will be quite different compared to the scenario where environmental conditions are the main drivers of traits variation. In this thesis, I provided insights on which evolutionary scenarios are more plausible by elucidating the importance of phylogenetic conservatism and evolutionary lability in functional strategies and their relationship with environmental conditions.

The eco-evolutionary perspective of this thesis has proven to be valuable to better understand ecological processes related to species assemblage, ecological strategies, and responses to environmental forcing. First, elucidating that phylogenetic conservatism in ecological strategies (here, including functional strategies and life history strategies) can be very useful to assess adaptive capability of species under a changing climate. Second, moving from a taxon-based community ecology and biogeography to a one based on functional syndromes can be highly insightful to close the gap between mechanisms and observed patterns in species distributions and abundances. Finally, a unified framework will serve to bring ecophysiologicals and evolutionary biologists into a common field, seeking to better understand living systems from an integrated perspective and across scales, from the micro evolutionary at local scale to the macroevolutionary at global scale.

6.2 PHYLOGENETIC NICHE CONSERVATISM IN FUNCTIONAL SYNDROMES

Our results show a predominant pattern of phylogenetic conservatism in functional trait syndromes which is related to the abiotic niche. This points that functional syndromes evolution is constrained and slow, leading to a pattern where closely related taxa tend to resemble each other in their functional strategies (Losos 2008). The fact that this conservatism is generally related to environmental conditions describing species abiotic niche suggests that adaptation under stabilizing selection may underlie macroevolutionary variability in trait syndromes (Hansen 1997). However, phylogenetic conservatism may indicate that even if adaptation occurs it may be not the only process shaping species assemblages. Being adapted to survive under a given set of conditions is a prerequisite determining species distributions and then, environmental filtering may be crucial to determine which species are present under a given set of conditions. Contrarily, in a scenario where evolutionary lability plays a more important role, we would expect rapid adaptation or plasticity to allow species to survive

under new conditions, with a lower importance of lineage-specific environmental filtering on species distributions.

Results reported in this thesis do not completely discard evolutionary lability, as phylogenetic conservatism in individual traits is not maximized. Some traits, such as photosynthetic capability present a labile evolution leading to rapid adaptation, while others, like embolism resistance, are more evolutionarily constrained. The underlying causal phenotype related to structural and physiological determinants of each trait may play an important role in determining to what degree traits can vary at different scales. For instance, embolism resistance depends on the structure and anatomy of the xylem, which is expected to be rather canalized (Lamy et al. 2014, Lobo et al. 2018, Pritzkow et al. 2020). This may contribute to the slower adaptive response of this trait, while other traits such as photosynthetic capacity can be modulated by the expression in living cells which are expected to be more responsive to external conditions related to resource availability. It is important to note that the macroecological perspective taken in this thesis (i.e., working at the species or supra-specific levels) may be undermining the role of local adaptation and plasticity, as a good representation of within-species variability is not included. Then, the take home message in this regard would be that trait syndromes present a significant degree of phylogenetic conservatism that can be highly informative and should not be overlooked. However, future work is needed to expand this framework by including within-species variability to better quantify evolutionary lability at smaller scales in time and space (e.g., local adaptation and phenotypic plasticity).

Importantly, the novel multivariate perspective taken in the current thesis elucidates how trait correlations may present a strong phylogenetic component. These patterns suggest that traits may be integrated into different modules that respond to selective pressures, maintaining the underlying trait relationships. Then, some traits may be tightly hardwired and may evolve together responding to external conditions, which would constrain the potential values that individual traits can take. This pattern may be underlined by a causal relationship between traits, constraining each other's values. In this case, evolutionary history takes a key role in shaping functional patterns, potentially producing deviations from the optimal relationship between individual traits and environmental conditions (keeping other trait values constant) that would not maximize performance but allow for survival and reproduction leading to successful strategies in a specific evolutionary context. In fact, the relationship between functional traits and environmental conditions has been shown to be rather weak (Anderegg 2022), while its relationship with phylogenies as shown in this thesis is generally strong.

Evolutionary history has shown to be highly informative when predicting traits at the species level, in line with previous findings (Swenson 2014, Anderegg et al. 2021). Moreover, by finding patterns in data, one can make decisions on which of the potential predictors may work better to predict missing values in functional traits. In the present thesis I present an algorithm that automatizes this process of selection and performs predictions using phylogenetic, environmental, and functional data available. This will allow to impute traits at different scales, helping to address the functional data scarcity problem (see chapter 3). In addition, this approach has great potential to elucidate how functional syndromes distribute and using the resulting, spatially explicit information to better assess climate change impacts on vegetation.

6.3 ECOLOGICAL CONSEQUENCES OF FUNCTIONAL STRATEGIES EVOLUTION

Once we better understand functional traits evolutionary patterns, it is then worth to see how they translate into ecological consequences affecting species performance, their distributions, and their response to environmental conditions. In his thesis I report the relationship between functional traits and life history traits from an evolutionary explicit perspective (chapter 4). Then, I show an example on the scaling from evolutionary patterns in trait syndromes to ecological consequences by exploring the spatial relationship between physiological hydraulic risk of species assemblages and drought-induced mortality at the global scale (chapter 5).

6.3.1 Functional strategies relationship with life history strategies

In this thesis I report that functional traits and life history traits are evolutionarily related in a case study for Amazon trees. I show how depending on the traits and the aspect of life history, relationships can be evolutionarily constrained and/or evolutionarily labile. Results showed how species with acquisitive leaves tend to be evolutionarily constrained to present a lower investment per unit offspring and lower survival, while species with conservative leaves are evolutionarily constrained to present a higher investment per unit offspring and higher survival. I show how size and growth conform to another module which presented a higher evolutionary lability. These patterns indicate that species performance may be at least partially determined by their functional trait syndromes, which then influence life history evolution, conforming to ecological strategies which are partially phylogenetically conserved, suggesting some degree of evolutionary constrains.

Labile modules may be able to rapidly respond to environmental changes over evolutionary timescales, while conserved ones may be more strongly determining the ecological niche, having a higher impact on species distributional ranges and abundances. This is shown in this thesis by the phylogenetic conserved relationships between functional trait syndromes and environmental conditions characterizing species niches. In a first case, I showed how hydraulic trait syndromes are related to variables describing water availability (chapter 2). In a second case I showed how functional trait syndromes representing leaf economics and hydraulics are related to aridity (chapter 3), both in a phylogenetically conserved manner. In contrast to most of the functional traits studied in this thesis, life history traits such as maximum growth rate present a lower phylogenetic conservatism, being likely to be more responsive to environmental changes at short evolutionary timescales (i.e., within genera), having an impact on community structure by influencing, for instance, species size distributions (chapter 4).

In this thesis I report how acquisitive species will occupy environmental spaces that meet their higher resource demand (e.g., higher water availability), rapidly producing a high quantity of relatively small seeds, related to a colonizer and fast behaviour referred as a pioneer strategy (Turner 2001). Conservative species will present a higher capability to tolerate stress and then, higher lifespan, with a delayed reproduction and a higher degree of investment per unit seed (chapter 4). According to these results, woody plant species are not expected to drastically change their functional strategies as quantified by leaf economic traits. Instead, they will respond to the environment by modulating those traits that present a higher lability, such as growth rates, which are disconnected from leaf economics. Then, under stressful conditions, species are expected to evolve to present a lower growth capability, which will have an impact on the maximum size that they can reach. When pushed towards its physiological limit, a stop in growth may happen as a consequence of a function-environment mismatch. When stress is beyond the physiological limits and/or is

maintained through time, these species are prone to present higher levels of mortality as a result of a dysfunction of some physiological processes (Hammond 2020).

Knowledge on functional strategies evolution can help elucidate how species will be able to respond to environmental forcing, especially when contextualized in a framework that relates physiology with performance. Scaling from the organ-specific physiological measures to effects at the whole-plant, population, community, and ecosystem-level has been shown to be a challenge (Mencuccini et al. 2019a). In this regard, understanding how functional traits are related and how they affect performance from an evolutionary perspective can pave the ground for future frameworks determining how function-environment mismatches are likely to affect species capability to maintain viable populations under different environmental scenarios and the ecological effects that may emerge.

6.3.2 Effects of functional strategies on vegetation responses to climate

Finally, in this thesis I attempt to develop a geographically explicit framework relating function-environment mismatches with species persistence. Here, I focus on a widely reported phenomena as it is global drought-induced mortality (DIM) in woody plants, specifically focusing in a well-known underlying physiological threshold related to hydraulic disfunction (Hammond 2020) (see chapter 5). The rationale behind this framework is the following: (1) drought-induced mortality has been mainly attributed to hydraulic failure, (2) we can characterize the risk to suffer hydraulic failure (hydraulic risk) of species by using functional traits, (3) functional traits determining hydraulic risk are phylogenetically conserved and related to species abiotic niche (see chapter 2) so we can successfully predict them for a high number of species, (4) we can calculate site-specific hydraulic metrics describing species-assemblage hydraulic risk by geographically referencing species-level hydraulic traits, (5) we expect communities with

a higher number of species under hydraulic risk to present a higher DIM when drought and heat waves strike, as these species will be more vulnerable to a decrease in water availability and rapid adaptation in functional traits determining hydraulic risk is not expected. In this thesis, I show how this rationale is confirmed and that newly derived hydraulic risk metrics predict spatial patterns of DIM at the global scale. By doing so, I demonstrate how functional traits can be aggregated from the organ to the community level and its usage improve our capability to understand and predict climate change impacts on vegetation worldwide.

Adaptive capability of crucial functional traits determining species responses to stress will strongly influence the fate of organisms, populations, and species under a changing world (Hammond 2020, McDowell et al. 2021). In this thesis, I have shown how woody plant functional strategies present a rather constrained evolution at the species level. I also showed how functional trait syndromes are related to a broad characterization of species niche, so plant function, and more concretely the hydraulic function, may be crucial in determining the environmental space that species can occupy, being under stabilizing selection, which leads to a predominant pattern of phylogenetic niche conservatism. If environmental conditions change, mismatches with hydraulic function could push some species outside the environmental space under which they can survive. This will have an impact on community- and ecosystem-level properties, such as a decrease in biodiversity which is expected to have negative impacts on ecosystem functioning and structure (Batllori et al. 2020, García-Valdés et al. 2020). Due to the dependence of human societies on living systems, it is of great urgency to further study how environmental changes will affect ecosystems, understanding the causal mechanisms and the *causa ultima* of their occurrence to better manage endangered ecosystems to ensure their persistence under future conditions.

6.4 CONCLUSIONS

I conclude that:

1. Hydraulic trait syndromes are phylogenetically conserved and related to water availability, pointing to a pattern of phylogenetic niche conservatism potentially underlined by stabilizing selection and environmental filtering.
2. Hydraulic traits are integrated with leaf economics in a phylogenetically conserved way and in response to aridity, pointing that aridity levels may act as an important selective pressure promoting the integration of different plant functions at the macroevolutionary scale.
3. Functional traits of Amazonian tree taxa describing resource uptake and process are integrated with life history traits describing growth, survival, and reproduction in a phylogenetically conserved way, while growth and size conform to an independent axis of variation which is more evolutionary labile.
4. Species-assemblages hydraulic risk is positively related with drought induced mortality at the global scale, Improving its prediction.
5. Implementing the proposed methodological framework can help elucidate the evolutionary basis of plant functional strategies and their ecological consequences at macroevolutionary and macroecological scales.

6.5 FUTURE DIRECTIONS

This thesis is mainly focused on a species- and supra-specific levels, and hence, it is based on a macroevolutionary and macroecological perspective. The study of specific lineages can complement results obtained in this thesis by specifically testing whether patterns reported here are universal or whether some exceptions may exist under specific evolutionary and ecological contexts. I acknowledge that working at the species and supra-specific levels present some drawbacks and that within-species variability can certainly buffer some of the patterns shown under the current framework by including local adaptation and phenotypic plasticity under different environmental conditions. These two aspects of trait syndromes variability are crucial to inform the current macroecological and macroevolutionary perspective with some microevolutionary insights at the local scale. Currently, there is not enough data available to include these aspects at global scale. However, meaningful examples already exist. For instance, recent studies showed how variability in vulnerability to embolism is mainly allocated at the interspecific level, being very low at the intra-specific level for the *Quercus* genera (Lobo et al. 2018, Skelton et al. 2019) and *Pinus* genera (Martínez-Vilalta et al. 2009, López et al. 2016). In fact, vulnerability to embolism has been shown to present a low genetic variability and phenotypic plasticity in *Pinus pinaster*, which points that this highly meaningful trait may be strongly canalized (Lamy et al. 2014). In contrast, specific leaf area and leaf size has been shown to present meaningful variability within species related to local adaptation to rainfall in the Mediterranean oak *Quercus suber* (Ramírez-Valiente et al. 2010). Then, further work on the characterization of intraspecific variability in trait suits will be of great interest to better understand vegetation responses to the environment, complementing the macroevolutionary perspective taken here.

Focusing on a micro-evolutionary perspective at local scale will also allow to close the gap between physiology and genetics. This is a challenging research field, as the expression of physiology is expected to have a complex genetic basis. However, recent advances in eco-physiology and genetics pave the ground for such studies and efforts in this direction are becoming more common (Pereira and Des Marais 2020). The determination of the phenotypical basis (i.e., biological structures resulting from genetic expression) of some crucial functional traits related, for instance, to drought tolerance and avoidance strategies could be a first step in this direction. Then, once the phenotypical basis of a given functional trait is well-known, the genetic basis may be easier to determine. With this knowledge, ecosystem management will have the tools to understand species responses to the environment in a more holistic and integrated way, understanding the mechanisms (physiology) impacting performance, their causal explanation (biological structures and specific genes) and their evolutionary background (phylogenetic structure of these functional traits and their phenotypic and genetic basis).

7 REFERENCES

- Ackerly, D. 2009. Conservatism and diversification of plant functional traits: Evolutionary rates versus phylogenetic signal. *Proceedings of the National Academy of Sciences* 106:19699–19706.
- Ackerly, D. D., and M. J. Donoghue. 1995. Phylogeny and ecology reconsidered. *The Journal of Ecology* 83:730.
- Ackerly, D. D., and M. J. Donoghue. 1998. Leaf size, sapling allometry, and Corner's rules: Phylogeny and correlated evolution in maples (*Acer*). *American Naturalist* 152:767–791.
- Ackerly, D. D., Dudley, Susan A, S. E. Sultan, J. Schmitt, J. S. Coleman, C. R. Linder, D. R. Sandquist, M. A. Geber, A. S. Evans, T. E. Dawson, and M. J. Lechowicz. 2000. The Evolution of Plant Ecophysiological Traits: Recent Advances and Future Directions. *BioScience* 50:979.
- Ackerly, D. D., and P. B. Reich. 1999. Convergence and correlations among leaf size and function in seed plants: A comparative test using independent contrasts. *American Journal of Botany* 86:1272–1281.
- Adams, H. D., M. J. B. Zeppel, W. R. L. Anderegg, H. Hartmann, S. M. Landhäusser, D. T. Tissue, T. E. Huxman, P. J. Hudson, T. E. Franz, C. D. Allen, L. D. L. Anderegg, G. A. Barron-Gafford, D. J. Beerling, D. D. Breshears, T. J. Brodribb, H. Bugmann, R. C. Cobb, A. D. Collins, L. T. Dickman, H. Duan, B. E. Ewers, L. Galiano, D. A. Galvez, N. Garcia-Forner, M. L. Gaylord, M. J. Germino, A. Gessler, U. G. Hacke, R. Hakamada, A. Hector, M. W. Jenkins, J. M. Kane, T. E. Kolb, D. J. Law, J. D. Lewis, J. M. Limousin, D. M. Love, A. K. Macalady, J. Martínez-Vilalta, M. Mencuccini, P. J. Mitchell, J. D. Muss, M. J. O'Brien, A. P. O'Grady, R. E. Pangle, E. A. Pinkard, F. I. Piper, J. A. Plaut, W. T. Pockman, J. Quirk, K. Reinhardt, F. Ripullone, M. G. Ryan, A. Sala, S. Sevanto, J. S. Sperry, R. Vargas, M. Vennetier, D. A. Way, C. Xu, E. A. Yopez, and N. G. McDowell. 2017. A multi-species synthesis of physiological mechanisms in drought-induced tree mortality. *Nature Ecology and Evolution* 1:1285–1291.
- Adler, P. B., R. Salguero-Gómez, A. Compagnoni, J. S. Hsu, J. Ray-Mukherjee, C. Mbeau-Ache, and M. Franco. 2014. Erratum: Functional traits explain variation in plant life history

strategies(Proc Natl Acad Sci USA (2014) 111, 2 (740-745)

DOI:10.1073/pnas.1315179111). Proceedings of the National Academy of Sciences of the United States of America 111:10019.

Alboukadel Kassambara, and Fabian Mundt. 2020. factoextra: Extract and Visualize the Results of Multivariate Data Analyses. R package version 1.0.7.

Allen, C. D., A. K. Macalady, H. Chenchouni, D. Bachelet, N. McDowell, M. Vennetier, T. Kitzberger, A. Rigling, D. D. Breshears, E. H. (Ted. Hogg, P. Gonzalez, R. Fensham, Z. Zhang, J. Castro, N. Demidova, J. H. Lim, G. Allard, S. W. Running, A. Semerci, and N. Cobb. 2010. A global overview of drought and heat-induced tree mortality reveals emerging climate change risks for forests. *Forest Ecology and Management* 259:660–684.

Anderegg, L. D. 2022. Why can't we predict traits from the environment? *New Phytologist*.

Anderegg, L. D. L., D. M. Griffith, J. Cavender- Bares, W. J. Riley, J. A. Berry, T. E. Dawson, and C. J. Still. 2021. Representing plant diversity in land models: An evolutionary approach to make 'Functional Types' more functional. *Global Change Biology*.

Anderegg, W. R. L. 2015. Spatial and temporal variation in plant hydraulic traits and their relevance for climate change impacts on vegetation. *New Phytologist* 205:1008–1014.

Anderegg, W. R. L., J. A. Berry, D. D. Smith, J. S. Sperry, L. D. L. Anderegg, and C. B. Field. 2012. The roles of hydraulic and carbon stress in a widespread climate-induced forest die-off. *Proceedings of the National Academy of Sciences of the United States of America* 109:233–237.

Anderegg, W. R. L., A. Flint, C. Y. Huang, L. Flint, J. A. Berry, F. W. Davis, J. S. Sperry, and C. B. Field. 2015. Tree mortality predicted from drought-induced vascular damage. *Nature Geoscience* 8:367–371.

Anderegg, W. R. L., T. Klein, M. Bartlett, L. Sack, A. F. A. Pellegrini, B. Choat, and S. Jansen. 2016. Meta-analysis reveals that hydraulic traits explain cross-species patterns of drought-induced tree mortality across the globe. *Proceedings of the National Academy of Sciences of the United States of America* 113:5024–5029.

- Anderegg, W. R. L., A. G. Konings, A. T. Trugman, K. Yu, D. R. Bowling, R. Gabbitas, D. S. Karp, S. Pacala, J. S. Sperry, B. N. Sulman, and N. Zenes. 2018a. Hydraulic diversity of forests regulates ecosystem resilience during drought. *Nature* 561:538–541.
- Anderegg, W. R. L., A. G. Konings, A. T. Trugman, K. Yu, D. R. Bowling, R. Gabbitas, D. S. Karp, S. Pacala, J. S. Sperry, B. N. Sulman, and N. Zenes. 2018b. Managing the Risks of Extreme Events and Disasters to Advance Climate Change Adaptation. A Special Report of Working Groups I and II of the Intergovernmental Panel on Climate Change. (Cambridge Univ. Press, Cambridge, 2012). *Nature* 561:538–541.
- Baas, P., F. W. Ewers, S. D. Davis, and E. A. Wheeler. 2004. Evolution of xylem physiology. *The Evolution of Plant Physiology*:273–295.
- Baker, T. R., R. T. Pennington, K. G. Dexter, P. V. A. Fine, H. Fortune-Hopkins, E. N. Honorio, I. Huamantupa-Chuquimaco, B. B. Klitgård, G. P. Lewis, H. C. de Lima, P. Ashton, C. Baraloto, S. Davies, M. J. Donoghue, M. Kaye, W. J. Kress, C. E. R. Lehmann, A. Monteagudo, O. L. Phillips, and R. Vasquez. 2017. Maximising Synergy among Tropical Plant Systematists, Ecologists, and Evolutionary Biologists. *Trends in Ecology and Evolution* 32:258–267.
- Baraloto, C., C. E. T. Paine, L. Poorter, J. Beauchene, D. Bonal, A. M. Domenach, B. Hérault, S. Patiño, J. C. Roggy, and J. Chave. 2010. Decoupled leaf and stem economics in rain forest trees. *Ecology Letters* 13:1338–1347.
- Batllori, E., F. Lloret, T. Aakala, W. R. L. Anderegg, E. Aynekulu, D. P. Bendixsen, A. Bentouati, C. Bigler, C. J. Burk, J. J. Camarero, M. Colangelo, J. D. Coop, R. Fensham, M. L. Floyd, L. Galiano, J. L. Ganey, P. Gonzalez, A. L. Jacobsen, J. M. Kane, T. Kitzberger, J. C. Linares, S. B. Marchetti, G. Matusick, M. Michaelia, R. M. Navarro-Cerrillo, R. B. Pratt, M. D. Redmond, A. Rigling, F. Ripullone, G. Sangüesa-Barreda, Y. Sasal, S. Saura-Mas, M. L. Suarez, T. T. Veblen, A. Vilà-Cabrera, C. Vincke, and B. Zeeman. 2020. Forest and woodland replacement patterns following drought-related mortality. *Proceedings of the National Academy of Sciences of the United States of America* 117:29720–29729.
- Berling, D. J., and C. K. Kelly. 1996. Evolutionary comparative analyses of the relationship

- between leaf structure and function. *New Phytologist* 134:35–51.
- Bhaskar, R., and D. D. Ackerly. 2006. Ecological relevance of minimum seasonal water potentials. *Physiologia Plantarum* 127:353–359.
- Blomberg. 2016. A primer phylogenetic Generalized Least Squares. Page (L. Z. Garamszegi, Ed.) *Modern Phylogenetic Comparative Methods and their Application in Evolutionary Biology*. Springer Berlin Heidelberg, Berlin, Heidelberg.
- Blomberg, S. P., and T. Garland. 2002. Tempo and mode in evolution: Phylogenetic inertia, adaptation and comparative methods. *Journal of Evolutionary Biology* 15:899–910.
- Blomberg, S. P., T. Garland, and A. R. Ives. 2003. Testing for phylogenetic signal in comparative data: Behavioral traits are more labile. *Evolution* 57:717–745.
- Bonan, G. B. 2008. Forests and Climate Change: Forcings, Feedbacks, and the Climate Benefits of Fiorests. *Science* 320:1444–1449.
- Brodribb, T., and R. S. Hill. 1999. The importance of xylem constraints in the distribution of conifer species. *New Phytologist* 143:365–372.
- Brodribb, T. J., and S. A. M. McAdam. 2017. Evolution of the stomatal regulation of plant water content. *Plant Physiology* 174:639–649.
- Brodribb, T. J., S. A. M. McAdam, G. J. Jordan, and S. C. V. Martins. 2014. Conifer species adapt to low-rainfall climates by following one of two divergent pathways. *Proceedings of the National Academy of Sciences* 111:14489–14493.
- Brodribb, T. J., J. Powers, H. Cochard, and B. Choat. 2020. Hanging by a thread? Forests and drought. *Science* 368:261–266.
- van Buuren, S., and K. Groothuis-Oudshoorn. 2011. mice: Multivariate imputation by chained equations in R. *Journal of Statistical Software* 45:1–67.
- De Cáceres, M., M. Mencuccini, N. Martin-StPaul, J.-M. M. Limousin, L. Coll, R. Poyatos, A.

- Cabon, V. Granda, A. Forner, F. Valladares, and J. Martínez-Vilalta. 2021a. Unravelling the effect of species mixing on water use and drought stress in Mediterranean forests: A modelling approach. *Agricultural and Forest Meteorology* 296.
- De Cáceres, M., M. Mencuccini, N. Martin-StPaul, J.-M. M. Limousin, L. Coll, R. Poyatos, A. Cabon, V. Granda, A. Forner, F. Valladares, and J. Martínez-Vilalta. 2021b. Unravelling the effect of species mixing on water use and drought stress in Mediterranean forests: A modelling approach. *Agricultural and Forest Meteorology* 296.
- Cai, J. 2019. humidity: Calculate Water Vapor Measures from Temperature and Dew Point. R package version 0.1.5.
- Canadell, J., R. B. Jackson, J. R. Ehleringer, H. A. Mooney, O. E. Sala, and E. D. Schulze. 1996. Maximum rooting depth of vegetation types at the global scale. *Oecologia* 108:583–595.
- Cavender-Bares, J., D. D. Ackerly, S. E. Hobbie, and P. A. Townsend. 2016. Evolutionary Legacy Effects on Ecosystems: Biogeographic Origins, Plant Traits, and Implications for Management in the Era of Global Change. Page Annual Review of Ecology, Evolution, and Systematics.
- Cayuela, L., Í. Granzow-de la Cerda, F. S. Albuquerque, and D. J. Golicher. 2012. Taxonstand: An r package for species names standardisation in vegetation databases. *Methods in Ecology and Evolution* 3:1078–1083.
- Chamberlain, S., V. Barve, D. Mcglinn, D. Oldoni, P. Desmet, L. Geffert, and K. Ram. 2023. rgbif: Interface to the Global Biodiversity Information Facility API. R package version 3.7.5.
- Chase, M. W., M. J. M. Christenhusz, M. F. Fay, J. W. Byng, W. S. Judd, D. E. Soltis, D. J. Mabberley, A. N. Sennikov, P. S. Soltis, P. F. Stevens, B. Briggs, S. Brockington, A. Chautems, J. C. Clark, J. Conran, E. Haston, M. Möller, M. Moore, R. Olmstead, M. Perret, L. Skog, J. Smith, D. Tank, M. Vorontsova, and A. Weber. 2016. An update of the Angiosperm Phylogeny Group classification for the orders and families of flowering plants: APG IV. *Botanical Journal of the Linnean Society* 181:1–20.

- Chave, J., D. Coomes, S. Jansen, S. L. Lewis, N. G. Swenson, and A. E. Zanne. 2009. Towards a worldwide wood economics spectrum. *Ecology Letters* 12:351–366.
- Chen, K., K. S. Burgess, X. Y. Yang, Y. H. Luo, L. M. Gao, and D. Z. Li. 2018. Functional trade-offs and the phylogenetic dispersion of seed traits in a biodiversity hotspot of the Mountains of Southwest China. *Ecology and Evolution* 8:2218–2230.
- Cheverud, J. M. 1996. Developmental integration and the evolution of pleiotropy. *American Zoologist* 36:44–50.
- Chhetri, H. B., D. Macaya-Sanz, D. Kainer, A. K. Biswal, L. M. Evans, J. G. Chen, C. Collins, K. Hunt, S. S. Mohanty, T. Rosenstiel, D. Ryno, K. Winkeler, X. Yang, D. Jacobson, D. Mohnen, W. Muchero, S. H. Strauss, T. J. Tschaplinski, G. A. Tuskan, and S. P. DiFazio. 2019. Multitrait genome-wide association analysis of *Populus trichocarpa* identifies key polymorphisms controlling morphological and physiological traits. *New Phytologist* 223:293–309.
- Choat, B., M. Ball, J. Luly, and J. Holtum. 2003. Pit membrane porosity and water stress-induced cavitation in four co-existing dry rainforest tree species. *Plant Physiology* 131:41–48.
- Choat, B., T. Brodribb, C. Brodersen, R. Duursma, R. López, and B. Medlyn. 2018a. Triggers of tree mortality under drought. *Nature* 558:531–539.
- Choat, B., T. J. Brodribb, C. R. Brodersen, R. A. Duursma, R. López, and B. E. Medlyn. 2018b. Triggers of tree mortality under drought. *Nature* 558:531–539.
- Choat, B., S. Jansen, T. J. Brodribb, H. Cochard, S. Delzon, R. Bhaskar, S. J. Bucci, T. S. Feild, S. M. Gleason, U. G. Hacke, A. L. Jacobsen, F. Lens, H. Maherali, J. Martínez-Vilalta, S. Mayr, M. Mencuccini, P. J. Mitchell, A. Nardini, J. Pittermann, R. B. Pratt, J. S. Sperry, M. Westoby, I. J. Wright, and A. E. Zanne. 2012. Global convergence in the vulnerability of forests to drought. *Nature* 491:752–755.
- Coelho de Souza, F., K. G. Dexter, O. L. Phillips, R. J. W. Brienen, J. Chave, D. R. Galbraith, G. Lopez Gonzalez, A. Monteagudo Mendoza, R. T. Pennington, L. Poorter, M. Alexiades, E. Álvarez-Dávila, A. Andrade, L. E. O. C. Aragão, A. Araujo-Murakami, E. J. M. M. Arets, G.

- A. Aymard C, C. Baraloto, J. G. Barroso, D. Bonal, R. G. A. Boot, J. L. C. Camargo, J. A. Comiskey, F. C. Valverde, P. B. de Camargo, A. Di Fiore, F. Elias, T. L. Erwin, T. R. Feldpausch, L. Ferreira, N. M. Fyllas, E. Gloor, B. Herault, R. Herrera, N. Higuchi, E. N. Honorio Coronado, T. J. Killeen, W. F. Laurance, S. Laurance, J. Lloyd, T. E. Lovejoy, Y. Malhi, L. Maracahipes, B. S. Marimon, B. H. Marimon-Junior, C. Mendoza, P. Morandi, D. A. Neill, P. N. Vargas, E. A. Oliveira, E. Lenza, W. A. Palacios, M. C. Peñuela-Mora, J. J. Pipoly, N. C. A. Pitman, A. Prieto, C. A. Quesada, H. Ramirez-Angulo, A. Rudas, K. Ruokolainen, R. P. Salomão, M. Silveira, J. Stropp, H. Ter Steege, R. Thomas-Caesar, P. van der Hout, G. M. F. van der Heijden, P. J. van der Meer, R. V. Vasquez, S. A. Vieira, E. Vilanova, V. A. Vos, O. Wang, K. R. Young, R. J. Zagt, and T. R. Baker. 2016. Evolutionary heritage influences Amazon tree ecology. *Proceedings. Biological sciences* 283.
- Crisp, M. D., M. T. K. Arroyo, L. G. Cook, M. A. Gandolfo, G. J. Jordan, M. S. McGlone, P. H. Weston, M. Westoby, P. Wilf, and H. P. Linder. 2009. Phylogenetic biome conservatism on a global scale. *Nature* 458:754–756.
- Crisp, M. D., and L. G. Cook. 2012. Phylogenetic niche conservatism: What are the underlying evolutionary and ecological causes? *New Phytologist* 196:681–694.
- Cruzan, M. B. 2018. *Evolutionary biology : a plant perspective*. New York, NY : Oxford University Press.
- Csardi, G., and T. Nepusz. 2006. The igraph software package for complex network research. *InterJournal, Complex Systems*.
- Cunningham, S. A., B. Summerhayes, and M. Westoby. 1999. Evolutionary divergences in leaf structure and chemistry, comparing rainfall and soil nutrient gradients. *Ecological Monographs* 69:569–588.
- Davies, T. J., E. M. Wolkovich, N. J. B. Kraft, N. Salamin, J. M. Allen, T. R. Ault, J. L. Betancourt, K. Bolmgren, E. E. Cleland, B. I. Cook, T. M. Crimmins, S. J. Mazer, G. J. McCabe, S. Pau, J. Regetz, M. D. Schwartz, and S. E. Travers. 2013. Phylogenetic conservatism in plant phenology. *Journal of Ecology* 101:1520–1530.

- DeBruine Lisa. 2021. faux: Simulation for Factorial Designs R package version 1.1.0. Zenodo.
- Delzon, S. 2015. New insight into leaf drought tolerance. *Functional Ecology* 29:1247–1249.
- Delzon, S., and H. Cochard. 2014. Recent advances in tree hydraulics highlight the ecological significance of the hydraulic safety margin. *New Phytologist* 203:355–358.
- Dexter, K., and J. Chave. 2016. Evolutionary patterns of range size, abundance and species richness in Amazonian angiosperm trees. *PeerJ* 2016:1–14.
- Díaz, S., J. Kattge, J. H. C. Cornelissen, I. J. Wright, S. Lavorel, S. Dray, B. Reu, M. Kleyer, C. Wirth, I. Colin Prentice, E. Garnier, G. Bönsch, M. Westoby, H. Poorter, P. B. Reich, A. T. Moles, J. Dickie, A. N. Gillison, A. E. Zanne, J. Chave, S. Joseph Wright, S. N. Sheremet'ev, H. Jactel, C. Baraloto, B. Cerabolini, S. Pierce, B. Shipley, D. Kirkup, F. Casanoves, J. S. Joswig, A. Günther, V. Falczuk, N. Rüger, M. D. Mahecha, and L. D. Gorné. 2016. The global spectrum of plant form and function. *Nature* 529:167–171.
- Dinerstein, E., D. Olson, A. Joshi, C. Vynne, N. D. Burgess, E. Wikramanayake, N. Hahn, S. Palminteri, P. Hedao, R. Noss, M. Hansen, H. Locke, E. C. Ellis, B. Jones, C. V. Barber, R. Hayes, C. Kormos, V. Martin, E. Crist, W. Sechrest, L. Price, J. E. M. Baillie, D. Weeden, K. Suckling, C. Davis, N. Sizer, R. Moore, D. Thau, T. Birch, P. Potapov, S. Turubanova, A. Tyukavina, N. De Souza, L. Pintea, J. C. Brito, O. A. Llewellyn, A. G. Miller, A. Patzelt, S. A. Ghazanfar, J. Timberlake, H. Klöser, Y. Shennan-Farpón, R. Kindt, J. P. B. Lillesø, P. Van Breugel, L. Graudal, M. Voge, K. F. Al-Shammari, and M. Saleem. 2017. An Ecoregion-Based Approach to Protecting Half the Terrestrial Realm. *BioScience* 67:534–545.
- Dixon, H. H. 1914. *Transpiration and the ascent of sap in plants*. Macmillan and co., limited, London.
- Dray, S., and A.-B. Dufour. 2007. The ade4 Package: Implementing the Duality Diagram for Ecologists. *Journal of Statistical Software* 22:1–20.
- Ehleringer, J. R., and R. K. Monson. 1993. VARIATION.

- Elith, J., C. H. Graham, R. P. Anderson, M. Dudík, S. Ferrier, A. Guisan, R. J. Hijmans, F. Huettmann, J. R. Leathwick, A. Lehmann, J. Li, L. G. Lohmann, B. A. Loiselle, G. Manion, C. Moritz, M. Nakamura, Y. Nakazawa, J. McC. M. Overton, A. Townsend Peterson, S. J. Phillips, K. Richardson, R. Scachetti-Pereira, R. E. Schapire, J. Soberón, S. Williams, M. S. Wisz, and N. E. Zimmermann. 2006. Novel methods improve prediction of species' distributions from occurrence data. *Ecography* 29:129–151.
- Eller, C. B., L. Rowland, M. Mencuccini, T. Rosas, K. Williams, A. Harper, B. E. Medlyn, Y. Wagner, T. Klein, G. S. Teodoro, R. S. Oliveira, I. S. Matos, B. H. P. Rosado, K. Fuchs, G. Wohlfahrt, L. Montagnani, P. Meir, S. Sitch, and P. M. Cox. 2020. Stomatal optimization based on xylem hydraulics (SOX) improves land surface model simulation of vegetation responses to climate. *New Phytologist* 226:1622–1637.
- Esquivel-Muelbert, A., T. R. Baker, K. G. Dexter, S. L. Lewis, R. J. W. Brienen, T. R. Feldpausch, J. Lloyd, A. Monteagudo-Mendoza, L. Arroyo, E. Álvarez-Dávila, N. Higuchi, B. S. Marimon, B. H. Marimon-Junior, M. Silveira, E. Vilanova, E. Gloor, Y. Malhi, J. Chave, J. Barlow, D. Bonal, N. Davila Cardozo, T. Erwin, S. Fauset, B. Hérault, S. Laurance, L. Poorter, L. Qie, C. Stahl, M. J. P. Sullivan, H. ter Steege, V. A. Vos, P. A. Zuidema, E. Almeida, E. Almeida de Oliveira, A. Andrade, S. A. Vieira, L. Aragão, A. Araujo-Murakami, E. Arets, G. A. Aymard C, C. Baraloto, P. B. Camargo, J. G. Barroso, F. Bongers, R. Boot, J. L. Camargo, W. Castro, V. Chama Moscoso, J. Comiskey, F. Cornejo Valverde, A. C. Lola da Costa, J. del Aguila Pasquel, A. Di Fiore, L. Fernanda Duque, F. Elias, J. Engel, G. Flores Llampazo, D. Galbraith, R. Herrera Fernández, E. Honorio Coronado, W. Hubau, E. Jimenez-Rojas, A. J. N. Lima, R. K. Umetsu, W. Laurance, G. Lopez-Gonzalez, T. Lovejoy, O. Aurelio Melo Cruz, P. S. Morandi, D. Neill, P. Núñez Vargas, N. C. Pallqui Camacho, A. Parada Gutierrez, G. Pardo, J. Peacock, M. Peña-Claros, M. C. Peñuela-Mora, P. Petronelli, G. C. Pickavance, N. Pitman, A. Prieto, C. Quesada, H. Ramírez-Angulo, M. Réjou-Méchain, Z. Restrepo Correa, A. Roopsind, A. Rudas, R. Salomão, N. Silva, J. Silva Espejo, J. Singh, J. Stropp, J. Terborgh, R. Thomas, M. Toledo, A. Torres-Lezama, L. Valenzuela Gamarra, P. J. van de Meer, G. van der Heijden, P. van der Hout, R. Vasquez Martinez, C. Vela, I. C. G. Vieira, and O. L. Phillips. 2019. Compositional response of Amazon forests to climate change. *Global Change Biology* 25:39–56.

- Etterson, J. R., and R. G. Shaw. 2001. Constraint to adaptive evolution in response to global warming. *Science* 294:151–154.
- Felsenstein, J. 1985. Confidence Limits on Phylogenies: An Approach Using the Bootstrap. *Evolution* 39:783.
- Felsenstein, J. 1988. Phylogenies and quantitative characters. *Annual review of ecology and systematics*. Vol. 19:445–471.
- Fick, S. E., and R. J. Hijmans. 2017. WorldClim 2: new 1-km spatial resolution climate surfaces for global land areas. *International Journal of Climatology* 37:4302–4315.
- Fischer, A. G. 1960. Latitudinal variations in organic diversity. *Evolution* 14:64–81.
- Flo, V., J. Martínez-Vilalta, M. Mencuccini, V. Granda, W. R. L. Anderegg, and R. Poyatos. 2021. Climate and functional traits jointly mediate tree water-use strategies. *New Phytologist* 231:617–630.
- Flores, O., E. Garnier, I. J. Wright, P. B. Reich, S. Pierce, S. Diaz, R. J. Pakeman, G. M. Rusch, M. Bernard-Verdier, B. Testi, J. P. Bakker, R. M. Bekker, B. E. L. Cerabolini, R. M. Ceriani, G. Cornu, P. Cruz, M. Delcamp, J. Dolezal, O. Eriksson, A. Fayolle, H. Freitas, C. Golodets, S. Gourlet-Fleury, J. G. Hodgson, G. Brusa, M. Kleyer, D. Kunzmann, S. Lavorel, V. P. Papanastasis, N. Pérez-Harguindeguy, F. Vendramini, and E. Weiher. 2014. An evolutionary perspective on leaf economics: Phylogenetics of leaf mass per area in vascular plants. *Ecology and Evolution* 4:2799–2811.
- Fortunel, C., P. V. A. Fine, and C. Baraloto. 2012. Leaf, stem and root tissue strategies across 758 Neotropical tree species. *Functional Ecology* 26:1153–1161.
- Garamszegi, L. Z. 2014. *Modern Phylogenetic Comparative Methods and Their Application in Evolutionary Biology: Concepts and Practice*. Page Systematic Biology.
- García-Valdés, R., H. Bugmann, and X. Morin. 2018. Climate change-driven extinctions of tree species affect forest functioning more than random extinctions. *Diversity and Distributions* 24:906–918.

- García-Valdés, R., A. Estrada, R. Early, V. Lehsten, and X. Morin. 2020. Climate change impacts on long-term forest productivity might be driven by species turnover rather than by changes in tree growth. *Global Ecology and Biogeography* 29:1360–1372.
- García-Valdés, R., J. Vayreda, J. Retana, and J. Martínez-Vilalta. 2021. Low forest productivity associated with increasing drought-tolerant species is compensated by an increase in drought-tolerance richness. *Global Change Biology*:1–15.
- Garnier, E., and G. Laurent. 1994. Leaf anatomy, specific mass and water content in congeneric annual and perennial grass species. *New Phytologist* 128:725–736.
- Geber, M. A., and L. R. Griffen. 2003. Inheritance and natural selection on functional traits. *International Journal of Plant Sciences* 164.
- Gleason, S. M., M. Westoby, S. Jansen, B. Choat, U. G. Hacke, R. B. Pratt, R. Bhaskar, T. J. Brodribb, S. J. Bucci, K. F. Cao, H. Cochard, S. Delzon, J. C. Domec, Z. X. Fan, T. S. Feild, A. L. Jacobsen, D. M. Johnson, F. Lens, H. Maherali, J. Martínez-Vilalta, S. Mayr, K. A. Mcculloh, M. Mencuccini, P. J. Mitchell, H. Morris, A. Nardini, J. Pittermann, L. Plavcová, S. G. Schreiber, J. S. Sperry, I. J. Wright, and A. E. Zanne. 2016. Weak tradeoff between xylem safety and xylem-specific hydraulic efficiency across the world's woody plant species. *New Phytologist* 209:123–136.
- Goolsby, E. W., J. Bruggeman, and C. Ané. 2017. Rphylopars: fast multivariate phylogenetic comparative methods for missing data and within-species variation. *Methods in Ecology and Evolution* 8:22–27.
- Green, J. K., J. Berry, P. Ciais, Y. Zhang, and P. Gentile. 2020. Amazon rainforest photosynthesis increases in response to atmospheric dryness:1–10.
- Grime, J. P. 1974. Vegetation classification by reference to strategies. *Nature* 252:497–499.
- Grime, J. P., and R. Hunt. 1975. Relative Growth-Rate: Its Range and Adaptive Significance in a Local Flora. *The Journal of Ecology* 63:393.
- Grime, J. P., K. Thompson, R. Hunt, J. G. Hodgson, J. H. C. Cornelissen, I. H. Rorison, G. A.

- F. Hendry, T. W. Ashenden, A. P. Askew, S. R. Band, R. E. Booth, C. C. Bossard, B. D. Campbell, J. E. L. Cooper, A. W. Davison, P. L. Gupta, W. Hall, D. W. Hand, M. A. Hannah, S. H. Hillier, D. J. Hodkinson, A. Jalili, Z. Liu, J. M. L. Mackey, N. Matthews, M. A. Mowforth, A. M. Neal, R. J. Reader, K. Reiling, W. Ross-Fraser, R. E. Spencer, F. Sutton, D. E. Tasker, P. C. Thorpe, and J. Whitehouse. 1997. Integrated Screening Validates Primary Axes of Specialisation in Plants. *Oikos* 79:259.
- Hadfield, J. D. 2010a. MCMCglmm for R. *Journal Of Statistical Software* 33.
- Hadfield, J. D. 2010b. MCMCglmm: MCMC Methods for Multi-Response GLMMs in R. *Journal of Statistical Software* 33:1–22.
- Hadfield, J. D., and S. Nakagawa. 2010. General quantitative genetic methods for comparative biology: Phylogenies, taxonomies and multi-trait models for continuous and categorical characters. *Journal of Evolutionary Biology* 23:494–508.
- Hammond, W. M. 2020. A Matter of Life and Death: Alternative Stable States in Trees, From Xylem to Ecosystems. *Frontiers in Forests and Global Change* 3:1–8.
- Hammond, W. M., B. Choat, D. M. Johnson, M. A. Ahmed, L. D. Anderegg, T. S. Barigah, F. de M. B. Barros, T. B. L. B. Beikircher, P. Bittencourt, C. J. Blackman, T. Brodribb, M. Brum, and S. Jansen. 2021. The global vulnerability of plant xylem. *AGU Fall Meeting 2021*.
- Hammond, W. M., A. P. Williams, J. T. Abatzoglou, H. D. Adams, and T. Klein. 2022. Global field observations of tree die-off reveal hotter-drought fingerprint for Earth ' s forests. *Nature Communications*.
- Hammond, W. M., K. Yu, L. A. Wilson, R. E. Will, W. R. L. Anderegg, and H. D. Adams. 2019. Dead or dying? Quantifying the point of no return from hydraulic failure in drought-induced tree mortality. *New Phytologist* 223:1834–1843.
- Hansen, T. F. 1997. Stabilizing Selection and the Comparative Analysis of Adaptation. *Evolution* 51:1341.
- Harrel, F. E. 2020. rms: Regression Modeling Strategies. R package version 6.1-0.

- Hartmann, H., C. F. Moura, W. R. L. Anderegg, N. K. Ruehr, Y. Salmon, C. D. Allen, S. K. Arndt, D. D. Breshears, H. Davi, D. Galbraith, K. X. Ruthrof, J. Wunder, H. D. Adams, J. Bloemen, M. Cailleret, R. Cobb, A. Gessler, T. E. E. Grams, S. Jansen, M. Kautz, F. Lloret, and M. O'Brien. 2018. Research frontiers for improving our understanding of drought-induced tree and forest mortality. *New Phytologist* 218:15–28.
- He, N., Y. Li, C. Liu, L. Xu, M. Li, J. Zhang, J. He, Z. Tang, X. Han, Q. Ye, C. Xiao, Q. Yu, S. Liu, W. Sun, S. Niu, S. Li, L. Sack, and G. Yu. 2020a. Plant Trait Networks: Improved Resolution of the Dimensionality of Adaptation. *Trends in Ecology and Evolution* 35:908–918.
- He, P., S. M. Gleason, I. J. Wright, E. Weng, H. Liu, S. Zhu, M. Lu, Q. Luo, R. Li, G. Wu, E. Yan, Y. Song, X. Mi, G. Hao, P. B. Reich, Y. Wang, D. S. Ellsworth, and Q. Ye. 2020b. Growing-season temperature and precipitation are independent drivers of global variation in xylem hydraulic conductivity. *Global Change Biology* 26:1833–1841.
- Head, A. W., J. S. Hardin, and S. C. Adolph. 2012. Methods for estimating peak physiological performance and correlating performance measures. *Environmental and Ecological Statistics* 19:127–137.
- Henery, M. L., and M. Westoby. 2001. Seed mass and seed nutrient content as predictors of seed output variation between species. *Oikos* 92:479–490.
- Hengl, T., J. Mendes de Jesus, G. B. M. Heuvelink, M. Ruiperez Gonzalez, M. Kilibarda, A. Blagotić, W. Shangquan, M. N. Wright, X. Geng, B. Bauer-Marschallinger, M. A. Guevara, R. Vargas, R. A. MacMillan, N. H. Batjes, J. G. B. Leenaars, E. Ribeiro, I. Wheeler, S. Mantel, and B. Kempen. 2017. SoilGrids250m: Global gridded soil information based on machine learning. *PLOS ONE* 12:e0169748.
- Hijmans, R. J. 2021. raster: Geographic Data Analysis and Modeling. R package version 3.4-10.
- Hijmans, R. J., S. Phillips, J. Leathwick, and J. Elith. 2017. dismo: Species Distribution Modeling. R package version 1.1-4.
- Hilker, T., A. I. Lyapustin, C. J. Tucker, F. G. Hall, R. B. Myneni, Y. Wang, J. Bi, Y. M. De

- Moura, and P. J. Sellers. 2014. Vegetation dynamics and rainfall sensitivity of the Amazon. *Proceedings of the National Academy of Sciences of the United States of America* 111:16041–16046.
- Housworth, E. A. A., E. P. P. Martins, and M. Lynch. 2004. The Phylogenetic Mixed Model. *The American Naturalist* 163:84–96.
- Hutchinson, G. E. 1957. Concluding Remarks. Pages 75–76 *SpringerBriefs in Applied Sciences and Technology*.
- IPPC. 2022. *Climate Change 2022: Impacts, Adaptation and Vulnerability*. Page Contribution of Working Group II to the Sixth Assessment Report of the Intergovernmental Panel on Climate Change [H.-O. Pörtner, D.C. Roberts, M. Tignor, E.S. Poloczanska, K. Mintenbeck, A. Alegría, M. Craig, S. Langsdorf, S. Löschke, V. Möller, A. Okem., Cambridge University Press. Cambridge University Press, Cambridge, UK and New York, NY, USA.
- Jacobsen, A. L., R. B. Pratt, F. W. Ewers, and S. D. Davis. 2007. Cavitation resistance among 26 chaparral species of southern california. *Ecological Monographs* 77:99–115.
- Jansen, S., B. Schuldt, and B. Choat. 2015. Current controversies and challenges in applying plant hydraulic techniques. *New Phytologist* 205:961–964.
- Jin, Y., and H. Qian. 2019. V.PhyloMaker: an R package that can generate very large phylogenies for vascular plants. *Ecography* 42:1353–1359.
- Johnson, D. M., J. C. Domec, Z. Carter Berry, A. M. Schwantes, K. A. McCulloh, D. R. Woodruff, H. Wayne Polley, R. Wortemann, J. J. Swenson, D. Scott Mackay, N. G. McDowell, and R. B. Jackson. 2018. Co-occurring woody species have diverse hydraulic strategies and mortality rates during an extreme drought. *Plant Cell and Environment* 41:576–588.
- Kannenbergh, S. A., J. S. Guo, K. A. Novick, W. R. L. Anderegg, X. Feng, D. Kennedy, A. G. Konings, J. Martínez-Vilalta, and A. M. Matheny. 2021. Opportunities, challenges and pitfalls in characterizing plant water-use strategies. *Functional Ecology*:1–14.

- Katoh, K., and D. M. Standley. 2013. MAFFT multiple sequence alignment software version 7: Improvements in performance and usability. *Molecular Biology and Evolution* 30:772–780.
- Kattge, J., G. Bönisch, S. Díaz, S. Lavorel, I. C. Prentice, P. Leadley, S. Tautenhahn, G. D. A. Werner, T. Aakala, M. Abedi, A. T. R. Acosta, G. C. Adamidis, K. Adamson, M. Aiba, C. H. Albert, J. M. Alcántara, C. Alcázar C, I. Aleixo, H. Ali, B. Amiaud, C. Ammer, M. M. Amoroso, M. Anand, C. Anderson, N. Anten, J. Antos, D. M. G. Apgaua, T. L. Ashman, D. H. Asmara, G. P. Asner, M. Aspinwall, O. Atkin, I. Aubin, L. Bastrup-Spohr, K. Bahalkeh, M. Bahn, T. Baker, W. J. Baker, J. P. Bakker, D. Baldocchi, J. Baltzer, A. Banerjee, A. Baranger, J. Barlow, D. R. Barneche, Z. Baruch, D. Bastianelli, J. Battles, W. Bauerle, M. Bauters, E. Bazzato, M. Beckmann, H. Beeckman, C. Beierkuhnlein, R. Bekker, G. Belfry, M. Belluau, M. Beloiu, R. Benavides, L. Benomar, M. L. Berdugo-Lattke, E. Berenguer, R. Bergamin, J. Bergmann, M. Bergmann Carlucci, L. Berner, M. Bernhardt-Römermann, C. Bigler, A. D. Bjorkman, C. Blackman, C. Blanco, B. Blonder, D. Blumenthal, K. T. Bocanegra-González, P. Boeckx, S. Bohlman, K. Böhning-Gaese, L. Boisvert-Marsh, W. Bond, B. Bond-Lamberty, A. Boom, C. C. F. Boonman, K. Bordin, E. H. Boughton, V. Boukili, D. M. J. S. Bowman, S. Bravo, M. R. Brendel, M. R. Broadley, K. A. Brown, H. Bruelheide, F. Brumnich, H. H. Bruun, D. Bruy, S. W. Buchanan, S. F. Bucher, N. Buchmann, R. Buitenwerf, D. E. Bunker, J. Bürger, S. Burrascano, D. F. R. P. Burslem, B. J. Butterfield, C. Byun, M. Marques, M. C. Scalon, M. Caccianiga, M. Cadotte, M. Cailleret, J. Camac, J. J. Camarero, C. Company, G. Campetella, J. A. Campos, L. Cano-Arboleda, R. Canullo, M. Carbognani, F. Carvalho, F. Casanoves, B. Castagnyrol, J. A. Catford, J. Cavender-Bares, B. E. L. Cerabolini, M. Cervellini, E. Chacón-Madriral, K. Chapin, F. S. Chapin, S. Chelli, S. C. Chen, A. Chen, P. Cherubini, F. Chianucci, B. Choat, K. S. Chung, M. Chytrý, D. Ciccarelli, L. Coll, C. G. Collins, L. Conti, D. Coomes, J. H. C. Cornelissen, W. K. Cornwell, P. Corona, M. Coyea, J. Craine, D. Craven, J. P. G. M. Cromsigt, A. Csecserits, K. Cufar, M. Cuntz, A. C. da Silva, K. M. Dahlin, M. Dainese, I. Dalke, M. Dalle Fratte, A. T. Dang-Le, J. Danihelka, M. Dannoura, S. Dawson, A. J. de Beer, A. De Frutos, J. R. De Long, B. Dechant, S. Delagrangé, N. Delpierre, G. Derroire, A. S. Dias, M. H. Diaz-Toribio, P. G. Dimitrakopoulos, M. Dobrowolski, D. Doktor, P. Dřevojan, N. Dong, J. Dransfield, S. Dressler, L. Duarte, E. Ducouret, S. Dullinger, W. Durka, R. Duursma, O. Dymova, A. E-Vojtkó, R. L. Eckstein, H. Ejtehadi, J. Elser, T. Emilio, K. Engemann, M. B. Erfanian, A. Erfmeier, A. Esquivel-Muelbert, G. Esser, M.

Estiarte, T. F. Domingues, W. F. Fagan, J. Fagúndez, D. S. Falster, Y. Fan, J. Fang, E. Farris, F. Fazlioglu, Y. Feng, F. Fernandez-Mendez, C. Ferrara, J. Ferreira, A. Fidelis, B. Finegan, J. Firn, T. J. Flowers, D. F. B. Flynn, V. Fontana, E. Forey, C. Forgiarini, L. François, M. Frangipani, D. Frank, C. Frenette-Dussault, G. T. Freschet, E. L. Fry, N. M. Fyllas, G. G. Mazzochini, S. Gachet, R. Gallagher, G. Ganade, F. Ganga, P. García-Palacios, V. Gargaglione, E. Garnier, J. L. Garrido, A. L. de Gasper, G. Gea-Izquierdo, D. Gibson, A. N. Gillison, A. Giroldo, M. C. Glasenhardt, S. Gleason, M. Gliesch, E. Goldberg, B. Göldel, E. Gonzalez-Akre, J. L. Gonzalez-Andujar, A. González-Melo, A. González-Robles, B. J. Graae, E. Granda, S. Graves, W. A. Green, T. Gregor, N. Gross, G. R. Guerin, A. Günther, A. G. Gutiérrez, L. Haddock, A. Haines, J. Hall, A. Hambuckers, W. Han, S. P. Harrison, W. Hattingh, J. E. Hawes, T. He, P. He, J. M. Heberling, A. Helm, S. Hempel, J. Hentschel, B. Hérault, A. M. Hereş, K. Herz, M. Heuertz, T. Hickler, P. Hietz, P. Higuchi, A. L. Hipp, A. Hiron, M. Hock, J. A. Hogan, K. Holl, O. Honnay, D. Hornstein, E. Hou, N. Hough-Snee, K. A. Hovstad, T. Ichie, B. Igić, E. Illa, M. Isaac, M. Ishihara, L. Ivanov, L. Ivanova, C. M. Iversen, J. Izquierdo, R. B. Jackson, B. Jackson, H. Jactel, A. M. Jagodzinski, U. Jandt, S. Jansen, T. Jenkins, A. Jentsch, J. R. P. Jespersen, G. F. Jiang, J. L. Johansen, D. Johnson, E. J. Jokela, C. A. Joly, G. J. Jordan, G. S. Joseph, D. Junaedi, R. R. Junker, E. Justes, R. Kabzems, J. Kane, Z. Kaplan, T. Kattenborn, L. Kavelenova, E. Kearsley, A. Kempel, T. Kenzo, A. Kerkhoff, M. I. Khalil, N. L. Kinlock, W. D. Kissling, K. Kitajima, T. Kitzberger, R. Kjøller, T. Klein, M. Kleyer, J. Klimešová, J. Klipel, B. Kloeppel, S. Klotz, J. M. H. Knops, T. Kohyama, F. Koike, J. Kollmann, B. Komac, K. Komatsu, C. König, N. J. B. Kraft, K. Kramer, H. Kreft, I. Kühn, D. Kumarathunge, J. Kuppler, H. Kurokawa, Y. Kurosawa, S. Kuyah, J. P. Laclau, B. Lafleur, E. Lallai, E. Lamb, A. Lamprecht, D. J. Larkin, D. Laughlin, Y. Le Bagousse-Pinguet, G. le Maire, P. C. le Roux, E. le Roux, T. Lee, F. Lens, S. L. Lewis, B. Lhotsky, Y. Li, X. Li, J. W. Lichstein, M. Liebergesell, J. Y. Lim, Y. S. Lin, J. C. Linares, C. Liu, D. Liu, U. Liu, S. Livingstone, J. Llusà, M. Lohbeck, Á. López-García, G. Lopez-Gonzalez, Z. Lososová, F. Louault, B. A. Lukács, P. Lukeš, Y. Luo, M. Lussu, S. Ma, C. Maciel Rabelo Pereira, M. Mack, V. Maire, A. Mäkelä, H. Mäkinen, A. C. M. Malhado, A. Mallik, P. Manning, S. Manzoni, Z. Marchetti, L. Marchino, V. Marcilio-Silva, E. Marcon, M. Marignani, L. Markesteijn, A. Martin, C. Martínez-Garza, J. Martínez-Vilalta, T. Mašková, K. Mason, N. Mason, T. J. Massad, J. Masse, I. Mayrose, J. McCarthy, M. L. McCormack, K. McCulloh, I. R. McFadden, B. J. McGill, M. Y. McPartland, J. S. Medeiros, B. Medlyn, P. Meerts, Z.

Mehrabi, P. Meir, F. P. L. Melo, M. Mencuccini, C. Meredieu, J. Messier, I. Mészáros, J. Metsaranta, S. T. Michaletz, C. Michelaki, S. Migalina, R. Milla, J. E. D. Miller, V. Minden, R. Ming, K. Mokany, A. T. Moles, A. Molnár, J. Molofsky, M. Molz, R. A. Montgomery, A. Monty, L. Moravcová, A. Moreno-Martínez, M. Moretti, A. S. Mori, S. Mori, D. Morris, J. Morrison, L. Mucina, S. Mueller, C. D. Muir, S. C. Müller, F. Munoz, I. H. Myers-Smith, R. W. Myster, M. Nagano, S. Naidu, A. Narayanan, B. Natesan, L. Negoita, A. S. Nelson, E. L. Neuschulz, J. Ni, G. Niedrist, J. Nieto, Ü. Niinemets, R. Nolan, H. Nottebrock, Y. Nouvellon, A. Novakovskiy, K. O. Nystuen, A. O'Grady, K. O'Hara, A. O'Reilly-Nugent, S. Oakley, W. Oberhuber, T. Ohtsuka, R. Oliveira, K. Öllerer, M. E. Olson, V. Onipchenko, Y. Onoda, R. E. Onstein, J. C. Ordonez, N. Osada, I. Ostonen, G. Ottaviani, S. Otto, G. E. Overbeck, W. A. Ozinga, A. T. Pahl, C. E. T. Paine, R. J. Pakeman, A. C. Papageorgiou, E. Parfionova, M. Pärtel, M. Patacca, S. Paula, J. Paule, H. Pauli, J. G. Pausas, B. Peco, J. Penuelas, A. Perea, P. L. Peri, A. C. Petisco-Souza, A. Petraglia, A. M. Petritan, O. L. Phillips, S. Pierce, V. D. Pillar, J. Pisek, A. Pomogaybin, H. Poorter, A. Portsmouth, P. Poschlod, C. Potvin, D. Pounds, A. S. Powell, S. A. Power, A. Prinzing, G. Puglielli, P. Pyšek, V. Raevel, A. Rammig, J. Ransijn, C. A. Ray, P. B. Reich, M. Reichstein, D. E. B. Reid, M. Réjou-Méchain, V. R. de Dios, S. Ribeiro, S. Richardson, K. Riibak, M. C. Rillig, F. Riviera, E. M. R. Robert, S. Roberts, B. Robroek, A. Roddy, A. V. Rodrigues, A. Rogers, E. Rollinson, V. Rolo, C. Römermann, D. Ronzhina, C. Roscher, J. A. Rosell, M. F. Rosenfield, C. Rossi, D. B. Roy, S. Royer-Tardif, N. Rüger, R. Ruiz-Peinado, S. B. Rumpf, G. M. Rusch, M. Ryo, L. Sack, A. Saldaña, B. Salgado-Negret, R. Salguero-Gomez, I. Santa-Regina, A. C. Santacruz-García, J. Santos, J. Sardans, B. Schamp, M. Scherer-Lorenzen, M. Schleuning, B. Schmid, M. Schmidt, S. Schmitt, J. V. Schneider, S. D. Schowanek, J. Schrader, F. Schrodte, B. Schuldt, F. Schurr, G. Selaya Garvizu, M. Semchenko, C. Seymour, J. C. Sfair, J. M. Sharpe, C. S. Sheppard, S. Sheremetiev, S. Shiodera, B. Shipley, T. A. Shovon, A. Siebenkäs, C. Sierra, V. Silva, M. Silva, T. Sitzia, H. Sjöman, M. Slot, N. G. Smith, D. Sodhi, P. Soltis, D. Soltis, B. Somers, G. Sonnier, M. V. Sørensen, E. E. Sosinski, N. A. Soudzilovskaia, A. F. Souza, M. Spasojevic, M. G. Sperandii, A. B. Stan, J. Stegen, K. Steinbauer, J. G. Stephan, F. Sterck, D. B. Stojanovic, T. Strydom, M. L. Suarez, J. C. Svenning, I. Svitková, M. Svitok, M. Svoboda, E. Swaine, N. Swenson, M. Tabarelli, K. Takagi, U. Tappeiner, R. Tarifa, S. Tauougourdeau, C. Tavsanoğlu, M. te Beest, L. Tedersoo, N. Thiffault, D. Thom, E. Thomas, K. Thompson, P. E. Thornton, W. Thuiller, L. Tichý, D. Tissue, M. G. Tjoelker, D. Y. P. Tng, J. Tobias, P. Török, T. Tarin, J. M. Torres-Ruiz, B.

- Tóthmérész, M. Treurnicht, V. Trivellone, F. Trollet, V. Trotsiuk, J. L. Tsakalos, I. Tsiripidis, N. Tyskland, T. Umehara, V. Usoltsev, M. Vadeboncoeur, J. Vaezi, F. Valladares, J. Vamosi, P. M. van Bodegom, M. van Breugel, E. Van Cleemput, M. van de Weg, S. van der Merwe, F. van der Plas, M. T. van der Sande, M. van Kleunen, K. Van Meerbeek, M. Vanderwel, K. A. Vanselow, A. Vårhammar, L. Varone, M. Y. Vasquez Valderrama, K. Vassilev, M. Vellend, E. J. Veneklaas, H. Verbeeck, K. Verheyen, A. Vibrans, I. Vieira, J. Villacís, C. Violle, P. Vivek, K. Wagner, M. Waldram, A. Waldron, A. P. Walker, M. Waller, G. Walther, H. Wang, F. Wang, W. Wang, H. Watkins, J. Watkins, U. Weber, J. T. Weedon, L. Wei, P. Weigelt, E. Weiher, A. W. Wells, C. Wellstein, E. Wenk, M. Westoby, A. Westwood, P. J. White, M. Whitten, M. Williams, D. E. Winkler, K. Winter, C. Womack, I. J. Wright, S. J. Wright, J. Wright, B. X. Pinho, F. Ximenes, T. Yamada, K. Yamaji, R. Yanai, N. Yankov, B. Yguel, K. J. Zanini, A. E. Zanne, D. Zelený, Y. P. Zhao, J. Zheng, J. Zheng, K. Ziemińska, C. R. Zirbel, G. Zizka, I. C. Zo-Bi, G. Zotz, and C. Wirth. 2020. TRY plant trait database – enhanced coverage and open access. *Global Change Biology* 26:119–188.
- De Kauwe, M. G., B. E. Medlyn, A. M. Ukkola, M. Mu, M. E. B. Sabot, A. J. Pitman, P. Meir, L. A. Cernusak, S. W. Rifai, B. Choat, D. T. Tissue, C. J. Blackman, X. Li, M. Roderick, and P. R. Briggs. 2020. Identifying areas at risk of drought-induced tree mortality across South-Eastern Australia. *Global Change Biology* 26:5716–5733.
- Kolb, K. J., and S. D. Davis. 1994. Drought Tolerance and Xylem Embolism in Co-Occurring Species of Coastal Sage and Chaparral. *Ecology* 75:648–659.
- Kunstler, G., A. Guyennon, S. Ratcliffe, N. Rüger, P. Ruiz-Benito, D. Z. Childs, J. Dahlgren, A. Lehtonen, W. Thuiller, C. Wirth, M. A. Zavala, and R. Salguero-Gomez. 2021. Demographic performance of European tree species at their hot and cold climatic edges. *Journal of Ecology* 109:1041–1054.
- Lamy, J. B., S. Delzon, P. S. Bouche, R. Alia, G. G. Vendramin, H. Cochard, and C. Plomion. 2014. Limited genetic variability and phenotypic plasticity detected for cavitation resistance in a Mediterranean pine. *New Phytologist* 201:874–886.
- Larter, M., S. Pfautsch, J. C. Domec, S. Trueba, N. Nagalingum, and S. Delzon. 2017. Aridity drove the evolution of extreme embolism resistance and the radiation of conifer genus

- Callitris. *New Phytologist* 215:97–112.
- Laughlin, D. C., S. Delzon, M. J. Clearwater, P. J. Bellingham, M. S. McGlone, and S. J. Richardson. 2020. Climatic limits of temperate rainforest tree species are explained by xylem embolism resistance among angiosperms but not among conifers. *New Phytologist*.
- Lecina-Diaz, J., M. Martínez-Vilalta, A. Alvarez, M. Banqué, J. Birkmann, D. Feldmeyer, J. Vayreda, and J. Retana. 2020. Characterizing forest vulnerability and risk to climate change hazards. *Frontiers in Ecology and the Environment*:1–8.
- Lens, F., S. M. Gleason, G. Bortolami, C. Brodersen, S. Delzon, and S. Jansen. 2022. Functional xylem characteristics associated with drought-induced embolism in angiosperms. *New Phytologist*:2019–2036.
- Lenth, R. V. 2021. emmeans: Estimated Marginal Means, aka Least-Squares Means. R package version 1.6.3.
- Leslie, A. B., J. Beaulieu, G. Holman, C. S. Campbell, W. Mei, L. R. Raubeson, and S. Mathews. 2018. An overview of extant conifer evolution from the perspective of the fossil record. *American Journal of Botany* 105:1531–1544.
- Li, S., F. Lens, S. Espino, Z. Karimi, M. Klepsch, H. J. Schenk, M. Schmitt, B. Schuldt, and S. Jansen. 2016. INTERVESSEL PIT MEMBRANE THICKNESS AS A KEY DETERMINANT of EMBOLISM RESISTANCE in ANGIOSPERM XYLEM. *IAWA Journal* 37:152–171.
- Liaw, A., and M. Wiener. 2002. Classification and Regression by randomForest. *R news* 2:18–22.
- Liu, H., S. M. Gleason, G. Hao, L. Hua, P. He, G. Goldstein, and Q. Ye. 2019a. Hydraulic traits are coordinated with maximum plant height at the global scale. *Science Advances* 5:eaav1332.
- Liu, H., S. M. Gleason, G. Hao, L. Hua, P. He, G. Goldstein, and Q. Ye. 2019b. Hydraulic traits are coordinated with maximum plant height at the global scale. *Science Advances*

5:eaav1332.

- Liu, Y., N. Holtzman, and A. Konings. 2020. Global ecosystem-scale plant hydraulic traits retrieved using model-data fusion. *Hydrology and Earth System Sciences Discussions*:1–30.
- Lobo, A., J. M. Torres-Ruiz, R. Burlett, C. Lemaire, C. Parise, C. Francioni, L. Truffaut, I. Tomášková, J. K. Hansen, E. D. Kjær, A. Kremer, and S. Delzon. 2018. Assessing inter- and intraspecific variability of xylem vulnerability to embolism in oaks. *Forest Ecology and Management* 424:53–61.
- López, R., F. J. Cano, B. Choat, H. Cochard, and L. Gil. 2016. Plasticity in vulnerability to cavitation of *pinus canariensis* occurs only at the driest end of an aridity gradient. *Frontiers in Plant Science* 7:1–10.
- Losos, J. B. 2008. Phylogenetic niche conservatism, phylogenetic signal and the relationship between phylogenetic relatedness and ecological similarity among species. *Ecology letters* 11:995–1003.
- Louca, S., and M. Doebeli. 2018. Efficient comparative phylogenetics on large trees. *Bioinformatics* 34:1053–1055.
- Lynch, M. 1991. *Methods for the analysis of comparative data in evolutionary biology*. *Evolution* 45:1065–1079.
- MacArthur, R. H., and E. O. Wilson. 1967. *The theory of island biogeography*. Princeton Univ. Press, N.J.
- Magallón, S., S. Gómez-Acevedo, L. L. Sánchez-Reyes, and T. Hernández-Hernández. 2015. A metacalibrated time-tree documents the early rise of flowering plant phylogenetic diversity. *New Phytologist* 207:437–453.
- Maherali, H., W. T. Pockman, and R. B. Jackson. 2004. Adaptive variation in the vulnerability of woody plants to xylem cavitation. *Ecology* 85:2184–2199.
- Makowski, D., M. Ben-Shachar, and D. Lüdtke. 2019. bayestestR: Describing Effects and their

- Uncertainty, Existence and Significance within the Bayesian Framework. *Journal of Open Source Software* 4:1541.
- Martin-StPaul, N., S. Delzon, and H. Cochard. 2017. Plant resistance to drought depends on timely stomatal closure. *Ecology Letters* 20:1437–1447.
- Martínez-Vilalta, J., H. Cochard, M. Mencuccini, F. Sterck, A. Herrero, J. F. J. Korhonen, P. Llorens, E. Nikinmaa, A. Nolé, R. Poyatos, F. Ripullone, U. Sass-Klaassen, and R. Zweifel. 2009. Hydraulic adjustment of Scots pine across Europe. *New Phytologist* 184:353–364.
- Martínez-Vilalta, J., R. Poyatos, D. Aguadé, J. Retana, and M. Mencuccini. 2014. A new look at water transport regulation in plants. *New Phytologist* 204:105–115.
- Martínez-Vilalta, J., E. Prat, I. Oliveras, and J. Piñol. 2002. Xylem hydraulic properties of roots and stems of nine Mediterranean woody species. *Oecologia* 133:19–29.
- Martínez-Vilalta, J., A. Sala, and J. Piol. 2004. The hydraulic architecture of Pinaceae - A review. *Plant Ecology* 171:3–13.
- Martínez-Vilalta, J., L. S. Santiago, R. Poyatos, L. Badiella, M. de Cáceres, I. Aranda, S. Delzon, A. Vilagrosa, and M. Mencuccini. 2021. Towards a statistically robust determination of minimum water potential and hydraulic risk in plants. *New Phytologist*.
- Mazer, S. J. 1990. Seed mass of Indiana Dune genera and families: Taxonomic and ecological correlates. *Evolutionary Ecology* 4:326–357.
- McDowell, N., W. T. Pockman, C. D. Allen, D. D. Breshears, N. Cobb, T. Kolb, J. Plaut, J. Sperry, A. West, D. G. Williams, and E. A. Yezzer. 2008. Mechanisms of plant survival and mortality during drought: why do some plants survive while others succumb to drought? *New Phytologist* 178:719–739.
- McDowell, N., G. Sapes, A. Pivovarov, H. Adams, C. D. Allen, W. R. L. Anderegg, M. Arend, D. D. Breshears, T. Brodrigg, B. Choat, H. Cochard, M. De Cáceres, M. G. De Kauwe, C. Grossiord, W. M. Hammond, H. Hartmann, G. Hoch, A. Kahmen, T. Klein, D. S. Mackay, M. Mantova, J. Martínez-Vilalta, B. E. Medlyn, M. Mencuccini, A. Nardini, R. S. Oliveira,

- A. Sala, D. T. Tissue, J. M. Torres-Ruiz, A. Trowbridge, A. T. Trugman, E. Wiley, and C. Xu. 2021. Mechanisms of woody plant mortality under rising drought, CO₂, and vapor pressure deficit. *Nature reviews*.
- Mencuccini, M., S. Manzoni, and B. Christoffersen. 2019a. Modelling water fluxes in plants: from tissues to biosphere. *New Phytologist* 222:1207–1222.
- Mencuccini, M., T. Rosas, L. Rowland, B. Choat, H. Cornelissen, S. Jansen, K. Kramer, A. Lapenis, S. Manzoni, Ü. Niinemets, P. B. Reich, F. Schrodte, N. Soudzilovskaia, I. J. Wright, and J. Martínez-Vilalta. 2019b. Leaf economics and plant hydraulics drive leaf : wood area ratios. *New Phytologist* 224:1544–1556.
- Merow, C., M. J. Smith, and J. A. Silander. 2013. A practical guide to MaxEnt for modeling species' distributions: What it does, and why inputs and settings matter. *Ecography* 36:1058–1069.
- Moles, A. T., and M. Westoby. 2006. Seed size and plant strategy across the whole life cycle. *Oikos* 113:91–105.
- Montzka, C., M. Herbst, L. Weihermüller, A. Verhoef, and H. Vereecken. 2017. A global data set of soil hydraulic properties and sub-grid variability of soil water retention and hydraulic conductivity curves. *Earth System Science Data Discussions*:1–25.
- Mundim, F. M., and E. G. Pringle. 2018. Whole-plant metabolic allocation under water stress. *Frontiers in Plant Science* 9:852.
- Muñoz-Sabater, J., E. Dutra, A. Agustí-Panareda, C. Albergel, G. Arduini, G. Balsamo, S. Boussetta, M. Choulga, S. Harrigan, H. Hersbach, B. Martens, D. G. Miralles, M. Piles, N. J. Rodríguez-Fernández, E. Zsoter, C. Buontempo, and J. N. Thépaut. 2021. ERA5-Land: A state-of-the-art global reanalysis dataset for land applications. *Earth System Science Data* 13:4349–4383.
- Nakagawa, S., and H. Schielzeth. 2013. A general and simple method for obtaining R² from generalized linear mixed-effects models. *Methods in Ecology and Evolution* 4:133–142.

- Needham, J. F., D. J. Johnson, K. J. Anderson-Teixeira, N. Bourg, S. Bunyavejchewin, N. Butt, M. Cao, D. Cárdenas, C. H. Chang-Yang, Y. Y. Chen, G. Chuyong, H. S. Dattaraja, S. J. Davies, A. Duque, C. E. N. Ewango, E. S. Fernando, R. Fisher, C. D. Fletcher, R. Foster, Z. Hao, T. Hart, C. F. Hsieh, S. P. Hubbell, A. Itoh, D. Kenfack, C. D. Koven, A. J. Larson, J. A. Lutz, W. McShea, J. R. Makana, Y. Malhi, T. Marthews, M. Bt. Mohamad, M. D. Morecroft, N. Norden, G. Parker, A. Shringi, R. Sukumar, H. S. Suresh, I. F. Sun, S. Tan, D. W. Thomas, J. Thompson, M. Uriarte, R. Valencia, T. L. Yao, S. L. Yap, Z. Yuan, H. Yuehua, J. K. Zimmerman, D. Zuleta, and S. M. McMahon. 2022. Demographic composition, not demographic diversity, predicts biomass and turnover across temperate and tropical forests. *Global Change Biology* 28:2895–2909.
- Neves, D. M., K. G. Dexter, T. R. Baker, F. Coelho de Souza, A. T. Oliveira-Filho, L. P. Queiroz, H. C. Lima, M. F. Simon, G. P. Lewis, R. A. Segovia, L. Arroyo, C. Reynel, J. L. Marcelo-Peña, I. Huamantupa-Chuquimaco, D. Villarroel, G. A. Parada, A. Daza, R. Linares-Palomino, L. V. Ferreira, R. P. Salomão, G. S. Siqueira, M. T. Nascimento, C. N. Fraga, and R. T. Pennington. 2020. Evolutionary diversity in tropical tree communities peaks at intermediate precipitation. *Scientific Reports* 10:1–8.
- Niinemets, Ü. 2010. Responses of forest trees to single and multiple environmental stresses from seedlings to mature plants: Past stress history, stress interactions, tolerance and acclimation. *Forest Ecology and Management* 260:1623–1639.
- Pagel, M. 1999. Inferring the historical patterns of biological evolution. *Nature* 401:877–884.
- Panchen, Z. A., R. B. Primack, B. Nordt, E. R. Ellwood, A. D. Stevens, S. S. Renner, C. G. Willis, R. Fahey, A. Whittemore, Y. Du, and C. C. Davis. 2014. Leaf out times of temperate woody plants are related to phylogeny, deciduousness, growth habit and wood anatomy. *New Phytologist* 203:1208–1219.
- Paradis, E., and K. Schliep. 2019. Ape 5.0: An environment for modern phylogenetics and evolutionary analyses in R. *Bioinformatics* 35:526–528.
- Parmesan, C., and G. Yohe. 2003. A globally coherent fingerprint of climate change impacts across natural systems. *Nature* 421:37–42.

- Pebesma, E. 2018. Simple Features for R: Standardized Support for Spatial Vector Data. *The R Journal* 10:439.
- Pennell, M. W., R. G. FitzJohn, and W. K. Cornwell. 2016. A simple approach for maximizing the overlap of phylogenetic and comparative data. *Methods in Ecology and Evolution* 7:751–758.
- Pennell, M. W., and L. J. Harmon. 2013. An integrative view of phylogenetic comparative methods: Connections to population genetics, community ecology, and paleobiology. *Annals of the New York Academy of Sciences* 1289:90–105.
- Pereira, C. G., and D. L. Des Marais. 2020. The genetic basis of plant functional traits and the evolution of plant-environment interactions. *International Journal of Plant Sciences* 181:56–74.
- Pérez-Navarro, M. Á., J. M. Serra-Diaz, J. Svenning, M. Á. Esteve-Selma, J. Hernández-Bastida, and F. Lloret. 2021. Extreme drought reduces climatic disequilibrium in dryland plant communities. *Oikos* 130:680–690.
- Peters, J. M. R., R. López, M. Nolf, L. B. Hutley, T. Wardlaw, L. A. Cernusak, and B. Choat. 2021. Living on the edge: A continental-scale assessment of forest vulnerability to drought. *Global Change Biology* 27:3620–3641.
- Phillips, S. J., and M. Dudík. 2008. Modeling of species distributions with Maxent: new extensions and a comprehensive evaluation. *Ecography*:161–175.
- Pianka Eric R. 1970. On r- and K-Selection. *American society of naturalists* 104:592–597.
- Poorter, L., S. J. Wright, H. Paz, D. D. Ackerly, R. Condit, G. Ibarra-Manríquez, K. E. Harms, J. C. Licona, M. Martínez-Ramos, S. J. Mazer, H. C. Muller-Landau, M. Peña-Claros, C. O. Webb, and I. J. Wright. 2008. Are functional traits good predictors of demographic rates? Evidence from five neotropical forests. *Ecology* 89:1908–1920.
- Poyatos, R., D. Aguadé, and J. Martínez-Vilalta. 2018a. Below-ground hydraulic constraints during drought-induced decline in Scots pine. *Annals of Forest Science* 75:100.

- Poyatos, R., O. Sus, L. Badiella, M. Mencuccini, and J. Martínez-Vilalta. 2018b. Gap-filling a spatially explicit plant trait database: Comparing imputation methods and different levels of environmental information. *Biogeosciences* 15:2601–2617.
- Pritzkow, C., V. Williamson, C. Szota, R. Trouvé, and S. K. Arndt. 2020. Phenotypic plasticity and genetic adaptation of functional traits influences intra-specific variation in hydraulic efficiency and safety. *Tree Physiology* 40:215–229.
- Qian, H., and Y. Jin. 2016. An updated megaphylogeny of plants, a tool for generating plant phylogenies and an analysis of phylogenetic community structure. *Journal of Plant Ecology* 9:233–239.
- R Core Team. 2020. R: A language and environment for statistical computing. R Foundation for Statistical Computing.
- Ramírez-Valiente, J. A., and J. Cavender-Bares. 2017. Evolutionary trade-offs between drought resistance mechanisms across a precipitation gradient in a seasonally dry tropical oak (*Quercus oleoides*). *Tree physiology* 37:889–901.
- Ramírez-Valiente, J. A., D. Sánchez-Gómez, I. Aranda, and F. Valladares. 2010. Phenotypic plasticity and local adaptation in leaf ecophysiological traits of 13 contrasting cork oak populations under different water availabilities. *Tree Physiology* 30:618–627.
- Ran, J. H., T. T. Shen, M. M. Wang, and X. Q. Wang. 2018. Phylogenomics resolves the deep phylogeny of seed plants and indicates partial convergent or homoplastic evolution between Gnetales and angiosperms. *Proceedings of the Royal Society B: Biological Sciences* 285.
- Reich, P. B. 2014. The world-wide “fast-slow” plant economics spectrum: A traits manifesto. *Journal of Ecology* 102:275–301.
- Reich, P. B., D. S. Ellsworth, M. B. Walters, J. M. Vose, C. Gresham, J. C. Volin, and W. D. Bowman. 1999. Generality of leaf trait relationships: A test across six biomes. *Ecology* 80:1955–1969.
- Reich, P. B., I. J. Wright, J. Cavender-Bares, J. M. Craine, J. Oleksyn, M. Westoby, and M. B.

- Walters. 2003. The Evolution of Plant Functional Variation: Traits, Spectra, and Strategies. *International Journal of Plant Sciences* 164:S143–S164.
- Revell, L. J. 2009. Size-correction and principal components for interspecific comparative studies. *Evolution* 63:3258–3268.
- Revell, L. J. 2012. phytools: An R package for phylogenetic comparative biology (and other things). *Methods in Ecology and Evolution* 3:217–223.
- Revell, L. J. 2013. Two new graphical methods for mapping trait evolution on phylogenies. *Methods in Ecology and Evolution* 4:754–759.
- Revell, L. J., L. J. Harmon, and D. C. Collar. 2008. Phylogenetic signal, evolutionary process, and rate. *Systematic biology* 57:591–601.
- Rosas, T., M. Mencuccini, J. Barba, H. Cochard, S. Saura-Mas, and J. Martínez-Vilalta. 2019. Adjustments and coordination of hydraulic, leaf and stem traits along a water availability gradient. *New Phytologist* 223:632–646.
- Ross, N. (n.d.). fasterize: Fast Polygon to Raster Conversion. R package version 1.0.3.
- Rowland, L., A. C. L. da Costa, D. R. Galbraith, R. S. Oliveira, O. J. Binks, A. A. R. Oliveira, A. M. Pullen, C. E. Doughty, D. B. Metcalfe, S. S. Vasconcelos, L. V. Ferreira, Y. Malhi, J. Grace, M. Mencuccini, and P. Meir. 2015. Death from drought in tropical forests is triggered by hydraulics not carbon starvation. *Nature*:1–13.
- Rowland, L., J. Martínez-Vilalta, and M. Mencuccini. 2021. Hard times for high expectations from hydraulics: predicting drought-induced forest mortality at landscape scales remains a challenge. *New Phytologist*:1685–1687.
- Rüger, N., L. S. Comita, R. Condit, D. Purves, B. Rosenbaum, M. D. Visser, S. J. Wright, and C. Wirth. 2018. Beyond the fast–slow continuum: demographic dimensions structuring a tropical tree community. *Ecology Letters* 21:1075–1084.
- Sala, A., D. R. Woodruff, and F. C. Meinzer. 2012. Carbon dynamics in trees: Feast or famine?

- Tree Physiology 32:764–775.
- Salguero-Gómez, R. 2017. Applications of the fast–slow continuum and reproductive strategy framework of plant life histories. *New Phytologist* 213:1618–1624.
- Salguero-gómez, R., O. R. Jones, S. P. Blomberg, D. J. Hodgson, P. A. Zuidema, and H. De Kroon. 2017. Erratum: Fast–slow continuum and reproductive strategies structure plant life-history variation worldwide (*Proc Natl Acad Sci USA* (2015) 113 (230–235) DOI: 10.1073/pnas.1506215112). *Proceedings of the National Academy of Sciences of the United States of America* 114:E9753.
- Salguero-Gómez, R., O. R. Jones, E. Jongejans, S. P. Blomberg, D. J. Hodgson, C. Mbeau-Ache, P. A. Zuidema, H. de Kroon, and Y. M. Buckley. 2016. Fast–slow continuum and reproductive strategies structure plant life-history variation worldwide. *Proceedings of the National Academy of Sciences* 113:230–235.
- Sanchez-Martinez, P., A. Marcer, M. Mayol, and M. Riba. 2021. Shaping the niche of *Taxus baccata*, a modelling exercise using biologically meaningful information. *Forest Ecology and Management* 501:119688.
- Sanchez-Martinez, P., J. Martínez-Vilalta, K. G. Dexter, R. A. Segovia, and M. Mencuccini. 2020. Adaptation and coordinated evolution of plant hydraulic traits. *Ecology Letters* 23:1599–1610.
- Saxton, K. E., and W. J. Rawls. 2006. Soil Water Characteristic Estimates by Texture and Organic Matter for Hydrologic Solutions. *Soil Science Society of America Journal* 70:1569–1578.
- Schluter, D., T. Price, A. T. Mooers, and D. Ludwig. 1997. EVOLUTION. *Evolution* 51.
- Scoffoni, C., D. S. Chatelet, J. Pasquet-Kok, M. Rawls, M. J. Donoghue, E. J. Edwards, and L. Sack. 2016. Hydraulic basis for the evolution of photosynthetic productivity. *Nature Plants* 2:1–8.
- Segovia, R. A., R. T. Pennington, T. R. Baker, F. C. de Souza, D. M. Neves, C. C. Davis, J. J.

- Armesto, A. T. Olivera-Filho, and K. G. Dexter. 2020. Freezing and water availability structure the evolutionary diversity of trees across the Americas. *Science Advances* 6:1–10.
- Serra-Diaz, J. M., B. J. Enquist, B. Maitner, C. Merow, and J. C. Svenning. 2017. Big data of tree species distributions: how big and how good? *Forest Ecosystems* 4:0–12.
- Skelton, R. P., L. D. L. Anderegg, P. Papper, E. Reich, T. E. Dawson, M. Kling, S. E. Thompson, J. Diaz, and D. D. Ackerly. 2019. No local adaptation in leaf or stem xylem vulnerability to embolism, but consistent vulnerability segmentation in a North American oak. *New Phytologist* 223:1296–1306.
- Skelton, R. P., A. G. West, and T. E. Dawson. 2015. Predicting plant vulnerability to drought in biodiverse regions using functional traits. *Proceedings of the National Academy of Sciences of the United States of America* 112:5744–5749.
- Smith, S. A., and J. W. Brown. 2018. Constructing a broadly inclusive seed plant phylogeny. *American Journal of Botany* 105:302–314.
- Smith, S. A., and B. C. O'Meara. 2012. TreePL: Divergence time estimation using penalized likelihood for large phylogenies. *Bioinformatics* 28:2689–2690.
- Sperry, J. S., and U. G. Hacke. 2002. Desert shrub water relations with respect to soil characteristics and plant functional type. *Functional Ecology* 16:367–378.
- Sperry, J. S., U. G. Hacke, and J. Pittermann. 2006. Size and function in conifer tracheids and angiosperm vessels. *American Journal of Botany* 93:1490–1500.
- Stahl, U., B. Reu, and C. Wirth. 2014. Predicting species' range limits from functional traits for the tree flora of North America. *Proceedings of the National Academy of Sciences* 111:13739–13744.
- Stamatakis, A., P. Hoover, and J. Rougemont. 2008. A rapid bootstrap algorithm for the RAxML web servers. *Systematic Biology* 57:758–771.
- Stearns, S. C. 1999. *The Evolution of Life Histories*. Oxford University Press, New York, NY.

- Stekhoven, D. J., and P. Bühlmann. 2012. Missforest-Non-parametric missing value imputation for mixed-type data. *Bioinformatics* 28:112–118.
- Stocker, T. F., Q. Dahe, G.-K. Plattner, L. V. Alexander, S. K. Allen, N. L. Bindoff, F.-M. Bréon, J. A. Church, U. Cubash, S. Emori, P. Forster, P. Friedlingstein, L. D. Talley, D. G. Vaughan, and S.-P. Xie. 2013. IPCC WG1AR5 Technical Summary:33–115.
- Sultan, S. E. 2000. Phenotypic plasticity for plant development, function and life history. *Trends in Plant Science* 5:537–542.
- Swenson, N. G. 2014. Phylogenetic imputation of plant functional trait databases. *Ecography* 37:105–110.
- Swenson, N. G., B. J. Enquist, J. Pither, A. J. Kerkhoff, B. Boyle, M. D. Weiser, J. J. Elser, W. F. Fagan, J. Forero-Montaña, N. Fyllas, N. J. B. Kraft, J. K. Lake, A. T. Moles, S. Patiño, O. L. Phillips, C. A. Price, P. B. Reich, C. A. Quesada, J. C. Stegen, R. Valencia, I. J. Wright, S. J. Wright, S. Andelman, P. M. Jørgensen, T. E. Lacher, A. Monteagudo, M. P. Núñez-Vargas, R. Vasquez-Martínez, and K. M. Nolting. 2012. The biogeography and filtering of woody plant functional diversity in North and South America. *Global Ecology and Biogeography* 21:798–808.
- Swenson, N. G., M. D. Weiser, L. Mao, M. B. Araújo, J. A. F. Diniz-Filho, J. Kollmann, D. Nogués-Bravo, S. Normand, M. A. Rodríguez, R. García-Valdés, F. Valladares, M. A. Zavala, and J. C. Svenning. 2017. Phylogeny and the prediction of tree functional diversity across novel continental settings. *Global Ecology and Biogeography* 26:553–562.
- Tank, D. C., J. M. Eastman, M. W. Pennell, P. S. Soltis, D. E. Soltis, C. E. Hinchliff, J. W. Brown, E. B. Sessa, and L. J. Harmon. 2015. Nested radiations and the pulse of angiosperm diversification: increased diversification rates often follow whole genome duplications. *New Phytologist* 207:454–467.
- Thomas, C. D., C. D. Thomas, A. Cameron, A. Cameron, R. E. Green, R. E. Green, M. Bakkenes, M. Bakkenes, L. J. Beaumont, L. J. Beaumont, Y. C. Collingham, Y. C. Collingham, B. F. N. Erasmus, B. F. N. Erasmus, M. F. De Siqueira, M. F. De Siqueira, A.

- Grainger, A. Grainger, L. Hannah, L. Hannah, L. Hughes, L. Hughes, B. Huntley, B. Huntley, A. S. Van Jaarsveld, A. S. Van Jaarsveld, G. F. Midgley, G. F. Midgley, L. Miles, L. Miles, M. a Ortega-Huerta, M. a Ortega-Huerta, a T. Peterson, a T. Peterson, O. L. Phillips, O. L. Phillips, S. E. Williams, and S. E. Williams. 2004. Extinction risk from climate change. *Nature* 427:145–8.
- Trabucco, A., and R. J. Zomer. 2018. Global Aridity Index and Potential Evapotranspiration (ET0) Climate Database v2. CGIAR Consortium for Spatial Information (CGIAR-CSI):10.
- Trugman, A. T., L. D. L. Anderegg, W. R. L. Anderegg, A. J. Das, and N. L. Stephenson. 2021. Why is Tree Drought Mortality so Hard to Predict? *Trends in Ecology and Evolution* 36:1–13.
- Trugman, A. T., L. D. L. Anderegg, J. D. Shaw, and W. R. L. Anderegg. 2020. Trait velocities reveal that mortality has driven widespread coordinated shifts in forest hydraulic trait composition. *Proceedings of the National Academy of Sciences*:201917521.
- Turner, I. M. 2001. *The Ecology of Trees in the Tropical Rain Forest*. Cambridge University Press, Cambridge.
- Tyree, M. T., and M. H. Zimmermann. 2002. *Xylem Structure and the Ascent of Sap*. Springer Berlin Heidelberg, Berlin, Heidelberg.
- Varela, S., R. P. Anderson, R. García-Valdés, and F. Fernández-González. 2014. Environmental filters reduce the effects of sampling bias and improve predictions of ecological niche models. *Ecography* 37:1084–1091.
- Venturas, M. D., J. S. Sperry, and U. G. Hacke. 2017. Plant xylem hydraulics: What we understand, current research, and future challenges. *Journal of Integrative Plant Biology* 59:356–389.
- Venturas, M. D., H. N. Todd, A. T. Trugman, and W. R. L. Anderegg. 2020. Understanding and predicting forest mortality in the western United States using long-term forest inventory data and modeled hydraulic damage. *New Phytologist* 230:1896–1910.

- Villemeireuil, P. De. 2012. How to use the MCMCglmm R package.
- Violle, C., M.-L. Navas, D. Vile, E. Kazakou, C. Fortunel, I. Hummel, and E. Garnier. 2007. Let the concept of trait be functional! *Oikos* 116:882–892.
- Volaire, F. 2018. A unified framework of plant adaptive strategies to drought: Crossing scales and disciplines. *Global Change Biology* 24:2929–2938.
- Wagner, G. P. 1996. Homologues, natural kinds and the evolution of modularity. *American Zoologist* 36:36–43.
- Weiser, M. D., B. J. Enquist, B. Boyle, T. J. Killeen, P. M. Jørgensen, G. Fonseca, M. D. Jennings, A. J. Kerkhoff, T. E. Lacher, A. Monteagudo, M. P. N. Vargas, O. L. Phillips, N. G. Swenson, and R. V. Martínez. 2007. Latitudinal patterns of range size and species richness of New World woody plants. *Global Ecology and Biogeography* 16:679–688.
- Westgate, M., M. Stevenson, P. Newman, B. Raymond, J. VanDerWal, and L. Belbin. 2023. ALA4R: Atlas of Living Australia (ALA) Data and Resources in R. R package version 1.9.1.
- Westoby, M., D. S. Falster, A. T. Moles, P. A. Vesk, and I. J. Wright. 2002. Plant ecological strategies: Some leading dimensions of variation between species. *Annual Review of Ecology and Systematics* 33:125–159.
- Westoby, M., M. Leishman, and J. Lord. 1996. Comparative ecology of seed size and dispersal. *Philosophical Transactions of the Royal Society B: Biological Sciences* 351:1309–1318.
- Willson, C. J., P. S. Manos, and R. B. Jackson. 2008. Hydraulic traits are influenced by phylogenetic history in the drought-resistant, invasive genus *Juniperus* (Cupressaceae). *American Journal of Botany* 95:299–314.
- Wolfe, B. T., J. S. Sperry, and T. A. Kursar. 2016. Does leaf shedding protect stems from cavitation during seasonal droughts? A test of the hydraulic fuse hypothesis. *New Phytologist* 212:1007–1018.
- Wright, I. J., N. Dong, V. Maire, I. C. Prentice, M. Westoby, S. Díaz, R. V. Gallagher, B. F.

- Jacobs, R. Kooyman, E. A. Law, M. R. Leishman, Ü. Niinemets, P. B. Reich, L. Sack, R. Villar, H. Wang, and P. Wilf. 2017. Global climatic drivers of leaf size. *Science* 357:917–921.
- Wright, I. J., P. B. Reich, M. Westoby, D. D. Ackerly, Z. Baruch, F. Bongers, J. Cavender-Bares, T. Chapin, J. H. C. Cornelissen, M. Diemer, J. Flexas, E. Garnier, P. K. Groom, J. Gulias, K. Hikosaka, B. B. Lamont, T. Lee, W. Lee, C. Lusk, J. J. Midgley, M.-L. Navas, Ü. Niinemets, J. Oleksyn, N. Osada, H. Poorter, P. Poot, L. Prior, V. I. Pyankov, C. Roumet, S. C. Thomas, M. G. Tjoelker, E. J. Veneklaas, and R. Villar. 2004. The worldwide leaf economics spectrum. *Nature* 428:821–827.
- Zanne, A. E., D. C. Tank, W. K. Cornwell, J. M. Eastman, S. A. Smith, R. G. Fitzjohn, D. J. McGlenn, B. C. O’Meara, A. T. Moles, P. B. Reich, D. L. Royer, D. E. Soltis, P. F. Stevens, M. Westoby, I. J. Wright, L. Aarssen, R. I. Bertin, A. Calaminus, R. Govaerts, F. Hemmings, M. R. Leishman, J. Oleksyn, P. S. Soltis, N. G. Swenson, L. Warman, and J. M. Beaulieu. 2014. Three keys to the radiation of angiosperms into freezing environments. *Nature* 506:89–92.
- Zheng, J., X. Zhao, H. Morris, and S. Jansen. 2019. Phylogeny Best Explains Latitudinal Patterns of Xylem Tissue Fractions for Woody Angiosperm Species Across China. *Frontiers in Plant Science* 10.
- Zizka, A., D. Silvestro, T. Andermann, J. Azevedo, C. Duarte Ritter, D. Edler, H. Farooq, A. Herdean, M. Ariza, R. Scharn, S. Svantesson, N. Wengström, V. Zizka, and A. Antonelli. 2019. CoordinateCleaner: Standardized cleaning of occurrence records from biological collection databases. *Methods in Ecology and Evolution* 10:744–751.

8 APPENDIXES

8.1 CHAPTER 2

8.1.1 Supplementary tables and figures

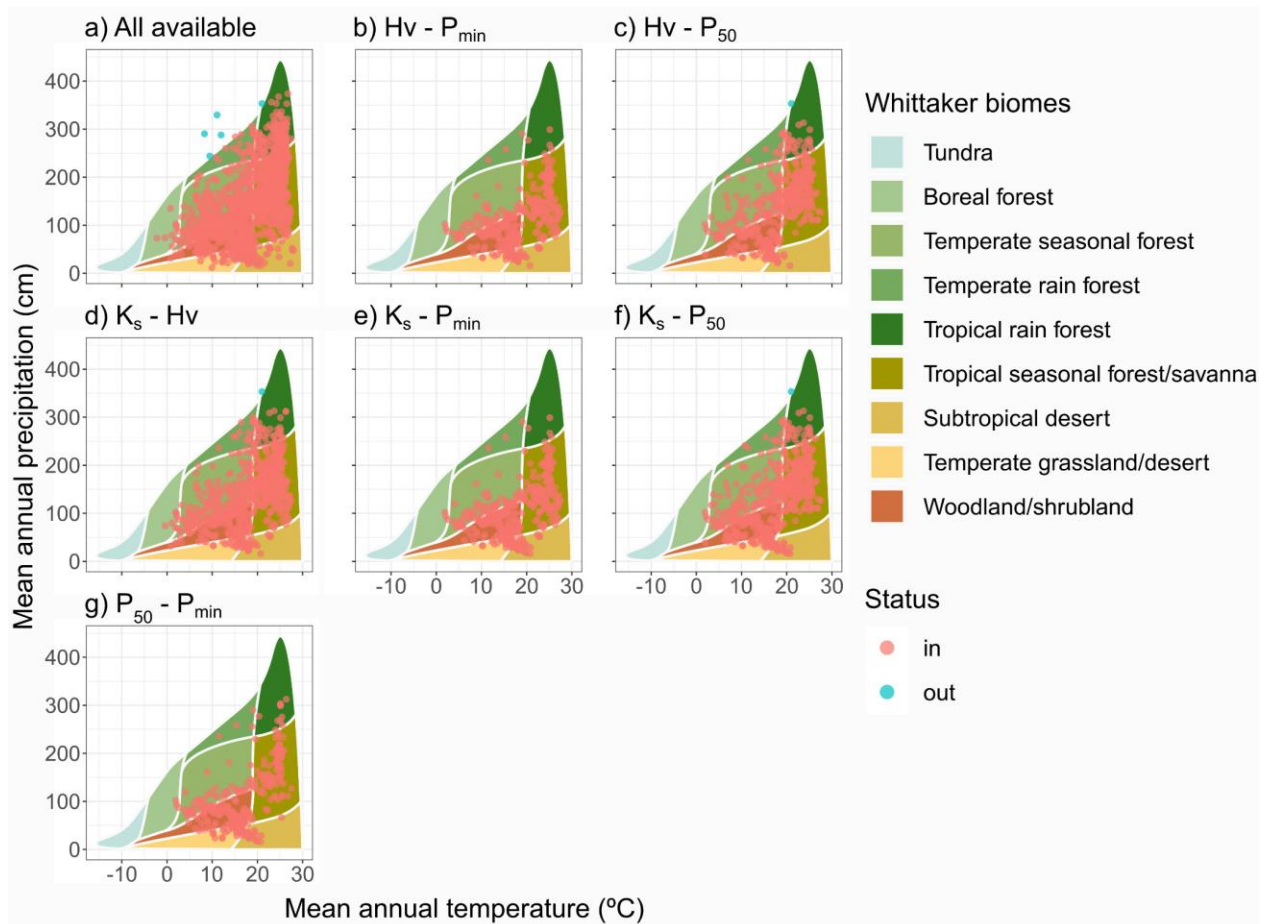
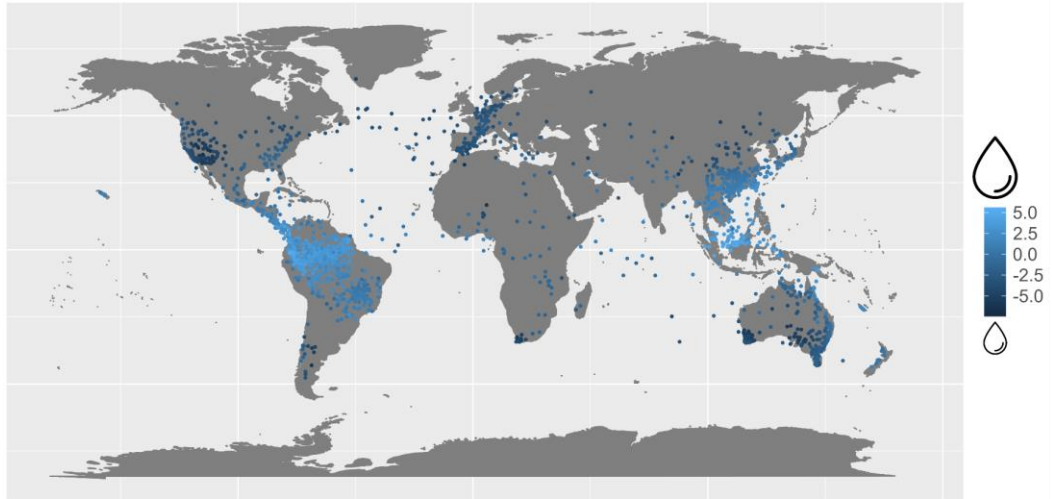
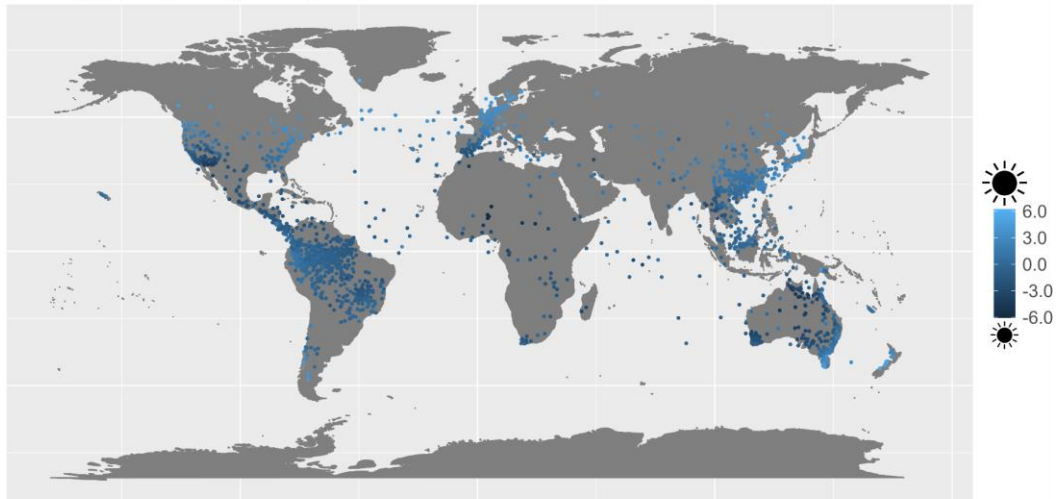


Figure S2.1 Whittaker diagrams for all observations available (once matched with the phylogeny) and observations used for each one of the evolutionary correlations calculations (which has been restricted to those species with complete observations for the two traits and with genus-level phylogenetic information available).

a) Water availability (PC1)



b) Energy input (PC2)



c) Soil depth

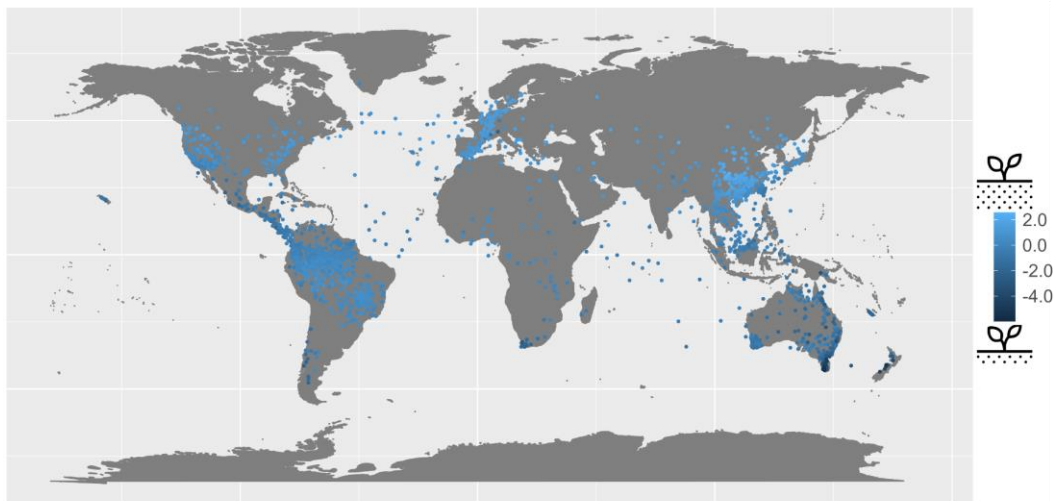


Figure S2.2 Species-mean coordinates are plotted for each species coloured by their environmental principal components mean values. Thus, some coordinates fall into the sea (presumably species present in both the Palearctic and the Nearctic realms). However, note that environmental variables were calculated for each occurrence of each species separately and then averaged to the species level.

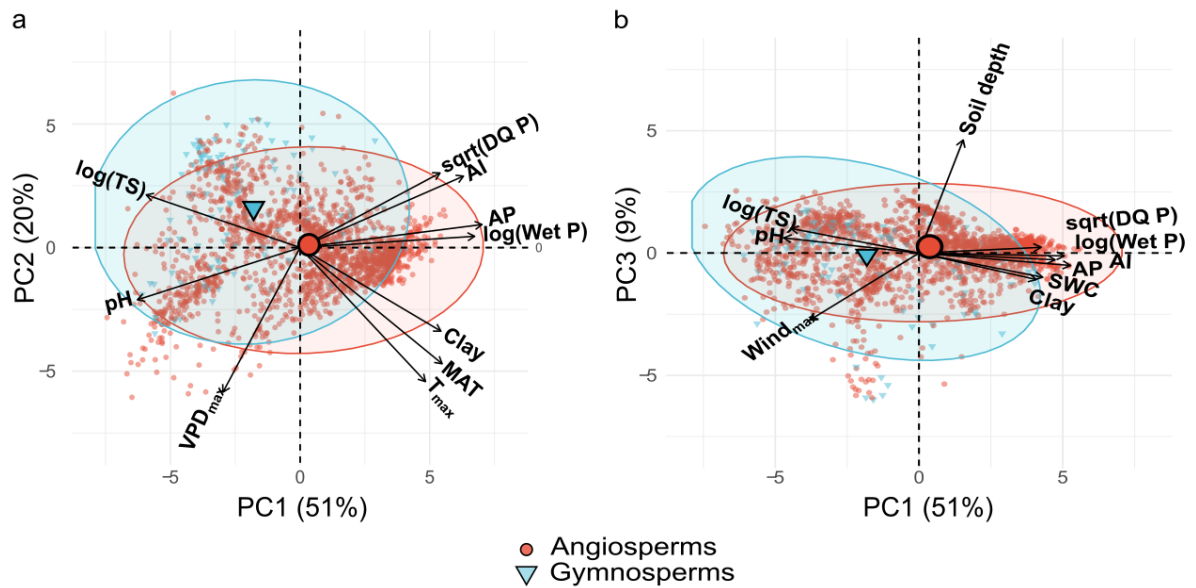
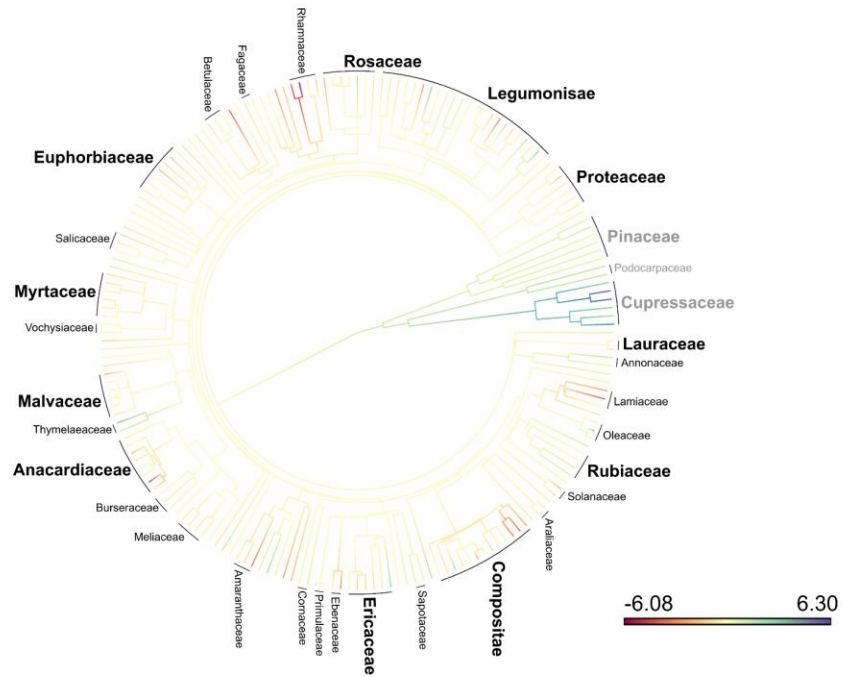


Figure S2.3 PCA biplots showing the contributions of the 10 most important environmental variables to the first two principal components, PC1 and PC2 (a) and to PC1 and PC3 (b), colouring species as angiosperms (red circles) or gymnosperms (light blue triangles). Environmental variance explained for each principal component is shown in percentage. log(TS): temperature seasonality (log. transformed); pH: soil pH measured at 60 cm; VPD_{max}: maximum vapour pressure deficit; T_{max}: mean of the monthly maximum temperatures; MAT: mean annual temperature; Clay: clay content in percentage measured at 60cm, log(Wet P): Precipitation of the wettest month (log. Transformed); AP: annual precipitation; AI: aridity index (which is actually a moisture index); sqrt(DQ P): dry quarter precipitation (square root transformed); Soil depth: absolute depth to bedrock, SWC: soil water content at 200cm, Wind_{max}: mean of the monthly maximum wind velocity.

a) Hydraulic Safety Margin, HSM



b) Hydraulic sufficiency, $\ln(K)$

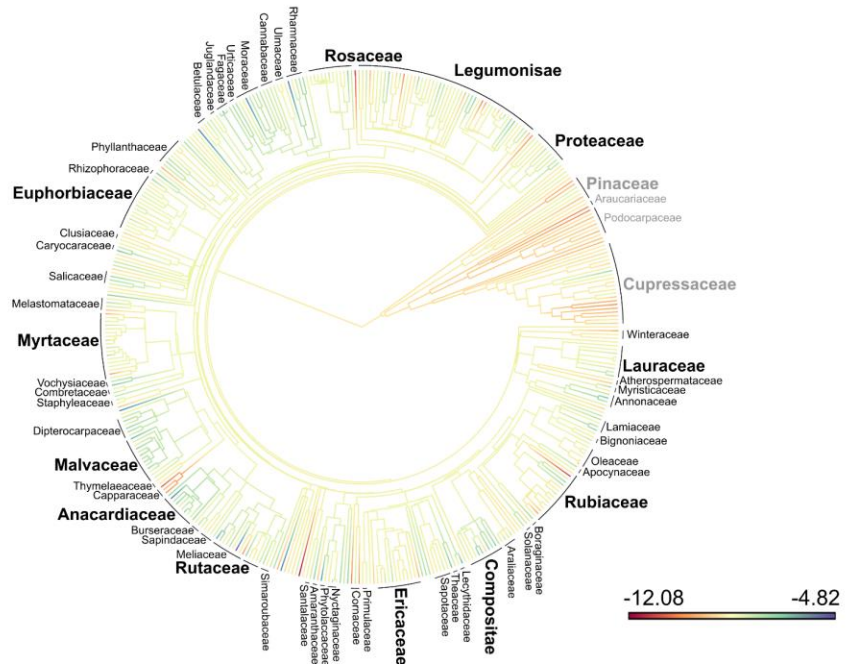
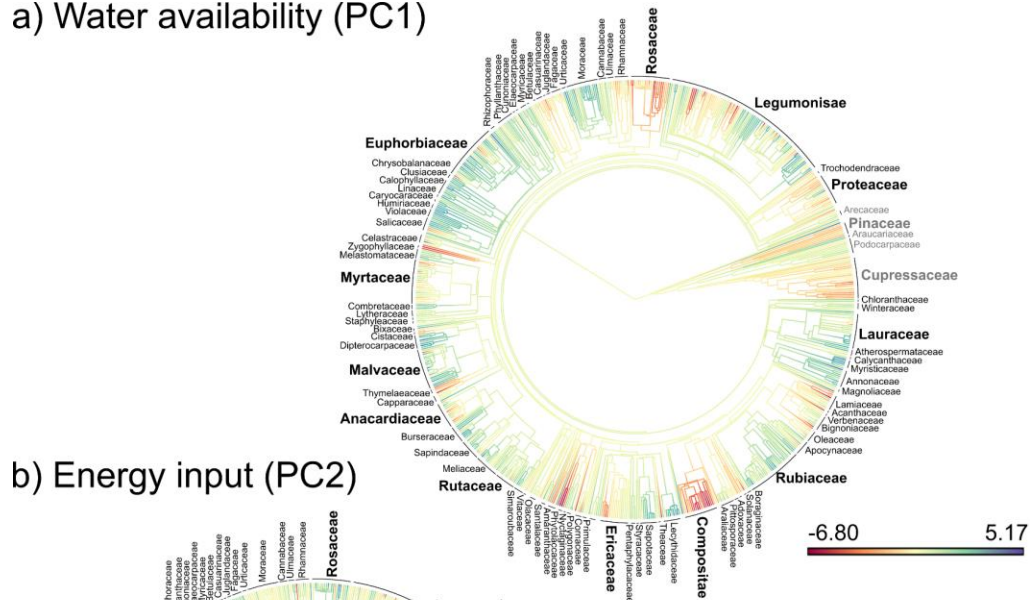
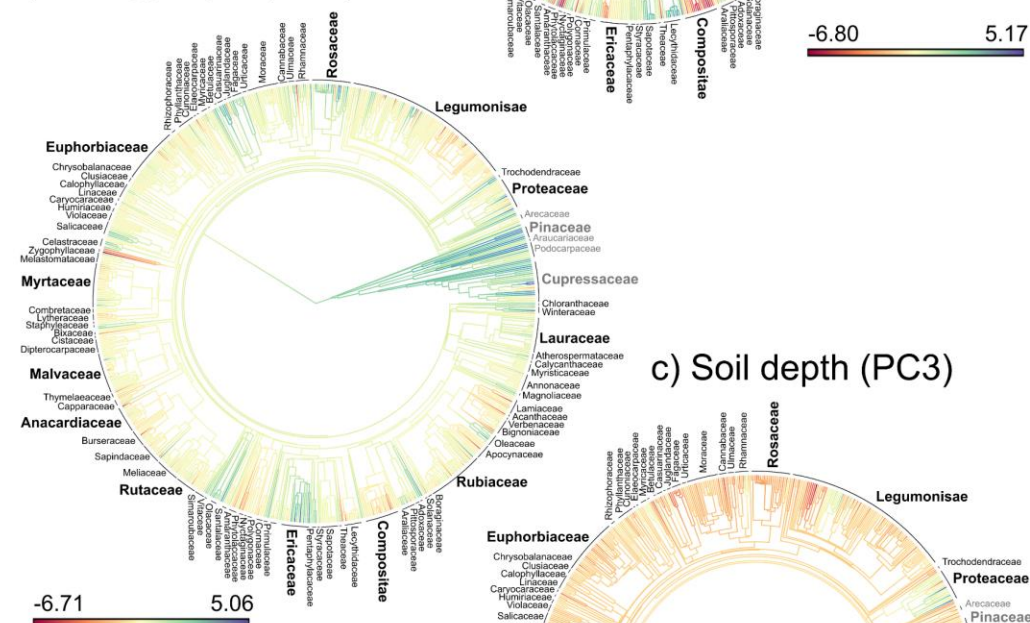


Figure S2.4 and S2.5 Phylogenetic reconstruction of ln-transformed hydraulic traits and environmental principal components, respectively. Families with more than one genus are shown in grey (gymnosperms) and black (angiosperms).

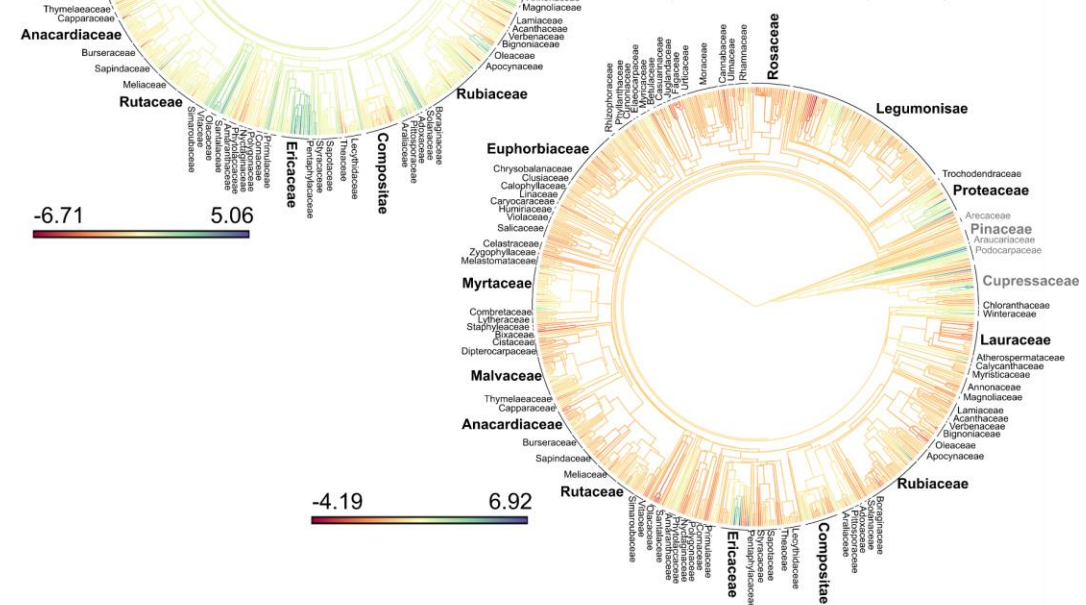
a) Water availability (PC1)



b) Energy input (PC2)



c) Soil depth (PC3)



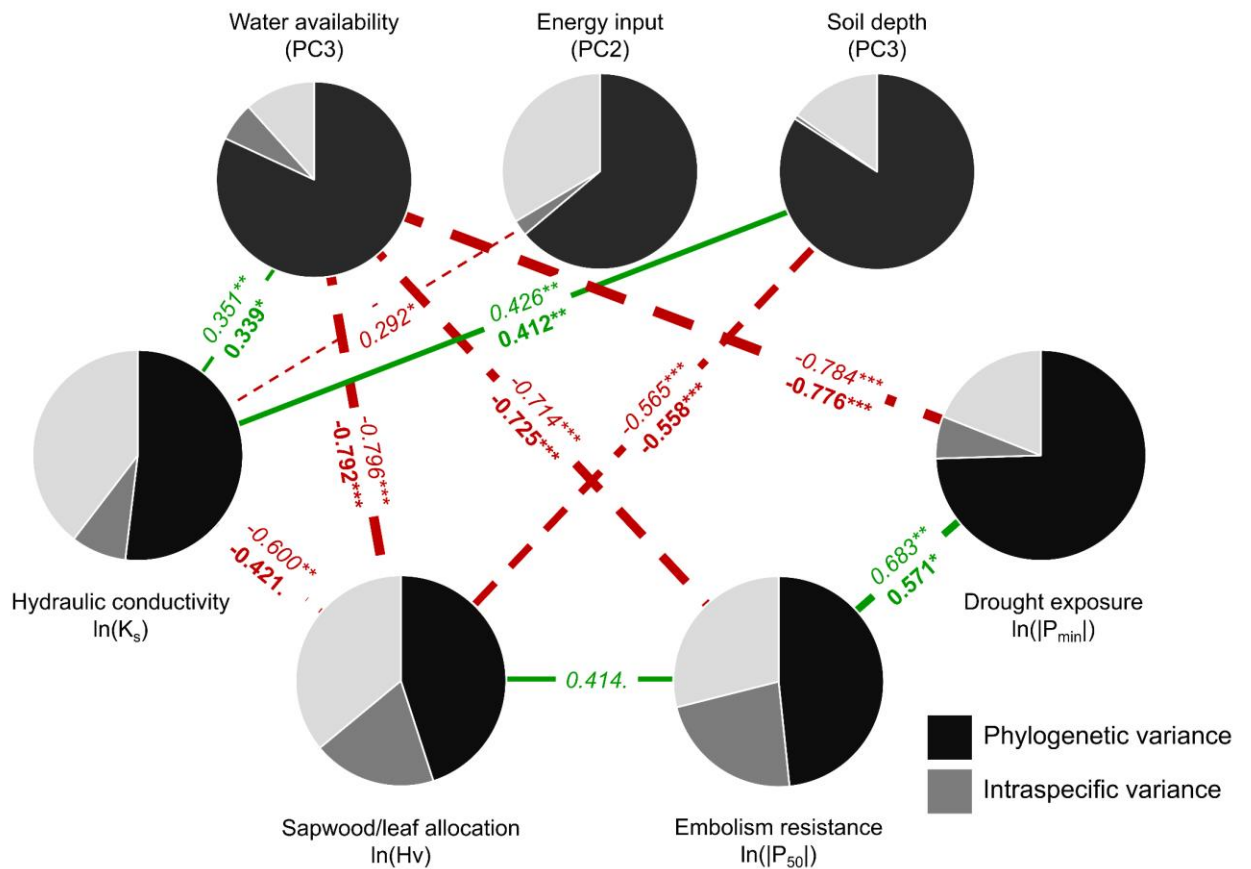


Figure S2.6 Correlated phylogenetic signals involving species-level hydraulic traits and environmental principal components using a species-level phylogeny. Environmental variables represent orthogonal PC axes and as such are not correlated. Lines represent significant evolutionary correlations. Red dashed lines represent negative correlations and green solid lines indicate positive correlations. Significant correlation coefficients are shown in italics and are proportional to the thickness of the line. Significant correlation coefficients between traits including environmental components and evolutionary affiliation as fixed effects are shown in bold (in the case of the relationships between environmental axes and traits, only evolutionary affiliation was considered as a fixed effect). P-values are also displayed for each coefficient. Signif. codes: “***”: P < 0.001; “**”: P < 0.01; “*”: P < 0.05 “.”: P < 0.1 “ ”: P > 0.1.

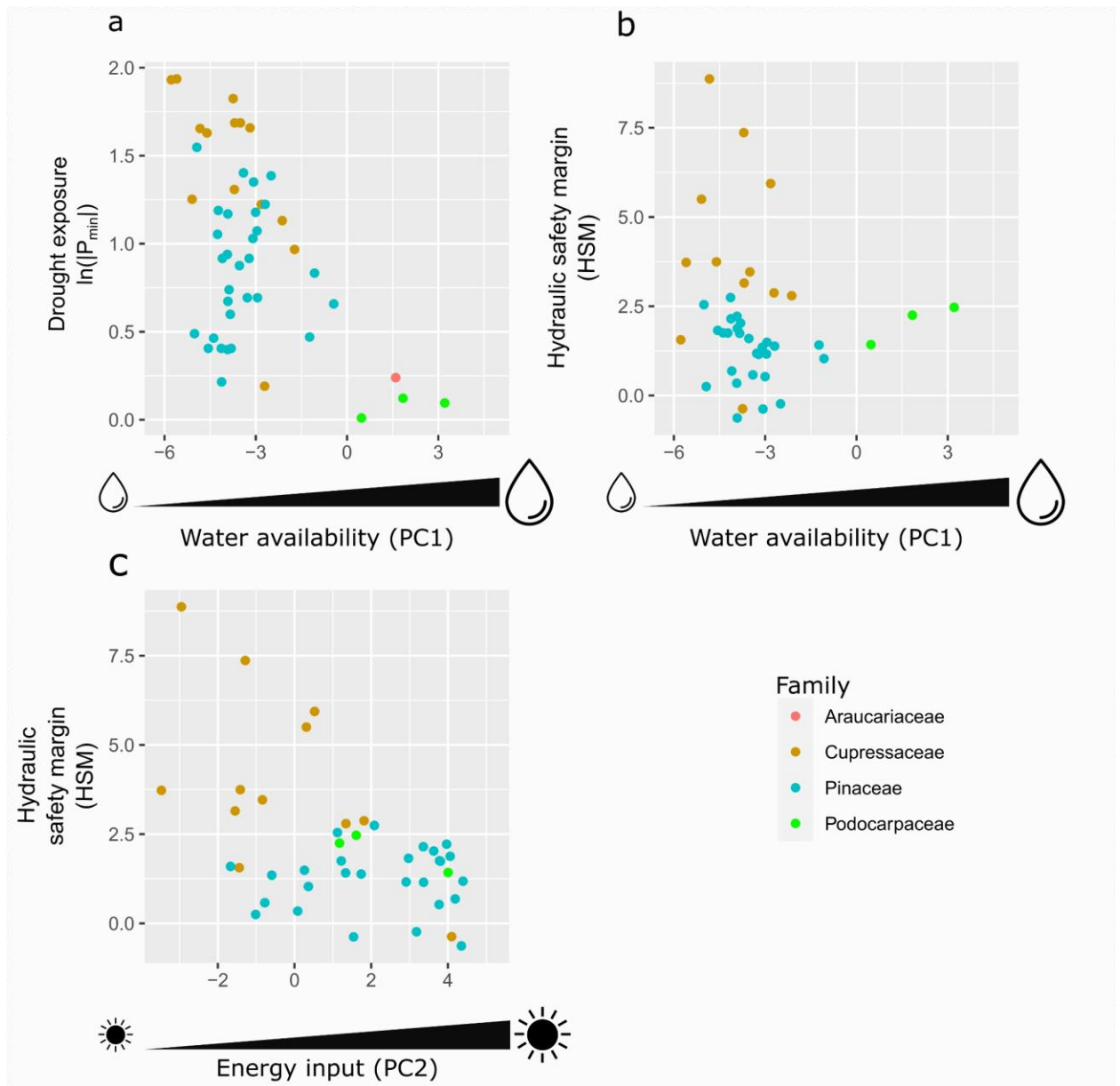


Figure S2.7 Gymnosperms observations for the relationships between HSM and P_{\min} with PC1 and the one between HSM and PC2. Species with HSM and P_{\min} data available are shown coloured by family. PC1 refers to the environmental principal component mainly explained by water availability, PC2 refers to the principal component mainly explained by decreasing energy input.

Table S2.1 Environmental variable and hydraulic traits nomenclature and number of whole dataset and major evolutionary affiliation observations. In the “Transformation” column, data transformations are specified when implemented.

Variable	Transformation	Abbreviation	Total observations	Angiosperms	Gymnosperms
Potential at the 50% loss of conductivity	Logarithmic of the absolute value	$\ln(P_{50})$	894	771	123
Maximum stem-specific hydraulic conductivity	Logarithmic	$\ln(K_s)$	1051	951	100
Leaf-specific hydraulic conductivity	Logarithmic	$\ln(K_l)$	845	769	76
Huber value (sapwood area:leaf area ratio)	Logarithmic	$\ln(H_v)$	1298	1223	75
Minimum water potential recorded	Logarithmic of the absolute value	$\ln(P_{min})$	553	505	48
Hydraulic Safety Margin ($\psi_{min-P50}$)		HSM	336	294	42
Precipitation warmest quarter	Square root	$\sqrt{WQ\ P}$	1937	1808	129
Precipitation wettest month	Logarithmic	$\ln(Wet\ P)$	1937	1808	129
Mean of the monthly maximum temperature		T_{max}	1937	1808	129
Temperature seasonality	Logarithmic	$\ln(TS)$	1937	1808	129
Annual precipitation		AP	1937	1808	129
Precipitation driest quarter	Square root	$\sqrt{DQ\ P}$	1937	1808	129
Mean annual temperature		MAT	1937	1808	129
Aridity index (which is actually a moisture index)		AI	1937	1808	129
Solar radiation		srad	1937	1808	129
Mean of the monthly maximum wind velocity		$wind_{max}$	1937	1808	129
Maximum vapour pressure deficit		VPD_{max}	1937	1808	129
Absolute depth to bed rock		Soil depth	1937	1808	129
pH measured at 60cm		pH	1937	1808	129
Clay content in percentage measured at 60cm		Clay	1937	1808	129
Sand content in percentage measured at 60cm		Sand	1937	1808	129
Soil water content at 200cm		SWC	1937	1808	129

Table S2.2 Contribution of environmental variables to the three environmental principal components. The highest contribution is highlighted for each variable. Sqrt(WQ P): Precipitation warmest quarter (square root transformed); log(Wet P): Precipitation wettest month (log. Transformed); T_{max}: Mean of the monthly maximum temperature; log(TS): Temperature seasonality (log. Transformed); AP: Annual precipitation; sqrt(DQ P): Precipitation driest quarter (square root Transformed); MAT: Mean annual temperature; AI: Aridity index (which is actually a moisture index); srad: Solar radiation; Wind_{max}: Mean of the monthly maximum wind velocity; VPD_{max}: Maximum vapour pressure deficit; Soil depth: Absolute depth to bedrock; pH: pH measured at 60cm; Clay: Clay content in percentage measured at 60cm; Sand: Sand content in percentage measured at 60cm; SWC: Soil water content at 200cm.

Variable	Contribution			Correlation		
	PC1	PC2	PC3	PC1	PC2	PC3
sqrt(WQ P)	7.200	2.273	0.125	0.766	0.269	0.042
log(Wet P)	10.192	0.121	0.031	0.912	0.062	-0.021
T_{max}	5.261	16.947	0.022	0.655	-0.734	-0.018
ln(TS)	7.906	2.624	2.283	-0.803	0.289	0.181
AP	11.069	0.502	0.588	0.950	0.126	-0.092
sqrt(DQ P)	6.551	5.256	2.105	0.731	0.409	-0.174
MAT	6.749	12.733	0.041	0.742	-0.636	-0.024
AI	8.932	4.820	0.173	0.853	0.391	-0.050
srad	0.077	20.291	11.520	-0.079	-0.803	-0.406
Wind_{max}	5.767	3.142	17.055	-0.686	0.316	-0.495
VPD_{max}	1.986	19.722	0.920	-0.402	-0.792	0.115
Soil Depth	0.942	1.405	48.430	0.277	-0.211	0.833
pH	8.843	2.569	0.873	-0.849	-0.286	0.112
Clay	6.636	6.592	2.668	0.736	-0.458	-0.196
Sand	4.496	0.825	10.945	-0.606	-0.162	-0.396
SWC	7.393	0.178	2.220	0.776	0.075	-0.178

Table S2.3 Reference table for all the models reported in the main text. All models were implemented with and without accounting for the phylogeny. In the fixed structure column, variables to the right of the “~” symbol are response variables, those to the left are predictors. Abbreviations: “env”(1): individual environmental principal component; env(3): three main environmental principal components; trait: individual hydraulic trait; Affiliation: major evolutionary affiliation (angiosperm or gymnosperm), “1” refer to the intercept.

Fixed structure	Description	Phylogeny used	Number of response variables
env(1) ~ 1		Genus-level	Uni-response
trait ~ 1	Phylogenetic signal	Genus-level	Uni-response
trait ~ env(1)		Genus-level	Uni-response
trait ~ env(1) + Affiliation		Genus-level	Uni-response
trait ~ env(1) * Affiliation	Uni-response environment models	Genus-level	Uni-response
trait , env(1) ~ 1		Genus-level	Bi-response
trait , env(1) ~ 1 + Affiliation		Genus-level	Bi-response
trait , trait ~ 1		Genus-level	Bi-response
trait , trait ~ 1 + Affiliation		Genus-level	Bi-response
trait , trait ~ 1 + env(3)		Genus-level	Bi-response
trait , trait ~ 1 + env(3) + Affiliation	Evolutionary correlations	Genus-level	Bi-response
trait , trait ~ 1 + env(3) * Affiliation		Genus-level	Bi-response
env(1) ~ 1		Species-level	Uni-response
trait ~ 1	Phylogenetic signal	Species-level	Uni-response
trait , env(1) ~ -1		Species-level	Bi-response
trait , env(1) ~ -1 + Affiliation		Species-level	Bi-response
trait , trait ~ -1	Evolutionary correlations	Species-level	Bi-response
trait , trait ~ -1 + env(3) * Affiliation		Species-level	Bi-response

Table S2.4 Non-phylogenetic model’s variance partition. Mean non-phylogenetic inter-generic (γ) and non-phylogenetic intra-generic (ϱ) variance in non-phylogenetic models without fixed effects. Note that phylogenetic variance (λ) is 0, as the phylogenetic effect was not considered.

variable	Phylogenetic (λ)	Inter-generic (γ)	Intra-generic (ϱ)
HSM	0	0.490	0.510
Ln(Hv)	0	0.514	0.486
Ln(Ki)	0	0.280	0.720
L(Ks)	0	0.459	0.541
Ln(P _{min})	0	0.621	0.379
Ln(P ₅₀)	0	0.636	0.364
PC1	0	0.787	0.213
PC2	0	0.483	0.517
PC3	0	0.641	0.359

Table S2.5 Uni-response models description. DICs and explained variances for phylogenetic and non-phylogenetic uni-response models. The fixed formula is shown in each case. DICs for the phylogenetic models are shown. “NP” refer to non-phylogenetic models (i.e., only including genus contingency as random effect) explained variances. R^2_c refer to the conditional and R^2_m refers to the marginal explained variances. Abbreviations: K_s : Xylem conductivity; P_{50} : xylem resistance to embolism; H_v : sapwood allocation relative to leaf area; P_{min} : drought exposure, HSM: hydraulic safety margin; K_j : and sufficiency; PC1: water availability; PC2: energy input and PC3: soil depth; Affiliation: evolutionary affiliation (angiosperm or gymnosperm).

Fixed effects formula	DIC	R^2_m	R^2_c	NP R^2_m	NP R^2_c
HSM ~ 1	1181	0	0.612	0	0.49
HSM ~ PC1 * Affiliation	1133	0.253	0.657	0.301	0.554
HSM ~ PC1 + Affiliation	1138	0.211	0.647	0.268	0.535
HSM ~ PC1	1139	0.065	0.625	0.026	0.519
HSM ~ PC2 * Affiliation	1133	0.246	0.623	0.28	0.509
HSM ~ PC2 + Affiliation	1142	0.184	0.658	0.237	0.54
HSM ~ PC2	1143	0.035	0.619	0.031	0.495
HSM ~ PC3 * Affiliation	1146	0.172	0.624	0.23	0.542
HSM ~ PC3 + Affiliation	1147	0.176	0.634	0.235	0.541
HSM ~ PC3	1150	0.006	0.618	0.02	0.528
ln(H_v) ~ 1	3147	0	0.641	0	0.514
ln(H_v) ~ PC1 + Affiliation	3013	0.166	0.549	0.187	0.479
ln(H_v) ~ PC1	3013	0.155	0.536	0.184	0.477
ln(H_v) ~ PC1 * Affiliation	3014	0.168	0.551	0.188	0.478
ln(H_v) ~ PC2 * Affiliation	3058	0.028	0.662	0.014	0.51
ln(H_v) ~ PC2	3060	0.002	0.646	0.001	0.509
ln(H_v) ~ PC2 + Affiliation	3060	0.028	0.657	0.013	0.509
ln(H_v) ~ PC3 + Affiliation	3066	0.045	0.615	0.04	0.477
ln(H_v) ~ PC3	3066	0.022	0.601	0.032	0.48
ln(H_v) ~ PC3 * Affiliation	3068	0.045	0.614	0.043	0.475
ln(K_i) ~ 1	2348	0	0.47	0	0.28
ln(K_i) ~ PC1 * Affiliation	2250	0.067	0.482	0.077	0.299
ln(K_i) ~ PC1	2252	0.002	0.447	0.002	0.282
ln(K_i) ~ PC1 + Affiliation	2254	0.069	0.463	0.077	0.296
ln(K_i) ~ PC2	2250	0.016	0.41	0.033	0.254
ln(K_i) ~ PC2 * Affiliation	2251	0.089	0.439	0.093	0.283
ln(K_i) ~ PC2 + Affiliation	2251	0.084	0.434	0.088	0.276
ln(K_i) ~ PC3	2250	0.002	0.454	0.008	0.297
ln(K_i) ~ PC3 + Affiliation	2252	0.072	0.462	0.077	0.304
ln(K_i) ~ PC3 * Affiliation	2253	0.075	0.47	0.077	0.304
ln(K_s) ~ 1	2795	0	0.608	0	0.459
ln(K_s) ~ ln(H_v)	2079	0.116	0.614	0.181	0.494
ln(K_s) ~ ln(H_v) * Affiliation	2081	0.166	0.64	0.23	0.506
ln(K_s) ~ ln(P_{50})	1581	0.041	0.634	0.074	0.499
ln(K_s) ~ ln(P_{50}) * Affiliation	1583	0.111	0.666	0.118	0.51

$\ln(K_s) \sim \text{PC1}$	2670	0.028	0.603	0.042	0.475
$\ln(K_s) \sim \text{PC1} + \text{Affiliation}$	2670	0.084	0.631	0.089	0.479
$\ln(K_s) \sim \text{PC1} * \text{Affiliation}$	2670	0.091	0.635	0.09	0.479
$\ln(K_s) \sim \text{PC2}$	2694	0.003	0.602	0.01	0.447
$\ln(K_s) \sim \text{PC2} + \text{Affiliation}$	2694	0.057	0.623	0.055	0.453
$\ln(K_s) \sim \text{PC2} * \text{Affiliation}$	2696	0.058	0.625	0.056	0.456
$\ln(K_s) \sim \text{PC3}$	2685	0.01	0.59	0.028	0.462
$\ln(K_s) \sim \text{PC3} + \text{Affiliation}$	2685	0.063	0.618	0.069	0.462
$\ln(K_s) \sim \text{PC3} * \text{Affiliation}$	2687	0.062	0.617	0.07	0.463
$\ln(P_{\min}) \sim 1$	828	0	0.812	0	0.621
$\ln(P_{\min}) \sim \ln(P_{50})$	431	0.279	0.738	0.299	0.71
$\ln(P_{\min}) \sim \ln(P_{50}) * \text{Affiliation}$	432	0.29	0.738	0.314	0.703
$\ln(P_{\min}) \sim \text{PC1} * \text{Affiliation}$	688	0.228	0.788	0.303	0.686
$\ln(P_{\min}) \sim \text{PC1}$	692	0.211	0.763	0.302	0.679
$\ln(P_{\min}) \sim \text{PC1} + \text{Affiliation}$	692	0.229	0.781	0.302	0.68
$\ln(P_{\min}) \sim \text{PC2} * \text{Affiliation}$	724	0.099	0.854	0.107	0.692
$\ln(P_{\min}) \sim \text{PC2}$	725	0.055	0.843	0.094	0.691
$\ln(P_{\min}) \sim \text{PC2} + \text{Affiliation}$	725	0.099	0.854	0.104	0.687
$\ln(P_{\min}) \sim \text{PC3} + \text{Affiliation}$	793	0.07	0.841	0.047	0.649
$\ln(P_{\min}) \sim \text{PC3}$	793	0.016	0.827	0.036	0.644
$\ln(P_{\min}) \sim \text{PC3} * \text{Affiliation}$	795	0.072	0.841	0.051	0.65
$\ln(P_{50}) \sim 1$	1426	0	0.71	0	0.636
$\ln(P_{50}) \sim \text{PC1} * \text{Affiliation}$	1396	0.193	0.635	0.23	0.605
$\ln(P_{50}) \sim \text{PC1}$	1397	0.069	0.617	0.097	0.588
$\ln(P_{50}) \sim \text{PC1} + \text{Affiliation}$	1397	0.194	0.636	0.231	0.606
$\ln(P_{50}) \sim \text{PC2} * \text{Affiliation}$	1402	0.116	0.725	0.148	0.635
$\ln(P_{50}) \sim \text{PC2} + \text{Affiliation}$	1403	0.108	0.719	0.141	0.631
$\ln(P_{50}) \sim \text{PC2}$	1403	0.001	0.694	0.002	0.623
$\ln(P_{50}) \sim \text{PC3} * \text{Affiliation}$	1394	0.107	0.728	0.141	0.637
$\ln(P_{50}) \sim \text{PC3} + \text{Affiliation}$	1397	0.105	0.725	0.144	0.636
$\ln(P_{50}) \sim \text{PC3}$	1397	0.003	0.699	0.002	0.628
$\text{PC1} \sim 1$	6985	0	0.891	0	0.787
$\text{PC2} \sim 1$	6723	0	0.697	0	0.483
$\text{PC3} \sim 1$	4707	0	0.85	0	0.641

Table S2.6 Mean of the evolutionary correlation (EC), credible interval (lower and upper HPD) and p-value reported by bi-response models. The fixed formula is shown in each case. Models are ordered by DIC values (from lower to higher) for each set of nested models (same response variables). Statistically significant evolutionary correlations are highlighted in bold and marginally significant in italics. Abbreviations: K_s : Xylem conductivity; P_{50} : xylem resistance to embolism; H_v : sapwood allocation relative to leaf area; P_{min} : drought exposure; PC1: water availability; PC2: energy input and PC3: soil depth; Affiliation: evolutionary affiliation (angiosperm or gymnosperm).

Variable 1	Variable 2	Fixed formula	EC	Lower HPD	Upper HPD	p-value	DIC
$\ln(H_v)$	$\ln(P_{min})$	$(\ln(H_v), \ln(P_{min})) \sim 1 + (PC1 + PC2 + PC3) * \text{Affiliation}$	-0.094	-0.681	0.436	0.752	1403
$\ln(H_v)$	$\ln(P_{min})$	$(\ln(H_v), \ln(P_{min})) \sim 1 + PC1 + PC2 + PC3$	-0.100	-0.636	0.486	0.736	1403
$\ln(H_v)$	$\ln(P_{min})$	$(\ln(H_v), \ln(P_{min})) \sim 1 + \text{Affiliation} + PC1 + PC2 + PC3$	-0.117	-0.624	0.462	0.664	1404
$\ln(H_v)$	$\ln(P_{min})$	$(\ln(H_v), \ln(P_{min})) \sim 1 + \text{Affiliation}$	0.222	-0.405	0.801	0.494	1571
$\ln(H_v)$	$\ln(P_{min})$	$(\ln(H_v), \ln(P_{min})) \sim 1$	0.217	-0.405	0.798	0.509	1571
$\ln(H_v)$	PC1	$(\ln(H_v), PC1) \sim 1$	-0.796	-0.913	-0.662	0.000	7475
$\ln(H_v)$	PC1	$(\ln(H_v), PC1) \sim 1 + \text{Affiliation}$	-0.792	-0.910	-0.657	0.000	7475
$\ln(H_v)$	PC2	$(\ln(H_v), PC2) \sim 1 + \text{Affiliation}$	0.145	-0.160	0.462	0.397	7296
$\ln(H_v)$	PC2	$(\ln(H_v), PC2) \sim 1$	0.156	-0.141	0.473	0.363	7296
$\ln(H_v)$	PC3	$(\ln(H_v), PC3) \sim 1 + \text{Affiliation}$	-0.558	-0.747	-0.363	0.000	5971
$\ln(H_v)$	PC3	$(\ln(H_v), PC3) \sim 1$	-0.565	-0.737	-0.367	0.000	5972
$\ln(K_s)$	$\ln(H_v)$	$(\ln(K_s), \ln(H_v)) \sim 1 + PC1 + PC2 + PC3$	-0.423	-0.805	-0.016	0.077	3843
$\ln(K_s)$	$\ln(H_v)$	$(\ln(K_s), \ln(H_v)) \sim 1 + \text{Affiliation} + PC1 + PC2 + PC3$	-0.423	-0.795	-0.005	0.079	3843
$\ln(K_s)$	$\ln(H_v)$	$chind(\ln(K_s), \ln(H_v)) \sim 1 + (PC1 + PC2 + PC3) * \text{Affiliation}$	-0.421	-0.827	-0.012	0.085	3853
$\ln(K_s)$	$\ln(H_v)$	$(\ln(K_s), \ln(H_v)) \sim 1$	-0.600	-0.868	-0.271	0.008	4058
$\ln(K_s)$	$\ln(H_v)$	$(\ln(K_s), \ln(H_v)) \sim 1 + \text{Affiliation}$	-0.588	-0.879	-0.247	0.010	4059
$\ln(K_s)$	$\ln(P_{min})$	$(\ln(K_s), \ln(P_{min})) \sim 1 + (PC1 + PC2 + PC3) * \text{Affiliation}$	0.019	-0.538	0.566	0.934	1571
$\ln(K_s)$	$\ln(P_{min})$	$(\ln(K_s), \ln(P_{min})) \sim 1 + \text{Affiliation} + PC1 + PC2 + PC3$	-0.013	-0.535	0.569	0.966	1572
$\ln(K_s)$	$\ln(P_{min})$	$(\ln(K_s), \ln(P_{min})) \sim 1 + PC1 + PC2 + PC3$	0.008	-0.512	0.555	0.970	1572
$\ln(K_s)$	$\ln(P_{min})$	$(\ln(K_s), \ln(P_{min})) \sim 1$	-0.080	-0.683	0.487	0.785	1768
$\ln(K_s)$	$\ln(P_{min})$	$(\ln(K_s), \ln(P_{min})) \sim 1 + \text{Affiliation}$	-0.066	-0.675	0.507	0.823	1768
$\ln(K_s)$	$\ln(P_{50})$	$(\ln(K_s), \ln(P_{50})) \sim 1 + \text{Affiliation} + PC1 + PC2 + PC3$	-0.046	-0.517	0.399	0.851	2489
$\ln(K_s)$	$\ln(P_{50})$	$(\ln(K_s), \ln(P_{50})) \sim 1 + PC1 + PC2 + PC3$	-0.098	-0.510	0.324	0.648	2489
$\ln(K_s)$	$\ln(P_{50})$	$(\ln(K_s), \ln(P_{50})) \sim 1 + (PC1 + PC2 + PC3) * \text{Affiliation}$	-0.019	-0.475	0.408	0.917	2495
$\ln(K_s)$	$\ln(P_{50})$	$(\ln(K_s), \ln(P_{50})) \sim 1$	-0.317	-0.665	0.055	0.114	2596
$\ln(K_s)$	$\ln(P_{50})$	$(\ln(K_s), \ln(P_{50})) \sim 1 + \text{Affiliation}$	-0.274	-0.639	0.165	0.211	2596
$\ln(K_s)$	PC1	$(\ln(K_s), PC1) \sim 1 + \text{Affiliation}$	0.339	0.093	0.578	0.010	6343
$\ln(K_s)$	PC1	$(\ln(K_s), PC1) \sim 1$	0.351	0.110	0.594	0.009	6343
$\ln(K_s)$	PC2	$(\ln(K_s), PC2) \sim 1 + \text{Affiliation}$	-0.275	-0.570	0.003	0.069	6315
$\ln(K_s)$	PC2	$(\ln(K_s), PC2) \sim 1$	-0.292	-0.576	-0.007	0.048	6315
$\ln(K_s)$	PC3	$(\ln(K_s), PC3) \sim 1 + \text{Affiliation}$	0.412	0.144	0.683	0.008	5216
$\ln(K_s)$	PC3	$(\ln(K_s), PC3) \sim 1$	0.426	0.185	0.706	0.005	5216
$\ln(P_{min})$	PC1	$(\ln(P_{min}), PC1) \sim 1 + \text{Affiliation}$	-0.776	-0.908	-0.624	0.000	2636
$\ln(P_{min})$	PC1	$(\ln(P_{min}), PC1) \sim 1$	-0.784	-0.907	-0.620	0.000	2636

$\ln(P_{\min})$	PC2	$(\ln(P_{\min}), PC2) \sim 1$	-0.232	-0.566	0.129	0.214	2744
$\ln(P_{\min})$	PC2	$(\ln(P_{\min}), PC2) \sim 1 + \text{Affiliation}$	-0.249	-0.594	0.124	0.195	2745
$\ln(P_{\min})$	PC3	$(\ln(P_{\min}), PC3) \sim 1 + \text{Affiliation}$	0.115	-0.236	0.452	0.539	1916
$\ln(P_{\min})$	PC3	$(\ln(P_{\min}), PC3) \sim 1$	0.126	-0.208	0.480	0.471	1917
$\ln(P_{50})$	$\ln(Hv)$	$(\ln(P_{50}), \ln(Hv)) \sim 1 + PC1 + PC2 + PC3$	0.060	-0.423	0.507	0.818	1834
$\ln(P_{50})$	$\ln(Hv)$	$(\ln(P_{50}), \ln(Hv)) \sim 1 + \text{Affiliation} + PC1 + PC2 + PC3$	0.061	-0.413	0.511	0.779	1835
$\ln(P_{50})$	$\ln(Hv)$	$(\ln(P_{50}), \ln(Hv)) \sim 1 + (PC1 + PC2 + PC3) * \text{Affiliation}$	0.053	-0.404	0.531	0.831	1843
$\ln(P_{50})$	$\ln(Hv)$	$(\ln(P_{50}), \ln(Hv)) \sim 1$	0.414	0.052	0.790	0.070	1927
$\ln(P_{50})$	$\ln(Hv)$	$(\ln(P_{50}), \ln(Hv)) \sim 1 + \text{Affiliation}$	0.385	-0.043	0.777	0.121	1927
$\ln(P_{50})$	$\ln(P_{\min})$	$(\ln(P_{50}), \ln(P_{\min})) \sim 1 + (PC1 + PC2 + PC3) * \text{Affiliation}$	0.571	0.213	0.860	0.015	745
$\ln(P_{50})$	$\ln(P_{\min})$	$(\ln(P_{50}), \ln(P_{\min})) \sim 1 + \text{Affiliation} + PC1 + PC2 + PC3$	0.552	0.168	0.863	0.030	751
$\ln(P_{50})$	$\ln(P_{\min})$	$(\ln(P_{50}), \ln(P_{\min})) \sim 1 + PC1 + PC2 + PC3$	0.556	0.168	0.833	0.015	751
$\ln(P_{50})$	$\ln(P_{\min})$	$(\ln(P_{50}), \ln(P_{\min})) \sim 1 + \text{Affiliation}$	0.702	0.428	0.917	0.000	834
$\ln(P_{50})$	$\ln(P_{\min})$	$(\ln(P_{50}), \ln(P_{\min})) \sim 1$	0.683	0.386	0.914	0.006	834
$\ln(P_{50})$	PC1	$(\ln(P_{50}), PC1) \sim 1 + \text{Affiliation}$	-0.725	-0.885	-0.537	0.000	4476
$\ln(P_{50})$	PC1	$(\ln(P_{50}), PC1) \sim 1$	-0.714	-0.875	-0.524	0.000	4477
$\ln(P_{50})$	PC2	$(\ln(P_{50}), PC2) \sim 1$	0.050	-0.316	0.460	0.803	4487
$\ln(P_{50})$	PC2	$(\ln(P_{50}), PC2) \sim 1 + \text{Affiliation}$	0.015	-0.344	0.400	0.978	4488
$\ln(P_{50})$	PC3	$(\ln(P_{50}), PC3) \sim 1 + \text{Affiliation}$	-0.110	-0.456	0.208	0.570	3677
$\ln(P_{50})$	PC3	$(\ln(P_{50}), PC3) \sim 1$	-0.097	-0.426	0.229	0.573	3678

8.1.2 Supplementary methods

8.1.2.1 Phylogenetic mixed model description

Phylogenetic mixed models are commonly used in quantitative genetics (the so called “animal” model), being useful for comparative analyses as they allow to incorporate a range of variance structures for the random effects, including shared ancestry through a phylogeny (Housworth et al. 2004). The general model structure is defined as follows:

$$y = \mu + \beta x + p + g + e \quad (1)$$

Where μ is the grand mean, interpreted as the root ancestor state, β is the slope for the covariate x (fixed effect, in green), p and g are the variability caused by the genus-level phylogeny and the genus contingency effects (random effects, in red), and e is the residual error (Housworth *et al.* 2004; Villemereuil & Nakagawa 2014). Both fixed (β) and random (r , which is $p + g$) effects and the residuals (e) are expected to come from a multivariate normal distribution as it follows:

$$\begin{bmatrix} \beta \\ r \\ e \end{bmatrix} \sim N \left(\begin{bmatrix} \beta_0 \\ 0 \\ 0 \end{bmatrix}, \begin{bmatrix} B & 0 & 0 \\ 0 & G & 0 \\ 0 & 0 & R \end{bmatrix} \right) \quad (2)$$

Where β is the fixed effect parameter to estimate, β_0 is the prior means for the fixed effects with prior (co)variance matrix B , and G and R are the expected (co)variances of the random effects and the residuals respectively (Hadfield 2010a, Hadfield and Nakagawa 2010). G and R are unknown, and must be estimated from the data by assuming they are structured in a way that can be parametrized by few parameters, as it has been exemplified below for the G case:

$$G = \begin{bmatrix} V_{G_1} \otimes A_{G_1} & 0 \\ 0 & V_{G_2} \otimes A_{G_2} \end{bmatrix} \quad (3)$$

Where the (co)variance matrices (V) are matrices with one parameter to be estimated per response variable and the structured matrices (A) refer to the phylogenetic structure (A_{G_1}) and genus contingency (A_{G_2}). The Kronecker product (\otimes) allows for possible dependence between random effects (Hadfield 2010a, Hadfield and Nakagawa 2010).

In multi-response models, the (co)variance matrix of the previous equation is reformulated including the covariance estimates in the off-diagonal and the respective variances in the diagonal as follows:

$$V_{G1} = \begin{bmatrix} \sigma_{u_1}^2 & \sigma_{u_1, u_2} \\ \sigma_{u_2, u_1} & \sigma_{u_2}^2 \end{bmatrix} \quad (4)$$

Where $\sigma_{u_1}^2$ is the variance for the first response variable (V_1) and $\sigma_{u_2}^2$ the variance for the second response variable (V_2), while σ_{u_1, u_2} and σ_{u_2, u_1} are the same covariance estimate (C).

8.1.2.2 Phylogenetic indexes calculation

The phylogenetic signal or phylogenetic heritability it is calculated as follows (Villemereuil & Nakagawa 2014):

$$\lambda = \frac{\sigma_p^2}{\sigma_p^2 + \sigma_g^2 + \sigma_e^2} \quad (5)$$

Where σ_p^2 is the variance of the phylogenetic effect (V_{G1}), σ_g^2 is the variance of the cross-genus effect (V_{G2}) and σ_e^2 is the residual error (Villemereuil & Nakagawa 2014). Cross-genera variance (i.e. non-phylogenetic variation among genera or genus lability) has been calculated as follows:

$$\gamma = \frac{\sigma_g^2}{\sigma_p^2 + \sigma_g^2 + \sigma_e^2} \quad (6)$$

And finally, intra-genus variability including measurement error has been calculated as follows:

$$\rho = \frac{\sigma_e^2}{\sigma_p^2 + \sigma_g^2 + \sigma_e^2} \quad (7)$$

Note also that $\gamma + \rho + \lambda = 1$ (Housworth et al. 2004). The three indexes were calculated for the whole Markov chain random effects and residual samples (once burned and thinned), so the output is a statistical distribution from which the mean and 95% credible intervals can be calculated.

8.1.2.3 Phylogenetic covariation calculation

From the phylogenetic variances and covariance in equation 4, the evolutionary correlation between response variables can be calculated as follows (Villemereuil 2012):

$$r_{ev} = \frac{\sigma_{u_2, u_1}}{\sqrt{\sigma_{u_1}^2 \cdot \sigma_{u_2}^2}} \quad (8)$$

8.1.2.4 Model specifications

MCMCglmm implements a Bayesian approach, estimating the posterior distribution of parameters, from which 95% credible intervals can be obtained (Hadfield 2010a). I set independent normal prior distributions for fixed effects and non-informative Inverse-Gamma prior distributions for random effects and residual variances (Villemereuil & Nakagawa 2014). Less informative expanded priors were also used, and highly similar results were obtained.

Uni-response models random effects variance priors were set as $V = 1$, $\nu = 0.002$. For bi-response models, the random effects variances priors were set as $V = \text{diag}(2)/2$, $\nu = 2$. To achieve convergence, each model was run for 8,000,000 iterations with a 1,000,000 burn-in and a thinning interval of 4,000, reaching an effective sample size between 1,000 and 2,000 in all estimated parameters. When models did not converge, I increased the number of iterations until convergence were achieved. Thinning intervals and the final number of iterations were progressively increased until autocorrelations between samples were found to be < 0.1 . Convergence of all models was assessed by plots of chain mixing and by the Heidenberg stationary test as a diagnostic. All reported models had a low degree of autocorrelation between iterations and passed the convergence diagnostic, both for fixed and random effects (i.e., the sampled chains were stationary).

Literature cited

Hadfield, J.D. (2010). MCMCglmm for R. *J. Stat. Softw.*, 33.

Hadfield, J.D. & Nakagawa, S. (2010). General quantitative genetic methods for comparative biology: Phylogenies, taxonomies and multi-trait models for continuous and categorical characters. *J. Evol. Biol.*, 23, 494–508.

Housworth, E.A., Martins, E.P. & Lynch, M. (2004). The Phylogenetic Mixed Model. *Am. Nat.*, 163, 84–96.

Villemereuil, P. (2012). How to use the MCMCglmm R package.

Villemereuil, P. & Nakagawa, S. (2014). General Quantitative Genetic Methods for Comparative Biology. In: (*Modern Phylogenetic Comparative Methods and Their Application in Evolutionary Biology: Concepts and Practice*), {[Garamszegi, L.Z.]} Springer, New York, USA. 287-303.

8.1.3 Analyses using a species-level phylogeny

Species-level phylogeny was obtained by pruning the phylogenetic tree reported by Smith & Brown (2018) available in the R package *V.PhyloMaker* (Jin and Qian 2019) by using the *ape* R package (Paradis and Schliep 2019) only keeping species with hydraulic data available in each case, obtaining the same number of observations compared to the genus-level analyses. Some bi-response models implemented using the genus-level phylogeny were also conducted using the species-level phylogeny. As I had only one value per specie, no extra random effect was included, so variance partition was reduced to phylogenetic signal calculation.

Table S2.7 Phylogenetic signal results Variance partitioning for the six hydraulic traits and three environmental principal components related to water availability (PC1), energy input (PC2) and soil depth (PC3). Legend: N: number of species used in each case (for which both phylogenetic and hydraulic data were available), phylogenetic variance (phylogenetic signal, λ) and non-phylogenetic intraspecific variance plus measurement error (ϱ). Mean and lower and upper 95% credible intervals (HPD) are shown for each component.

variable	N	λ	λ Lower HPD	λ Upper HPD	ϱ	ϱ Lower HPD	ϱ Upper HPD
HSM	195	0.456	0.228	0.680	0.544	0.320	0.772
Ln(Hv)	842	0.654	0.539	0.774	0.346	0.226	0.461
Ln(K_v)	616	0.610	0.456	0.753	0.390	0.247	0.544
Ln(K_s)	763	0.681	0.569	0.792	0.319	0.208	0.431
Ln(P_{min})	358	0.876	0.799	0.940	0.124	0.060	0.201
ln(P₅₀)	693	0.709	0.594	0.817	0.291	0.183	0.406
PC1	1329	0.963	0.951	0.975	0.037	0.025	0.049
PC2	1329	0.845	0.796	0.889	0.155	0.111	0.204
PC3	1329	0.907	0.882	0.934	0.093	0.066	0.118

Table S2.8 Evolutionary correlations results. Mean of the evolutionary correlation (EC), credible interval (lower and upper HPD) and p-value reported by bi-response models. In the fixed structure column, variables to the right of the “~” symbol are response variables, those to the left are predictors. Abbreviations: “env” (1): individual environmental principal component; env(3): three main environmental principal components; trait: individual hydraulic trait; Affiliation: major evolutionary affiliation (angiosperm or gymnosperm).

Fixed structure	Variable 1	Variable 2	EC	Lower HPD	Upper HPD	p-value
trait, trait ~ 1 + env(3) * Affiliation5	ln(Hv)	ln(P _{min})	0.134	-0.365	0.695	0.641
trait, trait ~ 1	ln(Hv)	ln(P _{min})	0.607	0.261	0.915	0.014
trait, env(1) ~ 1	log(Hv)	PC1	-0.807	-0.908	-0.699	0.000
trait, env(1) ~ 1 + Affiliation	log(Hv)	PC1	-0.816	-0.922	-0.714	0.000
trait, env(1) ~ 1	log(Hv)	PC2	-0.090	-0.334	0.191	0.495
trait, env(1) ~ 1 + Affiliation	log(Hv)	PC2	-0.092	-0.376	0.164	0.501
trait, env(1) ~ 1 + Affiliation	ln(Hv)	PC3	-0.492	-0.689	-0.304	0.000
trait, env(1) ~ 1	ln(Hv)	PC3	-0.493	-0.691	-0.304	0.000
trait, trait ~ 1 + env(3) * Affiliation	ln(K _s)	ln(Hv)	-0.630	-0.851	-0.359	0.000
trait, trait ~ 1	ln(K _s)	ln(Hv)	-0.589	-0.815	-0.348	0.000
trait, trait ~ -1 + env(3) * Affiliation	ln(K _s)	ln(P _{min})	-0.217	-0.663	0.226	0.349
trait, trait ~ 1	ln(K _s)	ln(P _{min})	-0.366	-0.703	0.012	0.090
trait, trait ~ -1 + env(3) * Affiliation	ln(K _s)	ln(P ₅₀)	-0.236	-0.579	0.172	0.223
trait, trait ~ 1	ln(K _s)	ln(P ₅₀)	-0.420	-0.674	-0.104	0.015
trait, env(1) ~ 1	ln(K _s)	PC1	0.225	0.000	0.421	0.043
trait, env(1) ~ 1 + Affiliation	ln(K _s)	PC1	0.225	0.006	0.452	0.067
trait, env(1) ~ 1 + Affiliation	ln(K _s)	PC2	-0.185	-0.434	0.065	0.160
trait, env(1) ~ 1	ln(K _s)	PC2	-0.196	-0.439	0.092	0.155
trait, env(1) ~ 1 + Affiliation	ln(K _s)	PC3	0.106	-0.132	0.350	0.395
trait, env(1) ~ 1	ln(K _s)	PC3	0.105	-0.147	0.338	0.423
trait, env(1) ~ 1 + Affiliation	ln(P _{min})	PC1	-0.734	-0.861	-0.599	0.000
trait, env(1) ~ 1	ln(P _{min})	PC1	-0.743	-0.868	-0.590	0.000
trait, env(1) ~ 1 + Affiliation	ln(P _{min})	PC2	-0.266	-0.573	0.041	0.127
trait, env(1) ~ 1	ln(P _{min})	PC2	-0.254	-0.567	0.040	0.118
trait, env(1) ~ 1 + Affiliation	ln(P _{min})	PC3	0.215	-0.032	0.462	0.101
trait, env(1) ~ 1	ln(P _{min})	PC3	0.223	-0.032	0.453	0.097
trait, trait ~ -1 + env * Affiliation	log(P ₅₀)	ln(Hv)	0.211	-0.256	0.663	0.429
trait, trait ~ 1	ln(P ₅₀)	ln(Hv)	0.622	0.370	0.839	0.001
trait, trait ~ -1 + env(3) * Affiliation	ln(P ₅₀)	ln(P _{min})	0.773	0.582	0.926	0.000
trait, env(1) ~ 1	ln(P ₅₀)	ln(P _{min})	0.794	0.636	0.923	0.000
trait, env(1) ~ 1 + Affiliation	ln(P ₅₀)	PC1	-0.466	-0.658	-0.254	0.000
trait, env(1) ~ 1	ln(P ₅₀)	PC1	-0.465	-0.661	-0.257	0.000
trait, env(1) ~ 1 + Affiliation	ln(P ₅₀)	PC2	0.022	-0.250	0.305	0.902
trait, env(1) ~ 1	ln(P ₅₀)	PC2	0.032	-0.225	0.343	0.837
trait, env(1) ~ 1 + Affiliation	ln(P ₅₀)	PC3	-0.147	-0.417	0.102	0.262
trait, env(1) ~ 1	ln(P ₅₀)	PC3	-0.144	-0.390	0.118	0.279

Literature cited

Jin, Y., & Qian, H. (2019). V.PhylMaker: an R package that can generate very large phylogenies for vascular plants. *Ecography*, 42(8), 1353–1359.

Paradis, E., & Schliep, K. (2018). ape 5.0: an environment for modern phylogenetics and evolutionary analyses in R. *Bioinformatics* 35: 526-528.

Smith, S. A., & Brown, J. W. (2018). Constructing a broadly inclusive seed plant phylogeny. *Am. J. Bot.*, 105(3), 302–314.

8.1.4 Evolutionary correlations reported by genus-level phylogenetic models using observations available for the species-level phylogeny and evolutionary correlations reported by species-level phylogeny pruned at the genus level.

For bivariate models including two traits as response variable, only models without fixed effects and models including the three environmental components and its interaction with major evolutionary affiliation (angiosperm or gymnosperm) were implemented.

Table S2.9 Significant evolutionary correlations (i.e., when the credible interval for the estimated correlation do not include zero) reported by models using a genus-level phylogeny including only observations available for the species-level phylogenetic analyses to check for effects of the different species coverage between phylogenies. Mean of the evolutionary correlation (EC), credible interval (lower and upper HPD) and p-value reported by bi-response models. In the fixed structure column, variables to the right of the “~” symbol are response variables, those to the left are predictors. Abbreviations: “env”(1): individual environmental principal component; env(3): three main environmental principal components; trait: individual hydraulic trait; Affiliation: major evolutionary affiliation (angiosperm or gymnosperm).

Fixed structure	var1	var2	EC	Lower HPD	Upper HPD	p-value
trait, env(1) ~ 1 + Affiliation	ln(Hv)	PC1	-0.779	-0.926	-0.634	0.000
trait, env(1) ~ 1	ln(Hv)	PC1	-0.787	-0.921	-0.647	0.000
trait, env(1) ~ 1 + Affiliation	ln(Hv)	PC3	-0.499	-0.749	-0.250	0.001
trait, env(1) ~ 1	ln(Hv)	PC3	-0.510	-0.749	-0.260	0.001
trait, trait ~ 1	ln(K _s)	ln(Hv)	-0.501	-0.850	-0.101	0.049
trait, trait ~ 1 + env(3) * Affiliation	ln(K _s)	ln(Hv)	-0.603	-0.861	-0.297	0.003
trait, trait ~ 1	ln(K _s)	ln(P ₅₀)	-0.394	-0.709	-0.022	0.054
trait, env(1) ~ 1 + Affiliation	ln(K _s)	PC2	-0.316	-0.602	-0.011	0.049
trait, env(1) ~ 1	ln(K _s)	PC2	-0.341	-0.618	-0.056	0.024
trait, env(1) ~ 1 + Affiliation	ln(K _s)	PC3	0.350	0.045	0.633	0.031
trait, env(1) ~ 1	ln(K _s)	PC3	0.355	0.065	0.651	0.021
trait, env(1) ~ 1 + Affiliation	ln(P _{min})	PC1	-0.779	-0.926	-0.623	0.000
trait, env(1) ~ 1	ln(P _{min})	PC1	-0.783	-0.928	-0.621	0.000
trait, trait ~ 1	ln(P ₅₀)	ln(Hv)	0.495	0.126	0.816	0.014
trait, trait ~ 1	ln(P ₅₀)	ln(P _{min})	0.485	0.065	0.836	0.054
trait, trait ~ 1 + env(3) * Affiliation	ln(P ₅₀)	ln(P _{min})	0.598	0.233	0.888	0.008
trait, env(1) ~ 1 + Affiliation	ln(P ₅₀)	PC1	-0.628	-0.863	-0.394	0.000
trait, env(1) ~ 1	ln(P ₅₀)	PC1	-0.618	-0.831	-0.374	0.001

Table S2.10 Significant evolutionary correlations (i.e., when the credible interval for the estimated correlation do not include zero) reported by models using a species-level phylogeny pruned at genus-level to check for effects of differences in the topology between phylogenies. Mean of the evolutionary correlation (EC), credible interval (lower and upper HPD) and p-value reported by bi-response models. In the fixed structure column, variables to the right of the “~” symbol are response variables, those to the left are predictors. Abbreviations: “env”(1): individual environmental principal component; env(3): three main environmental principal components; trait: individual hydraulic trait; Affiliation: major evolutionary affiliation (angiosperm or gymnosperm).

Fixed structure	Variable 1	Variable 2	EC	Lower HPD	Upper HPD	p-value
trait, env(1) ~ 1 + Affiliation	ln(Hv)	PC1	-0.817	-0.924	-0.685	0.000
trait, env(1) ~ 1	ln(Hv)	PC1	-0.824	-0.936	-0.696	0.000
trait, env(1) ~ 1 + Affiliation	ln(Hv)	PC3	-0.439	-0.705	-0.158	0.008
trait, env(1) ~ 1	ln(Hv)	PC3	-0.451	-0.711	-0.159	0.012
trait, trait ~ 1	ln(K _s)	ln(Hv)	-0.535	-0.844	-0.178	0.018
trait, trait ~ 1 + env(3) * Affiliation	ln(K _s)	ln(Hv)	-0.626	-0.877	-0.330	0.002
trait, trait ~ 1	ln(K _s)	ln(P ₅₀)	-0.398	-0.749	-0.016	0.069
trait, env(1) ~ 1 + Affiliation	ln(K _s)	PC2	-0.326	-0.626	-0.013	0.046
trait, env(1) ~ 1	ln(K _s)	PC2	-0.332	-0.688	-0.037	0.068
trait, env(1) ~ 1	ln(K _s)	PC3	0.334	0.005	0.647	0.045
trait, env(1) ~ 1 + Affiliation	ln(P _{min})	PC1	-0.774	-0.924	-0.614	0.000
trait, env(1) ~ 1	ln(P _{min})	PC1	-0.783	-0.933	-0.619	0.000
trait, trait ~ 1	ln(P ₅₀)	ln(Hv)	0.505	0.131	0.814	0.024
trait, trait ~ 1	ln(P ₅₀)	ln(P _{min})	0.493	0.066	0.858	0.054
trait, trait ~ 1 + env(3) * Affiliation	ln(P ₅₀)	ln(P _{min})	0.591	0.177	0.906	0.034
trait, env(1) ~ 1 + Affiliation	ln(P ₅₀)	PC1	-0.609	-0.856	-0.349	0.001
trait, env(1) ~ 1	ln(P ₅₀)	PC1	-0.595	-0.831	-0.342	0.001

8.2 CHAPTER 3

8.2.1 Supplementary tables and figures

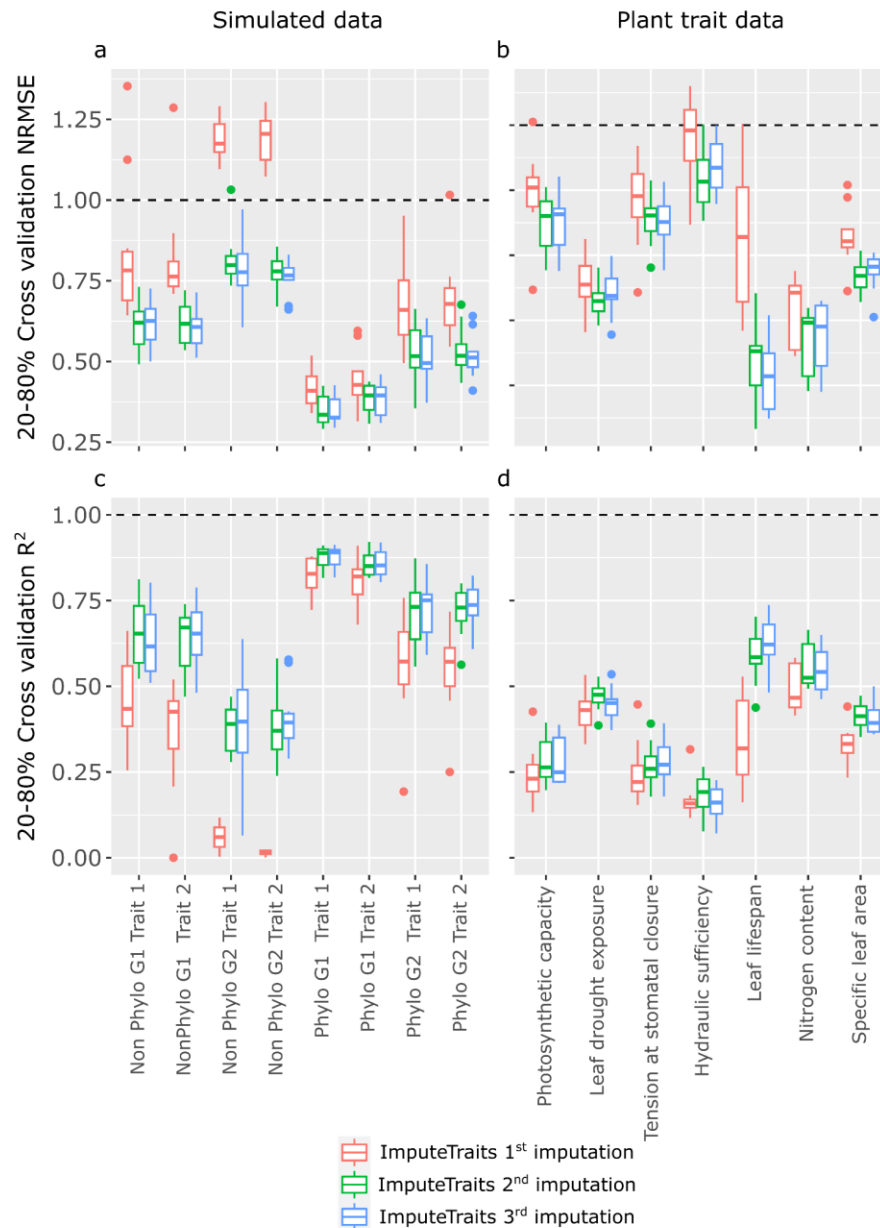


Figure S3.1 Predictive performance *imputeTraits* different rounds.-Predictive performance of the three rounds of the imputation framework for simulated traits. a) and b) Normalized root mean square, c) and d) R².

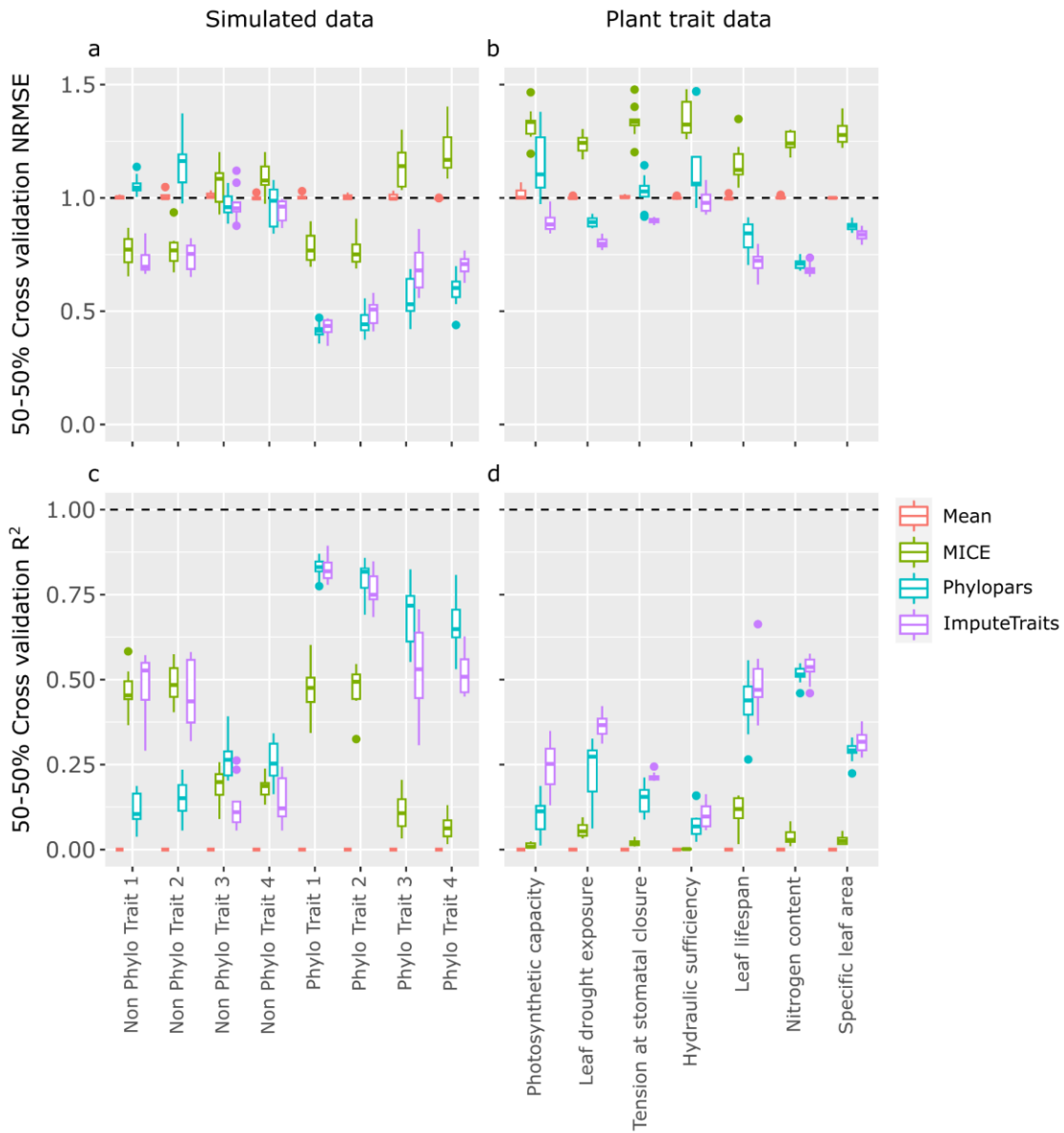


Figure S3.2 Predictive performance cross validation 50-50%. Predictive performance of the imputation framework. Results for mean imputation (red), *MICE* imputation (blue), *phylopars* imputation (green) and *imputeTraits* imputation (purple) are shown. a and c) normalized root mean square error (NRMSE) for simulated and leaf traits, respectively. B, d) R² for simulated and leaf traits, respectively. NRMSE and R² were calculated from a cross validation procedure using 50% of the data to train models and 50% to test.

Table S3.1 Variance-covariance matrix used to simulate traits covariation (either phylogenetic or non-phylogenetic). Off diagonal elements represent expected total correlation between traits. The diagonal refers to the phylogenetic signal of traits simulated under a Brownian motion model (“Phylo” traits). This matrix was used to simulate both Phylo and Non Phylo traits (the first one, simulated to show the correlation in a phylogenetically structured way).

	Trait 1	Trait 2	Env	Trait 3	Trait 4
Trait 1	1	0.9	0.8	0	0
Trait 2	0.9	1	0.8	0	0
Env	0.8	0.8	1	0	0
Trait 3	0	0	0	1	0.9
Trait 4	0	0	0	0.9	1

Table S3.2 Simulated data characteristics and expectations. “Phylo” stands for traits expected to present phylogenetic signal, “Non Phylo” stands for traits not expected to present phylogenetic signal. “Env” indicate those traits that were used as if they were environmental predictors.

	Expected phylogenetic signal	Expected strong correlation with	Expected type of correlation	Expected to be partially explained by
Phylo Trait 1	Yes	Phylo Trait 2, <i>Phylo Env</i>	Phylogenetic	<i>Phylo Env</i>
Phylo Trait 2	Yes	Phylo Trait 1, <i>Phylo Env</i>	Phylogenetic	<i>Phylo Env</i>
Phylo Trait 3	Yes	Phylo Trait 4	Phylogenetic	
Phylo Trait 4	Yes	Phylo Trait 3	Phylogenetic	
Non Phylo Trait 1	No	Non Phylo Trait 2, <i>Non Phylo Env</i>	Non-Phylogenetic	<i>Non Phylo Env</i>
Non Phylo Trait 2	No	Non Phylo Trait 1, <i>Non Phylo Env</i>	Non-Phylogenetic	<i>Non Phylo Env</i>
Non Phylo Trait 3	No	Non Phylo Trait 4	Non-Phylogenetic	
Non Phylo Trait 4	No	Non Phylo Trait 3	Non-Phylogenetic	
<i>Phylo Env</i>	Yes	Phylo Trait 1, Phylo Trait 2	Phylogenetic	
<i>Non Phylo Env</i>	No	Non Phylo Trait 1, Non Phylo Trait 2	Non-Phylogenetic	

8.2.2 Supplementary methods

To include more than one environmental variable or one or more non-continuous environmental variables into the presented framework I compare mixed linear models including the phylogeny as a random effect with models including the phylogeny as a random effect and the environmental factors as fixed effect. I do not include multiple environmental variables as response variables as in the methodology presented in the main text because the computation of the variance covariance matrix with more than three variables can be challenging and a high number of observations is needed (J. Hadfield, personal communication). Under this framework, I use uniresponse models to report variance results and biresponse models to report covariance results. Uniresponse models allow to estimate the phylogenetic variance (VAR_u), the non-phylogenetic variance (VAR_e) (which sum to total variance, VAR_t). Biresponse models allow to estimate, for a pair of traits (response variables, T1 and T2) the phylogenetic covariance ($COV_u^{T1, T2}$), the non-phylogenetic covariance ($COV_e^{T1, T2}$). Then, specific environmental variables expected to be related with traits are included in the previous models as fixed effects. By doing so, I can estimate the non-attributed phylogenetic variance (VAR_{phylo}) and covariance (COV_{phylo}) (i.e., not related to the environmental variables considered and related to the phylogeny) as well as the residual variance (VAR_{res}) and covariance (COV_{res}) (i.e., not related to the phylogeny nor to the environmental variables considered). Then, from these estimates and the ones calculated by the initial uni- and biresponse models, I can calculate the amount of variance and covariance related only to phylogeny (**non-attributed phylogenetic conservatism**), only the environmental variables (*labile environmental effect*) and to both the phylogeny and environmental variables (**environmental phylogenetic conservatism**) as follows:

1. **Non – environmental phylogenetic variance** = $\frac{VAR_{phylo}^{T1}}{VAR_{total}^{T1}}$
2. **Non – environmental phylogenetic covariance** = $\frac{COV_{phylo}^{T1, T2}}{\sqrt{VAR_{total}^{T1} * VAR_{total}^{T2}}}$
3. **Labile environmental variance** = $\frac{VAR_e^{T1} - VAR_{res}^{T1}}{VAR_{total}^{T1}}$
4. **Environmental phylogenetic variance** = $\frac{VAR_u^{T1} - VAR_{phylo}^{T1}}{VAR_{total}^{T1}}$
5. **Environmental phylogenetic covariance** = $\frac{COV_u^{T1, T2} - COV_{phylo}^{T1, T2}}{\sqrt{VAR_{total}^{T1} * VAR_{total}^{T2}}}$

Variance partition is performed by the function *computeVariancePartition*. The same approach is then applied to covariances by the function *computeCovariancePartition* (see methods in chapter 3).

8.3 CHAPTER 4

8.3.1 Supplementary tables and figures

Table S4.1 Number of observations per trait and phylogenetic signal values for individual traits and principal components.

Trait	N	Phylogenetic signal	P-value
Specific leaf area (SLA)	483	0.351	<0.001
Wood density (WD)	483	0.771	<0.001
Leaf N content (N)	481	0.760	<0.001
Leaf P content (P)	418	0.417	<0.001
Leaf C content (C)	391	0.451	<0.001
Maximum diameter (D_{\max})	445	0.592	<0.001
Maximum growth rate (GR_{\max})	368	0.434	<0.001
Mortality rate (MR)	219	0.301	<0.001
Seed mass (SM)	533	0.787	<0.001
Functional PC1	197	0.450	<0.001
Functional PC2	197	0.507	<0.001
Life history PC1	197	0.422	<0.001
Life history PC2	197	0.507	<0.001
Integrative PC1	197	0.607	<0.001
Integrative PC2	197	0.506	<0.001

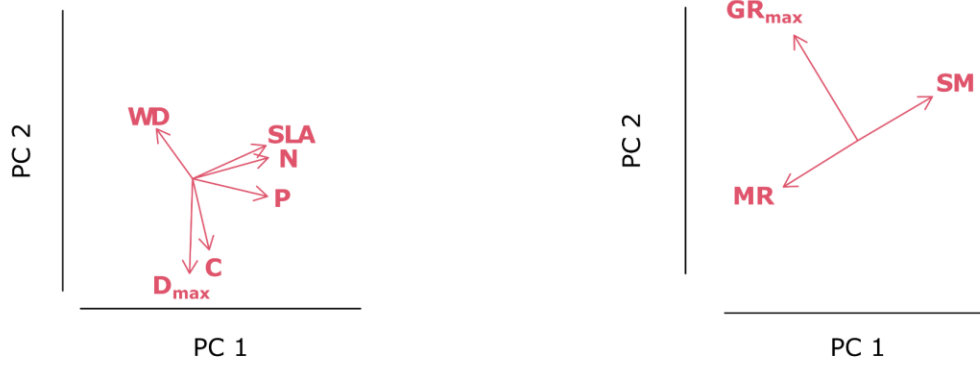
Table S4.2 Correlation results. See table S1 for traits abbreviations.

Trait 1	Trait 2	N	Total correlation	Phylogenetic correlation	Labile correlation	P-value total correlation	P-value phylogenetic correlation	P-value labile correlation
SLA	WD	483	-0.324	-0.316	-0.007	0.000	0.000	0.867
N	WD	481	-0.228	-0.237	0.009	0.002	0.005	0.688
P	WD	418	-0.352	-0.328	-0.024	0.000	0.000	0.556
C	WD	391	-0.088	-0.058	-0.030	0.287	0.570	0.447
D _{max}	WD	445	-0.074	-0.022	-0.051	0.362	0.835	0.121
GR _{max}	WD	368	-0.448	-0.274	-0.174	0.000	0.005	0.000
MR	WD	219	-0.428	-0.244	-0.184	0.000	0.030	0.005
SM	WD	533	0.191	0.176	0.015	0.007	0.042	0.513
N	SLA	483	0.627	0.327	0.301	0.000	0.000	0.000
P	SLA	416	0.576	0.334	0.242	0.000	0.000	0.000
C	SLA	391	0.029	0.007	0.022	0.719	0.961	0.662
D _{max}	SLA	389	-0.167	-0.171	0.004	0.021	0.055	0.907
GR _{max} x	SLA	332	0.194	0.066	0.128	0.005	0.771	0.070
MR	SLA	212	0.325	0.298	0.027	0.000	0.007	0.722
SLA	SM	438	-0.362	-0.322	-0.040	0.000	0.000	0.401
P	N	421	0.678	0.490	0.188	0.000	0.000	0.000
C	N	393	0.013	-0.097	0.110	0.875	0.298	0.002
D _{max}	N	390	-0.150	-0.174	0.024	0.075	0.096	0.498
GR _{max}	N	335	0.273	0.237	0.036	0.002	0.016	0.442
MR	N	212	0.359	0.372	-0.012	0.000	0.004	0.742
N	SM	435	-0.309	-0.309	0.000	0.000	0.000	0.952
C	P	385	0.284	-0.025	0.309	0.000	0.765	0.000
D _{max}	P	352	-0.058	-0.078	0.020	0.515	0.501	0.649
GR _{max}	P	313	0.236	0.184	0.052	0.005	0.093	0.343
MR	P	208	0.441	0.521	-0.079	0.000	0.000	0.188
P	SM	383	-0.218	-0.313	0.095	0.007	0.002	0.006
C	D _{max}	334	0.157	0.160	-0.003	0.065	0.133	0.940
C	GR _{max} x	302	-0.051	-0.035	-0.016	0.520	0.704	0.766
C	MR	202	-0.191	-0.190	0.000	0.027	0.059	0.998
C	SM	358	0.117	0.032	0.085	0.195	0.748	0.015
D _{max}	GR _{max}	368	0.596	0.330	0.266	0.000	0.001	0.000
D _{max}	MR	219	-0.435	-0.366	-0.070	0.000	0.001	0.334
D _{max}	SM	416	0.172	0.148	0.023	0.042	0.161	0.499
GR _{max}	MR	212	0.280	-0.039	0.319	0.002	0.679	0.001
GR _{max}	SM	355	-0.235	-0.176	-0.058	0.003	0.097	0.180
MR	SM	219	-0.511	-0.336	-0.175	0.000	0.013	0.007
Functi onal PC1	Functi onal PC2	197	-0.059	-0.147	0.088	0.542	0.219	0.158
Functi onal PC1	Life history PC1	197	0.449	0.432	0.017	0.000	0.000	0.896
Functi onal PC1	Life history PC2	197	-0.047	-0.102	0.055	0.630	0.400	0.389

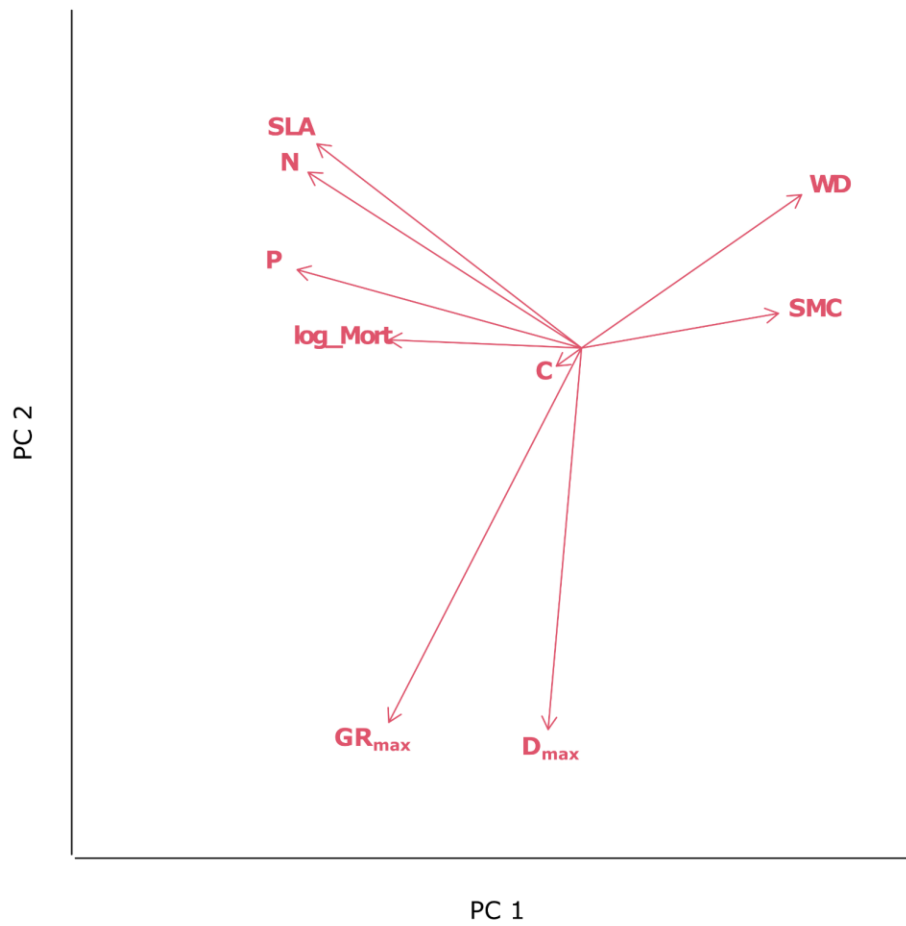
Functional PC1	Integrative PC1	197	0.919	0.524	0.396	0.000	0.000	0.000
Functional PC1	Integrative PC2	197	0.146	0.129	0.016	0.144	0.303	0.830
Functional PC2	Life history PC1	197	-0.089	-0.243	0.154	0.288	0.013	0.029
Functional PC2	Life history PC2	197	0.722	0.407	0.315	0.000	0.000	0.000
Functional PC2	Integrative PC1	197	-0.076	-0.196	0.120	0.450	0.126	0.047
Functional PC2	Integrative PC2	197	-0.858	-0.454	-0.404	0.000	0.000	0.000
Life history PC1	Life history PC2	197	-0.107	-0.287	0.180	0.338	0.029	0.022
Life history PC1	Integrative PC1	197	0.733	0.431	0.302	0.000	0.000	0.000
Life history PC1	Integrative PC2	197	0.051	0.329	-0.278	0.605	0.013	0.000
Life history PC2	Integrative PC1	197	-0.064	-0.200	0.136	0.536	0.141	0.024
Life history PC2	Integrative PC2	197	-0.928	-0.486	-0.442	0.000	0.000	0.000
Integrative PC1	Integrative PC2	197	0.089	0.193	-0.104	0.381	0.146	0.078

Figure S4.1 Phylogenetic PCA.

a) Functional traits phylo. PCA (1st and 2nd PCs) b) Life history traits phylo. PCA (1st and 2nd PCs)



c) Unified phylo. PCA (1st and 2nd PCs)



8.4 CHAPTER 5

8.4.1 Supplementary tables and figures

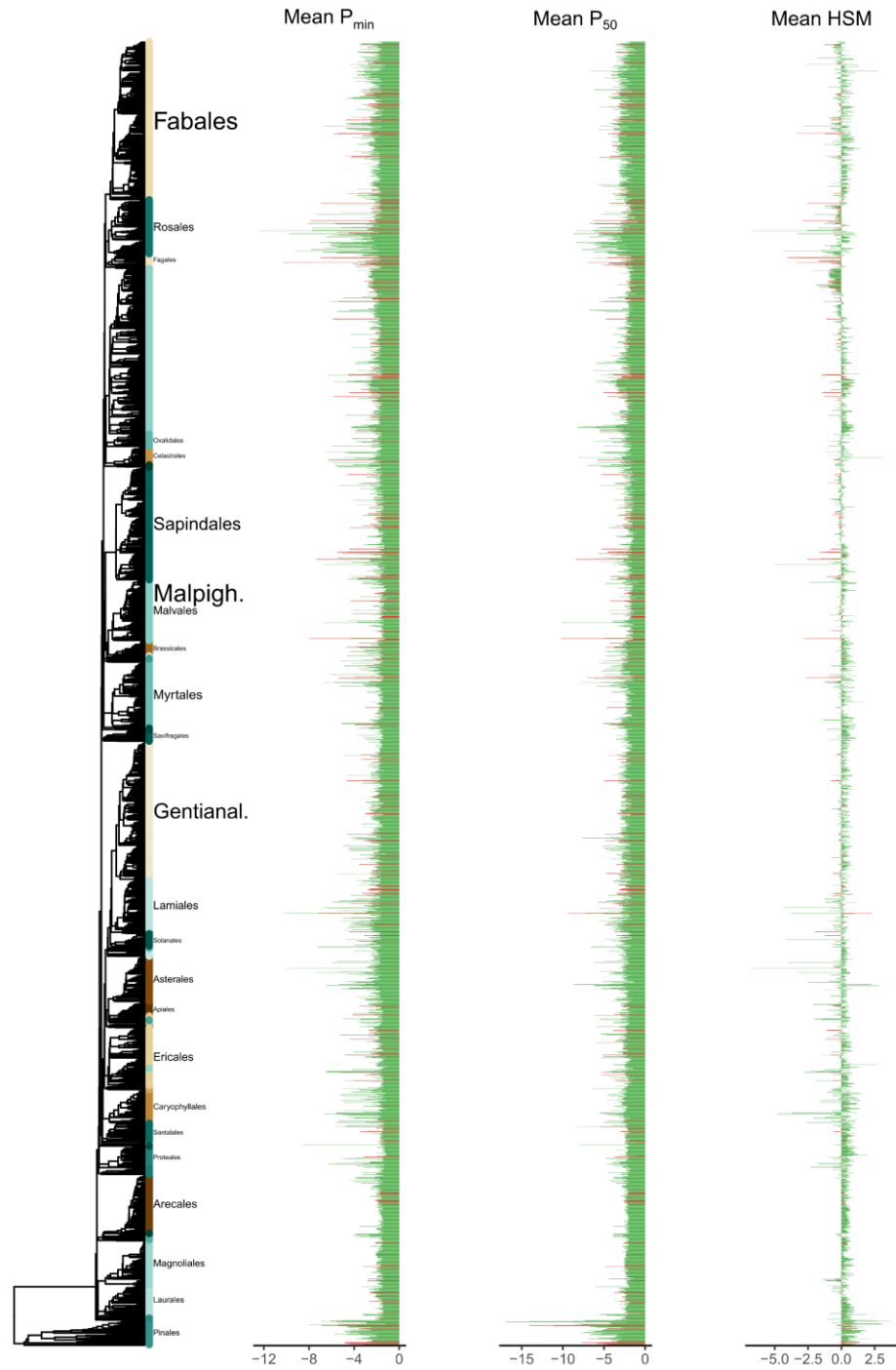


Figure S5.1 Hydraulic trait means values calculated from imputation results obtained by iterating the predictive model 100 times. Values were aggregated at genus level by calculating the mean for genera with more than one species. In red, genera with observed mortality. Order names are shown proportional to the number of species and marked in the phylogeny by different colours at the tips.

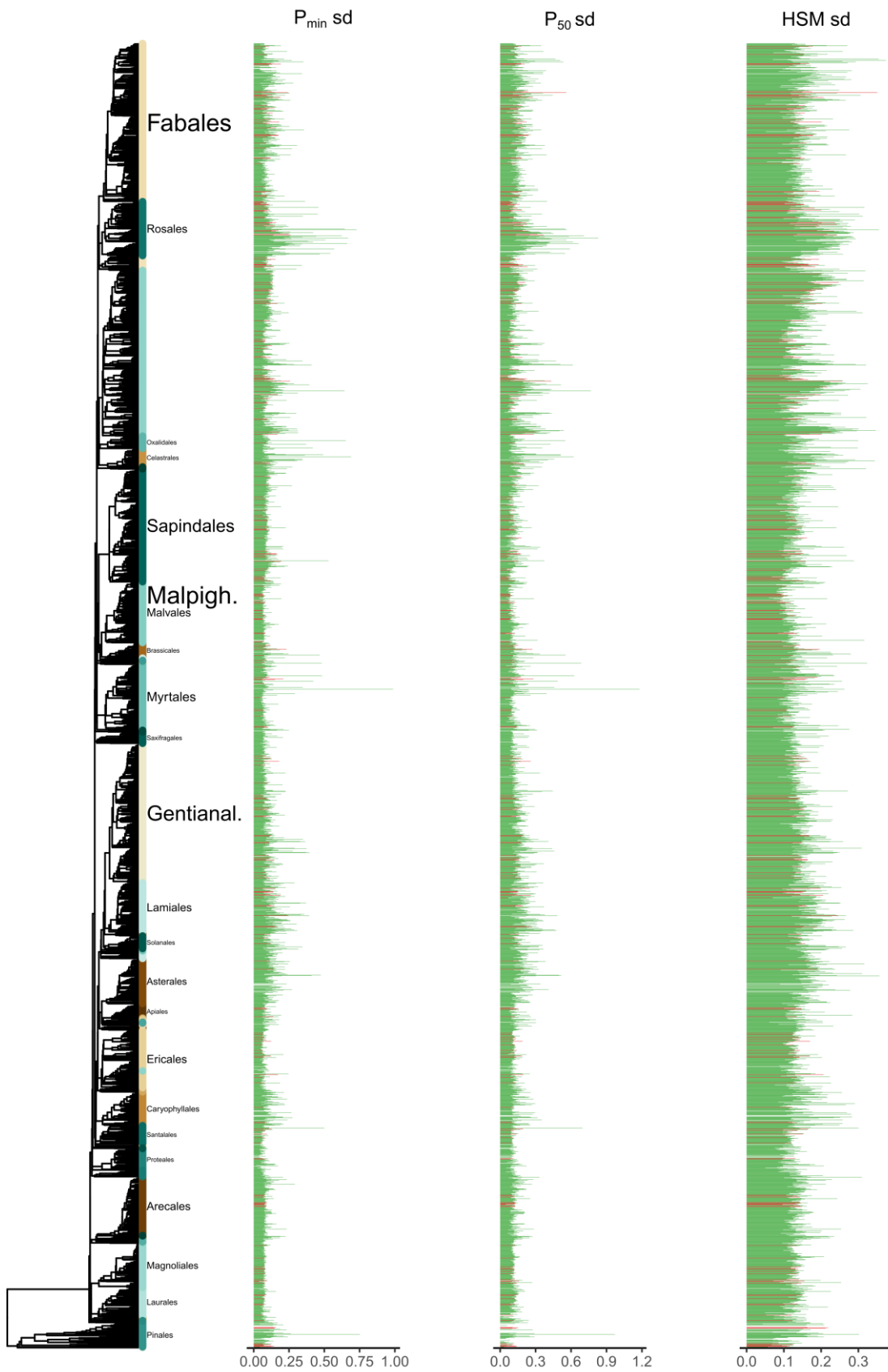
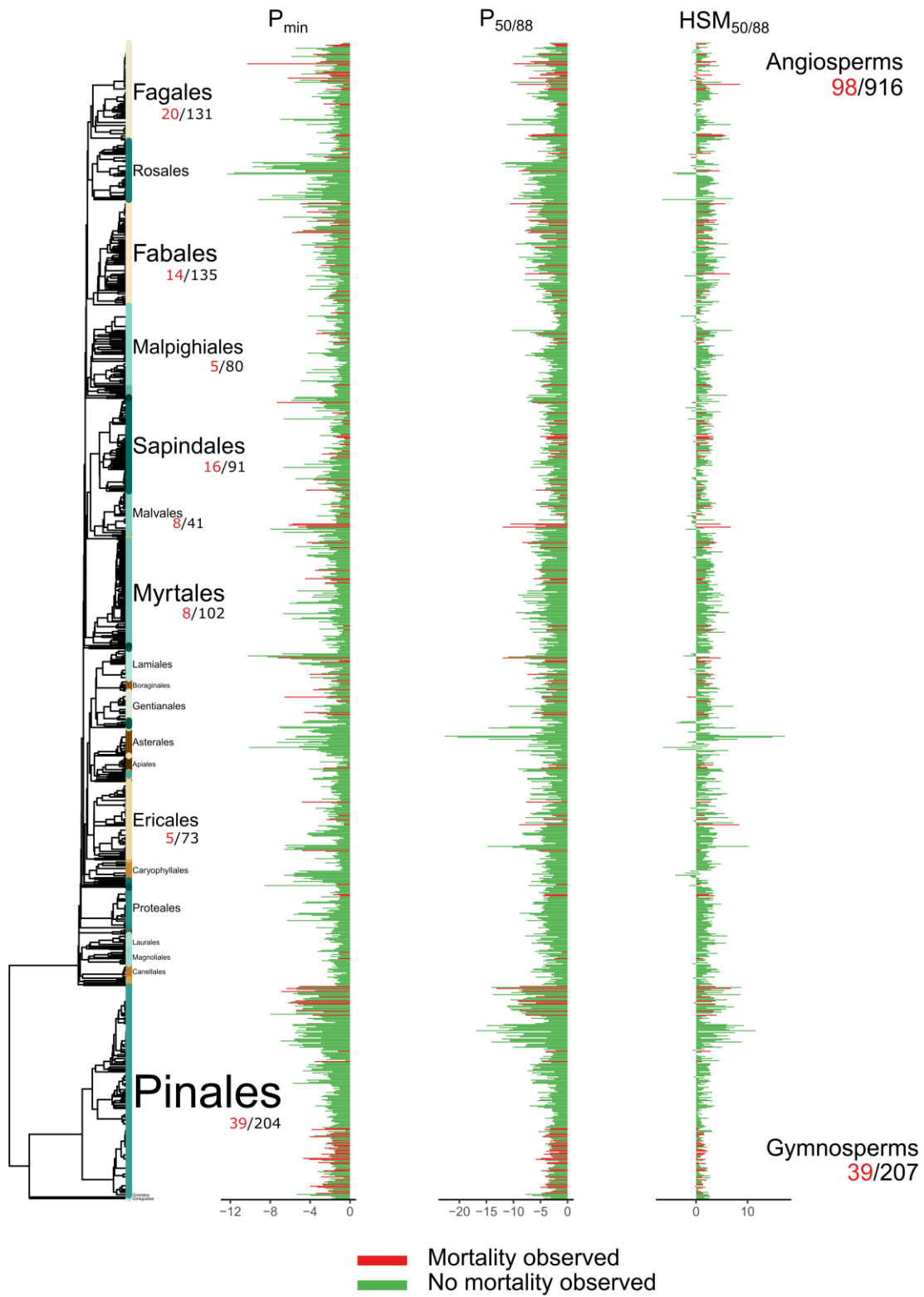


Figure S5.2 Hydraulic trait standard deviation calculated from imputation results obtained by iterating the predictive model 100 times. Values are aggregated at the genus level by calculating the mean for genera with more than one species. In red, are species with observed mortality. Order names are shown proportional to the number of species and marked in the phylogeny by different colours at the tips.



Number of species with HSM < 0:165 (0.4%)
 Number of species with HSM < 0.5: 523 (1.2%)
 Number of species with HSM < 1: 2,185 (4.8%)

Figure S5.3 Phylogenetic distribution of observed and imputed hydraulic traits for species with observed data for P_{\min} and/or $P_{50/88}$. Imputed values represent the mean of 100 predicted values per species resulting from 100 iterations of the predictive model. In red, species with observed mortality and in green species without observed mortality. The most important order names are shown with size proportional to the number of species represented. The total number of species with trait data is shown in black and the number in red is the number of those species that have an observed mortality event. The number and percentage of species showing hydraulic safety margin ($HSM_{50/88}$) values below zero, 0.5 and 1 are also shown.

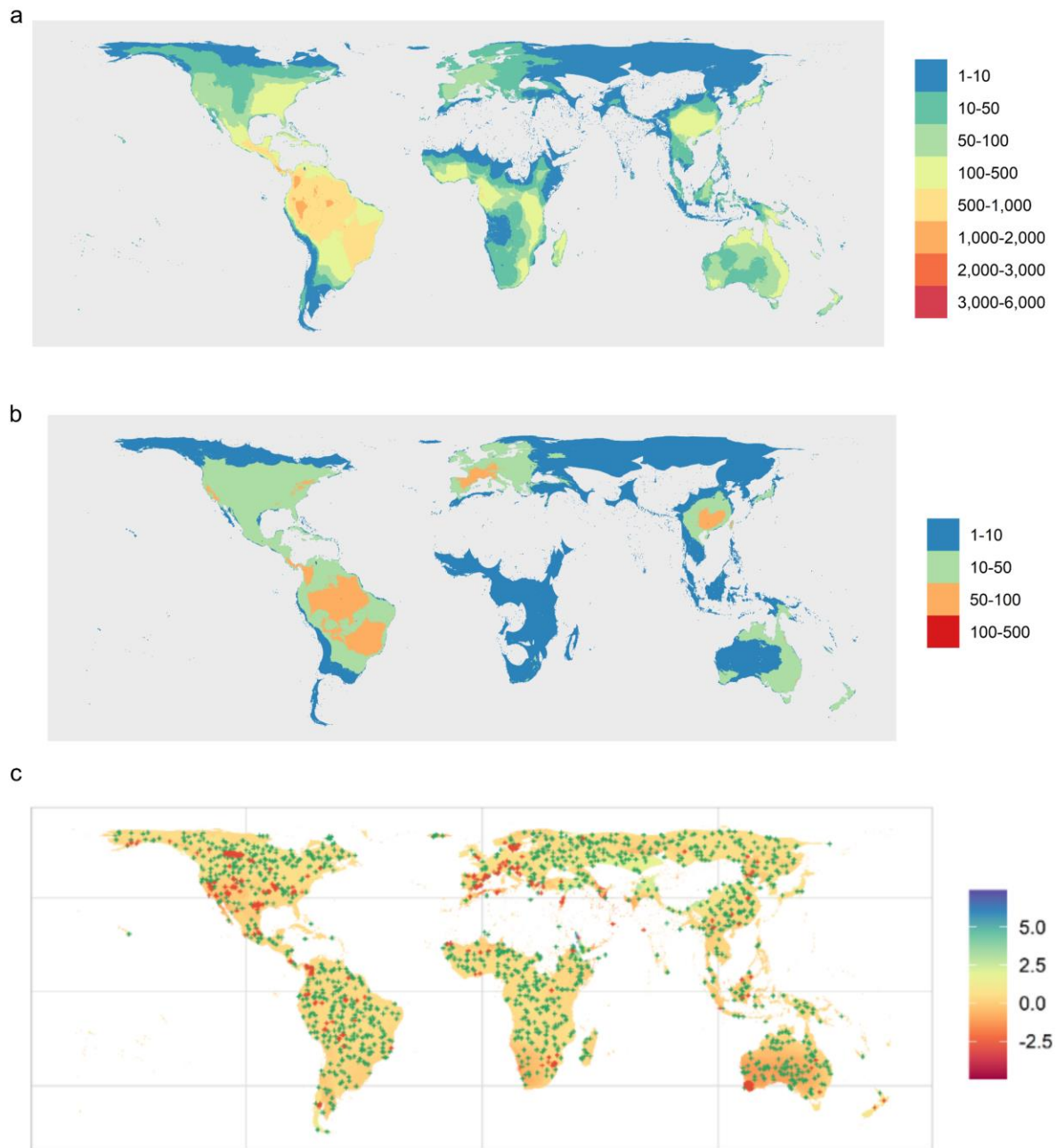


Figure S5.4 Geographical coverage of species range distribution data for: a) the number of species for which imputation was implemented and b) for species with observed traits data. c) Mortality points distribution and one of the background sets used in generalized linear models (red and green, respectively) plotted on HSM mean map.

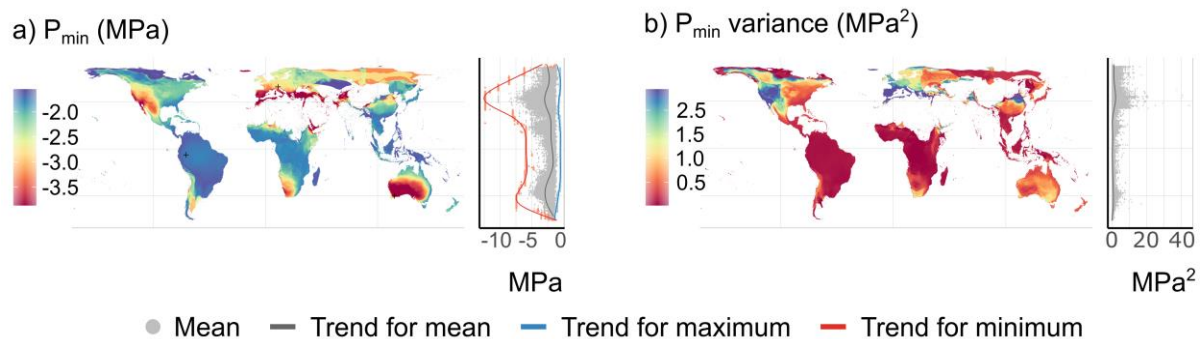


Figure S5.5 Geographical distribution of projected species-assemblage P_{\min} means and range and latitudinal patterns (a and b, respectively). Scatterplots show pixel values per latitude as circles and absolute minimum and maximum values by latitude (i.e., accounting for all species-level values present in a pixel) as red and blue triangles in a. Trend lines for pixel values and absolute maximum and minimum values in a are shown following a GAM methodology.

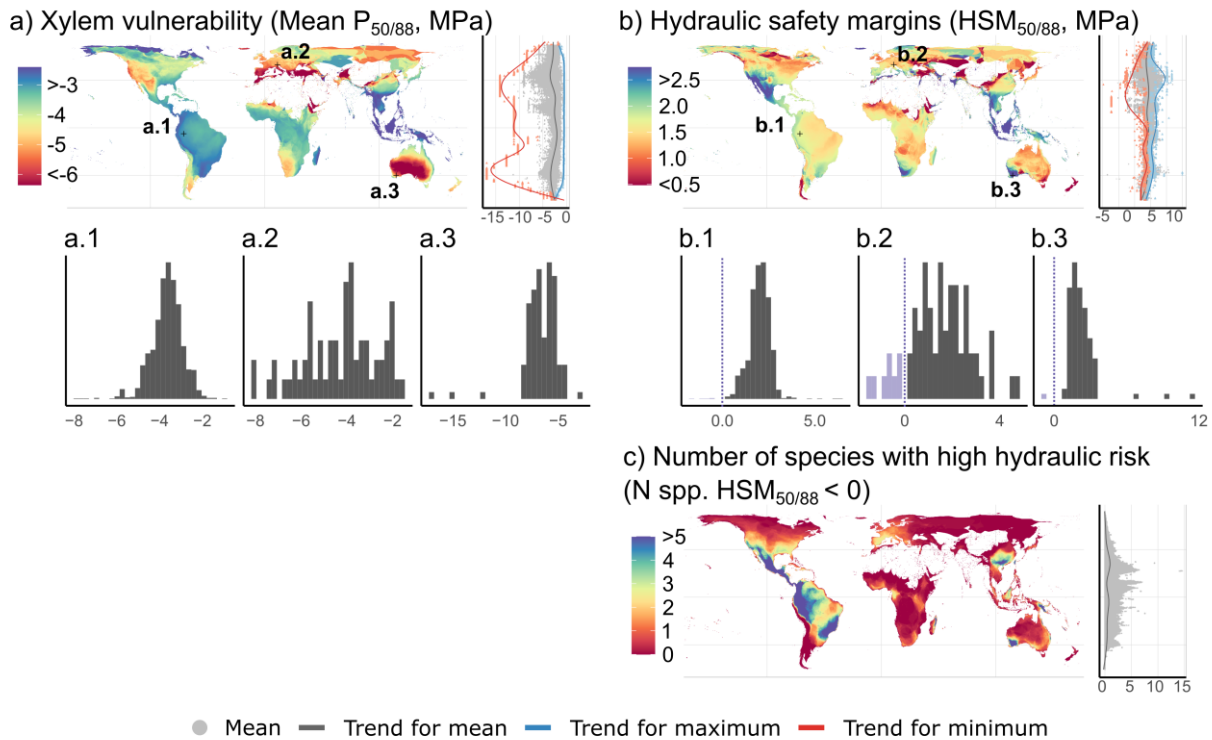


Figure S5.6 Geographical distribution of projected species-assemblage hydraulic metrics and corresponding latitudinal patterns. a, b: Mean $P_{50/88}$ and $HSM_{50/88}$, respectively and c: number of species with negative $HSM_{50/88}$ values. The distribution of species-level values from which metrics are calculated for a sample of three representative pixels is shown in histograms in a and b. Scatterplots show the distribution of pixel values by latitude using circles, absolute minimum and maximum values by latitude (i.e., accounting for all species-level values present in a pixel) as red and blue triangles, respectively. Trend lines for pixel values and absolute maximum and minimum values for scatterplots in a and b are shown following a GAM methodology.

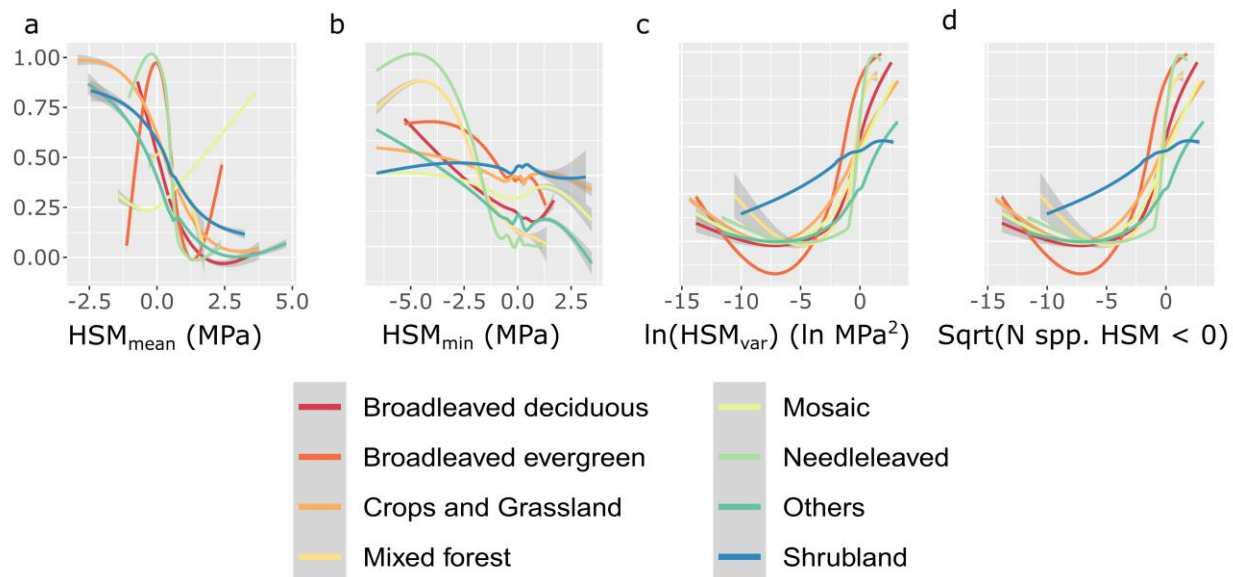


Figure S5.7 Relationship between drought-induced mortality occurrence and species-assembly hydraulic metrics representing a) mean HSM; b) minimum HSM; c) HSM variability and d) number of species with HSM < 0 including their interaction with functional type distribution. Results summarize 100 iterations of each model from which R^2 and test AUC mean and standard deviation were calculated. In each iteration, a different set of background points was sampled. Mean response curves for individual species-assembly metrics for each functional type and performance of multiple generalized linear models are shown.

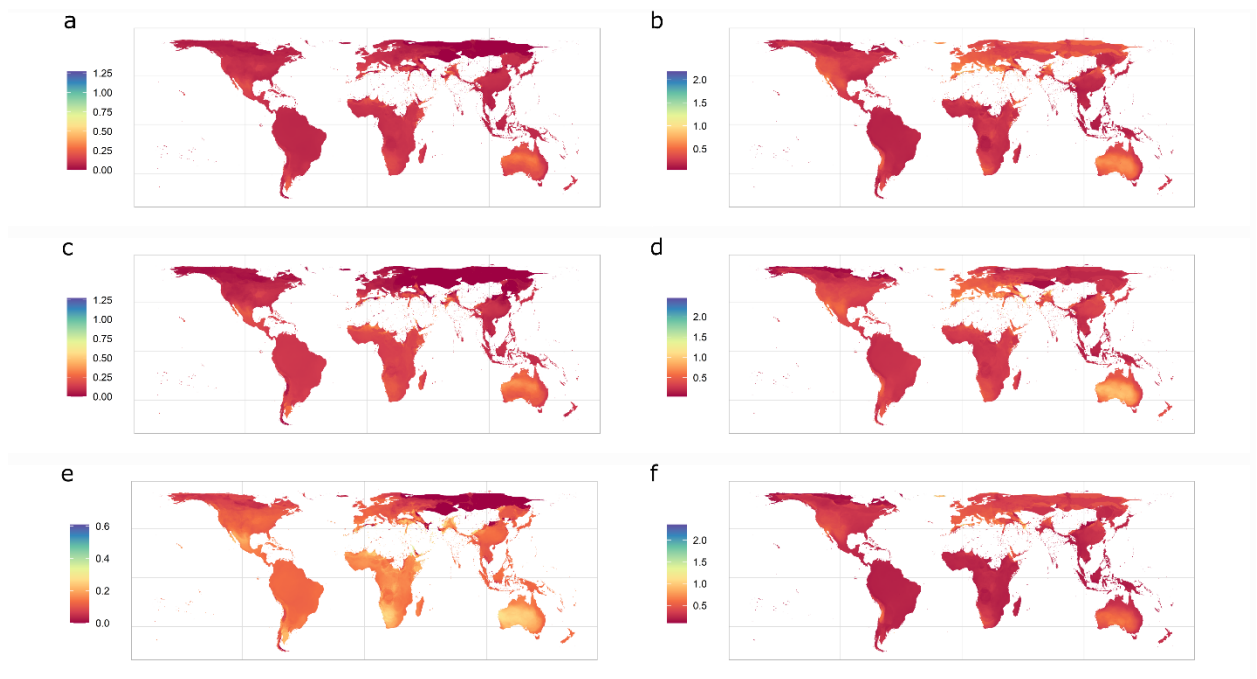


Figure S5.8 Mean of standard deviations resulting from 100 iterations of the predictive models (left column) and from 100 iterations of the predictive models randomly excluding 20% of the species with observed traits in each case (right column) for P_{\min} (first row), P_{50} (second row) and HSM (third row).

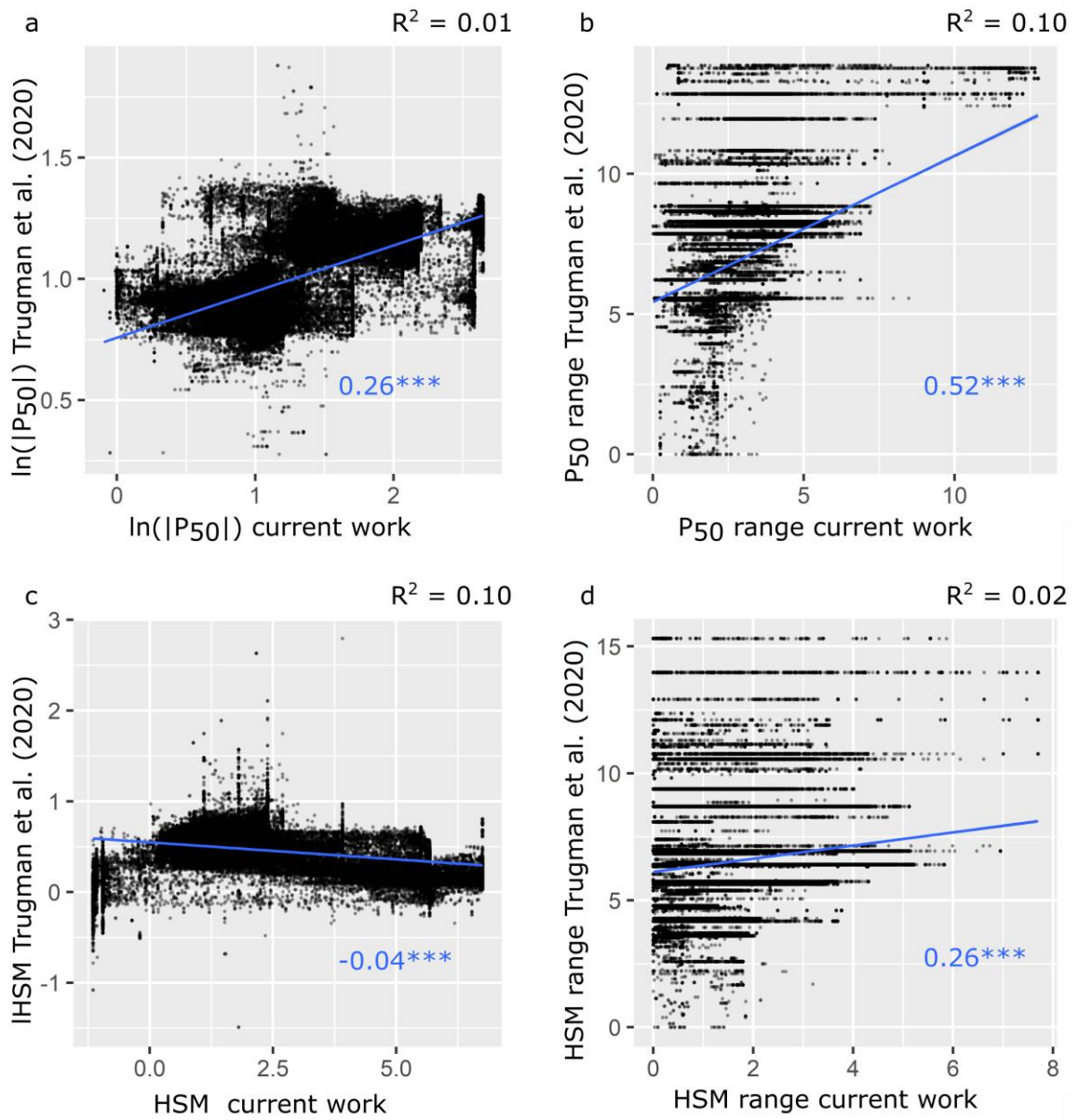


Figure S5.9 Comparison between P₅₀ and HSM mean and range projections calculated here with previous results including plot-level data(Trugman et al. 2020) for the United States of America. Linear regressions coefficients and R² are shown.

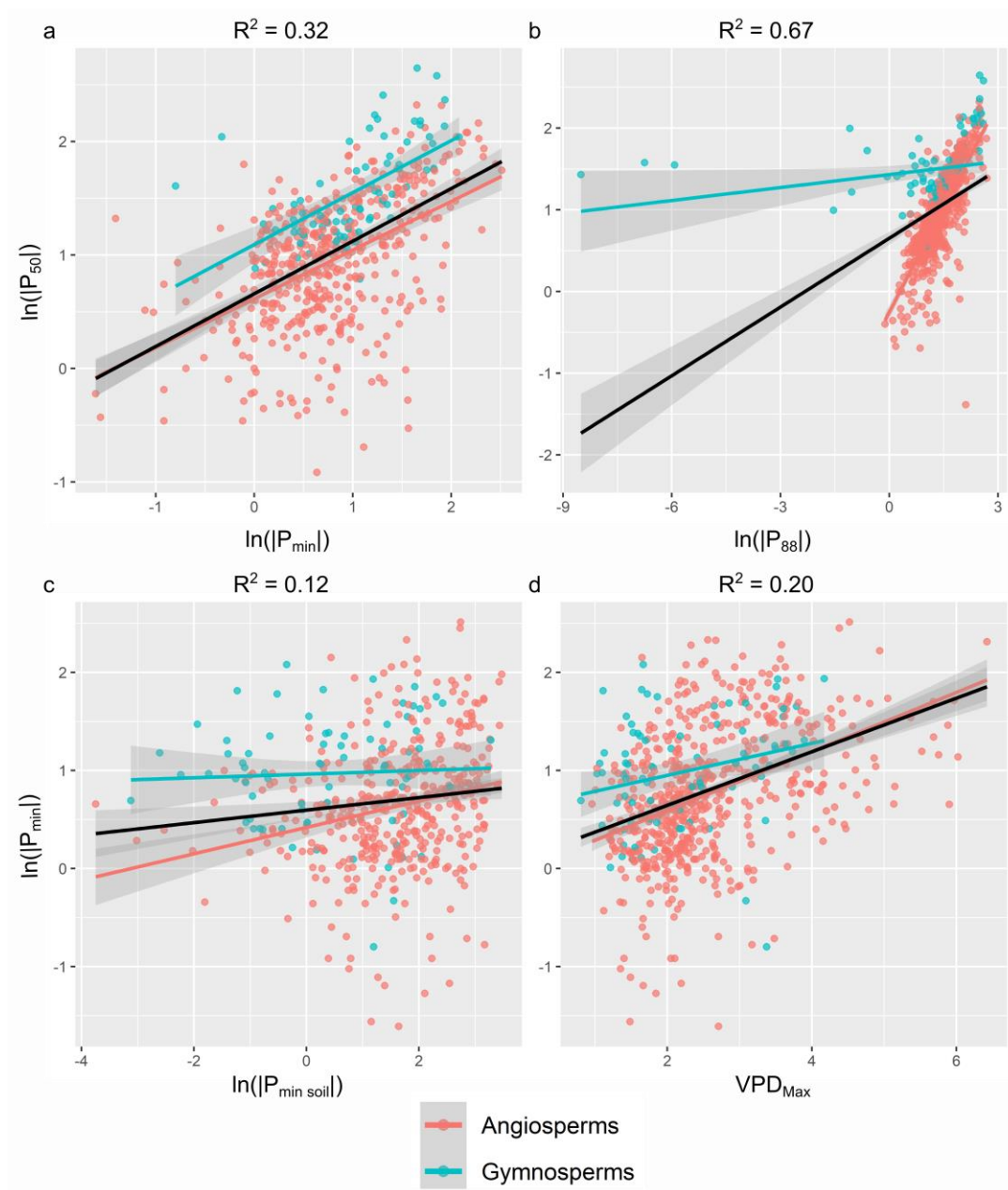


Figure S5.10 Relationship between variables as calculated by linear models including evolutionary affiliation as a factor (angiosperms and gymnosperms) for: a) water potential at 50% loss of conductivity (P_{50}) and minimum xylem water potential (P_{min}) (\ln -transformation of the absolute values), b) P_{50} and water potential at 88% loss of conductivity (P_{88}) (\ln -transformation of the absolute values), c) P_{min} and estimated minimum soil water potential ($P_{min\ soil}$) and d) P_{min} and maximum vapour pressure deficit.

Table S5.1 Random forest models performance. R^2 results for different combinations of predictors and different percentages of data used to train and test models. Model refers to the model tested indicating the variable predicted (bi when both are predicted at the same time), the number of climate (climate_n) and phylogenetic predictors (phylo_n) and whether evolutionary affiliation (angiosperms vs. gymnosperms) was included as an explanatory factor (group), in this order. In bold, the models used for the final prediction.

Model	Variable	N environmental PCs	N phylogenetic PCs	Evolutionary affiliation	Hydraulic trait covariance	R^2 (10% test)	R^2 sd (10% test)	R^2 (20% test)	R^2 sd (20% test)	R^2 (30% test)	R^2 sd (30% test)	R^2 (50% test)	R^2 sd (50% test)	R^2 (70% test)	R^2 sd (70% test)
P50_climate_3	P ₅₀	3	0	No	No	0.11	0.055	0.106	0.038	0.102	0.029	0.095	0.021	0.084	0.017
Pmin_climate_3	P _{min}	3	0	No	No	0.369	0.094	0.35	0.064	0.355	0.052	0.334	0.032	0.318	0.03
bi_climate_3	P _{min}	3	0	No	Yes	0.512	0.123	0.469	0.092	0.441	0.066	0.364	0.051	0.281	0.058
bi_climate_3	P ₅₀	3	0	No	Yes	0.304	0.123	0.277	0.081	0.25	0.072	0.183	0.05	0.116	0.038
P50_climate_10	P ₅₀	10	0	No	No	0.154	0.071	0.154	0.046	0.143	0.032	0.136	0.025	0.12	0.02
Pmin_climate_10	P _{min}	10	0	No	No	0.415	0.096	0.377	0.06	0.375	0.052	0.364	0.037	0.335	0.03
bi_climate_10	P _{min}	10	0	No	Yes	0.544	0.102	0.499	0.074	0.465	0.061	0.399	0.047	0.337	0.043
bi_climate_10	P ₅₀	10	0	No	Yes	0.35	0.122	0.309	0.087	0.263	0.067	0.198	0.047	0.133	0.035
P50_phylo_5	P ₅₀	0	5	No	No	0.473	0.088	0.465	0.059	0.453	0.053	0.433	0.031	0.402	0.027
Pmin_phylo_5	P _{min}	0	5	No	No	0.333	0.108	0.3	0.084	0.297	0.061	0.249	0.05	0.191	0.04
bi_phylo_5	P _{min}	0	5	No	Yes	0.457	0.137	0.422	0.099	0.4	0.071	0.311	0.058	0.237	0.049
bi_phylo_5	P ₅₀	0	5	No	Yes	0.5	0.108	0.471	0.102	0.45	0.066	0.387	0.053	0.332	0.048
P50_phylo_20	P ₅₀	0	20	No	No	0.474	0.097	0.461	0.064	0.451	0.051	0.438	0.034	0.409	0.028
Pmin_phylo_20	P _{min}	0	20	No	No	0.341	0.134	0.313	0.082	0.306	0.058	0.267	0.049	0.206	0.038
bi_phylo_20	P _{min}	0	20	No	Yes	0.438	0.131	0.428	0.095	0.396	0.082	0.338	0.049	0.258	0.047

bi_phylo_20	P ₅₀	0	20	No	Yes	0.485	0.159	0.464	0.093	0.454	0.071	0.397	0.052	0.349	0.045
P50_phylo_50	P ₅₀	0	50	No	No	0.455	0.106	0.475	0.062	0.462	0.047	0.44	0.038	0.411	0.028
Pmin_phylo_50	P _{min}	0	50	No	No	0.345	0.13	0.311	0.077	0.31	0.067	0.271	0.047	0.206	0.041
bi_phylo_50	P _{min}	0	50	No	Yes	0.439	0.14	0.42	0.096	0.387	0.088	0.336	0.047	0.269	0.041
bi_phylo_50	P ₅₀	0	50	No	Yes	0.485	0.123	0.481	0.091	0.44	0.063	0.398	0.047	0.352	0.038
P50_phylo_100	P ₅₀	0	100	No	No	0.487	0.088	0.482	0.058	0.461	0.052	0.452	0.03	0.425	0.026
Pmin_phylo_100	P _{min}	0	100	No	No	0.341	0.126	0.318	0.077	0.304	0.069	0.264	0.038	0.206	0.032
bi_phylo_100	P _{min}	0	100	No	Yes	0.44	0.119	0.412	0.105	0.373	0.068	0.326	0.05	0.249	0.042
bi_phylo_100	P ₅₀	0	100	No	Yes	0.456	0.132	0.429	0.097	0.429	0.073	0.395	0.044	0.357	0.043
P50_climate_3_phylo_5_group	P ₅₀	3	5	Yes	No	0.573	0.101	0.558	0.068	0.556	0.054	0.535	0.029	0.498	0.028
Pmin_climate_3_phylo_5_group	P _{min}	3	5	Yes	No	0.467	0.115	0.468	0.086	0.456	0.06	0.43	0.039	0.401	0.031
bi_climate_3_phylo_5_group	P _{min}	3	5	Yes	Yes	0.588	0.122	0.559	0.082	0.525	0.066	0.475	0.056	0.399	0.049
bi_climate_3_phylo_5_group	P ₅₀	3	5	Yes	Yes	0.551	0.123	0.528	0.1	0.515	0.071	0.459	0.055	0.399	0.046
P50_climate_5_phylo_5_group	P ₅₀	5	5	Yes	No	0.567	0.101	0.564	0.063	0.563	0.047	0.532	0.035	0.507	0.026
Pmin_climate_5_phylo_5_group	P _{min}	5	5	Yes	No	0.489	0.101	0.491	0.076	0.485	0.052	0.457	0.039	0.425	0.029
bi_climate_5_phylo_5_group	P _{min}	5	5	Yes	Yes	0.594	0.118	0.581	0.079	0.551	0.061	0.496	0.051	0.44	0.04
bi_climate_5_phylo_5_group	P ₅₀	5	5	Yes	Yes	0.547	0.13	0.537	0.091	0.526	0.069	0.476	0.054	0.403	0.045
P50_climate_10_phylo_10_group	P ₅₀	10	10	Yes	No	0.579	0.094	0.575	0.057	0.57	0.046	0.538	0.035	0.509	0.021
Pmin_climate_10_phylo_10_group	P _{min}	10	10	Yes	No	0.483	0.108	0.485	0.069	0.464	0.059	0.458	0.036	0.422	0.031
bi_climate_10_phylo_10_group	P _{min}	10	10	Yes	Yes	0.575	0.117	0.564	0.078	0.559	0.062	0.505	0.046	0.434	0.046
bi_climate_10_phylo_10_group	P ₅₀	10	10	Yes	Yes	0.558	0.139	0.541	0.087	0.521	0.071	0.489	0.044	0.411	0.038
P50_climate_10_phylo_20_group	P ₅₀	10	10	Yes	No	0.569	0.094	0.557	0.066	0.56	0.056	0.542	0.037	0.501	0.028
Pmin_climate_10_phylo_20_group	P _{min}	10	20	Yes	No	0.491	0.101	0.47	0.08	0.47	0.06	0.443	0.043	0.406	0.037

bi_climate_10_phylo_20_group	P _{min}	10	20	Yes	Yes	0.578	0.126	0.578	0.105	0.544	0.067	0.492	0.048	0.435	0.041
bi_climate_10_phylo_20_group	P ₅₀	10	20	Yes	Yes	0.551	0.129	0.54	0.087	0.517	0.068	0.458	0.05	0.405	0.04
P50_climate_10_phylo_50_group	P ₅₀	10	50	Yes	No	0.572	0.103	0.567	0.067	0.556	0.051	0.533	0.035	0.496	0.026
Pmin_climate_10_phylo_50_group	P _{min}	10	50	Yes	No	0.473	0.13	0.463	0.077	0.459	0.059	0.436	0.045	0.39	0.04
bi_climate_10_phylo_50_group	P _{min}	10	50	Yes	Yes	0.547	0.134	0.528	0.093	0.511	0.077	0.478	0.048	0.411	0.046
bi_climate_10_phylo_50_group	P ₅₀	10	50	Yes	Yes	0.534	0.128	0.507	0.098	0.492	0.071	0.452	0.053	0.391	0.04
P50_climate_10_phylo_100_group	P ₅₀	10	100	Yes	No	0.557	0.101	0.557	0.062	0.546	0.051	0.524	0.039	0.49	0.025
Pmin_climate_10_phylo_100_group	P _{min}	10	100	Yes	No	0.467	0.111	0.45	0.079	0.449	0.064	0.414	0.046	0.373	0.045
bi_climate_10_phylo_100_group	P _{min}	10	100	Yes	Yes	0.545	0.118	0.512	0.098	0.496	0.07	0.457	0.052	0.389	0.042
bi_climate_10_phylo_100_group	P ₅₀	10	100	Yes	Yes	0.497	0.132	0.49	0.097	0.469	0.076	0.441	0.048	0.385	0.039

Table S5.2 Prediction of DIM occurrence. Pseudo-R² test AUC mean and standard deviation and mean model AIC (summary of 100 iterations with different background points) for logistic models with mortality occurrence as a response variable (binary). In the model column, model formula is shown.

Model	Mean R ²	R ² standard deviation	Mean test AUC	Test AUC standard deviation	AIC
p ~ ln(aridity index)	0.011	0.006	0.590	0.042	1384.780
p ~ annual precipitation	0.016	0.006	0.555	0.036	1381.321
p ~ maximum temperature	0.019	0.008	0.594	0.045	1378.893
p ~ HSM mean	0.067	0.014	0.683	0.032	1341.226
p ~ HSM mean * biome	0.346	0.024	0.772	0.038	1116.217
p ~ HSM mean * functional type	0.189	0.017	0.683	0.036	1268.188
p ~ HSM min	0.264	0.022	0.750	0.033	1171.312
p ~ HSM min * biome	0.369	0.022	0.793	0.030	1091.891
p ~ HSM min * functional type	0.340	0.019	0.766	0.029	1125.860
p ~ sqrt(Number spp. HSM<0)	0.357	0.017	0.817	0.020	1865.168
p ~ sqrt(Number spp. HSM<0) * biome	0.434	0.020	0.826	0.025	1022.707
p ~ sqrt(Number spp. HSM<0) * functional type	0.470	0.014	0.836	0.019	1680.722
p ~ ln(HSM variance)	0.236	0.019	0.751	0.033	1197.921
p ~ ln(HSM variance) * biome	0.343	0.022	0.779	0.033	1118.953
p ~ ln(HSM variance) * functional type	0.460	0.010	0.828	0.021	1699.935

Table S5.3 Relationship of hydraulic risk and mortality. Variables significance (mean of ANOVA test results for 100 models with different background points in each case) for logistic models with mortality occurrence as a response variable (binary). In the column “variable”, interaction is shown by “:”. Significance codes: “***”: $p < 0.0001$; “**”: $p < 0.001$, “*”: $p < 0.05$; NS: non-significant.

Model	Variable	df	Deviance mean	Resid. df mean	Resid. dev mean	Pr. Chi mean	Deviance sd	Resid dev sd	Pr. Chi sd	Pr. Chi mean significance
p ~ HSM mean	HSM mean	1	51.841	1000	1337.226	0	10.68	10.68	0	***
p ~ HSM mean * biome	biome	6	224.773	994	1112.043	0	18.204	22.217	0	***
p ~ HSM mean * biome	HSM mean	1	52.251	1000	1336.816	0	15.478	15.478	0	***
p ~ HSM mean * biome	HSM mean: biome	6	23.826	988	1088.217	0.003	6.522	24.153	0.005	*
p ~ HSM mean * functional type	functional type	7	32.082	993	1303.737	0.001	7.046	10.295	0.003	**
p ~ HSM mean * functional type	HSM mean	1	53.248	1000	1335.819	0	9.469	9.469	0	***
p ~ HSM mean * functional type	HSM mean:functional type	7	67.549	986	1236.188	0	11.375	14.468	0	***
p ~ HSM min	HSM min	1	221.755	1000	1167.312	0	20.287	20.287	0	***
p ~ HSM min * biome	biome	6	92.65	994	1074.169	0	12.602	21.822	0	***
p ~ HSM min * biome	HSM min	1	222.248	1000	1166.818	0	20.534	20.534	0	***
p ~ HSM min * biome	HSM min: biome	6	10.278	988	1063.891	0.21	4.536	22.378	0.211	NS
p ~ HSM min * functional type	functional type	7	15.65	993	1149.341	0.081	5.166	18.708	0.118	NS
p ~ HSM min * functional type	HSM min	1	224.076	1000	1164.991	0	19.102	19.102	0	***
p ~ HSM min * functional type	HSM min:functional type	7	55.481	986	1093.86	0	12.066	19.581	0	***
p ~sqrt(Number spp. HSM<0)	ln(Number spp. HSM<0)	1	539.894	1730	1861.168	0	29.675	29.675	0	***
p ~sqrt(Number spp. HSM<0) * biome	biome	6	205.52	1724	1659.295	0	18.323	27.404	0	***
p ~sqrt(Number spp. HSM<0) * biome	sqrt(Number spp. HSM<0)	1	536.247	1730	1864.815	0	27.112	27.112	0	***
p ~sqrt(Number spp. HSM<0) * biome	sqrt(Number spp. HSM<0): biome	6	58.909	1718	1600.386	0	10.15	28.109	0	***
p ~sqrt(Number spp. HSM<0) * functional type	functional type	7	46.522	1723	1817.921	0	8.821	26.094	0	***
p ~sqrt(Number spp. HSM<0) * functional type	sqrt(Number spp. HSM<0)	1	536.619	1730	1864.443	0	26.715	26.715	0	***
p ~sqrt(Number spp. HSM<0) * functional type	sqrt(Number spp. HSM<0):functional type	7	169.199	1716	1648.722	0	19.237	27.167	0	***

p ~ ln(HSM variance)	ln(HSM variance)	1	195.146	1000	1193.921	0	17.592	17.592	0	***
p ~ ln(HSM variance) * biome	biome	6	81.35	994	1112.946	0	14.655	20.848	0	***
p ~ ln(HSM variance) * biome	ln(HSM variance)	1	194.77	1000	1194.297	0	17.899	17.899	0	***
p ~ ln(HSM variance) * biome	ln(HSM variance): biome	6	21.994	988	1090.953	0.006	5.394	22.255	0.014	*
p ~ ln(HSM variance) * functional type	functional type	7	111.59	1723	1820.328	0	15.037	24.614	0	***
p ~ ln(HSM variance) * functional type	ln(HSM variance)	1	469.144	1730	1931.918	0	23.493	23.493	0	***
p ~ ln(HSM variance) * functional type	ln(HSM variance):functional type	7	152.393	1716	1667.935	0	16.624	20.322	0	***

Table S5.4 Relationship of hydraulic risk and mortality including aridity index as a covariable. Variables significance (mean of the ANOVA test results for 100 models with different background points in each case) for logistic models with mortality occurrence as a response variable (binary) including a climate index as predictor (aridity index). In the column “variable”, interaction is shown by “:”. Significance codes: “***”: $p < 0.0001$; “**”: $p < 0.001$, “*”: $p < 0.05$; NS: $p > 0.05$.

Model	Variable	df	Deviance mean	Resid. df mean	Resid. dev mean	Pr. Chi mean	Deviance sd	Resid dev sd	Pr. Chi sd	Pr. Chi mean significance
p ~ HSM mean + ln(aridity index)	HSM mean	1	53.534	1000.000	1335.533	0.000	10.598	10.598	0.000	***
p ~ HSM mean + ln(aridity index)	ln(aridity index)	1	3.053	999.000	1332.480	0.223	2.994	10.306	0.214	NS
p ~ HSM mean * biome + ln(aridity index)	biome	6	211.323	994.000	1125.997	0.000	18.644	18.498	0.000	***
p ~ HSM mean * biome + ln(aridity index)	HSM mean	1	51.746	1000.000	1337.321	0.000	9.426	9.426	0.000	***
p ~ HSM mean * biome + ln(aridity index)	HSM mean:biome	6	21.390	987.000	1103.398	0.005	4.441	18.717	0.006	*
p ~ HSM mean * biome + ln(aridity index)	ln(aridity index)	1	1.210	993.000	1124.787	0.434	1.390	18.695	0.283	NS
p ~ HSM mean * functional type + ln(aridity index)	functional type	7	32.952	993.000	1303.902	0.001	7.681	11.205	0.002	**
p ~ HSM mean * functional type + ln(aridity index)	HSM mean	1	52.213	1000.000	1336.854	0.000	9.682	9.682	0.000	***
p ~ HSM mean * functional type + ln(aridity index)	HSM mean:functional type	7	61.136	985.000	1232.568	0.000	11.531	15.708	0.000	***
p ~ HSM mean * functional type + ln(aridity index)	ln(aridity index)	1	10.198	992.000	1293.704	0.014	5.132	10.846	0.036	.
p ~ ln(HSM variance) + ln(aridity index)	ln(aridity index)	1	7.026	999.000	1188.284	0.038	3.566	15.967	0.078	.
p ~ ln(HSM variance) + ln(aridity index)	ln(HSM variance)	1	193.757	1000.000	1195.310	0.000	16.515	16.515	0.000	***
p ~ ln(HSM variance) * biome + ln(aridity index)	biome	6	81.768	994.000	1110.967	0.000	12.346	20.381	0.000	***
p ~ ln(HSM variance) * biome + ln(aridity index)	ln(aridity index)	1	1.393	993.000	1109.574	0.425	1.661	20.705	0.298	NS
p ~ ln(HSM variance) * biome + ln(aridity index)	ln(HSM variance)	1	196.332	1000.000	1192.735	0.000	16.900	16.900	0.000	***
p ~ ln(HSM variance) * biome + ln(aridity index)	ln(HSM variance):biome	6	21.237	987.000	1088.337	0.009	5.625	23.029	0.017	*
p ~ ln(HSM variance) * functional type + ln(aridity index)	functional type	7	112.556	1723.000	1823.255	0.000	15.843	24.798	0.000	***

p ~ ln(HSM variance) * functional type + ln(aridity index)	ln(aridity index)	1	0.883	1722.000	1822.372	0.534	1.235	24.904	0.296	NS
p ~ ln(HSM variance) * functional type + ln(aridity index)	ln(HSM variance)	1	465.251	1730.000	1935.811	0.000	26.478	26.478	0.000	***
p ~ ln(HSM variance) * functional type + ln(aridity index)	ln(HSM variance):functional type	7	152.823	1715.000	1669.549	0.000	15.838	22.053	0.000	***
p ~ HSM min + ln(aridity index)	HSM min	1	220.492	1000.000	1168.575	0.000	19.283	19.283	0.000	***
p ~ HSM min + ln(aridity index)	ln(aridity index)	1	0.646	999.000	1167.930	0.564	0.830	19.157	0.271	NS
p ~ HSM min * biome + ln(aridity index)	biome	6	92.926	994.000	1074.115	0.000	14.567	21.186	0.000	***
p ~ HSM min * biome + ln(aridity index)	HSM min	1	222.026	1000.000	1167.041	0.000	19.720	19.720	0.000	***
p ~ HSM min * biome + ln(aridity index)	HSM min:biome	6	10.618	987.000	1062.268	0.168	3.806	22.782	0.164	NS
p ~ HSM min * biome + ln(aridity index)	ln(aridity index)	1	1.228	993.000	1072.887	0.460	1.554	21.716	0.301	NS
p ~ HSM min * functional type + ln(aridity index)	functional type	7	16.154	993.000	1151.774	0.069	5.272	18.874	0.092	NS
p ~ HSM min * functional type + ln(aridity index)	HSM min	1	221.139	1000.000	1167.928	0.000	19.708	19.708	0.000	***
p ~ HSM min * functional type + ln(aridity index)	HSM min:functional type	7	57.426	985.000	1093.693	0.000	10.881	18.582	0.000	***
p ~ HSM min * functional type + ln(aridity index)	ln(aridity index)	1	0.655	992.000	1151.119	0.540	0.761	19.016	0.256	NS
p ~ sqrt(Number spp. HSM<0) + ln(aridity index)	ln(aridity index)	1	41.829	1729.000	1824.266	0.000	12.322	30.667	0.000	***
p ~ sqrt(Number spp. HSM<0) + ln(aridity index)	sqrt(Number spp. HSM<0)	1	534.967	1730.000	1866.095	0.000	29.005	29.005	0.000	***
p ~ sqrt(Number spp. HSM<0) * biome + ln(aridity index)	biome	6	208.016	1724.000	1654.678	0.000	21.649	27.566	0.000	***
p ~ sqrt(Number spp. HSM<0) * biome + ln(aridity index)	ln(aridity index)	1	10.868	1723.000	1643.811	0.014	5.655	29.018	0.038	.
p ~ sqrt(Number spp. HSM<0) * biome + ln(aridity index)	sqrt(Number spp. HSM<0)	1	538.368	1730.000	1862.694	0.000	24.858	24.858	0.000	***
p ~ sqrt(Number spp. HSM<0) * biome + ln(aridity index)	sqrt(Number spp. HSM<0):biome	6	54.857	1717.000	1588.953	0.000	11.422	29.192	0.000	***
p ~ sqrt(Number spp. HSM<0) * functional type + ln(aridity index)	functional type	7	46.839	1723.000	1813.096	0.000	8.278	28.769	0.000	***
p ~ sqrt(Number spp. HSM<0) * functional type + ln(aridity index)	ln(aridity index)	1	39.652	1722.000	1773.444	0.000	10.485	27.221	0.000	***
p ~ sqrt(Number spp. HSM<0) * functional type + ln(aridity index)	sqrt(Number spp. HSM<0)	1	541.126	1730.000	1859.935	0.000	30.292	30.292	0.000	***
p ~ sqrt(Number spp. HSM<0) * functional type + ln(aridity index)	sqrt(Number spp. HSM<0):functional type	7	138.170	1715.000	1635.274	0.000	18.109	27.114	0.000	***

Table S5.5 Biome reclassification and number of mortality observations per biome and per functional type.

Aggregated biome	Biomes included	Number of total mortality points (1 per km²)	Number of aggregated mortality points (1 per 10km²)
Boreal	Tundra, Boreal Forests/Taiga,	39	34
Desert and xeric	Deserts & Xeric Shrublands	44	20
Mediterranean	Mediterranean Forests, Woodlands & Scrub,	292	139
Others	Montane Grasslands & Shrublands, Flooded Grasslands & Savannas, Mangroves,	4	4
Temperate	Temperate Grasslands, Savannas & Shrublands, Temperate Conifer Forests, Temperate Broadleaf & Mixed Forests	357	223
Tropical and subtropical dry	Tropical & Subtropical Grasslands, Savannas & Shrublands, Tropical & Subtropical Dry Broadleaf Forests, Tropical & Subtropical Coniferous Forests	73	42
Tropical and subtropical moist	Tropical & Subtropical Moist Broadleaf Forests,	73	55

Table S5.6 Trends in the relationship between species assemblages hydraulic metrics and DIM occurrence as reported by applying the emmeans R package(Lenth 2021) to generalized linear models results.

Model	Factor	Trend mean	St error mean	P value mean	Trend sd	St error sd	P value sd	Mean p value significance
p ~ HSM mean * biome	Boreal	-0.345	0.772	0.616	0.391	0.057	0.250	NS
p ~ HSM mean * biome	Desert and xeric	-0.029	0.312	0.695	0.157	0.026	0.200	NS
p ~ HSM mean * biome	Mediterranean	-1.395	0.689	0.174	1.089	0.126	0.263	NS
p ~ HSM mean * biome	Others	1.412	1.483	0.421	1.170	0.492	0.203	NS
p ~ HSM mean * biome	Temperate	-2.473	0.338	0.000	0.307	0.014	0.000	***
p ~ HSM mean * biome	Tropical and subtropical dry	-1.886	0.922	0.068	0.531	0.066	0.084	NS
p ~ HSM mean * biome	Tropical and subtropical moist	-0.869	0.812	0.349	0.534	0.053	0.268	NS
p ~ HSM mean * functional type	Broadleaved deciduous	-2.257	0.823	0.014	0.595	0.091	0.021	.
p ~ HSM mean * functional type	Broadleaved evergreen	-6.622	0.936	0.000	0.866	0.090	0.000	***
p ~ HSM mean * functional type	Crops and Grassland	-1.489	0.334	0.000	0.275	0.021	0.001	**
p ~ HSM mean * functional type	Mixed forest	-1.321	1.363	0.383	1.014	0.188	0.255	NS
p ~ HSM mean * functional type	Mosaic	0.686	0.388	0.095	0.163	0.030	0.068	NS
p ~ HSM mean * functional type	Needleleaved	-8.505	0.953	0.000	0.936	0.106	0.000	***
p ~ HSM mean * functional type	Others	-1.338	0.616	0.050	0.423	0.082	0.047	.
p ~ HSM mean * functional type	Shrubland	-1.117	0.516	0.075	0.418	0.054	0.102	NS
p ~ HSM min * biome	Boreal	-0.416	0.288	0.202	0.168	0.023	0.153	NS
p ~ HSM min * biome	Desert and xeric	-0.493	0.134	0.003	0.152	0.017	0.009	*
p ~ HSM min * biome	Mediterranean	-1.043	0.282	0.022	0.351	0.041	0.082	.
p ~ HSM min * biome	Others	0.209	0.576	0.688	0.203	0.158	0.161	NS
p ~ HSM min * biome	Temperate	-0.705	0.076	0.000	0.048	0.003	0.000	***
p ~ HSM min * biome	Tropical and subtropical dry	0.085	0.073	0.294	0.035	0.002	0.202	NS
p ~ HSM min * biome	Tropical and subtropical moist	-0.323	0.070	0.000	0.029	0.001	0.000	***
p ~ HSM min * functional type	Broadleaved deciduous	-0.422	0.138	0.008	0.130	0.016	0.011	*
p ~ HSM min * functional type	Broadleaved evergreen	-0.248	0.068	0.016	0.071	0.003	0.070	.
p ~ HSM min * functional type	Crops and Grassland	-0.139	0.064	0.070	0.046	0.002	0.099	NS
p ~ HSM min * functional type	Mixed forest	-1.279	0.431	0.007	0.405	0.101	0.010	*
p ~ HSM min * functional type	Mosaic	-0.120	0.094	0.285	0.064	0.005	0.237	NS
p ~ HSM min * functional type	Needleleaved	-2.108	0.236	0.000	0.232	0.035	0.000	***
p ~ HSM min * functional type	Others	-0.442	0.118	0.001	0.098	0.011	0.002	**
p ~ HSM min * functional type	Shrubland	0.004	0.073	0.574	0.059	0.003	0.262	NS
p ~ sqrt(N spp. HSM < 0) * biome	Boreal	1.058	0.321	0.003	0.192	0.016	0.004	*
p ~ sqrt(N spp. HSM < 0) * biome	Desert and xeric	0.656	0.170	0.000	0.095	0.011	0.001	**
p ~ sqrt(N spp. HSM < 0) * biome	Mediterranean	1.526	0.296	0.000	0.270	0.035	0.000	***
p ~ sqrt(N spp. HSM < 0) * biome	Others	0.133	2.281	0.790	0.804	16.627	0.182	NS

p ~ sqrt(N spp. HSM < 0) * biome	Temperate	0.832	0.080	0.000	0.039	0.002	0.000	***
p ~ sqrt(N spp. HSM < 0) * biome	Tropical and subtropical dry	0.251	0.098	0.023	0.051	0.002	0.045	.
p ~ sqrt(N spp. HSM < 0) * biome	Tropical and subtropical moist	1.449	0.280	0.000	0.141	0.023	0.000	***
p ~ sqrt(N spp. HSM < 0) * functional type	Broadleaved deciduous	0.755	0.157	0.000	0.090	0.009	0.000	***
p ~ sqrt(N spp. HSM < 0) * functional type	Broadleaved evergreen	2.381	0.324	0.000	0.196	0.021	0.000	***
p ~ sqrt(N spp. HSM < 0) * functional type	Crops and Grassland	0.397	0.078	0.000	0.046	0.002	0.000	***
p ~ sqrt(N spp. HSM < 0) * functional type	Mixed forest	1.367	0.415	0.002	0.342	0.088	0.002	*
p ~ sqrt(N spp. HSM < 0) * functional type	Mosaic	0.346	0.138	0.028	0.075	0.005	0.052	.
p ~ sqrt(N spp. HSM < 0) * functional type	Needleleaved	2.280	0.264	0.000	0.137	0.018	0.000	***
p ~ sqrt(N spp. HSM < 0) * functional type	Others	0.641	0.155	0.000	0.087	0.007	0.000	**
p ~ sqrt(N spp. HSM < 0) * functional type	Shrubland	0.332	0.109	0.011	0.082	0.004	0.023	.
p ~ ln(HSM variance) * biome	Boreal	0.649	0.248	0.014	0.104	0.013	0.013	.
p ~ ln(HSM variance) * biome	Desert and xeric	1.032	0.414	0.031	0.302	0.046	0.053	.
p ~ ln(HSM variance) * biome	Mediterranean	2.817	0.561	0.000	0.457	0.070	0.000	***
p ~ ln(HSM variance) * biome	Others	2.198	1.300	0.104	0.612	0.210	0.050	NS
p ~ ln(HSM variance) * biome	Temperate	1.406	0.159	0.000	0.080	0.004	0.000	***
p ~ ln(HSM variance) * biome	Tropical and subtropical dry	0.008	0.130	0.704	0.061	0.007	0.183	NS
p ~ ln(HSM variance) * biome	Tropical and subtropical moist	1.172	0.266	0.000	0.103	0.008	0.000	***
p ~ ln(HSM variance) * functional type	Broadleaved deciduous	1.181	0.290	0.000	0.153	0.019	0.000	**
p ~ ln(HSM variance) * functional type	Broadleaved evergreen	3.604	0.436	0.000	0.175	0.017	0.000	***
p ~ ln(HSM variance) * functional type	Crops and Grassland	0.552	0.129	0.000	0.069	0.004	0.000	**
p ~ ln(HSM variance) * functional type	Mixed forest	3.790	1.361	0.009	1.251	0.378	0.012	*
p ~ ln(HSM variance) * functional type	Mosaic	0.704	0.254	0.013	0.152	0.015	0.021	.
p ~ ln(HSM variance) * functional type	Needleleaved	3.036	0.359	0.000	0.182	0.016	0.000	***
p ~ ln(HSM variance) * functional type	Others	0.869	0.281	0.003	0.103	0.015	0.003	*
p ~ ln(HSM variance) * functional type	Shrubland	0.121	0.138	0.416	0.101	0.007	0.275	NS

